



UNIVERSITAT POLITÈCNICA DE CATALUNYA
ESCOLA TÈCNICA SUPERIOR D'ENGINYERS
DE CAMINS, CANALS I PORTS



DEPARTAMENT DE RESISTÈNCIA DE MATERIALS I
ESTRUCTURES A L'ENGINYERIA

PLASTICITY AND DAMAGE OF FRAMED STRUCTURES

DOCTORAL THESIS

By:

JEOVAN FALEIRO DE FREITAS

Advisors:

Prof. ALEX H. BARBAT
Prof. SERGIO OLLER

Barcelona, July 2006

Esta tesis fue leída el día en la Escuela Técnica Superior de Ingenieros de Caminos, Canales y Puertos de Barcelona, obteniendo la calificación de

El Presidente,

El Secretario,

El Vocal,

El Vocal,

El Vocal,

To my wife and son

Acknowledgements

A number of people have directly and indirectly contributed to this thesis. I would especially like to thank:

Prof. Alex Barbat, my doctorate supervisor, for allowing me to taste real academic freedom for the first time and for helping me to enter the world of "publish or perish".

Prof. Sergio Oller, my other doctorate supervisor, for his friendship and support these past few years as I struggled to shift paradigms.

Prof. Pratini, for the first opportunity in the academic life.

Prof. Lineu, for encouraging me to pursue a doctorate in the first instance and for helping me secure the CAPES studentship.

My Brazilians, Argentine, Catalans, Chilean, Colombian, Mexican, Spanish and Venezuelan friends for their friendship and by the endless hours of intense and always highly rewarding philosophical discussion. (We should have drunk more)

My wife, Eliane, for all her love, support, and help during these long four years. (We both learn that a "book" is an object and we will always have Paris, London, Oslo, Rome... to go back)

My baby son Caio, who without knowing, was one of the motivations to make this thesis.

My parents, for instilling in me the love of wisdom and for helping me at every step on the journey towards enlightenment. Words cannot express ...

U2, Rolling Stones and Legião Urbana for providing inspirational musical accompaniment as I composed the various chapters of this thesis.

This work was supported by a CAPES Studentship.

Contents

<i>Acknowledgements</i>	iii
<i>Contents</i> i	
<i>List of Figures</i> v	
<i>Abstract</i> xi	
<i>Resumen</i> xiii	
Chapter 1 Introduction.....	1
1.1 General	1
1.2 Motivation	3
1.3 Objectives of the thesis.....	5
1.4 Contents of the thesis	6
Chapter 2 State of the Art	9
2.1 Introduction.....	9
2.2 Lumped and moment-curvature models.....	10
2.2.1 Moment-curvature models.....	10
2.2.2 Lumped Models.....	13
2.2.3 Stiffness models	16
2.3 Plastic-Damage models for reinforced concrete structures.....	21
2.4 Global damage in structures	26
2.4.1 Damage indices based on maximum deformation	26
2.4.2 Damage indices based on energy dissipation	30
Chapter 3 Formulation of Planar Frames	33
3.1 Introduction.....	33
3.2 Degrees of Freedom	35
3.3 Support Conditions	38
3.4 Generalized Deformations	39
3.5 Cinematic Equations	40
3.6 Generalized Stresses and Internal Forces.....	44
3.6.1 External Force.....	45

3.6.2	Inertial Force	46
3.6.3	Internal Forces.....	46
3.7	Dynamic equilibrium equation	49
3.8	Nonlinear Dynamic Analysis	49
3.8.1	Global stiffness matrix	51
3.8.2	Mass matrix	53
3.8.3	Damping matrix.....	55
3.9	Incremental equilibrium equations.....	56
3.9.1	Equilibrium Condition.....	57
3.9.2	Implicit solution: Newmark's method	59
3.10	Numerical Implementation.....	60
Chapter 4	Elastoplastic constitutive model for frames	65
4.1	Introduction.....	65
4.2	Yield Function for Plastic Hinge	67
4.3	Elastoplastic frames.....	68
4.3.1	Perfect Elastoplastic Frames	70
4.3.2	Elastoplastic Frames with Kinematic Hardening	74
4.3.3	Elastoplastic Frames with axial force	76
Chapter 5	Concentrated Damage Constitutive Model for Frames.....	83
5.1	Introduction.....	83
5.2	Elements of continuum damage mechanics	85
5.2.1	Strain-based Isotropic Continuum Damage Model	88
5.3	Concentrated Damage Constitutive Model.....	91
5.4	Damage evolution law of the Concentrated Damage Model.....	95
5.4.1	Free energy potential	96
5.4.2	Free Energy for Flexural Force	96
5.4.3	Free Energy for Axial Force	98
5.4.4	Free Energy for Frame Member	99
5.4.5	Undamaged energy norm and damage evolution	100
5.5	Local, plastic and global damage indexes.....	103
5.5.1	Local damage index	103
5.5.2	Plastic Damage index.....	104
5.5.3	Global damage index	105
5.6	Integration of the constitutive equation.....	106
5.7	Unilateral damage model.....	106
5.7.1	Undamaged energy norm and damage evolution for unilateral damage	108
5.7.2	Integration of the constitutive equation for unilateral damage.....	110

Chapter 6	Elastoplastic-Damage Model for Frames	113
6.1	Introduction.....	113
6.2	Characteristics of Reinforced Concrete Behaviour	114
6.2.1	Uncracked section.....	116
6.2.2	Crack propagation in the elastic section.....	118
6.2.3	Ultimate strength.....	119
6.3	Plastic-Damage model	122
6.3.1	Thermodynamic references.....	123
6.3.2	Internal variable evolution laws.....	124
6.3.3	Integration of the constitutive equation for plastic-damage model.....	126
6.4	Member damage index	128
Chapter 7	Numerical examples.....	131
7.1	Introduction.....	131
7.2	Example 1: Model validation using a simple framed structure.....	131
7.3	Example 2: Model validation using a simply reinforced concrete beam. 137	
7.4	Example 3: Model validation using a reinforced concrete framed structure	140
7.4.1	Comparison between local, plastic and member damage indexes	144
7.5	Example 4: Model validation using dynamic analysis of a reinforced concrete framed structure.....	146
7.6	Example 5: Pushover and dynamic analysis of a reinforced concrete frame	154
7.7	Example 6: Model validation using a reinforced concrete framed structure subjected to a synthetic earthquake accelerogram.	158
Chapter 8	Conclusions and Recommendations for Further Work	167
8.1	Conclusions of the research.....	167
8.2	Main contributions	169
8.3	Future research lines	170
Appendix 1	Element Flexibility and Stiffness Matrix	173
A1.1	Introduction.....	173
A1.2	Flexibility coefficient and flexibility matrix.....	175
A1.3	Stiffness coefficient and Stiffness matrix.....	180
A1.4	Flexibility and stiffness relation.....	187
A1.4.1	Frame Elements with internal hinges	190
A1.5	Stiffness and Flexibility Matrices of Beam-Columns.....	191

A1.5.1	Differential equations of the Beam-Columns	192
A1.5.2	Stiffness matrix	193
A1.6	Generalized Stress and Stiffness relationship	195
Appendix 2	One-Dimensional Plasticity.	197
A2.1	Introduction.....	197
A2.2	Uniaxial Elastoplasticity	198
A2.3	Simple elastoplastic constitutive models	202
A2.3.1	Flow theory.....	203
A2.3.2	Isotropic Hardening	205
A2.3.3	Kinematic Hardening law.	207
A2.3.4	Return-Mapping Algorithms.....	209
Appendix 3	Plastic Analysis Theory	213
A3.1	Introduction.....	213
A3.2	Bending stresses and strains in beam-column	214
A3.2.1	Bending in the elastic range	215
A3.2.2	Bending in plastic range	216
A3.3	Moment-Curvature diagram of a beam-column	217
A3.4	Plastic Hinge	219
A3.5	Theory of Plastic Analysis.....	223
A3.5.1	Statical Approach	225
A3.5.2	Kinematic Approach.....	225
References	227

List of Figures

Figure 2.1 – Elastoplastic model.	11
Figure 2.2 – Clough model.	11
Figure 2.3 – Takeda’s model.....	12
Figure 2.4 - Loading-unloading behaviour – Simulated behaviours and Experimental behaviour	21
Figure 3.3 - Generalized displacements of a node i	37
Figure 3.4 – Improper or insufficient support conditions.	38
Figure 3.5 – Improper internal connections.....	38
Figure 3.6 - The generalized deformations at the ends i and j	40
Figure 3.7 - Generalized deformations into a frame element due to an infinitesimal increment du_1	40
Figure 3.8 - Generalized deformations into a frame element due to an infinitesimal increment du_2	41
Figure 3.9 - Generalized deformations into a frame element due to an infinitesimal increment du_3	41
Figure 3.10 - Generalized stress of a member.....	48
Figure 3.11 - Lumped Mass for a frame element: a) Uniform mass; b) Triangular mass; and c) Generic mass.	54
Figure 3.12 – Beam subjected to unitary angular acceleration and virtual translation.	54
Table 3.1 – Nonlinear time integration scheme.....	63
Figure 4.1 – Elastoplastic model for Frames.....	67
Figure 4.2 – Plastic hinge and moment-plastic rotation for perfect plasticity.	68
Figure 4.3 – Lumped plastic model for Frames.....	69
Figure 4.4 – Moment-moment diagram of the elastic domain and admissible states	70

Figure 4.5 – The final moment obtained through the Return-Mapping procedure	73
Table 4.1 – Return-Mapping Algorithm for Perfect Elastoplastic Frames.	74
Figure 4.6 – Plastic hinge with kinematic hardening.	75
Table 4.2 – Return-Mapping algorithm for Elastoplastic Frames with Kinematic Hardening.....	76
Figure 4.7 – Yield Surface in $m - n$ space: a) without hardening effect; b) with hardening.	77
Figure 4.8 – Return-Mapping algorithm: a) one function outside the yield surface; b) both functions outside the yield surface.....	81
Table 4.3 – Return-Mapping algorithm for Elastoplastic Frames with Axial Force	82
Figure 5.1 – One-dimensional damage element.....	85
Figure 5.2 – Schematic illustration of the strain equivalence principle.....	86
Figure 5.3 – Schematic illustration of the hypothesis of the stress equivalence proposed by (Simo and Ju, 1987).	87
Figure 5.4 – Damage in beam-column elements: a) Cracking at the end, of one reinforce concrete beam, b) The concentrated damage model for beam-column.	91
Figure 5.5 - Flexibility Damage parameters.....	92
Table 5.1 – Procedure to the determination of the evolution of the damage parameters.	106
Figure 5.6 – Unilateral damage model, the damage evolution at hinges i and j : a) due to positive actions at hinges; b) due to negative actions at hinges.....	107
Table 5.2 – Procedure to determine of the evolution of the damage parameters for the unilateral damage.	111
Figure 6.1 – Pure bending of a beam.	114
Figure 6.2 – Schematic stress-strain curves of concrete and steel.....	115
Figure 6.3 – Typical moment-deformation of reinforced concrete structure: phase <i>I</i> and <i>II</i> define the serviceability limit states; phase <i>III</i> defines the ultimate state.....	116

Figure 6.4 – Uncracked behaviour of reinforced concrete.....	117
Figure 6.5 – Crack propagation within the elastic range.	118
Figure 6.6 – Ultimate strength condition.....	120
Figure 6.7 – Singly reinforced rectangular beam	120
Figure 6.8 - Doubly reinforced rectangular cross section.	121
Figure 6.9 - Loading-unloading behaviour – Simulated behaviours and Experimental behaviour	122
Table 6.1 - Procedure to determine of the damage and plastic parameters.....	127
Figure 7.1 - Geometry of the studied frame.	
a) Geometry and cross section	
b) numeration of the nodes of for frame with 3 elements ,	
c) numeration of the nodes of for frame with 20 elements;	
d) FE mesh using Timoshenko 3-noded beams elements,	
e) FE mesh using 2D 8-noded quadrilateral elements.	132
Figure 7.2 - Comparison of the force-displacement curve for FEM results with results obtained by using the proposed plastic-damage model.	133
Figure 7.3 – Moment on the column base versus displacement at the left upper corner.....	134
Figure 7.4 – Evolution of the global damage index (GDI) and the concentrated damage at the base and at the top of the column.	135
Figure 7.5 - Evolution of the global damage index (GDI), local and plastic damage on the first element.....	136
Figure 7.6 – Plastic and local damage evolution on the elements of the frame modeled with 20 elements.....	136
Figure 7.7 - Simply supported beam:	
a) Description of the geometrical and section of the beam;	
b) the beam modeled by means of beams elements	137
Figure 7.8 - Comparison of the numerical and experimental results.....	138
Figure 7.9 - Evolution of the global, local and plastic damage indexes in the beams elements.	139
Figure 7.10 - Description of the geometrical and mechanical characteristics of the frame of Example 3.....	140
Figure 7.11 - Comparison of the experimental results with results obtained by using the frame analysis with the proposed plastic-damage model and a finite element model.....	141

Figure 7.12 – Evolution of the global, local and plastic damage indexes in the first floor.....	142
Figure 7.13 - Evolution of the global, local and plastic damage indexes in the second floor	143
Figure 7.14 – Sequence of formation of the plastics hinge within the frame.....	144
Figure 7.15 – Evolution of the damage indexes at first column of the first storey.	145
Figure 7.16 - Evolution of the damage indexes in the beam of the first storey. ...	146
Figure 7.17 - Geometry and sections of the studied frame.....	147
Figure 7.18 – Third floor displacement, in elastic, plastic, damage and plastic-damage behaviour.....	148
Figure 7.19 –Comparison of the global damage indexes evolution.....	149
Figure 7.20- Evolution of the member damage indexes a) at the second column and b) at the first beam of the first floor	150
Figure 7.21 - Moment-plastic rotation a) in the second column and b) in the first beam of the first floor	151
Figure 7.22 - Evolution of the global and member damage indexes for beams and columns at the first floor.	152
Figure 7.23 - Evolution of the global and member damage indexes for beams and columns at at the second floor.....	152
Figure 7.24 - Evolution of the global and member damage indexes for beams and columns at the third floor.....	153
Figure 7.25 – Sequence of plastic hinges developments within the frame.....	154
Figure 7.26 - Geometry and sections of the studied frame.....	154
Figure 7.27 – Dynamic Load.	155
Figure 7.28 – Pushover loading pattern.	156
Figure 7.29 – Base shear versus global structural drift.	156
Figure 7.30 – Global damage evolution.....	157
Figure 7.31 – Geometry and sections of the studied frame.	158
Figure 7.32 – Synthetic seismic accelerogram.	159

Figure 7.33 – Fifth floor displacement, in elastic, damage, plastic and plastic-damage behaviour.	160
Figure 7.34 – Evolution of the global damage index and of the concentrated damage at the base and top of columns of the first floor.	161
Figure 7.35 – Evolution of the global and member damage (MDI) indexes for the first floor:	
a) columns;	
b) beams.	162
Figure 7.36 – Evolution of the global and member damage (MDI) indexes for the fifth floor:	
a) columns;	
b) beams.	162
Figure 7.37 - Moment-plastic rotation at the base of the first column of the first floor.....	163
Figure 7.38 - Moment-plastic rotation at the base of the second column of the first floor.....	164
Figure 7.39 - Sequence of formation of the plastic hinges within the frame.....	165
Figure 7.40 – Deformed configuration at:	
a) 1.0 seconds;	
b) 1.5 seconds; and	
c) 2.0 seconds.	166
FigureA 1.3 – Deflection displacement and rotation of the beam’s neutral axis..	181
Figure A1.4 – Stresses in a beam-	
a) normal stresses $\sigma_x(x, y)$;	
b) shear stresses $\sigma_{xy}(x, y)$	182
Figure A1.5 – Balance of forces and moments into a section dx of beam.	183
Figure A1.6 – Beam subjected to end moments and moment diagram.....	187
Figure A1.7 – Frame structures with an internal hinge and the moment diagram.	190
Figure A1.8 – Symmetric buckling mode of a fixed-fixed column.....	192
Figure A2.1 - Typical stress-strain curve of low-carbon steel	198
Figure 2.2 - Stress-strain curve for ductile metals.....	199
Figure A2.3 - Stress-strain curve for brittle materials.	200
Figure A2.4 – Stress-strain response of elastic-perfectly plastic material.	201

Figure A2.5 – Perfect Plasticity.....	202
Figure A2.6 – Schematic representation of the mechanical response of one-dimensional elastoplastic model.....	203
Figure A2.7 – Uniaxial stress-strain diagram of a material with isotropic hardening.....	206
Figure A2.8 – Uniaxial stress-strain diagram of kinematic hardening behaviour.....	208
Figure A2.9 – The final stress obtained by return mapping.....	210
Figure A3.1 – Simple supported beam:	
a) uniform load,	
b) deformed shape.....	214
Figure A3.2 – Rectangular cross section under pure bending:	
a) the cross section,	
b) the stress and strain at the elastic limit state,	
c) stress and strain at an elastoplastic state,	
d) the stress and strain at an increase of the elastoplastic state,	
e) stress and strain at the limit state.....	214
Figure A3.3 - Stress strain and moment curvature in a beam.....	218
Figure A3.4 – Beam loaded at midspan	219
Figure A3.5 - – Bending moment and deflection at $P \leq P_e$	219
Figure A3.6 – Bending moment and deflection at $P_e \leq P < P_p$	220
Figure A3.7 - – Bending moment and deflection at $P_p \leq P < P_l$	220
Figure A3.8 - – Bending moment and deflection at $P \cong P_p$	221
Figure A3.9 – Idealized plastic hinge.	222
Figure A3.10 – Mechanism of formation and motion.	224

Abstract

Faleiro, J. (2006). *Plasticity and Damage on Framed Structures*. Barcelona, Ph.D. – Technical University of Catalonia (UPC) - Spain

The objective of this thesis is to develop an improved analytical model for predicting the plastic-damage response of multi-storey reinforced concrete frames, in accordance with the classic theories of Continuum Damage Mechanics and of classic Theories of Plasticity. What distinguishes this work from others is the fact the complete plastic-damage constitutive model, as well as the global damage, is here implemented into a frame analysis algorithm, where the frame is described by elastic beams and columns with two inelastic hinges at its ends.

The behaviour of the reinforced concrete is described throughout by means of continuum constitutive equations rates. We assume that the reinforced concrete presents two distinguished phases: the cracking of the concrete and the yielding of the reinforcement. The concrete cracking phase is described by means of Continuum Damage Mechanics, while the yielding of steel is described by means of the Plasticity Theory. Both, damage and plasticity, are solved simultaneously by means of an uncoupled plastic-damage model proposed for framed structures. With this model, we can describe adequately the behaviour of the reinforced concrete elements.

The elastoplastic behaviour of the frame is give by means of plastic hinges in agreement with the classical Plastic Analysis Theory. The evolution of the plastic hinges is obtained by yield functions for beams and columns. The damage in the hinges is obtained by means of the concentrated damage concepts, based on isotropic strain damage. To obtain the damage of a frame member, a new evaluation method is developed, based on a member damage index, which also leads to a meaningful global damage index of the whole structure. Those parameters are based on continuum mechanics principles in which the label “member damage” is applied only to damage indices describing the state of frame member while the “global” damage index refers to the state of the whole structure. Both damages indices are independent of the chosen constitutive models for the structural material.

A numerical procedure for predicting the damage indices of the structures using matrix structural analysis, Plastic Theory and Continuum Damage model is also developed. The method is adequate for the prediction of the failure mechanisms. In order to illustrate the effectiveness of the method, several numerical

analyses of framed structures are presented in which various kinds of materials and structural shapes are considered. Several loading conditions are studied: pushover loads, loading-unloading cyclic and dynamic loads. The agreement with experimental data and finite element analysis is also discussed.

The obtained results endorse the proposed plastic-damage model as an effective tool for numerical simulation of the collapse of frames. Its implementation under a matrix analysis program gives an efficient tool, computationally economic, which it is a valuable alternative to other types of analysis, such as those based on multi-layer models, when these appear to be too expensive or impractical due the size and complexity of the structure.

According to the results obtained, it can be observed that the proposed plastic-damage model shows a good precision in comparison with results obtained by means of finite element models. When comparing with the results obtained by means of experimental tests, the results with the proposed plastic-damage model are better than those obtained by means of finite element models. The proposed model it has been demonstrated that under cyclic or dynamic loads can represent with sufficient accuracy the real behaviour of reinforced concrete.

Finally, the global damage index, together with the member and the concentrated damage indexes, provide accurate quantitative measure for evaluating the state of any component of a damaged structure and of the overall structural behaviour. It is an excellent tool for the seismic damage evaluation, reliability, and safety assessment of existing structures and can be used in the evaluation of the repair or retrofitting strategies

Keywords: Damage estimation; Global damage; Matricial Analysis; Plastic-damage model; Reinforced concrete frames.

Resumen

Faleiro, J. (2006). *Plasticity and Damage on Framed Structures*. Barcelona, Ph.D. – Technical University of Catalonia (UPC) - Spain

El objetivo de esta tesis es desarrollar un modelo analítico mejorado para predecir la respuesta plástica-dañada de estructuras porticadas de hormigón armado, de acuerdo con las teorías clásicas de Mecánica del Daño Continuo y de la clásica Teoría Plástica. Qué distingue este trabajo de otros es que el modelo plástico-daño, así como el índice de daño global, es aquí implementado en un algoritmo para el calculo matricial, donde el pórtico es formado por vigas y columnas elásticas compuestas por dos rotulas plásticas en las extremidades.

El comportamiento del hormigón armado se describe por medio del incremento en las ecuaciones constitutivas. Asumimos que el hormigón armado presenta dos fases distinguidas: el agrietamiento del hormigón y la fluencia del acero. La fase de agrietamiento del hormigón es descrita a través de la Mecánica de Daño Continuo, mientras que la fluencia del acero es descrita a través la Teoría Plástica. Ambos efectos, daños y plasticidad, se solucionan simultáneamente por medio de un modelo plástico-daño desacoplado, propuesto para las estructuras aporticadas. Con este modelo, podemos describir adecuadamente el comportamiento de los elementos de hormigón armado.

El comportamiento elastoplástico del pórtico es obtenido por medio de las rotulas plásticas en de acuerdo con la clásica Teoría de Análisis Plástico. La evolución de las rotulas plásticas es obtenida por medio de funciones de fluencia para vigas y columnas. El daño en las rotulas es evaluado por medio del concepto de daño concentrado, basado en los modelos de constitutivos de isotrópico de daño. Para obtener el daño en uno de los elementos del pórtico, se desarrolla un nuevo método de evaluación, basado en un índice de daño del miembro, lo cuál también conduce a un índice global del daño de toda estructura. Esos parámetros se basan en los principios de la mecánica de los medios continuos, donde la etiqueta “daños del miembro” se aplica solamente a los índices de los daños que describen el estado del miembro del pórtico mientras que el índice “global” del daño refiere al estado de la estructura total.

Un procedimiento numérico para predecir los índices de los daños de la estructura a través del método matricial de análisis de estructuras, Teoría de la Plasticidad y Mecánica del Daño Continuo es desarrollado. El método es adecuado para la predicción de los mecanismos de falla de la estructura. Para ilustrar la efi-

caja del método, se realiza varios análisis numéricos de estructuras aporricadas en las cuales se consideran las varios tipos de materiales y formas estructurales. Se estudian varias condiciones de cargamento: cargas de ruptura (pushover), cargas cíclicas y cargas dinámicas. También se hace la comparación con datos experimentales y con el método de elementos finitos.

Los resultados obtenidos endosan el modelo plástico-daño propuesto como una herramienta eficaz para la simulación numérica del colapso de pórticos. La implementación del modelo en un programa basado en el análisis matricial resulta en una excelente herramienta, que se puede ser una alternativa valida para sustituir otros tipos de análisis, tales como aquellos que se basan en modelos de múltiples capas, cuando éstas aparecen ser demasiado costosa o impráctica debido al tamaño y la complejidad de la estructura.

De acuerdo con los resultados obtenidos, se observa que el modelo plástico-daño propuesto demuestra una buena precisión en comparación con los resultados obtenidos por medio de modelos de elementos finitos. Cuando comparado con los testes experimentales, los resultados obtenidos con el modelo plástico-daño propuesto son mejores que los resultados obtenidos por medio del método de elementos finitos. El modelo propuesto ha demostrado que bajo cargas cíclicas o dinámicas puede representar con suficiente exactitud el real comportamiento del hormigón armado.

Finalmente, el índice global del daño, en conjunto con los índices de daños de los miembros y los índices de daños concentrados, proporciona la medida cuantitativa exacta para evaluar el estado de cualquier componente de una estructura dañada y bien como el comportamiento estructural total. Es una excelente herramienta para la evaluación de los daños sísmicos, la confiabilidad, y el de seguridad de las estructuras y puede ser utilizado en la evaluación de las estrategias de reparación o de modificación.

Palabras Claves: Valoración del daño, Daño global, Análisis matricial, Modelo plástico-daño, Pórticos de hormigón armado.

Chapter 1

Introduction

1.1 General

Conceptually, structural analysis performs the computation of deformations, deflections, and internal forces or stresses within structures, either for design or for performance evaluation of existing structures. Structural analysis needs input data such as loads, structural geometry, bearing conditions and material's properties. Output quantities may include reactions, stresses and displacements. Advanced structural analysis may include the effects of vibrations, stability and non-linear behaviours (i.e. plasticity, damage, etc.).

Three approaches can be used to perform the analysis of structures:

- The mechanics of materials approach (also known as strength of materials);

- The elasticity theory approach which is actually a special case of the more general field of continuum mechanics and;
- The finite element approach.

The first two make use of analytical formulation leading to closed-form solutions. The third, actually a numerical method for solving differential equations, is very widely used in structural analysis. The equations solved by the Finite Element Method are generated starting from theories of mechanics such as elasticity theory and strength of materials. Analytical formulations apply mostly to simple linear elastic models, while the finite-element method is computer-oriented, applicable to structures of arbitrary size and complexity. Regardless of approach, the formulation is based on the same three fundamental relations: equilibrium, constitutive and compatibility. The solutions are approximate when any of these relations are only approximately satisfied, or only an approximation of reality.

Each method has noteworthy limitations. The method of mechanics of materials is limited to very simple structural elements under relatively simple loading conditions. The structural elements and loading conditions, however, are sufficient to solve many useful engineering problems. The theory of elasticity allows the solution of structural elements of general geometry under general loading conditions, in principle. Analytical solutions, however, are limited to relatively simple cases. The solution of elasticity problems also requires solving of a system of partial differential equations, which is considerably more mathematically demanding than the solution of mechanics of materials problems, which require at most the solution of an ordinary differential equation. The Finite Element Method is, perhaps, the most restrictive and most useful at the same time. This method itself relies upon the other two mentioned structural theories. However, it allows to solve the differential equations, even with highly complex geometry and loading conditions, with the restriction that there is always some numerical error. Effective and reliable use of this method requires a solid understanding of its limitations.

In the Finite Element Method, a structure is considered to be an assembly of elements or components with various types of connection between them. Thus, a continuous system, such as a plate or a shell, is modelled as a discrete system with a finite number of elements interconnected at finite number of nodes. The behaviour of individual elements is characterised by the element's stiffness or flexibility relation, which altogether leads to the system's stiffness or flexibility relation. To establish the element's stiffness or flexibility relation, we can use the mechanics of materials approach for simple one-dimensional bar elements and the elasticity approach for more complex two- and three-dimensional elements.

The analytical and computational developments are performed by means of matrix algebra.

Early application of matrix methods were for articulated frameworks with truss, beam and column elements; later, more advanced matrix methods, referred to as "finite element analysis", model an entire structure with one-, two-, and three-dimensional elements, which can be used for framed (beams) systems together with continuous systems such as a pressure vessel, plates, shells, and three-dimensional solids. Computer software for structural analysis typically uses matrix finite-element analysis, which can be further classified into two main approaches: Direct Stiffness Method and Flexibility Method.

As one of the methods of structural analysis, the Direct Stiffness Method, also known as the displacement method or matrix stiffness method, is particularly suitable for computer-automated analysis of complex structures including the statically indeterminate type. The Direct Stiffness Method is the most common implementation of the Finite Element Method. During the historic review of the Direct Stiffness Method, Felippa (2000) observed that between 1934 and 1938 A. R. Collar and W. J. Duncan published the first papers with the representation and terminology for matrix systems that are used today, introducing various approaches for analysis of complex airplane frames. Afterwards, various others researchers expanded these approaches, including elasticity theory, energy principles in structural mechanics, flexibility method and matrix stiffness method. It was through analysis of these methods that the Direct Stiffness Method emerged as an efficient method, ideally suited for computer implementation.

The Direct Stiffness Method was specifically developed to be effectively and easily implemented into computer software to evaluate complicated structures that contain a large number of elements. Today, nearly every available finite element solver is based on the Direct Stiffness Method. While each program utilizes the same process, many have been streamlined to reduce computation time and reduce the required memory. In order to achieve this, shortcuts have been developed.

1.2 Motivation

Whereas two and three dimensional continuum are essential in civil engineering to model structures such as dams, shells and foundations, most of the civil engineering structures are constituted by one-dimensional "rod" elements such as beams, girders, or columns, usually called elements of a framed structure. For those elements, "displacements" and internal "forces" are somehow more

complex than those encountered in Continuum Finite Elements. In this case, the matrix structural analysis method is used to obtain the solution of the structure. Matrix Structural Analysis can be thought of as a subset of the Finite Element Method.

Hence, contrarily to Finite Element, where displacement is mostly synonymous with translation, in one dimensional frame elements and depending on the type of structure, generalized displacements may include translation and/or flexural and/or torsional rotation. Similarly, "internal forces" are not stresses, but rather axial and shear forces and/or bending or torsional moments. Those concepts are far more relevant in the analysis/design of most civil engineering structures.

One of the difficulties of using Finite Elements to framed structures is the complexity of describing the structure, which will require much time in this process and, if the analysis includes nonlinear dynamics effects, this analysis could be computationally expensive and, in some cases, impossible. Perhaps the main inconvenience in using Finite Elements is that most of the results obtained will be useless or of little practical utility for the structural designer.

Nevertheless, in Matrix Structural Analysis, the nonlinear analysis of frames is usually limited to the plastic analysis by means of the lumped (concentrated) plasticity models. Initially conceived for steel framed structures, the lumped plastic models use the concept that the plastic effects can be concentrated at special locations called plastic hinges. In framed structures, the plastic hinges are assumed to be located at the end of the member. This behaviour can be observed especially under lateral loads, by the fact that the members have the tendency of plastifying (or forming plastic hinges) near the ends. The plasticity then gradually spreads along the length of the member, as a consequence of the plastification of successive cross sections. However, for many-rolled steel cross sectional shapes, the spread of plasticity along the length of the member is not very significant and the deformation is concentrated at or very near the end cross sections.

Plastic theory can be used as a mathematical framework to treat permanent strains. However, in particular geomaterials such as concrete, permanent strains are caused by microcracking, which leads to permanent stiffness degradation. In those cases, the plasticity theory itself is not satisfactory to represent the stiffness degradation and, therefore, it is necessary to use another tool, the Continuum Damage Mechanics.

Using the works of Kachanov (1958), Continuum Damage Mechanics became one of the most studied subjects in Solids Mechanics. The main idea is defining a new damage internal variable, which describes the evolution of microcracks and microvoids and their influence on the behaviour of the material. This simple and general idea has been used for modelling, until local fracture, most of the construction materials. Initially introduced for metals, Continuum Damage Mechanics was later adapted to materials such as concrete, as observed by Oller (2001b). Currently, plasticity and damage are coupled in some models, as proposed by Simo and Ju (1987) and by Luccioni (2003). This approach has the advantage of allowing the development of constitutive independent laws, which simulate materials where the plastic deformation is not significant, as in the case of concrete, ceramic and ceramic composites

Using the lumped plasticity model, Cipolina *et al.* (1995) adapted the damage models to the analysis of frames starting from the assumption that the damage is concentrated in plastic hinges, being this called as a concentrated damage model. A value of the concentrated damage at the hinge equal to 1 reflects the complete loss of strength, while a value 0 means no damage. However, this method has the disadvantage that it only refers to the damage at the hinge, and does not take into account the effect of cumulative plastic deformations under cyclic loading. Another drawback is that, once the concentrated damage index is located at the ends of the frame member, it is not possible to determine the real damage state of the member.

1.3 Objectives of the thesis

One of the primary objectives of this thesis is to develop a global damage evaluation method based on continuum mechanics principles. In this work, the label “member damage” will be applied only to damage indices describing the state of the frame member, while the “global” damage indices will refer to the state of the whole structure. Both member and global damage indices developed herein are independent of the chosen constitutive models for the structural material. This feature converts the proposed member and global damage indices into a powerful general tool for structural assessment. Moreover, it can be applied directly to both static and dynamic analysis and to estimate the damage produced by seismic actions in reinforced concrete building structures.

The main objective of this thesis is to formulate a new procedure to use plastic-damage models in frame analysis, with application to reinforced concrete structures, in accordance with the classic theories of Continuum Damage Mechanics and classic Theories of Plasticity. These theories will give support to the im-

plementation of the member and global damage indices. Once developed the plastic-damage model, the results of the numerical analysis with this model should be in a good agreement with other models developed by means of Finite Element method. The proposed model has also to show a good accuracy in comparison with results obtained for reinforced concrete structures by means of experimental test. The results obtained by means of the proposed model have to be sufficiently clear, simples and describe the behaviour of a reinforced concrete frame without the necessity of a pos-process analysis.

Additionally, the proposed model within a Matrix Analysis program has to be computationally efficient to be able to solve complex structures, even in the case of a nonlinear behaviour when subjected to dynamic loads.

Finally, what will distinguishes this work from others is the fact that the complete plastic-damage constitutive model, as well as the global damage, is here implemented into a frame analysis algorithm based on Matrix Structural Analysis formulation an not on the Finite Element method.

The general objective of the thesis is splitted in the following items:

- Development of a Plastic-Damage model for reinforced concrete in framed structures;
- Development of a Member and Global damage indexes for framed structures.
- Development of a nonlinear program based on Matrix Analysis methods for framed structures;
- Development of a nonlinear algorithms to solve the proposed Plastic-Damage model;
- Convalidation of the model through the comparison of the results obtained by means of the proposed model with results obtained by means of Finite Elements method and/or experimental tests of reinforced concrete framed structures.

1.4 Contents of the thesis

A state of the art about the lumped and moment-curvature models is made; plastic-damage models for reinforced concrete structures and methods for evaluation of the global damage in structures are included in the stat of the art.

The kinematic equations for plane frame analysis are developed, where the cinematic behaviour of the plane frames are described, independently of the forces involved then we characterize the external forces and how they are applied in the frame structure. We introduce the concept of generalized stress as well as the concept of inertial forces and how we obtain the relationship between the external force, generalized stress and inertial forces.

Then describe aspects related to the nonlinear dynamic analysis method. The proposed nonlinear analysis method is applicable to the static and dynamic nonlinear analysis of structures but only the implementation of the method in the context of the nonlinear analysis of frames is developed herein.

We introduce the concepts of elastoplastic behaviour applied to framed structure by means of the plastic hinge and we introduce yield functions for the beam-column plastic models and all the procedures necessary to implement those functions in a matrix frame analysis program. We describes the formulation of the lumped damage model based on the concepts of the isotropic strain damage, followed by the member and global damage evaluation method starting from the principles of continuum mechanics principles. Then discuss the behaviour of reinforced concrete structures, followed by the description of one plastic-damage model for reinforced concrete frame structure.

We present the numerical results obtained by means of the proposed Plastic-Damage model, implemented into a frame analysis computer program based on the matricial methods.

The summary, future lines of research and conclusions are then presented.

Finally, three appendixes are included: the first describes the classical stiffness and flexibility method; the second reviews the principal concepts in plasticity, applied to the uniaxial stress; the third one review the elastoplastic concepts that are necessary in the plastic theory and the procedures used to determine the limit (plastic) load in accordance with the theory of plastic analysis.

Chapter 2

State of the Art

2.1 Introduction

Much effort has been devoted in the last thirty years to development of models of inelastic response of reinforced concrete under cyclic loads and dynamic loads. Numerous models incorporating information from experimental investigations and on-field observations of the behaviour of the reinforced concrete structural elements have been proposed. These range from the simple second-order-elastic-plastic analysis to refined fiber or layer models based on sophisticated descriptions of the cyclic stress-strain behaviour of concrete and reinforced steel. Due to extension of models, we confine our review of previous studies to the following topics:

- Lumped and moment-curvature models;
- Plastic-Damage models for reinforced concrete structures

- Methods for evaluation of the global damage in structures

In the first topic, more than a review, we give a brief history of the evolution of the lumped methods, focussing our attention only on the case of framed analysis, without distinguishing between static, cyclic or dynamic models. In the second topic, we concentrate our attention on plastic-damage models applied to reinforced concrete. In the last topic, we proceed with a review of the works where the procedure to obtain the global damage of the structure by means of the global damage indices.

Due to fact that our work is based on matricial analysis, inside each topic, we limited the review to models where its application could be extended or adapted for matricial frame analysis.

2.2 Lumped and moment-curvature models

2.2.1 Moment-curvature models

Nonlinear (cyclic or dynamic) analysis of a reinforced concrete structure requires two types of mathematical modelling: (a) modelling for the distribution of stiffness along a member; and (b) modelling for the force-deformation relationship under stress reversals.

A hysteresis model must be able to provide the stiffness and resistance under any displacement history. At the same time, the basic characteristics need to be defined by the member geometry and material properties. The current state of knowledge is sufficient to define flexural hysteresis models. However, it is not sufficient to determine the degree of stiffness degradation due to the deterioration of shear-resisting and rebar-concrete bond mechanisms.

a) Bilinear Model or Elastoplastic model.

The elastic-perfectly plastic moment-curvature model was used by many investigators because the model was simple. In dynamic analysis, the maximum displacement of an elastoplastic simple system was found to be practically the same as that of an elastic system having the same initial period of vibration as long as the period was longer than 0.5 s. A finite positive slope was assigned to the post yield stiffness to account for the strain-hardening characteristic, and the model was called a bilinear model. The bilinear model does not represent the degradation of loading and unloading stiffnesses with increasing displacement amplitude reversals (Figure 2.1), and the model is not suited for a refined nonlinear analysis of a reinforced concrete structure.

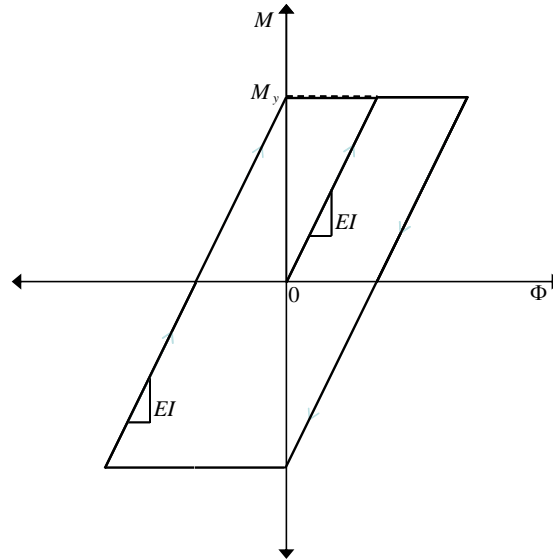


Figure 2.1 – Elastoplastic model.

b) Clough's Model.

A qualitative model for the reinforced concrete was developed by Clough and Benuska (1967) (well known as Clough's model), who incorporated the stiffness degradation in the elastoplastic model: the response point during loading moved toward the previous maximum response point. The unloading slope remained parallel to the initial elastic slope. This small modification improved the capability to simulate the flexural behaviour of the reinforced concrete. Compared with the elastoplastic model, less energy is absorbed per cycle beyond yielding by Clough's degrading model.

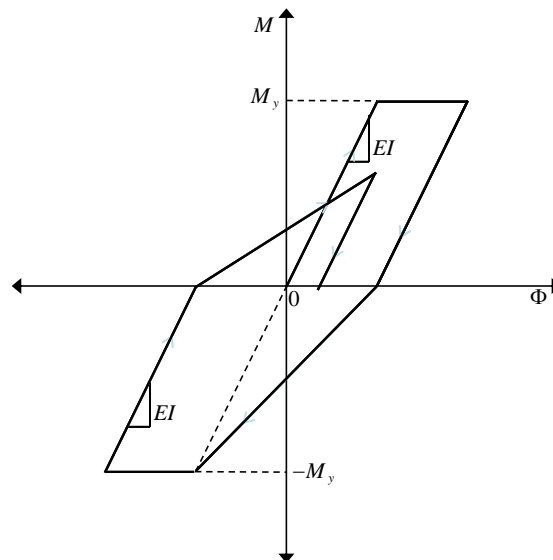


Figure 2.2 – Clough model.

From the response analysis of a series of single-degree-of-freedom systems, Clough concluded that: (i) the degrading stiffness model did not cause any significant change in the ductility demand of long-period structures (period longer than 0.6 s) compared with the elastoplastic model; on the other hand, (ii) the degrading stiffness model required significantly larger ductility from short-period structures than the corresponding elastoplastic systems; and (iii) the response waveform of a degrading stiffness model was distinctly different from that of an ordinary elastoplastic model. The model is relatively simple, and has been used extensively in nonlinear analysis with the inclusion of strain-hardening characteristics (Figure 2.2).

c) Takeda's model.

A more refined and sophisticated hysteretic model was developed by Takeda *et al.* (1970) (called Takeda's model) on the basis of experimental observation. This model included stiffness changes at flexural cracking and yielding, and also strain-hardening characteristics. The unloading stiffness was reduced by an exponential function of the previous maximum deformation. Takeda *et al.* also prepared a set of rules for load reversals within the outermost hysteretic loop. These are major improvements over the Clough model. Failure or extensive damage caused by shear or bond deterioration was not considered in the model. The Takeda model, similar to the Clough model, simulates dominantly flexural behaviour (Figure 2.3). Simplified Takeda hysteretic models were proposed by Otani and Sozen (1972) and by Powell (1975), using a bilinear backbone curve.

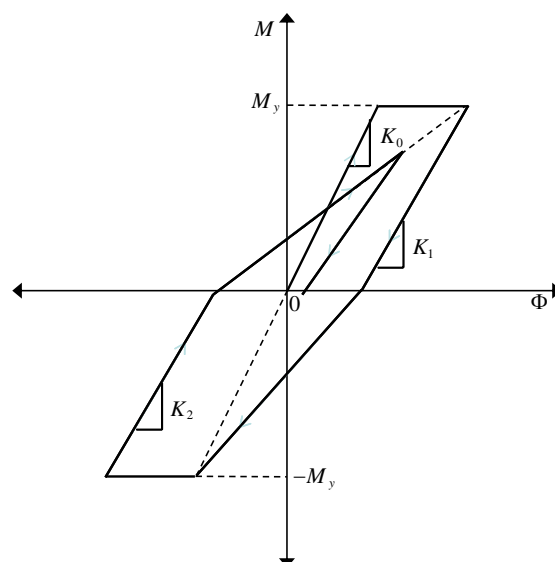


Figure 2.3 – Takeda's model.

2.2.2 Lumped Models

Under seismic excitation, or cyclic loads, the inelastic behaviour of reinforced concrete frames often concentrates at the ends of the beam-column. Thus, an early approach to modelling this behaviour was by means of zero length plastic hinges in the form of nonlinear springs located at the member ends. Depending on the formulation, these models consist of several springs that are connected in series or in parallel:

a) Clough and Johnston's model.

The earliest parallel component element was introduced by Clough and Johnston (1966) and allowed for a bilinear moment rotation relation: the element consists of two parallel elements, one elastic-perfectly plastic to represent yielding and the other perfectly elastic to represent strain-hardening. The stiffness matrix of the member is the sum of the stiffness of the components. The elastic modulus of the first component is equal to the strain hardening modulus $p \cdot EI$ of the moment curvature relation, where EI is the pre-yield section stiffness. The elastic modulus of the elastoplastic component is equal to $q \cdot EI$ where $q = 1 - p$.

b) Cohn and Franchi's model

Based on these concepts, Cohn and Franchi (1979) present a model consistent with the traditional assumption of plastic hinge (only plastic rotation), bar hinge (only axial deformation), and generalized plastic hinge (combined axial force and bending moment), through a rigid-plastic spring system to obtain the solution of the structure. The compatible equation is considered as the sum of q^{el} (elastic response of the external load) and q^{ep} (elastic response to the given plastic deformations q^p). The normality rule of the plastic deformation is expressed as $\dot{\mathbf{q}}^p = [\mathbf{N}] \dot{\lambda}$, where $[\mathbf{N}]$ is a matrix whose rows are outward unit normal vectors to yield planes, and the rate plastic multiplier $\dot{\lambda}$ rules the Kuhn-Tucker conditions ($\dot{\lambda} > 0$; $\Phi \dot{\lambda} = 0$; $\dot{\Phi} \dot{\lambda} = 0$) with Φ being the plastic potential vector. However, one of the shortcomings of this model is the difficulty of accounting for the stiffness deterioration of reinforced concrete elements during cyclic load reversals.

c) Giberson's model

The series model was formally introduced by Giberson (1967), although it had been reportedly used earlier. Its model consists of a linear elastic element with one equivalent nonlinear rotational spring attached to each end. The inelastic deformations of the member are lumped into the end springs. This model allows the phenomenological representation of the hysteresis behaviour of reinforced

concrete members. A major advantage of the model is that inelastic member-end deformation depends solely on the moment acting at the end so that any moment-rotation hysteretic model can be assigned to the spring. This fact is also a weakness of the model because the member-end rotation should be dependent on the curvature distribution along the member, hence dependent on moments at both member ends.

d) Filippou and Issa's model

Using these concepts, Filippou and Issa (1998) present a model to reinforced concrete beam element, where the element is composed of a number of sub-elements connected in series and represented by different sources of hysteretic behaviour of reinforced concrete beams. Their model is divided in two sub-elements: one describes the inelastic behaviour along the beam accounting for the gradual spread of inelastic deformations at the beam-ends, while the fixed-end rotations that arise at the beam-column interface due to bond deterioration and slippage of reinforced bars in the beam-column joint region are controlled by another model. In this model, the plastic length is calculated in terms of the bending moment and shear force at the beam end. The flexibility matrix of the beam is obtained by $[\mathbf{F}] = [\mathbf{f}_{el}] + [\mathbf{f}_{pl}] + [\mathbf{f}_{jnt}]$, in where $[\mathbf{f}_{el}]$, $[\mathbf{f}_{pl}]$ and $[\mathbf{f}_{jnt}]$ are, respectively, the elastic matrix, the flexibility matrix of either the concentrated rigid plastic or the spread rigid-plastic element and the flexibility matrix of the rotational joints of the element. Due to the complexity of evaluation of the flexibility matrix, this model is limited to analysis of subparts of a structure.

e) Riva and Cohn's model

Developing a model based on a moment-rotation constitutive law, Riva and Cohn (1990) obtain a model able to represent the behaviour of concrete structures. In this lumped-plasticity approach, the structure is discretized by linear-elastic elements; with behavioural nonlinearity lumped at rigid-plastic joints. In this model, the moment curvature law $M - \phi$ and the plastic hinge length l_p are influenced by:

- Material parameters: the $\sigma - \varepsilon$ law for concrete in compression and in tension, the $\sigma - \varepsilon$ law for reinforced steel and the bond slip law for reinforced steel.
- Geometric Parameters: the shape of the section, the mechanical percentage of tension steel q , the mechanical percentage of compression steel;

- Loading parameters: the duration of loading, the axial loading, the loading repletion and the loading reversal.

The mechanical percentage of tension steel is expressed as $q = \frac{A_s f_y}{b w d f_c}$, where f_y is the reinforced steel stress at the limiting strain, f_c is the concrete compressive stress, d is the effective depth of the steel, $b w$ is the section web width, and A_s is the reinforcing area. The plastic hinge length variable is defined as $l_p = \frac{1}{\phi - \phi_{el}} \int_0^z [\phi(x) - \phi_{el}(x)] dx$, where ϕ_{el} is the elastic curvature at distance of the critical section from the contra flexure point z . Once defined those parameters, which influence the moment curvature law $M - \phi$ and the plastic hinge length l_p , the model is based on the solution of the relationship between l_p / z and ϕ_p / ϕ_{py} , where ϕ_p and ϕ_{py} are plastic curvature and the plastic curvature at yielding of a critical section, respectively. This relationship is characterized by three behaviour states: a post-cracking state ($\phi_p / \phi_{py} \leq 1$); a post-yielding state, up to the reinforced strain hardening ($1 < \phi_p / \phi_{py} \leq 7$); and finally by the post strain-hardening state ($\phi_p / \phi_{py} > 7$), in which the plastic hinge length increases up to the final state.

Therefore, the moment-plastic rotation θ_p is derived from a moment-curvature relationship multiplied by the plastic curvature ϕ_p and an equivalent plastic hinge length l_p , $\theta_p = \phi_p l_p$. This expression requires an evaluation of the variable z , which for statically determined beams is assumed to be constant. However, for hyperstatic beams its value varies throughout the loading history, and is also a function of the reinforcement distribution in the beam. This model was limited only to first-order, flexural, static actions in beam elements. The number of nodes necessary to describe the behaviour of the structure depends on the number of potential critical sections. In this mesh discretization, the position of the reinforcement is not indicated, because the influence of the reinforced steel is obtained by the mechanical percentage of tension steel q , used to obtain the plastic hinge length.

Several other lumped plasticity constitutive models have been proposed to date. Such models include cyclic stiffness degradation in flexure shear, Clough and Benuska (1967) and Takeda *et al.* (1970), pinching under reversal, Banon *et al.* (1981) and fixed rotations at the beam-column joint interface due to bar pull-out, as proposed by Otani (1974) or by Filippou and Issa (1998). Typically, axial-flexural coupling is neglected.

However, for reinforced concrete frame, the parameters for these models depend not only on the section characteristics, but also on the load deformation history, thus limiting the generality of the approach, and a consistent and rational

method for the selection of model parameters requires special algorithms for ensuring a least squares fit between analytical and experimental data.

2.2.3 Stiffness models

In most lumped plasticity models, the axial force-bending moment interaction is described by a yield surface for the stress resultants and an associated flow rule according to the tenets of classical plasticity theory defined by Prager and Hodge (1951) or by Massonnet and Save (1966). The response is assumed to be linear for stress states that fall within the yield surface, in which case the flexural and axial stiffness of the member are uncoupled and independent of the end loads. With the introduction of multiple yield and loading surfaces and corresponding hardening rules, multi-linear constitutive representations that include cracking and cyclic stiffness degradation, the determination of the stiffness of the structure concentrated the efforts of some authors.

a) Argyris's model

Argyris *et al.* (1982) introduce a stiffness matrix for elastoplastic element, which consisted in a substitution of the sum process by four element stiffness matrices (one elastic matrix and three elastoplastic). The elastoplastic stiffness is redefined in terms of the existence or not of the plastic hinges on the extremities of the element. In this model, the plastic deformations are assumed to be restricted to the cross-sections at the ends of the members. For 2D elements, the plastic interaction curves for the plastic rotation at the beam-ends are defined in terms of the bending moment at the joint and the axial force as $\phi = \left| \frac{M}{M_y} \right| + \left(\frac{N}{N_y} \right)^2 - 1 = 0$, where M_y and N_y are the bending moment limit and the axial limit of a member, respectively.

b) Chen and Chan's stiffness model

Still based on the concept of definition of the plasticity inside the stiffness of the element, Chen and Chan (1995) present a model where the lumped plasticity is employed through connection springs at the two ends of the element. The formation of the plastic hinge is simulated in the analysis by setting the tangential stiffness of the connection spring to zero. The evolution of the spring stiffness is defined as $R = \alpha / [L(\frac{\gamma}{1-\phi} - 1)]$; where L , α and γ are the length of the member length, sharpness and the initial stress indexes, respectively. The plastic rotation

ϕ is defined as $\phi = \left| \frac{N}{N_y} \right|^{1.3+0.002(L/\gamma)} + \left| \frac{M}{M_y} \right|$, for the compressive loading case, and

$\phi = \left| \frac{N}{N_y} \right|^{1.3} + \left| \frac{M}{M_y} \right|$, for the tensile loading case. The term l/r is the slenderness ratio of the member. Although the stiffness is explicitly derived, the computational effort can be considerable to calculate the stiffness at each load step. Another inconvenience is that this model allows only the analysis of steel frames, and it cannot be adapted for reinforcement concrete structures.

c) Jirásek's stiffness model

Jirásek (1997) presents a model in which he describes the stiffness of beam elements with embedded softening hinges. The linear moment-rotation law is written in rate form as $\dot{\theta} = c\dot{M}$, where c is the inverse slope of the corresponding straight line. In virgin load, $c = 0$, for unloading or reloading $c = c_u \geq 0$, and for softening, $c = c_s = -\theta_f/M_y < 0$, where θ_f is the complete rotation at complete failure.. The tangential stiffness is defined as

$$[\mathbf{D}] = k \begin{bmatrix} 2 - \gamma_2 & 1 \\ 1 & 2 - \gamma_1 \end{bmatrix}, \text{ where } k = \frac{6EI}{L} \frac{1}{3 - 2\gamma_1 - 2\gamma_2 + \gamma_1\gamma_2}.$$

The parameter γ relates with the parameter c by $\gamma = -c \frac{6EI}{L}$, and its evolution depends on the specific constitutive model used, as well as on the loading history. Therefore, the value of the θ_f is defined as $\theta_f > M_y \frac{L}{4EI}$, in the case where there is one active plastic hinge in the beam, and $\theta_f > M_y \frac{L}{2EI}$ when both plastic hinges are active. However, the value θ_f also depends of the type of structure which will be analyzed, and at sufficiently large value of θ_f , the solution can become stable, and the model can no longer detect the formation of additional inelastic hinges.

d) Makode's stiffness model

In the works of Makode, Makode *et al.* (1999a) and Makode *et al.* (1999b), he develops a model which take into account the changes in the structural properties during the loading process, extended for elastic-plastic hinge considerations, using a submatrix formulation at each load step. The general member matrix $[\bar{\mathbf{K}}^m]$ is obtained through the sum of the linear elastic stiffness matrix $[\mathbf{K}^m]$ plus a geometric stiffness matrix $[\mathbf{K}_G^m]$, which is expressed in terms of the axial load on structure. The parameters of the geometric matrix are determined in terms of whether the axial force is present or not, and due to the presence of the plastic hinge at one or at both ends. This formulation requires the reanalysis of frame structures with the reformulation of the global stiffness matrix at each load in-

crement. Therefore, this model is only suitable for those situations where a limited number of members change at each step load.

e) Kondoh and Atluri's stiffness model

Using explicitly derived tangent stiffness, Kondoh and Atluri (1987) develop a procedure where the stiffness of each element was obtained in terms of the plastic-hinge method, with allowance to the formation of the hinge at any location or locations along the beam. The incremental plastic flow condition $f(M, N) = 0$ is given by $\frac{\partial f}{\partial N} \Delta N + \frac{\partial f}{\partial M} \Delta M = 0$ at x_1 equal to the plastic hinge location l_p . Thus, the stiffness, as well the tangent-stiffness affected by plasticity, is explicitly evaluated by two integrals over the length of the beam

$$\int_0^L \frac{\partial W}{\partial N} v dx_1 = \int_0^L \frac{\Delta N}{EA} \Delta v dx_1 + \Delta \lambda \left(\frac{\partial f}{\partial N} \Delta v \right)_{x_1=l_p} \quad \text{and}$$

$$\int_0^L \frac{\partial W}{\partial M} \mu dx_1 = \int_0^L \frac{\Delta M}{EI} \Delta \mu dx_1 + \Delta \lambda \left(\frac{\partial f}{\partial M} \Delta \mu \right)_{x_1=l_p}, \quad \text{where } W = \frac{1}{2} \left(\frac{N^2}{EA} + \frac{M^2}{EI} \right) \text{ is the complementary energy density, and } \Delta \lambda \text{ is plastic multiplier.}$$

The same concept was extended into space-frames by Kondoh *et al.* (1986) and by Shi and Atluri (1998), where the tangent stiffness matrix is obtained in terms of a stress approach and plastic-hinge method. However, these models are limited to steel frame structures. Nevertheless, Taylor (2004) observe that the inconvenience of these methods was that the plastified hinge did not remain within the yield surface during the load process, although a return-mapping algorithm is used.

f) Other's models

With the development of the finite elements method, the flexibility-based fiber elements becomes one of the most popular techniques for nonlinear analysis of reinforced concrete members. In these models, the element is subdivided into longitudinal fibers, which allows each fiber to be defined with a different properties and material. The constitutive relation of the section is not specified explicitly, but is derived by integration of the response of the fibers, which follow the uniaxial stress-strain relation of the particular material. Kwak and Filippou (1997) present a model where the monotonic behaviour of reinforced concrete beams and beam-column sub-assemblages is analysed by means of fiber elements. The concrete and reinforcing bars are represented by separate material models which are combined together with a model of the interaction between the reinforced bar and concrete through bond-slip to describe the behaviour of the composite reinforced

material. Taucer *et al.* (1991) presents a good review of the theories and procedures of fiber models. However, for framed structures, the fiber model is still computationally expensive.

g) Flórez-López's model

The basic advantage of the lumped model is its simplicity, which reduces storage requirements and computational cost and improves the numerical stability of the computations. Most lumped models, however, oversimplify certain important aspects of the hysteretic behaviour of reinforced concrete members, and are therefore limited in applicability. With the purpose of improving the lumped models, Flórez-López (1993) developed a damage model based in the continuum damage mechanics for analysis of framed structures, where the loss of stiffness is characterized by the damage state on the loading history. His assumption is that all inelastic behaviour is concentrated at the ends of the beam-column, formulating the loss of the stiffness in the member $[\mathbf{S}]$ through damage parameters d_i, d_j and d_a , includes the stiffness matrix of a member. So

$[\mathbf{S}(d_i, d_j, d_a)] = [\mathbf{S}^0]([\mathbf{1}] + [\mathbf{R}]^{-1}[\mathbf{S}^0])^{-1}$, where $[\mathbf{1}]$ is an identity matrix and $[\mathbf{R}]$ is a diagonal matrix, with diagonal elements equal to $R_{1,1} = \frac{1-d_i}{d_i} S_{1,1}$, $R_{2,2} = \frac{1-d_j}{d_j} S_{2,2}$ and $R_{3,3} = \frac{1-d_a}{d_a} S_{3,3}$. The evolution of the damage parameters is given by

$$d_i \begin{cases} = 0 \Rightarrow h_i < 0 \\ > 0 \Rightarrow h_i = 0 \end{cases}; \quad d_j \begin{cases} = 0 \Rightarrow h_j < 0 \\ > 0 \Rightarrow h_j = 0 \end{cases} \quad \text{and} \quad d_a \begin{cases} = 0 \Rightarrow h_a < 0 \\ > 0 \Rightarrow h_a = 0 \end{cases}, \quad \text{where the damage}$$

function is defined as $h(G, d) = G - K(d) \leq 0$, while G is the thermodynamic force conjugated to the damage, and $K(d)$ is the hardening or softening function of damage.

Expanding Flórez-López concepts, Cipolina *et al.* (1995) presented a general formulation for frame analysis based on a lumped plasticity model combined with continuum damage mechanics for reinforced concrete frames. The energy dissipation is assumed as concentrated only in the hinges, while beam-column remains elastic. Thus, the energy dissipation due to damage and plasticity is defined as $\xi = \{\dot{\mathbf{D}}\}^T \{\mathbf{G}\} + \{\dot{\Phi}^p\}^T \{\mathbf{M}\} + \{\dot{\mathbf{a}}\}^T \{\boldsymbol{\beta}\} \geq 0$, where $\{\mathbf{D}\}^T = \{d_i \quad d_j \quad d_a\}$ is the damage parameters vector, $\{\mathbf{G}\}^T = \{G_i \quad G_j \quad G_a\}$ is thermodynamic force vector conjugated to the damage, $\{\Phi^p\}^T = \{\phi_i^p \quad \phi_j^p \quad \delta^p\}$ is the generalized plastic deformations vector and $\{\mathbf{M}\}^T = \{M_i \quad M_j \quad N\}$ is the generalized stress vector. The term $\{\dot{\mathbf{a}}\}^T \{\boldsymbol{\beta}\}$ is the forces conjugated to plastic hardening. The plastic deformation evolution laws are given by $\dot{\phi}_i^p = \dot{\lambda}_i^p \frac{\partial f_i}{\partial M_i}$; $\dot{\phi}_j^p = \dot{\lambda}_j^p \frac{\partial f_j}{\partial M_j}$ and $\dot{\delta}^p = \dot{\lambda}_i^p \frac{\partial f_i}{\partial N} + \dot{\lambda}_j^p \frac{\partial f_j}{\partial N}$,

where $f_i \leq 0$ and $f_j \leq 0$ are the plastic hinge functions of hinges i and j , respectively. Likewise, the damage evolution is given by $\dot{d}_i = \dot{\lambda}_i^d \frac{\partial g_i}{\partial G_i}$; $\dot{d}_j = \dot{\lambda}_j^d \frac{\partial g_j}{\partial G_j}$ and $\dot{d}_a = \dot{\lambda}_i^d \frac{\partial g_i}{\partial G_a} + \dot{\lambda}_j^d \frac{\partial g_j}{\partial G_a}$, where $g_i \leq 0$ and $g_j \leq 0$ are the damage hinge functions.

This model requires an ‘inelastic corrector’ to control the evolution of the plastic ($\dot{\lambda}_i^p$ and $\dot{\lambda}_j^p$) and damage ($\dot{\lambda}_i^d$ and $\dot{\lambda}_j^d$) multipliers. Therefore, the consistent tangent matrix is obtained by a linear system of matrix equations, derivatives of generalized stress, internal variables, and inelastic multipliers with respect to generalized deformations. The solution of this linear system can be computationally expensive, for complex structures or under dynamic loads. Furthermore, in cyclic loads, the damage tends to keep the value reached during the first cyclic. This occurs due to the assumption that the damage model is a function of the maximum value of the energy release rate.

Later, Flórez-López (1995) and Thomson *et al.* (1998) presented a model for hysteretic behaviour of reinforced concrete frames, which allows the characterization of the unsymmetrical cross section with different yield capabilities, influence of the axial force, stiffness degradation and plastic deformation due the yield of reinforcement. In this model, using the fracture mechanics concepts, the damage evolution law at both hinges is defined as $\dot{d} = (G^\alpha / R^\alpha \frac{\partial R}{\partial d}) \langle G \rangle$ if $G \geq G_{cr}$ or $\dot{d} = 0$ otherwise; where, $\langle \bullet \rangle$ indicates the MacAuley brackets, $R(d)$ is the crack resistance term, G is the energy release rate, $G_{cr} = R(0)$ is the critical value or “crack resistance”, while α is a constant introduced due to the fatigue law. This constant can take values between 0 and ∞ , and it is assumed to be independent of the member properties of the axial load. The damage relating its influences on the plasticity-yield through the kinetic coupling process as proposed by Lemaitre and Lippmann (1996), given a yield function as $f(M, d) = \left| \frac{M}{1-d} - X \right| - M_y = 0$, in which $X = c\phi^p$ is an internal hardening variable, usually defined as a function of a plastic modulus c and in terms of the ϕ^p plastic rotation at the hinge.

Although these models present goods results modelling the low cyclic fatigues, they cannot capture decrease of the strength of the member due to the buckling of the longitudinal reinforcement at high values. This model also has a disadvantage when determining the model parameters due to its dependence on the load and deformation history.

All referenced works are based on the Finite Element Method to obtain the solution of their proposal model. In the case of the fiber methods, usually, only part or joints of the structure are analysed, due to the difficulty of describing the entire framed structure.

2.3 Plastic-Damage models for reinforced concrete structures

The response of a reinforced concrete structure is determined in part by the material response of the plain concrete of which it is composed. Thus, analysis and prediction of structural response to static or dynamic loading requires prediction of concrete response to variable load histories. The fundamental characteristics of concrete behaviour are established through experimental testing of plain concrete specimens subjected to specific, relatively simple load histories. Continuum mechanics provides a framework for developing an analytical model that describes these fundamental characteristics. Experimental data provide additional information for refinement and calibration of the analytical model. In some damage models, during the loading-unloading process, a zero stress corresponds to a zero strain and the value of the damage is thus overestimated (Figure 2.4b). An elastic plastic relation is not valid either, even with softening, (Figure 2.4a), as the unloading curve follows the elastic slope. A correct plastic-damage model should be one capable of representing the softening behaviour; the damage law reproduces the decreasing of the elastic modulus, while the plasticity effect accounts for the irreversible strains (Figure 2.4c).

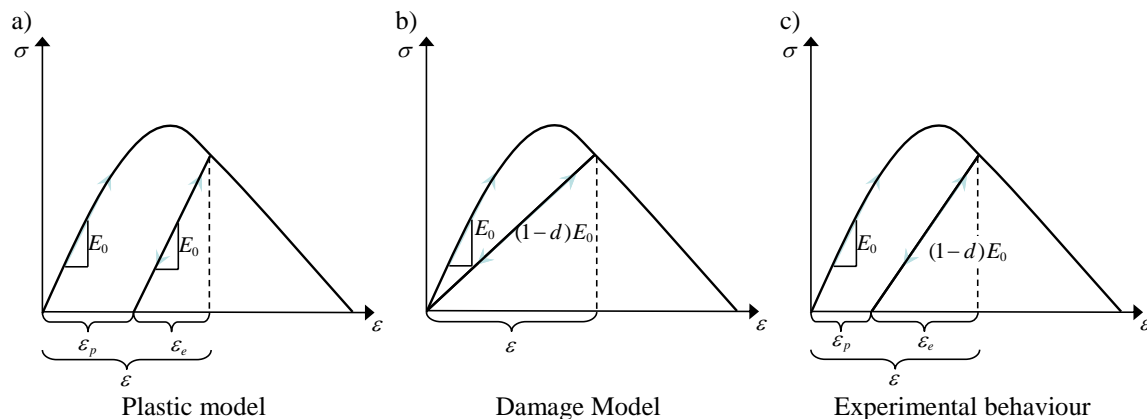


Figure 2.4 - Loading-unloading behaviour – Simulated behaviours and Experimental behaviour

Given that concrete displays the characteristics of both a plastic material and a damaging material, it is appropriate to develop models that incorporate both mechanisms of response. This phenomenological behaviour at the macroscopic level can be modeled by classical plasticity, as formulated by Chen (1994) or by Jirásek and Bazant (2002). On the other hand, Karsan and Jirsa (1969) observe that the microcracking process also causes stiffness degradation, which can be observed in concrete subjected to cyclic loading. Modelling the stiffness degradation is difficult to represent with classical plasticity. In continuum damage

mechanics, the degradation can be modelled by defining the relationship between stresses and effective stresses. Comprehensive reviews on continuum damage mechanics are given by Kachanov (1986) and Lemaitre and Chaboche (1990). Several models for concrete based on continuum damage mechanics have been developed, i.e., Mazars (1986); Mazars and Pijaudier-Cabot (1989) or Cervera *et al.* (1995). However, without inelastic (or plastic) strains the continuum damage mechanics theory cannot provide an appropriate dilatancy control, which is very important for simulating plain and reinforced concrete structures under multiaxial loading.

a) Simo and Ju's model

In the plastic-damage approach, Simo and Ju (1987) and Lubliner *et al.* (1989) proposed that stiffness degradation is imbedded in a plasticity model. In the coupled elastoplastic-damage model proposed by Simo and Ju (1987), the effective-stress concept in continuum damage mechanics is introduced to represent stiffness degradation. In this model, the free energy potential has the following form $\Psi(\varepsilon, \sigma^p, \mathbf{q}, d) = (1-d)\Psi^0(\varepsilon) - \varepsilon : \sigma^p + \Xi(\mathbf{q}, \sigma^p)$, where d is the damage parameter, \mathbf{q} a suitable set of internal plastic variables and σ^p is the plastic relaxation stress tensor. $\Xi(\mathbf{q}, \sigma^p)$ denoted as plastic potential function, and $\Psi^0(\varepsilon)$ is the initial elastic stored energy function. The advantage of this model is that the damage in stiffness degradation, which originally is coupled in the constitutive relations, can be decoupled from the plastic deformation by linearizing the evolution equations, given the elastic-damage tangent as $\mathbf{C}(\varepsilon, d) = [(1-d)\frac{\partial^2\Psi^0(\varepsilon)}{\partial\varepsilon^2} - \frac{H}{\bar{\tau}}\sigma^0 \otimes \sigma^0]$, where $\bar{\tau} = \sqrt{2\Psi^0(\varepsilon)}$ and $H(\bar{\tau}, d)$ is the damage evolution function. Therefore, the yield condition is given as $f\left(\frac{\partial\Psi^0(\varepsilon)}{\partial\varepsilon} - \sigma^p, \mathbf{q}\right) \leq 0$. However, as seen in other models based on continuum damage mechanics, calibration of the parameters determining the evolution of a yield surface with experimental data is difficult because most experimental data are based on the stress.

b) Lubliner's model

In a model proposed by Lubliner *et al.* (1989), a fracture-energy-based scalar damage variable is used to represent all damage states. In addition to the damage variable, the model introduces elastic and plastic degradation variables to simulate the degradation of elastic stiffness. The degradation variables are coupled with the plastic deformation in the constitutive relations, making it convenient to calibrate the parameters with experimental results. The model proposed by Lubliner has the following characteristics:

- The shape of the yield surface is assumed to remain constant and is defined by a modified Mohr-Coulomb criterion;
- The evolution of elastic domain is defined by a hardening rule that is calibrated on the basis of experimental data;
- The plastic strain is defined based on an associated flow rule, while the damage is assumed to be isotropic and defined by a single scalar damage variable which measure the accumulated damage.

c) Luccioni's model

Following the same principle, Luccioni *et al.* (1995) assume the existence of three spaces: a real damage anisotropic space, a fictitious damaged isotropic space and a fictitious undamaged isotropic space. The problem is solved in the fictitious damaged space for isotropic materials. Afterwards, Luccioni *et al.* (1996) presented a coupled plastic-damage model through a simultaneous solution of the plastic and the damage problem. In this model, the total free energy is expressed as $\Psi(\varepsilon^e, \alpha, \beta) = \Psi^e(\varepsilon^e, \beta) + \Psi^p(\alpha)$ where an elastic part Ψ^e and a plastic part Ψ^p , corresponding to the elastic and plastic process, respectively, while α and β represent groups of internal variables plastic and non-plastic, respectively. The plastic process is described by a generalization of classical theory, taking into account many aspects of geometrical behaviour, in a way that the yield function is defined as $F(\boldsymbol{\sigma}, \alpha) = f(\boldsymbol{\sigma}) - K(\boldsymbol{\sigma}, \alpha) \leq 0$, where $f(\boldsymbol{\sigma})$ is the equivalent tension defined in damaged space, $K(\boldsymbol{\sigma}, \alpha)$ is the equivalent yielding threshold and $\alpha(\kappa^p, \varphi, K)$ is a set of internal variables, where κ^p is the plastic damage variable.

Likewise, the damage threshold is described by a damage function $G^d = \bar{\boldsymbol{\sigma}}(\boldsymbol{\sigma}) - f_c(\boldsymbol{\sigma}, \kappa^d) \leq 0$, in which $\bar{\boldsymbol{\sigma}}(\boldsymbol{\sigma})$ is the equivalent tension defined in the damage space evaluated by yielding functions (Tresca, Von-Mises, Mohr-Coulomb, etc.), $f_c(\boldsymbol{\sigma}, \kappa^d)$ is the equivalent damage threshold and κ^d is the degradation variable. The evolution of permanent strains and damage is obtained from the simultaneous solution of the consistency conditions for both plastic and damage functions, i.e. $\dot{F} = 0$ and $\dot{G}^d = 0$, and the secant constitutive law is written as $\boldsymbol{\sigma} = (1 - d)\mathbf{C}^0 : (\boldsymbol{\varepsilon} - \boldsymbol{\varepsilon}^p)$.

d) Oller's model

Developing a procedure to evaluate the damage of reinforced concrete structure subjected to seismic actions, Oller *et al.* (1992) presents a local damage index constitutive model, based on Kachanov's theory, applied to the case of 2D and 3D Timoshenko beam elements. The damage function is give by

$F = G(\bar{\sigma}) - G(f_c) \leq 0$, where $f_c = (\Psi_c^0 E^0)^{1/2}$ is the compression strength, $\bar{\sigma} = [nr + (1-r)(\sum_{i=1}^3 (\sigma_i^0)^2)^{1/2}]$, with $n = f_c / f_t$ and $r = (\sum_{i=1}^3 \langle \sigma_i^0 \rangle) / (\sum_{i=1}^3 |\sigma_i^0|)$. The evolution of damage is defined as $\dot{d} = \frac{dG(\bar{\sigma})}{d\bar{\sigma}} \dot{\bar{\sigma}}$ and the dissipation is obtained as $\dot{\Xi}_m = \Psi^0 \frac{dG(\bar{\sigma})}{d\bar{\sigma}} \frac{\partial \bar{\sigma}}{\partial \sigma^0} \mathbf{C}^0 \dot{\varepsilon}$. The temporal variation of the stress tensor is given by $\delta \boldsymbol{\sigma} = \mathbf{C}^d : \delta \boldsymbol{\varepsilon}$, where \mathbf{C}^d is the unsymmetric tangent constitutive tensor, expressed as $\mathbf{C}^d = \mathbf{C}^s - \frac{1}{1-d} \frac{\partial G(\bar{\sigma})}{\partial \bar{\sigma}} \left[\left(\frac{\partial G(\bar{\sigma})}{\partial \sigma^0} : \mathbf{C}^0 \right) \otimes \boldsymbol{\sigma} \right]$, in which \mathbf{C}^0 is the stiffness tensor of the material in the initial undamaged state, $\mathbf{C}^s = -\mathbf{C}^0 \delta d$ is the secant stiffness tensor. With respect to reinforcement, in this model the steel bars are represented by two or three dimensional steel layers or fibers having its behaviour simulate by means of an elastoplastic constitutive model, with a classical Von Mises yield surface and associated plasticity, as described by Malvern (1969) and Lubliner (1990). However, the coupled relations give a complicated and unstable numerical algorithm, which causes spurious plastic unloading during iteration.

e) Other's models

Because a quasi-brittle material under cyclic loading undergoes several damage states, such as tensile cracking, compressive failure, and stiffness degradation, an assumption of a single damage variable is not adequate. To account for different damage responses, multiple hardening (or damage) variables can be used, as described in Mazars (1986); Ohtani and Chen (1988) and Mazars and Pijaudier-Cabot (1989). Isotropic continuum damage mechanics models with multiple damage variables cannot represent the different effects of damage on the tensile and compressive strengths because the damage variables eventually contribute to the same isotropic evolution for both strengths.

When cyclic loading ranges between the tensile and the compressive, the recovery of degraded stiffness is observed during unloading from the tensile region to the compressive region. The stiffness recovery is a consequence of closing the previously opened cracks. Cervera *et al.* (1995) observe that several models for simulating the stiffness recovery have been suggested in the context of isotropic and anisotropic damage models. A rate dependent damage model for concrete at dynamics loads is presented by Dubé *et al.* (1996), where the rate dependent is derived from a rate independent damage model simply by changing the expression of the damage evolution equation, while the plastic multiplier is modified compared to a standard rate independent plasticity model. In this model, the energy release rate $Y = \frac{1}{2} [(\boldsymbol{\sigma} : \mathbf{D}^0 : \boldsymbol{\sigma}) / (1-d)^2]$ and the strain $\boldsymbol{\varepsilon} = [(\mathbf{D}^0 : \boldsymbol{\sigma}) / (1-d)]$ are defined as variables associated to damage and to the stress., with $\mathbf{D}^0 = (\mathbf{C}^0)^{-1}$ is the compliance of undamaged material. The evolution of damage requires the definitions

of a loading function $f(Y, Z) = Y - Y_0 - Z$, with Y_0 being the parameter which defines the threshold of damage and Z is the hardening-softening controlling variable. The evolution law is prescribed in associated plasticity by $\dot{d} = \dot{\lambda} \frac{\partial f}{\partial Y}$ and $z = -\dot{\lambda} \frac{\partial f}{\partial Z}$, in where z is a equivalent cumulated plastic strain and λ is the damage multiplier, which is evaluated as $\dot{\lambda} = \frac{1}{m} \left(\frac{\langle f \rangle}{Y_0} \right)^n$, with m and n defined as the positive parameters to fit the response of the model to experimental data corresponding to several loading rates. With this model is possible to simulate a viscoplasticity behaviour, characterized by points in the stress (or strain) space outside the elastic domain.

Extending the model proposed by Oller *et al.* (1992) by the consideration of the influence of the viscosity, thus the including damping effects, Barbat *et al.* (1997) presents a local damage index constitutive model, based on Kachanov's theory, applied to the case of 2D and 3D Timoshenko beam elements. Each point of the material undergoes the same deformation ε , so that the total stress σ_{tot} of the system is the sum of a non-viscous stress σ and a viscous stress σ_{vis} , i.e., $\sigma_{tot} = \sigma + \sigma_{vis} = \mathbf{C}^s : \varepsilon + \eta^s : \dot{\varepsilon}$. The secant constitutive η^s is defined in this model as $\eta^s = \alpha \mathbf{C}^s$, where $\mathbf{C}^s = -\mathbf{C}^0 \delta d$ is the secant stiffness tensor and α is the relaxation time, defined as the time needed by the elasto-viscous system to reach a stable configuration in the undamaged state. The viscous-elastic incremental strain-stress relation is defined as $\delta \sigma_{tot} = (\mathbf{I} - \mathbf{D}_{vis}) \mathbf{C}^0 \delta \varepsilon + \alpha \mathbf{C}^s \delta \varepsilon$, where the \mathbf{I} is the identity matrix of the same order as \mathbf{C}^0 and \mathbf{D}_{vis} is a non-symmetric matrix, defined as $\mathbf{D}_{vis} = d \mathbf{I} + \frac{dG(\bar{\sigma})}{d\bar{\sigma}} (\boldsymbol{\sigma}^0 + \boldsymbol{\sigma}_{vis}^0) \otimes \frac{d\bar{\sigma}}{d\boldsymbol{\sigma}^0}$.

The definition of the scalar monotonic function $G(\chi)$ can be defined as defined in Simo and Ju (1987), or alternatively as $G(\chi) = 1 - \frac{\bar{G}(\chi)}{\chi}$, as exposed in Oller *et al.* (1992) and Barbat *et al.* (1997), where $\bar{G}(\chi)$ describes a function so that it gives for $\chi = \chi^0$ the compression initial yield tension \bar{G}^0 and for $\chi \rightarrow \infty$ the final strength $\bar{G} \rightarrow 0$. This function can be defined as, i.e., the exponential function proposed by Oliver *et al.* (1990), $\bar{G}(\chi) = \chi^0 e^{A[1 - (\chi/\chi^0)]}$ which results in $G(\chi) = 1 - \frac{\chi^0}{\chi} e^{A[1 - (\chi/\chi^0)]}$. The parameter A can be expressed as proposed by Oller (2001b) as $A = 1 / \left(\frac{g_f}{(\bar{\sigma}^0)^2} - \frac{1}{2} \right)$, where g_f is the fracture energy density, the parameter derived from fracture mechanics as $g_f = G_f / l_c$ where G_f is the fracture energy and l_c is the characteristic length of the fractured domain proposed by Lubliner *et al.* (1989). Alternatively, Oller (2001b) describes the possibility to use a linear function as $G(\chi) = \left(1 - \frac{\chi^0}{\chi} \right) / (1 + A)$, where in this case the parameter A is expressed as $A = -\frac{1}{2} \frac{(\bar{\sigma}^0)^2}{g_f}$.

2.4 Global damage in structures

Damage analysis is a major research area nowadays and several models have been proposed for the definition of the degree of damage at either the member or the structure level, especially under seismic loading conditions.

In the models discussed in Section 2.3, the selection of appropriate damage parameters is very important for performance evaluation. Maximum values of member or joint rotations, curvature and ductility factors are also good indicators of damage because they can be directly related to the element deformation capacities. However, the maximum value alone of any of these parameters may not be sufficient to quantify the overall damage caused by cyclic reversal of deformation. Damage indices, which take into account both the maximum deformation and cyclic effects, have been developed for such cases.

2.4.1 Damage indices based on maximum deformation

In seismic engineering, the damage indices based on maximum deformation as classified as:

a) Ductility ratio.

The ductility ratio is defined as the ratio of the maximum deformation to the yield deformation. It has been used extensively in seismic analysis to evaluate the capacity of structures undergoing inelastic deformation and to develop inelastic response spectra, as commented by Newmark and Rosenblueth (1971). As a damage index, Ayala and Xianguo (1995) concludes that the ductility ratio may be unsatisfactory, especially when shear distortion in joints and beam bottom bars pullout are anticipated. As demonstrated by experimental studies, the ductility ratio does not account for the effect of the duration and frequency content of the ground motion. It is normally assumed that failure occurs when the ductility demand (response) exceeds the structural ductility (capacity), which is equal to the ratio of the ultimate deformation under monotonic static load to the yield deformation.

b) Interstorey drift.

The interstorey drift is the maximum relative displacement between two storeys normalized to the storey height. According to Sozen (1981) the percentage of damage to the structure is given by % of damage equal to 50% versus the maximum interstorey drift in percentage – 25 %. From the analysis of test data on components and small-scale structures, it was found that an interstorey drift value smaller than 1 per cent corresponds to damage of non-structural compo-

nents, while values of interstorey drift larger than 4 per cent may result in irreparable structural damage or collapse. Collapse is considered to occur when interstorey drift exceeds 6 per cent, as proposed by Roufaiel and Meyer (1981). Similar to the damage index based on the ductility ratio, the interstorey drift does not account for effects of cumulative damage due to repeated inelastic deformation. In addition, the relationship between damage and interstorey drift varies depending on the maximum deformation at collapse, which depends on the ductility class of the structure.

c) Slope ratio.

The slope ratio is a measure of damage due to stiffness degradation during seismic loading. It is defined as the ratio of the slope of the loading branch of the force-displacement diagram to the slope of the unloading branch. From tests on small-scale structural systems, Toussi and Yao (1982) determined that slope ratio with values of 1.0 and 0.2 correspond to safe structural behaviour and critically damaged structures, respectively.

d) Flexural damage ratio.

Roufaiel and Meyer (1981) suggested that the ratio of initial stiffness to the reduced secant stiffness at the maximum displacement can be used as a measure of damage. Banon and Veneziano (1982) observe that damage indices based on extreme inelastic deformations seem to be strongly correlated so that their predictions are usually similar. For example, the correlation coefficient between the two ratios, the ductility and flexural damage, have been found to be 0.95. The flexural damage index does not account for effects of cumulative damage caused by repeated load reversals.

Critical values of the ductility ratio, slope ratio and flexural damage ratio indices are determined from laboratory tests and field observations. Therefore, their use in the prediction of seismic damage for structures with characteristics significantly different from those used in the calibration process requires caution. Additional difficulties in the use of these damage indices relate to the differences between the characteristics of the expected earthquake and the earthquakes used in the calibration such as intensity, duration and frequency content.

Similarly, several models have been proposed for damage indices taking into account the maximum deformation and cumulative damage:

i. Cyclic Ductility.

Mahin and Bertero (1981) present a damage model based on cyclic deformation ductility or inelastic dissipation, defining a cyclic ductility as $\mu_c = \frac{x_{\max,c}}{x_y}$, where $x_{\max,c}$ is the maximum plastic excursion and x_y is the yield displacement. The damage function D_μ in terms of cyclic ductility is $D_\mu = \frac{\mu_c}{\mu_{u,mon}-1}$, where $\mu_{u,mon}$ is the ultimate ductility in a monotonic test.

ii. Park and Ang's local damage index.

In other models, the damage is a function of both cyclic deformation ductility and inelastic energy dissipation. As an example, the damage index developed by Park and Ang (1985) for reinforced concrete structures attempts to account for the damage caused by cyclic deformations into the post-yield level, in such a way that the damage function is the linear combination of the maximum displacement (deformation) ductility and the inelastic energy dissipation.

This model is expressed as $D_{pa} = \frac{x_{\max}}{x_{u,mon}} + \beta \frac{E_h}{F_y x_{u,mon}} = \frac{\mu_s + \beta(\mu_c - 1)}{\mu_{u,mon}}$, where β is a parameter that depends on the level on the shear and axial force in the member, and on the amount of the longitudinal, and transverse reinforcement, F_y is the yield strength of the structural model, and E_h is the total inelastic energy dissipation. The assumptions used in the development of the damage index expression are: (I) the contributions to damage of the extreme deformation and dissipated energy can be superimposed linearly, and (II) the related evolution in time of these components can be disregarded. The results obtained by Banon and Veneziano (1982) do not support these assumptions. In addition, the value of the constant β is not specified and has to be obtained by calibration using laboratory or field data. The behaviour of this index is strongly dependent on the hysteretic model of the elements.

iii. Chung, Meyer and Shinozuka's local damage index

Chung *et al.* (1987) proposed a damage index which contains damage modifiers that reflect the effect of the loading history. This index considers the difference in response of members to positive and negative moments. The effect of the loading history is taken into account by a damage modifier which includes the change in stiffness and the bending moment sustained up to the calculation cycle. The damage index definition does not explicitly account for the damage caused by the maximum deformation experienced by the element.

iv. Maximum softening

DiPasquale and Çakmak (1987) developed a damage model based on the evolution of the natural period of a time-varying linear system equivalent to the actual non-linear system for a series of non-overlapping time windows. This global damage index depends on a combined effect of stiffness degradation and plastic deformation. However, to compute the maximum softening it is necessary to have the input ground acceleration and the acceleration at another location such as at the top of the structure. The maximum softening index does not explicitly account for the dissipated hysteretic energy and strength deterioration, and does not provide information concerning the extent of local damage sustained by the members.

v. Final softening.

DiPasquale and Çakmak (1998) used the change in the fundamental period of the structure as a measure of the change in the stiffness caused by the earthquake. However, the instantaneous fundamental period includes the effect of the inertia and damping forces. The advantage of the final softening is that it can be evaluated from the initial natural period and the final period determined from vibration field-testing after the earthquake. In effect, it is not necessary to know the actual structural response.

However, the measured change in period could be caused by cracking of infill walls while the structural system may remain intact. The final period is affected by the changes in the fundamental mode of the structure due to inelastic response. These changes will cause a corresponding change in the modal mass leading to final softening index that is no longer representative of the global stiffness deterioration. A shortcoming of damage measurements based on the final softening is that local element and storey damage as well as the information contained in the response to the earthquake are not available. A recognized difficulty in the calculation of the final period is due to the idealization used in the analytical procedure.

The period calculation at the final time step of the earthquake loading may be affected by the randomness of the instantaneous tangent stiffness at the end of the dynamic load. In the inelastic hysteretic response range of reinforced concrete, the stiffness of the loading direction may be significantly different from the stiffness in the unloading direction. In addition, the stiffness at the zero load position may differ from the stiffness at the loaded positions.

However, these models cannot be applied to determine the damage of a substructure (e.g. a storey of a building) and its impact on the overall structure.

Another drawback is that these models require the evaluation of the fundamental frequency for each load increment, being computationally expensive.

2.4.2 Damage indices based on energy dissipation

The storey level damage and global damage indices are obviously functions of constituent elements. The attributes “local” and “global” are often associated with damage indices in current terminology. In general acceptance, a damage index is local when it refers to a single point, sections, members or structural parts, while it is considered global when it describes the state of the entire structure (Hanganu *et al.* (2002)). Although damage indices exposed above are adequate for seismic analysis, they cannot be applicable directly to other types of studies.

The definitions of global damage indices generally rely on weighted averages of “local” indices. They vary widely from member volume or quota of potential energy absorbed by the member, to esoteric criteria like the assignment by experts of relative importance factors to the various structural subparts.

In the technical literature, the term damage is also used to denote hysteresis rules, which account for the gradual strength and stiffness deterioration in the material or section behaviour as a result of inelastic deformation reversals. Such hysteretic rules for material models, which are expressed in terms of a stress-strain or section moment-curvature relation, are based on expressions that resemble the damage index. Several damage indices have been proposed in which damage is a function of ductility or inelastic energy dissipation, as example:

a) Local and global damage indices based potential energy.

Using the concepts of potential energy, Oller *et al.* (1992) present a formulation where the local damage is based on Kachanov’s theories, where the global damage is defined as the ratio between the potential energy that the structure cannot undertake in the damaged state $W_p = \int_V (1-d)\Psi^0 dV$, and the potential energy that the structure should undertake if it were undamaged $W_p^0 = \int_V \Psi^0 dV$. This relation can be expressed as $D = 1 - \frac{W_p}{W_p^0}$, or expanding $D = \int d\Psi^0 dV / \int \Psi^0 dV$. In a finite element scheme, in the case of a structure discretized with layered beams, the damage index of a beam point D_p is given by a similar expression obtained by integrating the free energy $\Psi(\varepsilon, d) = (1-d)\Psi^0(\varepsilon, d)$, over the cross-section of the beam, resulting in $D_p = 1 - \frac{\varepsilon\sigma}{\varepsilon\sigma^0}$, where ε and σ are the generalized strains and stress in the beam point, respectively. Therefore, the global damage can be performed over the beam elements or over a number of finite elements (e) as

$$D = \sum_{(e)} \mathbf{a}^{(e)T} \int_{V^{(e)}} \mathbf{B}^{(e)T} \boldsymbol{\sigma}_{tot}^{(e)} dV / \sum_{(e)} \mathbf{a}^{(e)T} \int_{V^{(e)}} \mathbf{B}^{(e)T} \boldsymbol{\sigma}_{tot}^0{}^{(e)} ds, \text{ where } \mathbf{a} \text{ is the mesh modal}$$

displacement vector, \mathbf{B} is the strain displacement matrix, $V^{(e)}$ is the volume of each finite element (e), $\boldsymbol{\sigma}_{tot}^{(e)}$ is the actual stress vector and $\boldsymbol{\sigma}_{tot}^0{}^{(e)}$ is the stress vector should the material preserve its original characteristics and undergo the actual strains. This model is also described in Barbat *et al.* (1997) and Hanganu *et al.* (2002). Based on continuum mechanics principles, the term "local" is applied only to damage indices describing the state of the material at particular points of the structure by means of the loss of its stiffness relative to the initial state, while the "global" damage indices refers to the state of finite volume of material, obtained through the integration of pointwise points. In another words, the local damage gives a response of the damage in a member at a microscale level, while the global damage index giving a macroscale responses of the damage in a member or the entire structure. Defining the global damage index by means of the potential energy considerations has the advantage of allowing the determination of the global damage for a part or member of the structure (such as floors, columns, etc.), through the sum over the group of the elements for which a value for the global damage index is sought. This model has also advantage that can be applied directly to both static and dynamic analysis.

b) Local and Global damage indices based on energy dissipation.

Oller *et al.* (1996) presents a local and global damage indices deduced from the local damage corresponding to each point of the structure. The local damage state in a point of the continuum is defined as thermodynamic state due to the nonlinear behaviour of the material. The global damage index is obtained by two formulations. In the first one, the global damage is defined by means of the dissipated energy and of the internal forces, as $D = \int dg^*(\boldsymbol{\sigma})dV / \int \alpha(x)g^*(\boldsymbol{\sigma})dV$, where $g^*(\boldsymbol{\sigma})$ is a function which measure the maximum dissipated energy in a point of the solid under traction or compression, and $\alpha(x)$ is a plastic variable of the solid. This global damage index also can be calculated over a cross-section of a point or group of elements. The second formulation is based on the concept of the norm of the internal force, as $D = 1 - (|F_{int}| / |F_{int}^e|)$, where F_{int} is the real response of the structure while F_{int}^e is the ideal elastic response. Both global damage indices are independent of the function used to obtain the local damage index.

c) Local and global damage indices based on moment at cross sections.

Oller and Barbat (2005) introduce a moment-curvature damage model for bridges. In this case, the maximum damage at the base of the cross-section of a pier is obtained by the reduction of the cross-sectional moment of inertia of the

bridge piers. Therefore, the maximum damage at the base cross section of a pier i is given by $D_i = \frac{M_e - M_{int}}{M_e}$, where M_{int} is the actual cross-section moment of inertia response and M_e is the idealist elastic response of the moment of inertia. This expression is deduced by following a similar process used to determine the global damage proposed in Oller *et al.* (1992). Thus, the mean global structural damage caused by the seismic action in the bridge is calculated as the average of the pier damage indices, as $D_m = \left(\sum_{i=1}^{np} D_i \right) / np$, where np is the number of piers of the bridge.

Chapter 3

Formulation of Planar Frames

3.1 Introduction

Safety and serviceability constitute the two primary requirements in structural design. For a structure to be safe, it must have adequate strength and ductility when resisting occasional extreme loads. To ensure that a structure will perform satisfactorily at working loads, functional or serviceability requirements also must be met. An accurate prediction of the behaviour of a structure subjected to these loads is indispensable in designing new structures and evaluating existing ones.

The behaviour of a structure is defined by the displacements and forces produced within the structure as a result of external influences. In general, structural theory consists of the essential concepts and methods for determining these effects. The process of determining them is known as *structural analysis*. If the assumptions inherent in the applied structural theory are in close agreement with actual conditions, such an analysis can often produce results that are in reasonable agreement with performance in service.

Structural theory is based primarily on the following set of laws and properties. These principles often provide sufficient relations for analysis of structures. The first principle is the *laws of mechanics*, which consist of the rules for static equilibrium and dynamic behaviour; followed by the *properties of materials*, once the material used in a structure has a significant influence on its behaviour. Strength and stiffness are two important material properties. These properties are obtained from experimental tests and may be used in the analysis either directly or in an idealized form. Finally, the structure must be ruled by the *laws of deformation*, which requires that structure geometry and any incurred deformation be compatible; i.e., the deformations of structural components are in agreement such that all components fit together to define the deformed state of the entire structure.

An understanding of basic mechanics is essential for comprehending structural theory. Mechanics is a part of physics that deals with the state of rest and the motion of bodies under the action of forces. For convenience, mechanics is divided into two parts: statics and dynamics.

Statics is that branch of mechanics that deals with bodies at rest or in equilibrium under the action of forces. In elementary mechanics, bodies may be idealized as rigid when the actual changes in dimensions caused by forces are small in comparison with the dimensions of the body. In evaluating the deformation of a body under the action of loads, however, the body is considered deformable.

Dynamics is that branch of mechanics which deals with bodies in motion. Dynamics is further divided into kinematics, the study of motion without regard to the forces causing the motion, and kinetics, the study of the relationship between forces and resulting motions.

In physics, kinematics is the branch of mechanics concerned with the motions of objects without being concerned with the forces that cause the motion. In this latter respect, it differs from kinetics, which is concerned with the forces that affect motion. For this reason, in this chapter, we will define all concepts and fundamentals kinematics equations that are involved to obtain the forces as well as the deformation in frame structures.

The combination of the concepts for statics, or dynamics, with those of mechanics of materials provides the essentials for predicting the basic behaviour of members in a structural system.

Structural members often behave in a complicated and uncertain way. To analyze the behaviour of these members, i.e., to determine the relationships between the external loads and the resulting internal stresses and deformations, certain idealizations are necessary. Through this approach, structural members are converted to such a form that an analysis of their behaviour in service becomes readily possible. These idealizations include mathematical models that represent the type of structural members being assumed and the structural support conditions. This discretization will be represented by the coordinate system of the structure, by the degrees of freedom of each member, and by the boundary conditions applied for each join.

After that, we will describe the cinematic behaviour of the plane frames, independently of the forces involved. The cinematic will lead us to the definition of some concepts: displacement and deformation. The displacement represents mathematically the behaviour of the structure, while the deformations will represent the changes in the form of the structure.

Finally, we will characterize the dynamic analysis applied in the frame structure. Therefore, we will introduce the concept of generalized stress as well as the concept of the inertial forces. The relationship between the external force, generalized stress and inertial forces will be obtained using the continuum mechanics concepts, more specifically by the principle of virtual work.

3.2 Degrees of Freedom

Let us consider a planar frame with b elements, connected in n nodes, consisting of beams and columns, where each of these components can take loads acting in any direction at any point along its length (see Figure 3.1).

The movement of the structure is studied during a time interval $[0, T]$. At time $t = 0$ the state of the structure is denoted by 'initial or undeformed configuration'; in other words, the coordinates, which define the original position of the n nodes, are well known. For those cases, $t > 0$, where the coordinates are not necessarily known, the configuration of the structure will be called 'deformed'.

For reference, a couple of orthogonal coordinate axes X and Y , to define the position of each node at any configuration, will be considered. During the movement of structure, this coordinate system is assumed stationary (Figure 3.1.b).

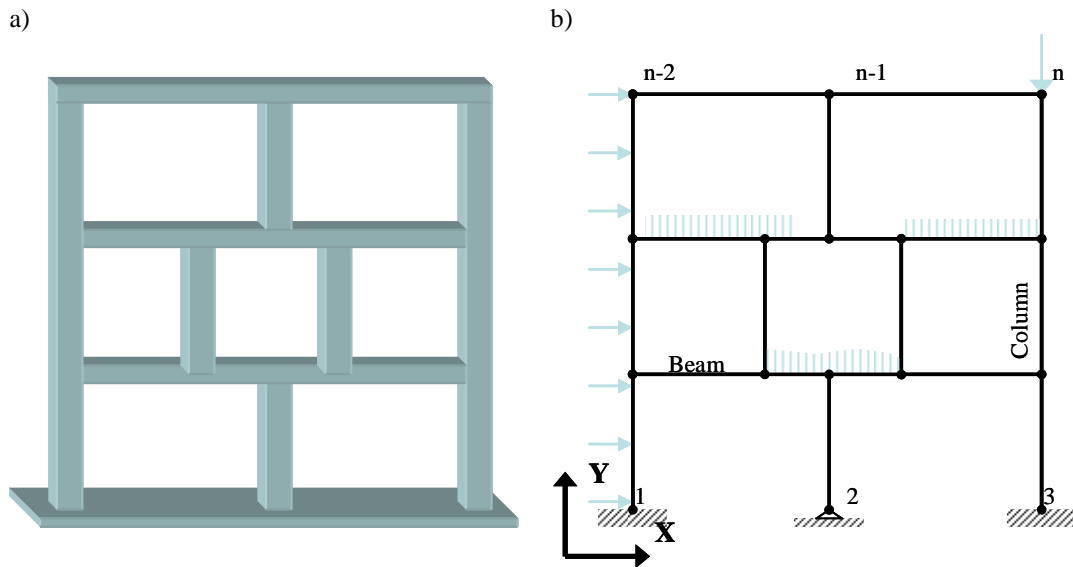


Figure 3.1 - A plane frame system defined: a) into beams and columns elements, b) into bars and nodes elements with loads.

Once a structure has been idealized (Figure 3.1.a), it must be discretized to lend itself to a mathematical representation, as shown in Figure 3.1.b. This discretization should uniquely define each node, and member. The node is characterized by its nodal id (node number), coordinates (local and global), boundary conditions and load (often defined separately).

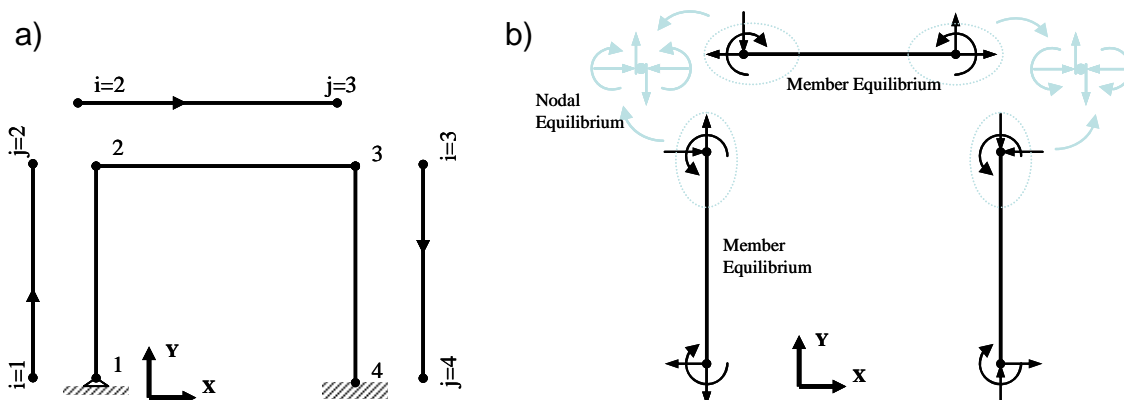


Figure 3.2 - Frame definitions: a) numeration and definition of direction and orientation of each element; b) Degrees of freedom of a member, nodal, and element equilibrium.

Nodes beam or column defines the frame elements, where joint i is the initial node, and joint j indicates the end of element, as shown in Figure 3.2.a. Conventionally, the direction and orientation of each element is given by the i - j node references.

Each joint has three independent generalized nodal displacements called degrees of freedom (Figure 3.2.b). The term *generalized* refers to translations as well as rotations; moreover, the displacements must be linearly independent and thus not related to each other. Usually there is the same number of degrees of freedom in local coordinates as in the global coordinate system. One notable exception is the truss element.

For example, the generalized nodal displacement in the i nodes can be defined as $\{\mathbf{u}_i\}^T = \{u_1 \ u_2 \ u_3\}$, where u_1, u_2 , and u_3 indicate the node displacement in the X direction, Y direction and the node rotation with respect to the initial configuration, represented in Figure 3.3. The same definition can be used for the case of node j .

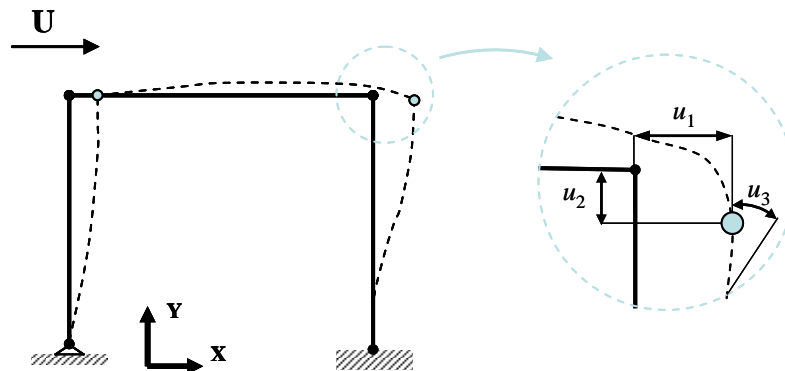


Figure 3.3 - Generalized displacements of a node i

For one b element, the generalized displacement vector for i - j nodes can be defined as:

$$\{\mathbf{u}_b\}^T = \{\mathbf{u}_i^T \ \mathbf{u}_j^T\} = \{u_1 \ u_3 \ u_2 \ u_4 \ u_5 \ u_6\} \quad (3.1)$$

This variable represents the local movement of the beam-column element in the frame as well as the degrees of freedom of the member.

Previously defined that every i and j of element b indicate one node, the global displacement $\{\mathbf{U}\}$ of the structure can be defined as:

$$\{\mathbf{U}\}^T = [\{\mathbf{u}_1\}^T \quad \{\mathbf{u}_2\}^T \quad \dots \quad \{\mathbf{u}_n\}^T] = [u_1 \quad u_2 \quad \dots \quad u_{3n}] \quad (3.2)$$

This vector defines all the structure movement. The positions $1, 2, \dots, 3n$ are known as the global degrees of freedom of the structure.

3.3 Support Conditions

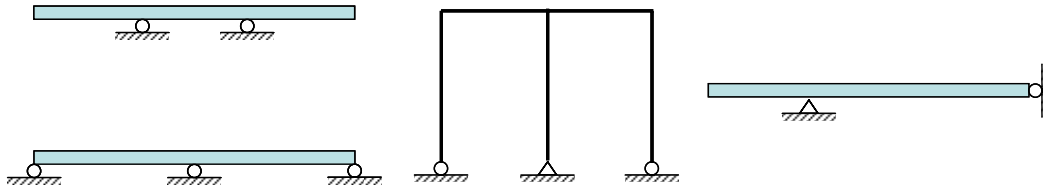


Figure 3.4 – Improper or insufficient support conditions.

In order to guarantee the frame stability, some node displacements are usually restricted. This implies that the displacement values are identified in the time interval $[0, T]$ and defined by the designer. Each restriction is related with at least one degree of freedom in the element. A frame is kinematically unstable if the support conditions are such that the whole structure is allowed to move as a mechanism (Figure 3.4) or if the internal connection conditions are such that part of the whole structure is allowed to move as a mechanism (Figure 3.5).

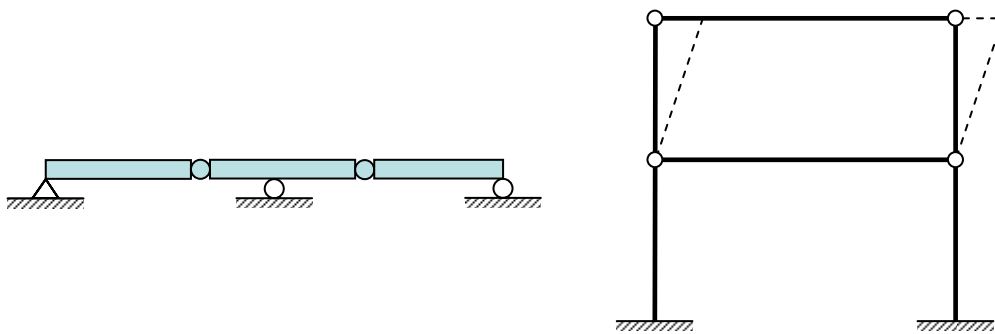


Figure 3.5 – Improper internal connections.

Generally, a stable frame is statically indeterminate. This occurs because the equilibrium equations are insufficient in number to determine all the unknown forces, and therefore they must be complemented with compatibility equations. The number of force unknowns is the sum of the number of reaction forces and the number of the internal member force unknowns, while the internal force is the sum of all degrees of freedom of all members. Alternatively, the equilibrium equations can be formulated in terms of displacements, and in this case, it has always enough equations to determine the unknown displacements (deflections and rotations).

Let us consider the existence of a vector that contains all the information of the degrees of freedom with restrictions, called ‘restriction vector’ $\{\mathbf{R}_u\}$. This vector will remain constant throughout analysis. This vector will be composed of zeros and one, zero indicating degrees of freedom not restricted, while one will indicate restricted degrees of freedom. For example, the structure in Figure 3.2 has twelve degrees of freedom (three for each node), however in the node 1 we have a hinge support, and at the node 4 we have one clamped (fixed) support, which means that the final degrees of freedom of the structure will be only seven. The restriction vector will have the following form:

$$\{\mathbf{R}_u\}^T = \left\{ \underbrace{1 \ 1 \ 0}_{\text{node 1}} \ \underbrace{0 \ 0 \ 0}_{\text{node 2}} \ \underbrace{0 \ 0 \ 0}_{\text{node 3}} \ \underbrace{1 \ 1 \ 1}_{\text{node 4}} \right\} \quad (3.3)$$

Alternatively, we can define displacements, accelerations, and velocity in the supports. The knowledge of these variables as well the initial conditions in the time $t=0$ will also allow us to determine the displacements in the supports through its integration in the time. The use of the accelerations instead of the displacements in the supports is typical of Seismic engineering problems, once it is the accelerations, and not the displacements, which are measured during earthquakes.

3.4 Generalized Deformations

The generalized displacement vector defined in 3.1 is not sufficient to characterize the deformation in the member or in the structure. For example, the movement of a member b can be the result of a non-zero generalized displacement vector $\{\mathbf{u}_b\}$.

For the measure of the deformation in member b the definition of a new variable will be necessary: the generalized deformations $\{\Phi_b\}$. For an element between the nodes i and j this variable is defined by Cipolina *et al.* (1995) as:

$$\{\Phi_b\}^T = \{\phi_i \ \phi_j \ \delta\} \quad (3.4)$$

where ϕ_i and ϕ_j indicate rotations of the member at the ends i and j with respect to the chord $i-j$, respectively, and δ is the elongation of the chord with respect to its length in the initial configuration, as indicated in Figure 3.6. This variable has the same meaning as the strain tensor used in continuum mechanics, and in the same way as in this theory, the deformation variables used are not the only way

to represent the movement, another variable can also be introduced which indicates the same concepts.

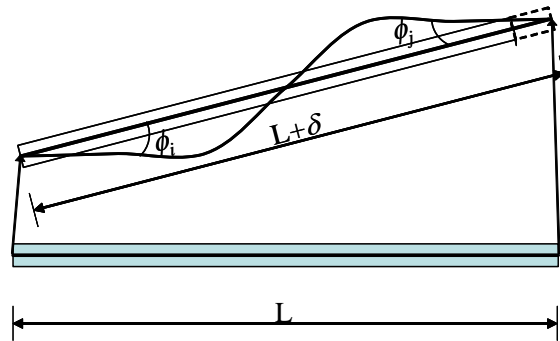


Figure 3.6 - The generalized deformations at the ends i and j .

3.5 Cinematic Equations

The cinematic equations make the interaction between the generalized deformations and the generalized displacements. With the aim of obtaining this expression, let us suppose one differential increment du_1 of the displacement in direction X in the node i of one member b of the structure, while all the others parameter remain constant or null (Figure.3.7).

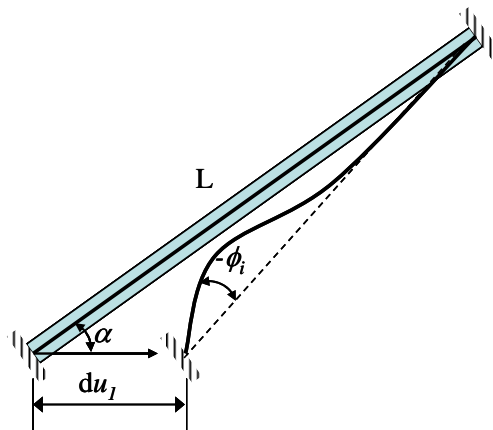


Figure.3.7 - Generalized deformations into a frame element due to an infinitesimal increment du_1

This displacement leads to differential increment of the generalized deformations, thus:

$$d\phi_i = -du_1 \frac{\sin \alpha}{L}; \quad d\phi_j = -du_1 \frac{\sin \alpha}{L} \quad d\delta = du_1 \cos \alpha \quad (3.5)$$

where L is the length of the chord $i-j$ and α is the angle of the chord with respect to the X axis in the original configuration, not necessarily the initial.

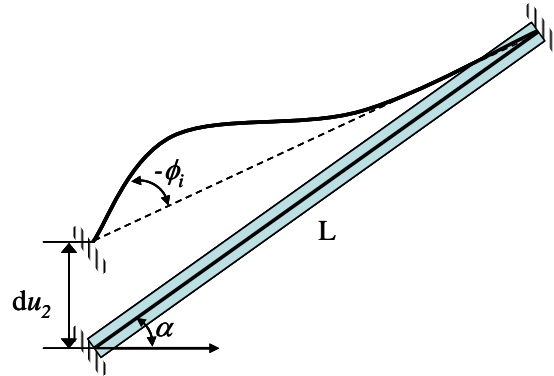


Figure 3.8 - Generalized deformations into a frame element due to an infinitesimal increment du_2

in the same way, a differential increment du_2 in the Y direction at the same node (Figure 3.8), resulting in an increment of the generalized deformations which can be expressed as:

$$d\phi_i = du_2 \frac{\cos \alpha}{L}; \quad d\phi_j = du_2 \frac{\cos \alpha}{L} \quad d\delta = du_2 \sin \alpha \quad (3.6)$$

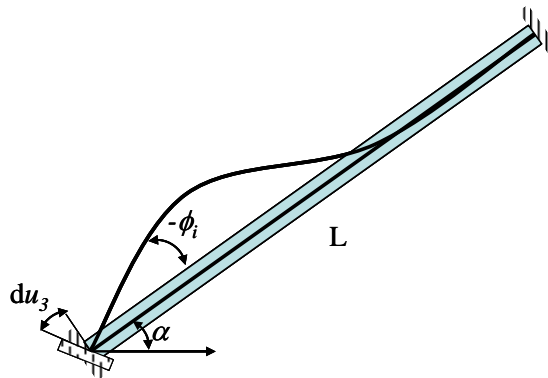


Figure 3.9 - Generalized deformations into a frame element due to an infinitesimal increment du_3

The increment of the generalized deformation due to a differential increment du_3 in the rotation of the node i (Figure 3.9) can be expressed as:

$$d\phi_i = du_3; \quad d\phi_j = 0 \quad d\delta = 0 \quad (3.7)$$

In the same way, we can obtain the generalized deformations in terms of the differential increments du_4 , du_5 or du_6 applied in the node j . Once those transformations are infinitesimal, it is possible to apply the superposition principle. Therefore, for a general case with displacement in all degrees of freedom of the member at the same time, the generalized deformation $\{\Phi_b\}$ can be expressed as:

$$\{d\Phi_b\} = [\mathbf{B}_1(\mathbf{q}_b)]\{d\mathbf{u}_b\} \quad (3.8)$$

Where the local transformation matrix $[\mathbf{B}_1(\mathbf{u}_b)]$ proposed by Flórez-López (1999) is defined as:

$$[\mathbf{B}_1(\mathbf{u}_b)] = \begin{bmatrix} \frac{-\sin \alpha}{L} & \frac{\cos \alpha}{L} & 1 & \frac{\sin \alpha}{L} & \frac{-\cos \alpha}{L} & 0 \\ \frac{-\sin \alpha}{L} & \frac{\cos \alpha}{L} & 0 & \frac{\sin \alpha}{L} & \frac{-\cos \alpha}{L} & 1 \\ \cos \alpha & \sin \alpha & 0 & -\cos \alpha & -\sin \alpha & 0 \end{bmatrix} \quad (3.9)$$

The definition of the displacement transformation matrix in terms of the generalized displacement vector $\{\mathbf{u}_b\}$ can be justified by the assumptions that $L = L(\mathbf{u}_b)$ as well $\alpha = \alpha(\mathbf{u}_b)$ are functions of the displacement in the structure.

When a member to change its initial configuration until a deformed configuration, due to the generalized displacements $\{\mathbf{u}_b\}$, going through a infinite number of transitory configurations. The cinematic equation which represents this movement can be obtained through the integration from the initial configuration until the final configuration, thus:

$$\{\Phi_b\} = \int_{\{0\}}^{\{\mathbf{u}_b\}} [\mathbf{B}_1(z)] \cdot \{dz\} \quad (3.10)$$

This nonlinear equation, for large displacements, leads to the relation between the deformation parameters from (3.4) and the displacements parameters (3.1), such as

$$\phi_i = u_3 - (\alpha_0 - \alpha(\mathbf{u})) \quad ; \quad \phi_j = u_6 - (\alpha_0 - \alpha(\mathbf{u})) \quad ; \quad \delta = L(\mathbf{u}) - L_0 \quad (3.11)$$

where

$$\alpha_0 = \arctan\left(\frac{\Delta Y_0}{\Delta X_0}\right) ; L_0 = \sqrt{(\Delta Y_0)^2 + (\Delta X_0)^2}$$

$$\alpha(\mathbf{u}) = \arctan\left(\frac{\Delta Y_0 + u_5 - u_2}{\Delta X_0 + u_4 - u_1}\right) ; L(\mathbf{u}) = \sqrt{(\Delta Y_0 + u_5 - u_2)^2 + (\Delta X_0 + u_4 - u_1)^2}$$
(3.12)

The equations (3.11) and (3.12) are obtained through purely geometric considerations.

However, one lineal expression can be obtained if the hypothesis of “small displacement” is assumed. This hypothesis consists in the assumption that all modifications in the displacement transformation matrix $[\mathbf{B}_1(\mathbf{u}_b)]$ are very small or insignificant, ($\alpha(\mathbf{u}_b) \cong \alpha_0$, and $L(\mathbf{u}_b) \cong L_0$). In this case, the transformation matrix remains constant throughout the process:

$$[\mathbf{B}_1(\mathbf{u}_b)] = [\mathbf{B}_b^0]$$
(3.13)

where, $[\mathbf{B}_b^0]$ is called the local displacement transformation matrix in the initial configuration. In this case, the integration of the cinematic equation (3.10) becomes:

$$\{\Phi_b\} = [\mathbf{B}_b^0] \cdot \{\mathbf{u}_b\}$$
(3.14)

In the same way, it is possible to describe the deformations in one member b in terms of the global displacement $\{\mathbf{U}\}$ of the structure. In such case, the local displacement transformation matrix $[\mathbf{B}_b^0]$ must be defined as a global displacement transformation matrix $[\mathbf{B}_b]$, adding zeros in the position, which does not correspond to the degrees of freedom of the beam-column element.

$$\mathbf{B}_b = \begin{bmatrix} 0 & \dots & \frac{-\sin \alpha}{l} & \frac{\cos \alpha}{l} & 1 & \dots & \frac{\sin \alpha}{l} & \frac{-\cos \alpha}{l} & 0 & \dots & 0 \\ 0 & \dots & \frac{-\sin \alpha}{l} & \frac{\cos \alpha}{l} & 0 & \dots & \frac{\sin \alpha}{l} & \frac{-\cos \alpha}{l} & 1 & \dots & 0 \\ 0 & \dots & \cos \alpha & \sin \alpha & 0 & \dots & -\cos \alpha & -\sin \alpha & 0 & \dots & 0 \end{bmatrix}$$

$$1, \dots, 3i-2, 3i-1, 3i, \dots, 3j-2, 3j-1, 3j, \dots, n$$
(3.15)

From now on, for small displacements, the generalized deformations $\{\Phi_b\}$ become one function in terms of the global displacement $\{\mathbf{U}\}$ as:

$$\{\Phi_b\} = [B_b]\{U\} \quad (3.16)$$

3.6 Generalized Stresses and Internal Forces

Before continuing with the definitions of the properties of the plain frames, we must remember some basic concepts of the Continuum Mechanics.

By definition, work is defined as the product of the force and displacement

$$W = \int_a^{def\ b} \mathbf{F}.ds \quad (3.17)$$

Energy can be defined as a quantity representing the ability or capacity to perform work. The change in energy is proportional to the amount of work performed. Since only the change of energy is involved, any datum can be used as basis for measure of energy. Hence, energy is neither created nor consumed.

As described by Malvern (1969), the first law of thermodynamics states definition is:

The time-rate of change of the total energy (i.e., sum of the kinetic or inertial energy and the internal energy) is equal to the sum of the rate of work done by the external forces and the change of the heat content per unit time:

$$\frac{d}{dt}(W_I + W_{int}) \stackrel{def}{=} W_e + H \quad (3.18)$$

where W_I is the kinetic or inertial energy, W_{int} the internal strain energy, W_e the external work, and H the heat input to the system.

In ideal elasticity, heat transfer is considered insignificant, and all of the input work is assumed converted into internal energy in the form of recoverable stored elastic strain energy, which can be recovered as work when it is unloaded. Thus, for an adiabatic system (no heat exchange), the equation (3.18) becomes:

$$W_I + W_{int} = W_e \quad (3.19)$$

For the case of purely elastic systems, the equality in the equation (3.19) is called a conservative system. When the plastic or damage (or damped) deformations occur, then we would have a nonconservative system.

We define the virtual work or “principle of virtual work” as fictitious work computed with a set of statically admissible forces and stresses assumed to remain constant while they do work on a set of infinitesimal, kinematically admissible displacements $\{\delta\mathbf{U}\}$. Thus:

$$\delta W_I + \delta W_{int} = \delta W_e \quad \forall \{\delta\mathbf{U}\} \quad (3.20)$$

Now we will analyze each term separately.

3.6.1 External Force

The external work for concentrated forces and moment is the sum of all external forces applied in the frame. These forces can be the loads along the element, the forces and moment applied on the nodes, thus:

$$\delta W_e = \underbrace{\int \delta u q dx}_{\text{loads along the element}} + \underbrace{\sum_i (\delta u_i) F_i}_{\text{loads on the node}} + \underbrace{\sum_i (\delta \Phi_i) m_i}_{\text{moments on the node}} \quad (3.21)$$

Assuming that the all loads along the element can be transformed into loads on the nodes, the equation (3.21) can be rewritten in terms of the infinitesimal displacements $\{\delta\mathbf{U}\}$ as:

$$\delta W_e = \{\delta\mathbf{U}\} \{\mathbf{F}_{ext}\} \quad (3.22)$$

The external load vector $\{\mathbf{F}_{ext}\}$ contains the external forces as well as reactions on supports.

$$\{\mathbf{F}_{ext}\}^T = \{ \underbrace{f_1, f_2, f_3}_{\text{forces on node 1}} \quad \dots \quad \underbrace{f_{3n-2}, f_{3n-1}, f_{3n}}_{\text{forces on node } n} \} \quad (3.23)$$

The terms $f_1, f_4, \dots, f_{3n-2}$ represent the forces in the X direction, applied on the nodes $1, 2, \dots, n$ respectively. The terms $f_2, f_5, \dots, f_{3n-1}$ represent the forces in the Y direction, applied on the nodes $1, 2, \dots, n$ respectively, while f_3, f_6, \dots, f_{3n} represent the moments on the same nodes.

The positions on the external load vector $\{\mathbf{F}_{ext}\}$ which match with the constrained degrees of freedom, the terms non-zero in the restriction vector $\{\mathbf{R}_u\}$, are called support “reactions”. These reactions are part of unknown variables of the analysis.

3.6.2 Inertial Force

The inertial force into a member b of a frame can be defined by the vector $\{\mathbf{f}_I\}$:

$$\{\mathbf{f}_I^b\}^T = (f_I^1 \quad f_I^2 \quad \dots \quad f_I^n) = [\mathbf{m}_b] \{\ddot{\mathbf{u}}_b\}^T \quad (3.24)$$

The term $\{\ddot{\mathbf{u}}_b\} = \{\frac{d^2\mathbf{u}_b}{dt^2}\}$ is called the generalized acceleration vector of the member while $[\mathbf{m}_b]$ represents the elemental mass matrix. Usually, the mass matrix is assumed to be one of data of the analysis.

So, the equation (3.24) can be rewritten in terms of the global acceleration of the frame $\{\ddot{\mathbf{U}}\} = \{\frac{d^2\mathbf{U}}{dt^2}\}$. In this case, the inertial force will be:

$$\{\mathbf{F}_I^b\}^T = (F_I^1 \quad F_I^2 \quad \dots \quad F_I^{3n}) = [\mathbf{m}_g]_b \{\ddot{\mathbf{U}}\}^T \quad (3.25)$$

The general mass matrix $[\mathbf{m}_g]$, defined in terms of the global displacements of the structure, is structured by the addition of zeros in the position, which does not correspond to the degrees of freedom of the beam-column element. The general inertial vector $\{\mathbf{F}_I\}$ is the sum of all inertial forces of the frame:

$$\{\mathbf{F}_I\} = \sum_{b=1}^{nelements} \{\mathbf{F}_I^b\} = \sum_{b=1}^{nelements} [\mathbf{m}_g]_b \{\ddot{\mathbf{U}}\} \Rightarrow \{\mathbf{F}_I\} = [\mathbf{m}] \{\ddot{\mathbf{U}}\} \quad (3.26)$$

here, $[\mathbf{m}] = \sum_{b=1}^{nelements} [\mathbf{m}_g]_b$ is called the mass matrix of the frame.

Thus, the virtual work of the inertial forces due to the virtual displacements $\{\delta\mathbf{U}\}$ can be defined as:

$$\delta W_I = \{\delta\mathbf{U}\} \{\mathbf{F}_I\} \quad (3.27)$$

3.6.3 Internal Forces

The internal virtual work can be written in terms of the stress tensor $\boldsymbol{\sigma}$, the strain tensor $\boldsymbol{\varepsilon}$, and the volume of the system Ω , thus:

$$\delta W_{int} \stackrel{def}{=} \int_{\Omega} \boldsymbol{\sigma} \delta \boldsymbol{\varepsilon} d\Omega \quad (3.28)$$

If now we assume that the internal virtual work is the sum of all internal work in the system, thus:

$$\delta W_{int} = \sum_{b=1}^{nelements} \delta w_b \quad (3.29)$$

where:

$$\delta w_b \stackrel{def}{=} \int_{\omega_b} \boldsymbol{\sigma}_b \delta \boldsymbol{\varepsilon}_b d\omega_b \quad (3.30)$$

being $\boldsymbol{\sigma}_b$ the stress tensor, $\boldsymbol{\varepsilon}_b$ the strain tensor, and ω_b the volume of a member b .

By definition, we assume that the only deformations analyzed in the beam-column element are the rotation and elongation (equation (3.4)). For this reason the equation (3.30) will be divided into three terms: two flexural forces and one axial force.

$$\delta w_b = \int_{\omega_i} \sigma_x \delta \varepsilon_x d\omega_i + \int_{\omega_j} \sigma_x \delta \varepsilon_x d\omega_j + \int_{\omega} \sigma \delta \varepsilon d\omega \quad (3.31)$$

By definition, the bending moment is the derivation along the area A of the stress σ_x plus the distance of the external face until the centroid y , so:

$$\begin{aligned} m_i &\stackrel{def}{=} \int_A \sigma_x y dA \Rightarrow \frac{m_i}{y} = \int_A \sigma_x dA \\ m_j &\stackrel{def}{=} \int_A \sigma_x y dA \Rightarrow \frac{m_j}{y} = \int_A \sigma_x dA \end{aligned} \quad (3.32)$$

The rotation increments and the strain increments are correlated by:

$$\delta \phi_i \stackrel{def}{=} \frac{\delta \varepsilon}{y} \Rightarrow y \delta \phi_i = \delta \varepsilon; \quad \delta \phi_i \stackrel{def}{=} \frac{\delta \varepsilon}{y} \Rightarrow y \delta \phi_i = \delta \varepsilon \quad (3.33)$$

The volume of a flexural beam-column member can be defined as:

$$d\omega_i = \int_0^L \int_A dA dx; \quad d\omega_j = \int_L^0 \int_A dA dx \quad (3.34)$$

where L is the length of the member.

While the volume of an axial beam-column member can be defined as:

$$d\omega = A dx \quad (3.35)$$

Rewriting the equation (3.31) in terms of the definitions (3.32),(3.33),(3.34) , and (3.35), we obtain

$$\delta w_b = \int_0^L m_i \delta \phi_i dx + \int_L^0 m_j \delta \phi_j dx + \int_0^L n \frac{\delta \delta}{A \sigma \delta \varepsilon} dx \quad (3.36)$$

rewritten as matrix form

$$\delta w_b = \{\delta \Phi_b\}^T \{\mathbf{M}_b\} \quad (3.37)$$

therefore the internal virtual work of the structure is:

$$\delta W_{int} = \sum_{b=1}^{nelements} \{\delta \Phi_b\}^T \{\mathbf{M}_b\} \quad (3.38)$$

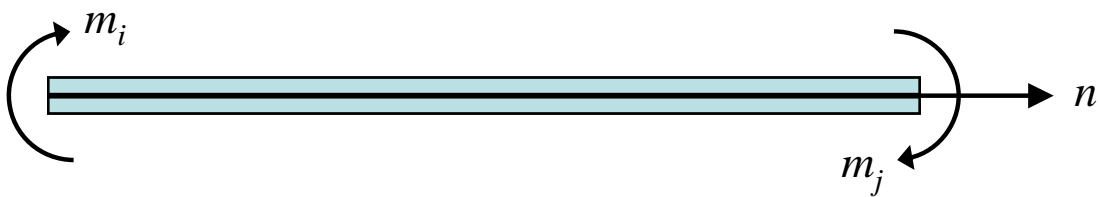


Figure 3.10 - Generalized stress of a member.

The generalized “effective” stress vector $\{\mathbf{M}_b\}$ of the b frame element is defined by Cipolina *et al.* (1995) as

$$\{\mathbf{M}_b\}^T = \{m_i \quad m_j \quad n\} \quad (3.39)$$

where it contains the final forces inside the member, where m_i and m_j are the moments at the ends of the member and n indicates the axial force. This variable has the same significance as the stress tensor used in continuum mechanics

3.7 Dynamic equilibrium equation

Replacing the equations (3.38), (3.22), and (3.27) into the virtual work expression (3.20), we obtain:

$$\{\delta\mathbf{U}\}\{\mathbf{F}_I\} + \sum_{b=1}^{nelements} \{\delta\Phi_b\}^T \{\mathbf{M}_b\} = \{\delta\mathbf{U}\}\{\mathbf{F}_{ext}\} \quad \forall \{\delta\mathbf{U}\} \quad (3.40)$$

once $\{\delta\Phi_b\}$ is the deformation due to the virtual infinitesimals displacements $\{\mathbf{U}\}$, it can be replaced by the cinematic equation (3.16), which leads to:

$$\{\delta\mathbf{U}\}\{\mathbf{F}_I\} + \{\delta\mathbf{U}\}^T \sum_{b=1}^{nelements} [\mathbf{B}_b]^T \{\mathbf{M}_b\} = \{\delta\mathbf{U}\}\{\mathbf{F}_{ext}\} \quad \forall \{\delta\mathbf{U}\} \quad (3.41)$$

Considering that equation (3.41) must be fulfilled for any virtual displacement, we obtain:

$$[\mathbf{m}]\{\ddot{\mathbf{U}}\} + \sum_{b=1}^{nelements} [\mathbf{B}_b]^T \{\mathbf{M}_b\} = \{\mathbf{F}_{ext}\} \quad (3.42)$$

which is the final equation of dynamic balance. Equation (3.42) is based on physical laws and is valid for both linear and nonlinear systems if equilibrium is formulated with respect to the deformed geometry of the structure.

3.8 Nonlinear Dynamic Analysis

To obtain the final response of the frame structure, we could simply use the equation (3.42), relating its dynamic resisting forces with the acceleration, velocity, or displacement vectors by means of linear influence coefficients. However, there are many instances in which the physical properties cannot be assumed to remain constant during the dynamic response. The stiffness influence coefficients may be altered by yielding or by the damage of the structural materials, or by significant changes of the axial forces in the members of the structure. Any such changes will be after the vibration characteristics of the system (since the simple

free-vibration concept cannot be applicable in a nonlinear system), and therefore the normal coordinate uncoupling of the equation of motion is not possible.

Let us analyze some aspects related to the nonlinear dynamic analysis method used. The proposed nonlinear analysis method is applicable to the static and dynamic nonlinear analysis of structures. We assume that the nonlinear static analysis of frames is just a special case of the dynamic analysis with no damping or inertia forces and with lateral forces applied as concentrated static forces at each floor.

The only generally applicable method for the analysis of arbitrary nonlinear system, which will be discussed in this chapter, is the numerical step-by-step integration of the coupled equations of motion. The response history is divided into short, equal time increments, and the response is calculated during each increment for a linear system having the properties determined at the beginning of the interval. Questions of accuracy and stability of the numerical integration scheme are only commented.

In section 3.7, we obtained the dynamic equilibrium equation, which can be rewritten as

$$[\mathbf{m}]\{\ddot{\mathbf{U}}\} + \{\mathbf{F}_{int}\} = \{\mathbf{F}_{ext}\} \quad (3.43)$$

where external vector forces $\{\mathbf{F}_{ext}\}$. Periodic loads, nonperiodic loads, impulsive loads or impactive loads, can define the external forces. Periodic loads vary cyclically with time. Nonperiodic loads do not have a specific pattern of variation with time. An "impulsive dynamic load" is when the load is independent of the motion of the structure, while impactive dynamic loads include the interaction of all external and internal forces, and thus depend on the motions of the structure and of the applied load. For example, in the case of earthquake loading, the external vector forces $\{\mathbf{F}_{ext}\}$ can be defined as

$$\{\mathbf{F}_{ext}(t)\} = -[\mathbf{m}]\{\ddot{\mathbf{U}}_g\} = -[\mathbf{m}]\{1\}\ddot{u}_g \quad (3.44)$$

here, \ddot{u}_g is the ground acceleration and $\{1\}$ is a vector with elements set to one. If the distributed loads along the elements are taken into account during the analysis, we could redefine the external forces as:

$$\{\mathbf{F}_{ext}(t)\} = -[\mathbf{m}]\{1\}\ddot{u}_g - \sum_{b=1}^{nelements} [\mathbf{B}_b]^T \{\mathbf{M}_b^0\} \quad (3.45)$$

where $\sum [\mathbf{B}_b] \{\mathbf{M}_b^0\}$ represents the contribution of the distributed loads along the elements. We assume that the initial generalized forces $\{\mathbf{M}_b^0\}$ will remain constant throughout the time.

Expressing the equation (3.43) in time, we obtain

$$[\mathbf{m}] \{\ddot{\mathbf{U}}(t)\} + \{\mathbf{F}_{int}(t)\} = \{\mathbf{F}_{ext}(t)\} \quad (3.46)$$

The difference between equation (3.43) and equation (3.42), is the fact that we now express the internal forces $\{\mathbf{F}_{int}\} = \{\mathbf{F}_{int}(\mathbf{U}, \dot{\mathbf{U}})\}$, an nonlinear function which contains the nonlinear terms of the structure, as plasticity and damage. It also can take into account the damping forces. Consequently, the internal forces can be expressed as:

$$\{\mathbf{F}_{int}\} = [\mathbf{K}]\{\mathbf{U}\} + [\mathbf{C}]\{\dot{\mathbf{U}}\} \quad (3.47)$$

here, $\{\dot{\mathbf{U}}\}$ is the relative velocity, $[\mathbf{K}]$ is the global stiffness matrix, linear or nonlinear, and $[\mathbf{C}]$ is the damping matrix. These matrices, as well the mass matrix $[\mathbf{m}]$, will be described in detail in the following.

3.8.1 Global stiffness matrix

The global stiffness matrix can be defined in two ways: elastic-linear or initial stiffness matrix $[\mathbf{K}^e]$, and nonlinear or tangent stiffness matrix $[\mathbf{K}_T]$

In the Appendix 1 we presented the complete derivation of the stiffness matrix of a beam-column element. In elastic-linear behaviour, the stiffness can be related with the generalized deformation $\{\Phi_b\}$ and the generalized stress vector $\{\mathbf{M}_b\}$ by:

$$\{\Phi_b\} = [\mathbf{F}_b] \{\mathbf{M}_b\} \quad (3.48)$$

once we have demonstrated that $[\mathbf{F}_b^e] = [\mathbf{S}_b^e]^{-1}$, the equation (3.48) becomes:

$$\{\mathbf{M}_b\} = [\mathbf{S}_b^e] \{\Phi_b\} \quad (3.49)$$

Since the generalized deformation $\{\Phi_b\}$ is defined in terms of the global displacement $\{\mathbf{U}\}$ of the structure and the global displacement transformation

matrix $[\mathbf{B}_b]$, the internal forces $\{\mathbf{F}_{int}\}$, equation (3.47), can now be expressed in terms of the stiffness matrix of a member as:

$$\left. \begin{aligned} \{\mathbf{M}_b\} &= [\mathbf{S}_b^e] \{\Phi_b\} \\ \{\Phi_b\} &= [\mathbf{B}_b] \{\mathbf{U}\} \end{aligned} \right\} \{\mathbf{F}_{int}\} = \left(\sum_{b=1}^{nelements} [\mathbf{B}_b]^T [\mathbf{S}_b^e] [\mathbf{B}_b] \right) \{\mathbf{U}\} + [\mathbf{C}] \{\dot{\mathbf{U}}\} \quad (3.50)$$

The quadratic matrix $[\mathbf{B}_b]^T [\mathbf{S}_b^e] [\mathbf{B}_b]$ is called the “element stiffness matrix”, and the sum of all stiffness matrices to obtain the global stiffness matrix is known as the assemble procedure. Equation (3.50) can be simplified by the substitution of the sum of all stiffness by a new variable, the global elastic stiffness matrix $[\mathbf{K}^e]$, so:

$$[\mathbf{K}^e] = \sum_{b=1}^{nelements} [\mathbf{B}_b]^T [\mathbf{S}_b] [\mathbf{B}_b] \quad (3.51)$$

In the procedure for assembling the global stiffness matrix $[\mathbf{K}^e]$, it will be necessary to take into account the positions in the matrix that correspond with the degrees of freedom with restrictions, the positions non-zero in the restriction vector $\{\mathbf{R}_u\}$. These considerations result in columns and rows that only contain zero.

However, in nonlinear frame analysis, frame members are decomposed into different subelements, which act in series. Each subelement represents a different source of inelastic deformation of frame members. Since each subelement has a unique hysteretic behaviour, changes of stiffness in the different subelements do not take place at the same instant. Consequently, equation (3.48) or (3.49), become nonlinear expressions, since the stiffness matrix $[\mathbf{S}_b]$ is no longer lineal, or the generalized deformation $\{\Phi_b\}$ becomes nonlinear functions of the of the inelastic deformation in the structure. Therefore, the global stiffness must be defined in terms of the generalized stress $\{\mathbf{M}_b\}$

$$[\mathbf{K}_T] = \sum_{b=1}^{nelements} [\mathbf{B}_b]^T \{\mathbf{M}_b\} \quad (3.52)$$

which results in the global tangent stiffness matrix $[\mathbf{K}_T]$. With this, we can assume that all nonlinearity of the structure will depend on the evolution of each generalized stress $\{\mathbf{M}_b\}$. However, each generalized stress depends of the generalized displacements $\{\mathbf{U}\}$. Consequently, we could define the tangent stiffness matrix depends on the generalized deformation, as

$$[\mathbf{K}_T] = [\mathbf{K}(\mathbf{U})] = \sum_{b=1}^{elements} [\mathbf{B}_b]^T \{\mathbf{M}_b(\mathbf{U})\} \quad (3.53)$$

Equation (3.53) will define the nonlinear evolution of the frame structure.

3.8.2 Mass matrix

The simplest procedure for defining the mass properties of any member is to assume that the entire mass is concentrated at each node of the element. This procedure is called “lumped-mass” (concentrated) method. Thus, the elemental lumped mass matrix $[\mathbf{m}_b^L]$, for the uniform case (Figure 3.11a), is defined by Clough and Penzien (1993) or by Paz (1992) as:

$$[\mathbf{m}_b^L] = \frac{\rho AL}{2} \begin{bmatrix} 1 & & & & \\ & 1 & & 0 & \\ & & 0 & & \\ & & & 1 & \\ & 0 & & & 1 \\ & & & & & 0 \end{bmatrix} \quad (3.54)$$

where ρ , A , and L indicate the material density, area and the length of the member, respectively. The off-diagonal terms $[\mathbf{m}_b^L]_{ij}$ of this matrix vanish because an acceleration of any mass point produces an inertia force at that point only. The inertia force at i due to a unit acceleration of point i is obviously equal to the mass concentrated at that point; thus the mass influence coefficient $[\mathbf{m}_b^L]_{ii} = [\mathbf{m}_b^L]_i$ in a lumped-mass system.

On the other hand, the mass associated with any rotational degrees of freedom will be zero because of the assumption that the mass is lumped in points, which have no rotational inertia. Once the lateral inertia forces and displacement constitute the dominant effect, mass is assigned to translational horizontal degrees of freedom only, and no rotational or vertical translational inertia is included. Thus the lumped-mass matrix is a diagonal matrix which will include zero diagonal elements for the rotational degree of freedom, in general.

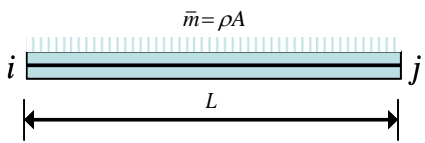
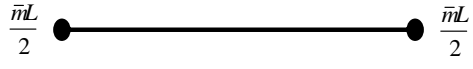
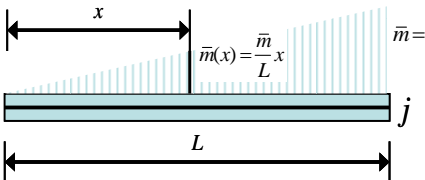
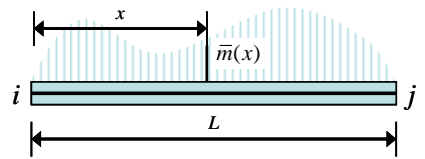
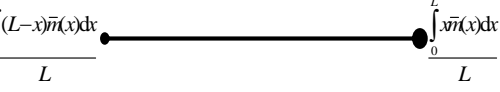
Distributed mass condition	Lumped Mass representation
a) 	
b) 	
c) 	

Figure 3.11 - Lumped Mass for a frame element: a) Uniform mass; b) Triangular mass; and c) Generic mass.

A further option to define the mass properties is by making use of the principle of virtual work method concept. It is possible to evaluate mass influence coefficients for each element of a structure in terms of the virtual displacements functions $\psi(x)$, as shown in Figure 3.12. This procedure is known as consistent mass matrix.

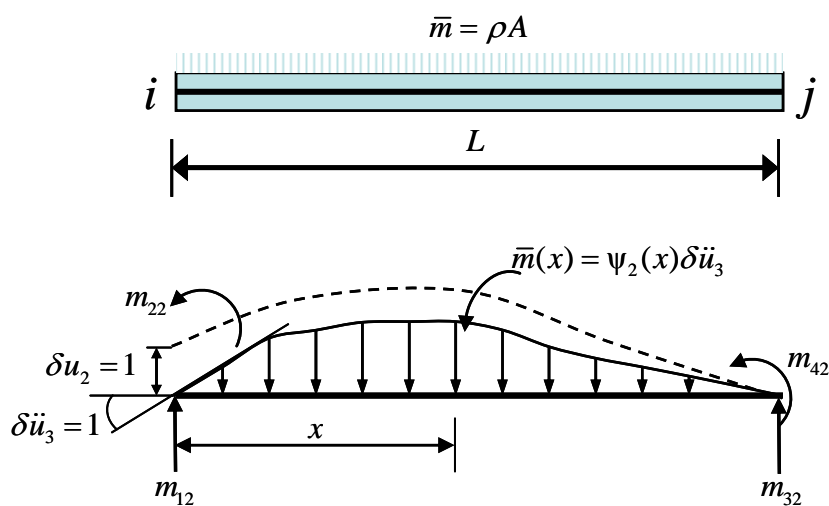


Figure 3.12 – Beam subjected to unitary angular acceleration and virtual translation.

Any mass influence coefficient $[\mathbf{m}_b^C]_{ij}$ of an arbitrary beam element can be evaluated by:

$$[\mathbf{m}_b^C]_{ij} = \int_0^L \bar{m}(x) \psi_i(x) \psi_j(x) dx \quad (3.55)$$

The term $\bar{m}(x)$ is the total mass of the member. When the mass coefficients are computed in this way, the result is called the consistent-mass matrix $[\mathbf{m}_b^C]$. In the special case of a beam with uniformly distributed mass, Flórez-López (1999) obtain:

$$[\mathbf{m}_b^C] = \frac{\bar{m}L}{420} \begin{bmatrix} 140c^2 + 156s^2 & & & & & & \\ -16cs & 156c^2 + 140s^2 & & & & & \\ & 22sL & -22cL & 4L^2 & & & \\ 70c^2 + 54s^2 & 16cs & 13sL & 140c^2 + 156s^2 & & & \\ 16cs & 54c^2 + 70s^2 & -13cL & -16cs & 156c^2 + 140s^2 & & \\ -13sL & 13cL & -3L^2 & 22sL & -22cL & 4L^2 & \end{bmatrix} \quad (3.56)$$

$c = \cos(\alpha) \quad ; \quad s = \sin(\alpha)$

The dynamic analysis of a consistent-mass matrix $[\mathbf{m}_b^C]$ generally requires considerably more computational effort than a lumped-mass matrix $[\mathbf{m}_b^L]$, for two reasons:

- a) The lumped-mass matrix $[\mathbf{m}_b^L]$ is diagonal, while the consistent-mass matrix $[\mathbf{m}_b^C]$ has many off-diagonal terms.
- b) The rotation degrees of freedom can be eliminated from a lumped-mass matrix $[\mathbf{m}_b^L]$, whereas all rotational and translational degrees of freedom must be included in a consistent-mass matrix $[\mathbf{m}_b^C]$.

As consequence, in frame analysis the use of consistent-mass matrix is not worth the effort, since the dynamic response is not much affected by the type of idealization, as observed by Filippou *et al.* (1992).

3.8.3 Damping matrix

In practice, evaluation of the damping matrix is almost impracticable. Energy dissipation in the form of damping is commonly idealized in linear elastic dynamic analysis as viscous or velocity proportional for convenience of solution.

In reality, damping forces may be proportional to the velocity or to some power of velocity.

Hysteretic damping is best accounted for directly by the hysteretic load-deformation relation. The most effective means of deriving a suitable damping matrix is to assume appropriate values of modal damping ratios for all significant modes of vibration of the structure, and then compute a damping matrix based on these damping ratios (Clough and Penzien (1993)). In our case, a Raleigh's type mass and stiffness proportional damping of the following form is used:

$$[\mathbf{C}] = \varphi[\mathbf{m}] + \mathcal{G}[\mathbf{K}] \quad (3.57)$$

in which φ and \mathcal{G} are arbitrary proportionally factors, derived by assuming suitable damping ratios for two modes of vibration. Using a normal coordinate transformation of the equations of motion the n th mode-damping ratio is $\xi_n = \varphi \frac{1}{2\omega_n} + \mathcal{G} \frac{\omega_n}{2}$, where ω_n is the circular frequency of the n th mode. For mass dependent damping, ξ_n is inversely proportional to the frequency such that higher modes have little damping.

Alternatively, the damping matrix, in nonlinear dynamic analysis, can also be expressed in proportion to the initial or current tangent stiffness of the structure according to Filippou *et al.* (1992) as

$$[\mathbf{C}_0] = \varphi[\mathbf{m}] + \mathcal{G}[\mathbf{K}^e] \quad (3.58)$$

or,

$$[\mathbf{C}] = \varphi[\mathbf{m}] + \mathcal{G}[\mathbf{K}_T] \quad (3.59)$$

In those cases where the damping force is considered in the analysis, only (3.58) will be used, since that equation (3.59) can lead to numerical problems and has no significant advantage over the first option.

3.9 Incremental equilibrium equations

The most general approach for the solution of dynamic response of structural systems is the direct numerical integration of the dynamic equilibrium equation (3.46). After the solution is defined at time zero, this involves the attempt to satisfy dynamic equilibrium at discrete points in time. Most methods use equal

time intervals at $\Delta t, 2\Delta t, 3\Delta t \dots n\Delta t$. The numerical techniques can fundamentally be classified as either explicit or implicit integration methods.

Explicit methods do not involve the solution of a set of linear equations at each step, as proposed by Oller (2001a). Basically, these methods use the differential equations at time t to predict a solution at time $t + \Delta t$. For most real structures, which contain stiff elements, a very small time step is required in order to obtain a stable solution. Therefore, all explicit methods are conditionally stable with respect to the size of the time step.

Implicit methods attempt to satisfy the differential equation at time $t + \Delta t$ after the solution at time t is found. These methods require the solution of a set of linear equations at each time step; however, larger time steps may be used. Implicit methods can be conditionally or unconditionally stable.

There exist a large number of accurate, higher-order, multi-step methods that have been developed for the numerical solution of differential equations. These multi-step methods assume that the solution is a smooth function in which the higher derivatives are continuous. The exact solution of many nonlinear structures requires that the accelerations, the second derivative of the displacements, are not smooth functions. This discontinuity of the acceleration is caused by the nonlinear hysteresis of most structural materials, contact between parts of the structure, and buckling of elements. Therefore, only single-step methods will be presented in this chapter. Based on a literature, our conclusion is that only single-step, implicit, unconditional stable methods are used for the step-by-step seismic analysis of practical structures.

3.9.1 Equilibrium Condition

The characteristic of the implicit methods is that, even the displacements $\{\mathbf{U}(t + \Delta t)\} = \{\mathbf{U}^{t+\Delta t}\}$ and the velocity $\{\dot{\mathbf{U}}(t + \Delta t)\} = \{\dot{\mathbf{U}}^{t+\Delta t}\}$ at the time $t + \Delta t$ can be obtained through linear approach in differences (Oller (2001a)):

$$\begin{cases} \{\dot{\mathbf{U}}\}^{t+\Delta t} = k_v \{\ddot{\mathbf{U}}\}^{t+\Delta t} \Delta t + f_v \left(\{\dot{\mathbf{U}}\}^t, \{\ddot{\mathbf{U}}\}^t, \dots \right) \\ \{\mathbf{U}\}^{t+\Delta t} = k_u \{\ddot{\mathbf{U}}\}^{t+\Delta t} \Delta t^2 + f_u \left(\{\dot{\mathbf{U}}\}^t, \{\ddot{\mathbf{U}}\}^t, \dots \right) \end{cases} \quad (3.60)$$

here, Δt is the time increment, and k_v and k_u are coefficients which depend on the solution method adopted.

Assuming that k_v and k_u are null, and that the acceleration $\{\ddot{\mathbf{U}}\}^{t+\Delta t}$ and velocity $\{\dot{\mathbf{U}}\}^{t+\Delta t}$ are defined in terms of the displacement $\{\mathbf{U}\}^{t+\Delta t}$ at the time $t + \Delta t$, the equation (3.46) can be solved by any interaction methods, as example the Newton-Raphson method, which give the approximate solution in the interaction $i+1$ through

$$0 = \{\Delta \mathbf{F}\}_{i+1}^{(t+\Delta t)} \cong \{\Delta \mathbf{F}\}_i^{(t+\Delta t)} + [\mathbf{J}]_i^{(t+\Delta t)} \left(\{\mathbf{U}\}_i^{(t+\Delta t)} - \{\mathbf{U}\}_i^{(t+\Delta t)} \right) \quad (3.61)$$

where $\{\Delta \mathbf{F}\}$ is the residual force in the interaction i . The Jacobian operator $[\mathbf{J}]$ can be obtained by

$$\begin{aligned} [\mathbf{J}]_i^{(t+\Delta t)} &= \left[\mathbf{J} \left(\{\mathbf{U}\}_i^{(t+\Delta t)} \right) \right] = \left(\frac{\partial \{\Delta \mathbf{F}\}}{\partial \{\mathbf{U}\}} \right)_i^{(t+\Delta t)} = \left(\frac{\partial \{\Delta \mathbf{F}\}}{\partial \{\mathbf{U}\}} \right)_i^{(t+\Delta t)} \\ [\mathbf{J}]_i^{(t+\Delta t)} &= \left([\mathbf{m}] \frac{\partial \{\ddot{\mathbf{U}}\}}{\partial \{\mathbf{U}\}} + \frac{\partial \{\mathbf{F}_{int}\}}{\partial \{\mathbf{U}\}} + \frac{\partial \{\mathbf{F}_{int}\}}{\partial \{\dot{\mathbf{U}}\}} \frac{\partial \{\dot{\mathbf{U}}\}}{\partial \{\mathbf{U}\}} - \frac{\partial \{\mathbf{F}_{ext}\}}{\partial \{\mathbf{U}\}} \right)_i^{(t+\Delta t)} \end{aligned} \quad (3.62)$$

in a way that the global tangent stiffness matrix is defined as $[\mathbf{K}_T] = \frac{\partial \{\mathbf{F}_{int}\}}{\partial \{\mathbf{U}\}}$, the damping forces can be defined as $[\mathbf{C}] = \frac{\partial \{\mathbf{F}_{int}\}}{\partial \{\dot{\mathbf{U}}\}}$. For small displacements, the influence of the position of the external force can be assumed null, so $\frac{\partial \{\mathbf{F}_{ext}\}}{\partial \{\dot{\mathbf{U}}\}} = 0$. consequently, the equation (3.62) can be rewritten as

$$[\mathbf{J}] = \left([\mathbf{m}] \frac{\partial \{\ddot{\mathbf{U}}\}}{\partial \{\mathbf{U}\}} + [\mathbf{K}_T] + [\mathbf{C}] \frac{\partial \{\dot{\mathbf{U}}\}}{\partial \{\mathbf{U}\}} \right) \quad (3.63)$$

If the problem is lineal elastic, the Jacobian operator becomes constant

$$[\mathbf{J}]_i^{(t+\Delta t)} = [\mathbf{J}]^{(0)} = [\mathbf{m}] \frac{\partial \{\ddot{\mathbf{U}}\}}{\partial \{\mathbf{U}\}} + [\mathbf{K}_0] + [\mathbf{C}_0] \frac{\partial \{\dot{\mathbf{U}}\}}{\partial \{\mathbf{U}\}} \quad (3.64)$$

and if the problem is almost static, where $\{\ddot{\mathbf{U}}\} = \{\dot{\mathbf{U}}\} = 0$ and $\{\mathbf{F}_{ext}\} \cong cte$, the Jacobian operator reduces to the stiffness matrix

$${}^i [\mathbf{J}]^{(t+\Delta t)} = \left[\mathbf{J} \left({}^i \{\mathbf{U}\}^{(t+\Delta t)} \right) \right] = \left(\frac{\partial \{\Delta \mathbf{F}\}}{\partial \{\mathbf{U}\}} \right)^{(t+\Delta t)} = {}^i [\mathbf{K}_T]^{(t+\Delta t)} \quad (3.65)$$

3.9.2 Implicit solution: Newmark's method

In frame analysis, some degrees of freedom with no associated mass can develop velocity dependent damping leading to modes with zero period. An integration method, which is unconditionally stable with respect to the integration step size, is indispensable in this case. The Newmark's method is one of the methods more used for its balanced relation between computational costs, precision and simplify of numerical implementation.

Expanding the equation (3.60) using Taylor's series provides:

$$\begin{cases} \{\mathbf{U}\}^{t+\Delta t} = \{\mathbf{U}\}^t + \{\dot{\mathbf{U}}\}^t \Delta t + \{\ddot{\mathbf{U}}\}^t \frac{\Delta t^2}{2} + \{\ddot{\ddot{\mathbf{U}}}\}^t \frac{\Delta t^3}{3} + \dots \\ \{\dot{\mathbf{U}}\}^{t+\Delta t} = \{\dot{\mathbf{U}}\}^t + \{\ddot{\mathbf{U}}\}^t \Delta t + \{\ddot{\ddot{\mathbf{U}}}\}^t \frac{\Delta t^2}{2} + \dots \end{cases} \quad (3.66)$$

Truncating these equations and expressing them in the following form:

$$\begin{cases} \{\mathbf{U}\}^{t+\Delta t} = \{\mathbf{U}\}^t + \{\dot{\mathbf{U}}\}^t \Delta t + \{\ddot{\mathbf{U}}\}^t \frac{\Delta t^2}{2} + \beta \{\ddot{\ddot{\mathbf{U}}}\}^t \Delta t^3 \\ \{\dot{\mathbf{U}}\}^{t+\Delta t} = \{\dot{\mathbf{U}}\}^t + \{\ddot{\mathbf{U}}\}^t \Delta t + \gamma \{\ddot{\ddot{\mathbf{U}}}\}^t \Delta t^2 \end{cases} \quad (3.67)$$

if the acceleration is assumed to be linear within the time step, we can write

$$\{\ddot{\ddot{\mathbf{U}}}\} = \frac{\{\ddot{\mathbf{U}}\}^{t+\Delta t} - \{\ddot{\mathbf{U}}\}^t}{\Delta t} \quad (3.68)$$

Replacing (3.68) into (3.67), we obtain Newmark's equations in standard form:

$$\begin{cases} \{\mathbf{U}\}^{t+\Delta t} = \{\mathbf{U}\}^t + \{\dot{\mathbf{U}}\}^t \Delta t + (\frac{1}{2} - \beta) \{\ddot{\mathbf{U}}\}^t \Delta t^2 + \beta \{\ddot{\ddot{\mathbf{U}}}\}^t \Delta t^3 \\ \{\dot{\mathbf{U}}\}^{t+\Delta t} = \{\dot{\mathbf{U}}\}^t + (1 - \gamma) \{\ddot{\mathbf{U}}\}^t \Delta t + \gamma \{\ddot{\ddot{\mathbf{U}}}\}^t \Delta t^2 \end{cases} \quad (3.69)$$

assuming that $\{\Delta \mathbf{U}\}^{t+\Delta t} = \{\dot{\mathbf{U}}\}^t \Delta t + (\frac{1}{2} - \beta) \{\ddot{\mathbf{U}}\}^t \Delta t^2 + \beta \{\ddot{\ddot{\mathbf{U}}}\}^t \Delta t^3$, we can now express the acceleration, velocity and displacement in the present time of process of temporary integration as

$$\begin{aligned}
\{\mathbf{U}\}^{t+\Delta t} &= \{\mathbf{U}\}^t + \{\Delta\mathbf{U}\}_i^{(t+\Delta t)} \\
\{\dot{\mathbf{U}}\}^{t+\Delta t} &= \left(\frac{\gamma}{\beta\Delta t}\right)\{\Delta\mathbf{U}\}_i^{(t+\Delta t)} + \left(1-\frac{\gamma}{\beta}\right)\{\dot{\mathbf{U}}\}^t + \left(1-\frac{\gamma}{2\beta}\right)\{\ddot{\mathbf{U}}\}^t \Delta t \\
\{\ddot{\mathbf{U}}\}^{t+\Delta t} &= \left(\frac{1}{\beta\Delta t^2}\right)\left(\{\mathbf{U}\}_i^{(t+\Delta t)} - \{\mathbf{U}\}^t - \{\dot{\mathbf{U}}\}^t \Delta t\right) - \left(\frac{1}{2\beta}-1\right)\{\ddot{\mathbf{U}}\}^t
\end{aligned} \tag{3.70}$$

The coefficients β and γ determine the stability of Newmark's method, which for zero damping the method is conditionally stable if

$$\gamma \geq \frac{1}{2}; \beta \geq \frac{1}{4}(0.5 + \gamma)^2 \text{ and } \Delta t \leq \frac{1}{\omega_{max} \sqrt{\frac{\gamma}{2} - \beta}} \tag{3.71}$$

where ω_{max} is the maximum frequency in the structural system. Otherwise, Newmark's method is unconditionally stable if

$$2\beta \geq \gamma \geq \frac{1}{2} \tag{3.72}$$

However, if γ is greater than $\frac{1}{2}$, errors are introduced. These errors are associated with numerical damping and period elongation. For large multi degree of freedom structural systems the time step limit given by equation (3.71) can be written in terms of the period as

$$\frac{\Delta t}{T_{min}} \leq \frac{1}{2\pi \sqrt{\frac{\gamma}{2} - \beta}} \tag{3.73}$$

Computer models of large real structures normally contain a large number of periods which are smaller than the integration time step; therefore, it is essential that the selection of the numerical integration method be unconditional for all time steps.

3.10 Numerical Implementation

For any frame structural program analysis, linear or nonlinear, these are generally the input data:

- (a) Determination of the geometry of the structure, defining the nodes coordinate and the connection table, which defines the members.
- (b) Properties of the member (area, inertia)
- (c) Properties of the materials (elastic modulus, plastic and damage parameters when necessary)
- (d) Loading history, static or dynamic, applied on the nodes, during the time interval $[0, T]$.
- (e) The displacements history or the restrictions imposed on the nodes, at the same interval.
- (f) The type of analysis: lineal or nonlinear.

As proposed by Barbat and Canet (1994), once having defined those parameters, we proceed with the nonlinear time integration scheme of dynamic equilibrium equation at time step $t + \Delta t$, where it is necessary solve i interactions of

$$[\mathbf{m}]\{\ddot{\mathbf{U}}\}_{i+1}^{(t+\Delta t)} + [\mathbf{C}]\{\dot{\mathbf{U}}\}_{i+1}^{(t+\Delta t)} + [\mathbf{K}_T]\{\Delta\mathbf{U}\}_{i+1}^{(t+\Delta t)} = \{\Delta\mathbf{F}\}_{i+1} \quad (3.74)$$

replacing (3.61) and (3.70) into (3.74) we obtain for the first interaction

$$[\mathbf{J}]_1 \{\Delta\mathbf{U}\}_1^{(t+\Delta t)} = \{\Delta\mathbf{F}\}_1 \quad (3.75)$$

with

$$[\mathbf{J}]_1 = \left([\mathbf{m}] \frac{\partial \{\ddot{\mathbf{U}}\}}{\partial \{\mathbf{U}\}} + [\mathbf{K}_T] + [\mathbf{C}] \frac{\partial \{\dot{\mathbf{U}}\}}{\partial \{\mathbf{U}\}} \right) = \left([\mathbf{m}] \frac{1}{\beta \Delta t^2} + [\mathbf{K}_T] + [\mathbf{C}] \frac{\gamma}{\beta \Delta t} \right) \quad (3.76)$$

$$\begin{aligned} \{\Delta\mathbf{F}\}_1^{(t+\Delta t)} = & \underbrace{\{\mathbf{F}_{ext}\}^{(t+\Delta t)} - \{\mathbf{F}_{int}\}_1^{(t+\Delta t)}}_{\{\mathbf{F}\}_0} + [\mathbf{m}] \left(\frac{1}{\beta \Delta t} \{\dot{\mathbf{U}}\}^{(t)} + \left(\frac{1}{2\beta} - 1 \right) \{\ddot{\mathbf{U}}\}^{(t)} \right) \\ & - [\mathbf{C}] \left(\left(1 - \frac{\gamma}{\beta} \right) \{\dot{\mathbf{U}}\}^{(t)} + \left(1 - \frac{\gamma}{2\beta} \right) \{\ddot{\mathbf{U}}\}^{(t)} \right) \end{aligned} \quad (3.77)$$

once obtained

$$\{\Delta \mathbf{U}\}_1^{(t+\Delta t)} = [\mathbf{J}]_1^{-1} : \{\Delta \mathbf{F}\}_1 \quad (3.78)$$

the displacements, velocity and accelerations can be calculated as:

$$\begin{aligned} \{\mathbf{U}\}_1^{(t+\Delta t)} &= \{\mathbf{U}\}_1^{(t)} + \{\Delta \mathbf{U}\}_1^{(t+\Delta t)} \\ \{\dot{\mathbf{U}}\}_1^{(t+\Delta t)} &= \left(\frac{\gamma}{\beta \Delta t}\right) \{\Delta \mathbf{U}\}_1^{(t+\Delta t)} + \left(1 - \frac{\gamma}{\beta}\right) \{\dot{\mathbf{U}}\}_1^{(t)} + \left(1 - \frac{\gamma}{2\beta}\right) \{\ddot{\mathbf{U}}\}_1^{(t)} \Delta t \\ \{\ddot{\mathbf{U}}\}_1^{(t+\Delta t)} &= \left(\frac{1}{\beta \Delta t^2}\right) \left(\{\Delta \mathbf{U}\}_1^{(t+\Delta t)} - \{\dot{\mathbf{U}}\}_1^{(t)} \Delta t\right) - \left(\frac{1}{2\beta} - 1\right) \{\ddot{\mathbf{U}}\}_1^{(t)} \end{aligned} \quad (3.79)$$

If the problem is nonlinear, the values obtained at (3.79) will not be the correct ones, consequently, for the second and subsequent i th interactions, the forces in the step $i+1$ must be calculated in terms of the last step.

$$\{\mathbf{F}\}_{i+1} = \{\mathbf{F}_{ext}\}_{i+1}^{(t+\Delta t)} - \{\mathbf{F}_{int}\}_{i+1}(\mathbf{U}_i^{(t+\Delta t)}, \dot{\mathbf{U}}_i^{(t+\Delta t)}) \quad (3.80)$$

moreover, if a change of stiffness occurs, the global tangent stiffness $[\mathbf{K}_T]$ must be redefined in terms of the generalized stress $\{\mathbf{M}_b\} = \{\mathbf{M}_b(\mathbf{U}_i^{(t+\Delta t)})\}$

$$[\mathbf{K}_T] = \sum_{b=1}^{nelements} [\mathbf{B}_b]^T \{\mathbf{M}_b(\mathbf{U}_i^{(t+\Delta t)})\} \quad (3.81)$$

which implies that the Jacobian matrix must be recalculated in the step $i+1$:

$$[\mathbf{J}]_{i+1} = \left([\mathbf{m}] \frac{1}{\beta \Delta t^2} + [\mathbf{K}_T] + [\mathbf{C}] \frac{\gamma}{\beta \Delta t} \right) \quad (3.82)$$

in addition, the residual forces are

$$\{\Delta \mathbf{F}\}_{i+1}^{(t+\Delta t)} = \underbrace{\{\mathbf{F}_{ext}\}_{i+1}^{(t+\Delta t)} - \{\mathbf{F}_{int}\}_i^{(t+\Delta t)}}_{\{\mathbf{F}\}_{i+1}} + [\mathbf{m}] \{\ddot{\mathbf{U}}\}_i^{(t+\Delta t)} - [\mathbf{C}] \{\dot{\mathbf{U}}\}_i^{(t+\Delta t)} \quad (3.83)$$

if the residual forces $\|\{\Delta \mathbf{F}\}_i^{(t+\Delta t)}\| > TOL$, it will be necessary to proceed by calculating:

$$\{\delta \mathbf{U}\}_{i+1}^{(t+\Delta t)} = [\mathbf{J}]_i^{-1} : \{\Delta \mathbf{F}\}_{i+1}^{(t+\Delta t)} \quad (3.84)$$

the displacements, velocity and accelerations in the step can be calculated as:

$$\begin{aligned} \{\mathbf{U}\}_{i+1}^{(t+\Delta t)} &= \{\mathbf{U}\}_i^{(t+\Delta t)} + \{\delta \mathbf{U}\}_{i+1}^{(t+\Delta t)} \\ \{\dot{\mathbf{U}}\}_{i+1}^{(t+\Delta t)} &= \left(\frac{\gamma}{\beta \Delta t} \right) \{\delta \mathbf{U}\}_{i+1}^{(t+\Delta t)} + \{\dot{\mathbf{U}}\}_i^{(t+\Delta t)} \\ \{\ddot{\mathbf{U}}\}_{i+1}^{(t+\Delta t)} &= \left(\frac{1}{\beta \Delta t^2} \right) \{\delta \mathbf{U}\}_{i+1}^{(t+\Delta t)} + \{\ddot{\mathbf{U}}\}_i^{(t+\Delta t)} \end{aligned} \quad (3.85)$$

This process continues until $\|\{\Delta \mathbf{F}\}_i^{(t+\Delta t)}\| \leq \text{TOL}$, or alternatively (Barbat and Canet (1994)) $\frac{|\{\delta \mathbf{U}\}_{i+1}^{(t+\Delta t)}|}{|\{\mathbf{U}\}_i^{(t+\Delta t)} + \{\delta \mathbf{U}\}_{i+1}^{(t+\Delta t)}|} \leq \text{tol}$. The Table 3.1 summarizes all the procedures described above.

As observed in expression (3.80) and (3.81), all nonlinear problems in frames depend on the solution of the generalized stress $\{\mathbf{M}_b\} = \{\mathbf{M}_b(\mathbf{U})\}$, once it is this variable which contains all nonlinearity effects, such as plasticity and damage. Consequently, the generalized stress can no longer be determined by equation (A1.94), described in Appendix 1, other equations being necessary where the nonlinear effects could be taken into account.

For this reason, in the following chapters we concentrate our attention on the analysis of behaviour of frame structures due to the plasticity and damage effects, with the aim of obtaining the expressions, as well as their nonlinear algorithms, which could be included in the calculation of the generalized stress.

Table 3.1 – Nonlinear time integration scheme

□ A. First iteration (passage from time instant t to time instant $t + \Delta t$)

- Update relevant matrices

$$[\mathbf{K}^e] = \sum_{b=1}^n [\mathbf{B}'_b] : [\mathbf{S}_b] : [\mathbf{B}_b] ; [\mathbf{K}_T] = \sum_{b=1}^n [\mathbf{B}'_b] : \{\mathbf{M}_b(\mathbf{U})\} ; [\mathbf{m}] = \sum_{b=1}^n (\mathbf{m}_g)_b$$

- Compute:

$$\{\mathbf{F}\}_1 = \{\mathbf{F}_{ext}\}^{(t+\Delta t)} - \{\mathbf{F}_{int}\}_1^{(t+\Delta t)} ; [\mathbf{J}]_1 = [\mathbf{m}] \frac{1}{\beta \Delta t^2} + [\mathbf{K}_T] + [\mathbf{C}] \frac{\gamma}{\beta \Delta t}$$

$$\{\Delta \mathbf{F}\}_1^{(t+\Delta t)} = \{\mathbf{F}_1\} + [\mathbf{m}] \left(\frac{1}{\beta \Delta t} \{\dot{\mathbf{U}}\}^{(t)} + \left(\frac{1}{2\beta} - 1 \right) \{\ddot{\mathbf{U}}\}^{(t)} \right) - [\mathbf{C}] \left(\left(1 - \frac{\gamma}{\beta} \right) \{\dot{\mathbf{U}}\}^{(t)} + \left(1 - \frac{\gamma}{2\beta} \right) \{\ddot{\mathbf{U}}\}^{(t)} \right)$$

- Calculate the first approximations for the time instant $t + \Delta t$:

$$\{\Delta \mathbf{U}\}_1^{(t+\Delta t)} = [\mathbf{J}]_1^{-1} : \{\Delta \mathbf{F}\}_1 \left\{ \begin{array}{l} \{\mathbf{U}\}_1^{(t+\Delta t)} = \{\mathbf{U}\}^{(t)} + \{\Delta \mathbf{U}\}_1^{(t+\Delta t)} \\ \{\dot{\mathbf{U}}\}_1^{(t+\Delta t)} = \left(\frac{\gamma}{\beta \Delta t}\right) \{\Delta \mathbf{U}\}_1^{(t+\Delta t)} + \left(1 - \frac{\gamma}{\beta}\right) \{\dot{\mathbf{U}}\}^{(t)} + \left(1 - \frac{\gamma}{2\beta}\right) \{\ddot{\mathbf{U}}\}^{(t)} \Delta t \\ \{\ddot{\mathbf{U}}\}_1^{(t+\Delta t)} = \left(\frac{1}{\beta \Delta t^2}\right) \left(\{\Delta \mathbf{U}\}_1^{(t+\Delta t)} - \{\dot{\mathbf{U}}\}^{(t)} \Delta t \right) - \left(\frac{1}{2\beta} - 1\right) \{\ddot{\mathbf{U}}\}^{(t)} \end{array} \right.$$

- B. Second and subsequent iterations (seeking the equilibrium for the time $t + \Delta t$)

Loop over global convergence iterations: n th iteration

- 1. Compute the members stresses and internal variables:

$$\{\mathbf{M}_b\}_{i+1} = \{\mathbf{M}(\mathbf{U}_i^{(t+\Delta t)})\}$$

- 2. Updates relevant matrices

$$[\mathbf{K}_T] = \sum_{b=1}^{nelements} [\mathbf{B}_b]^T \{\mathbf{M}_b(\mathbf{U}_i^{(t+\Delta t)})\}; [\mathbf{J}]_{i+1} = [\mathbf{m}] \frac{1}{\beta \Delta t^2} + [\mathbf{K}_T] + [\mathbf{C}] \frac{\gamma}{\beta \Delta t}$$

$$\{\mathbf{F}\}_{i+1} = \{\mathbf{F}_{ext}\}^{(t+\Delta t)} - \{\mathbf{F}_{int}(\mathbf{U}_i^{(t+\Delta t)}, \dot{\mathbf{U}}_i^{(t+\Delta t)})\}; \{\Delta \mathbf{F}\}_{i+1} = \{\mathbf{F}\}_{i+1} + [\mathbf{m}] \{\ddot{\mathbf{U}}\}_i^{(t+\Delta t)} - [\mathbf{C}] \{\dot{\mathbf{U}}\}_i^{(t+\Delta t)}$$

- 3. If the residual forces norm $\|\{\Delta \mathbf{F}\}_i^{(t+\Delta t)}\| \leq TOL$, end of iterations and back to A, and beginning of the computations in the next time step. If not, proceed calculating:

$$\{\delta \mathbf{U}\}_{i+1}^{(t+\Delta t)} = [\mathbf{J}]_i^{-1} : \{\Delta \mathbf{F}\}_{i+1} \left\{ \begin{array}{l} \{\mathbf{U}\}_{i+1}^{(t+\Delta t)} = \{\mathbf{U}\}_i^{(t+\Delta t)} + \{\delta \mathbf{U}\}_{i+1}^{(t+\Delta t)} \\ \{\dot{\mathbf{U}}\}_{i+1}^{(t+\Delta t)} = \left(\frac{\gamma}{\beta \Delta t}\right) \{\delta \mathbf{U}\}_{i+1}^{(t+\Delta t)} + \{\dot{\mathbf{U}}\}_i^{(t+\Delta t)} \\ \{\ddot{\mathbf{U}}\}_{i+1}^{(t+\Delta t)} = \left(\frac{1}{\beta \Delta t^2}\right) \{\delta \mathbf{U}\}_{i+1}^{(t+\Delta t)} + \{\ddot{\mathbf{U}}\}_i^{(t+\Delta t)} \end{array} \right.$$

- 4. Back to step 1

Chapter 4

Elastoplastic Constitutive Model for Frames

4.1 Introduction

In the previous chapters, we only mention the elastic relationship between forces and deformations, which are characterized by each load configuration, corresponding to one deformation configuration, in such a way that once the force is withdrawn or unloaded, the structure returns to its initial configuration, without residual deformations. In solid mechanics, this behaviour is called the “perfect plastic”. Traditionally, when subjected to service loads, structures must generally respond in an elastic manner. The standard design approach was to calculate the maximum stress according to the theory of elasticity, and make sure that it would

not exceed a certain allowable stress, which was set sufficiently smaller than the material strength or yield limit.

However, daily experience shows that only some structures fail at higher load at which the material strength or yield limit is exhausted at one point of the structure. Many structures redistribute stresses in such a way that the structure fails at higher load, beside the fact that there are some materials which can have residual deformations after important overloads. Increasing the yield limit is not a solution; once this limit is exceeded, the elastic models, linear or nonlinear, cannot correctly represent the structural behaviour.

Let us analyze the reason why the elasticity theory is unsatisfactory for analysis of structures. For the correct design of one structure by the elasticity theory, Massonnet and Save (1966) proposed two types of conditions must be satisfied:

- The equilibrium conditions
- The compatibility conditions, which impose on certain elements of the structure distributions of tensions characteristic of the elastic solid.

Although the first condition is imperative, the second condition can be transgressed when certain elements enter in plastic regime. This plastification can be observed in some laboratory tests, and there is no reason for not taking it into consideration during the analysis.

Thus, other models are necessary where the plastic behaviour is considered. One of first methods, based on the limit theorem, to obtain the plastic solution of structure is plastic analysis theory.

Although the plastic methods described in the Appendix 3 are still useful, they are not enough to represent all material properties and behaviour of one structure like hardening or softening. Furthermore, some structure could be almost impossible to solve, likewise multi-storey frames. Another inconvenience is that those methods do not allow us to determinate the residual or permanent deformations during the load-unload process.

For this reason, in this chapter we introduce the elastoplasticity concepts applied to frame structure. In the case of frame structure, the evolution of the plastic hinge will be given by yield functions for the beam-column, assuming that the plasticity is concentrated at the end of the cross section, leading to a sudden, and not gradual, plastification of the hinge. This concept is well known as the

Lumped Model. We also present some yield functions, which can be used for frame structures.

4.2 Yield Function for Plastic Hinge

In the Appendix 3, the plastic hinge is defined in terms of curvature. One of the first simplifications we can make in the moment-curvature diagram is to assume that the diagram is bilinear, two straight lines: one straight line with slope EI until the maximum moment, m_y , and the second straight line is horizontal and begins at moment equal to m_y . Therefore, when $m < m_y$ the behaviour of the beam section is elastic and equal to $m = m_y$, the beam section is completely plasticized, as shown in Figure 4.1.

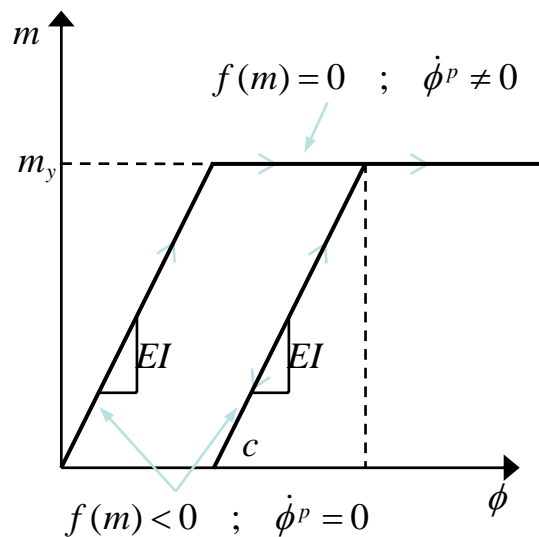


Figure 4.1 – Elastoplastic model for Frames.

We can observe that in the idealized moment-curvature diagram, the plastic deformation is concentrated into a single cross section. The difference between the actual and the idealized moment-curvature diagram is only significant for curvatures not much larger than the limiting elastic curvatures. For this reason the plasticized section can be replaced by a hinge, the plastic hinge, when, and only, the moment reaches m_y .

The behaviour of the plastic hinge cannot be described in terms of the moment and curvature, instead of this; it has to be described in terms of the moment and rotation. This behaviour can be expressed by a yield function, likewise the uniaxial stress models in the Appendix 2. For those situations where we suppose the perfect plasticity, Flórez-López (1999) proposed the yield function for plastic hinge as:

$$f(m) = |m| - m_y \quad (4.1)$$

where m_y is the plastic moment. The evolution of the plastic hinge, the plastic rotation ϕ^p , can be determined by the Kuhn-Tucker conditions, as

$$\begin{cases} d\phi^p = 0 & \Rightarrow & f(m) < 0 \quad \vee \quad df(m) < 0 \\ d\phi^p \neq 0 & \Rightarrow & f(m) = 0 \quad \wedge \quad df(m) = 0 \end{cases} \quad (4.2)$$

The Figure 4.2 represents the yield function of a plastic hinge for a simple supported beam. We can observe that, when the moment over the hinge is less than the plastic moment, the plastic rotations is null. In another words, the beam performance is elastic. When the plastic rotation is not null, $f(m) = 0$, the capacity of the beam to support the load P decreases, while the plastic rotation can increase infinitely. The increase of the load could be possible only in hyperstatic structures.

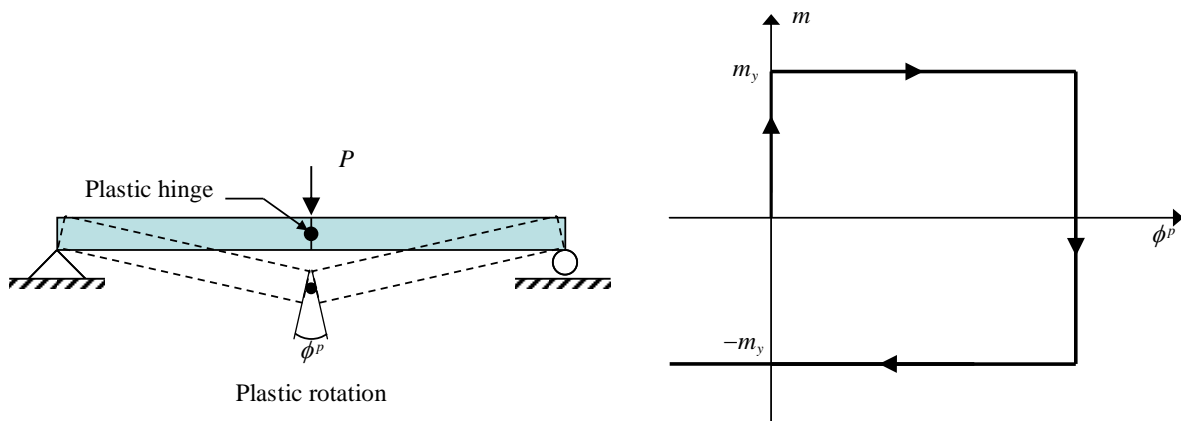


Figure 4.2 – Plastic hinge and moment-plastic rotation for perfect plasticity.

Similarly as to the uniaxial stress, the yield function can be defined in terms of the hardening, isotropic or kinematic. We can have functions that include the axial effect as well. In the next section, we describe some possible functions for frame structures.

4.3 Elastoplastic frames

In frame structures, particularly under lateral loads, the plasticization starts (or forms plastic hinges) at the ends of the member. The plasticity then gradually spreads along the length of the member, due to the plastification of successive cross sections. However, for many-rolled steel cross-sectional shapes, the spread of plasticity along the length of the member is not very significant, and the deforma-

tion is concentrated at or very near the end cross sections. For convenience in computation, we will assume that the inelastic behaviour is concentrated at the ends, the plastic hinges, instead of being spread along the length of the beam-column element. Further, the beam-column element is assumed to remain elastic between the plastic hinges. This assumption is well known as lumped plasticity approach.

The concept of zero-length plastic hinge is a mathematical abstraction, because it implies infinite curvatures. Nevertheless, the concept is computationally convenient, and is sufficiently accurate for many practical beam-column applications, where the plastic action is confined to small regions at the ends.

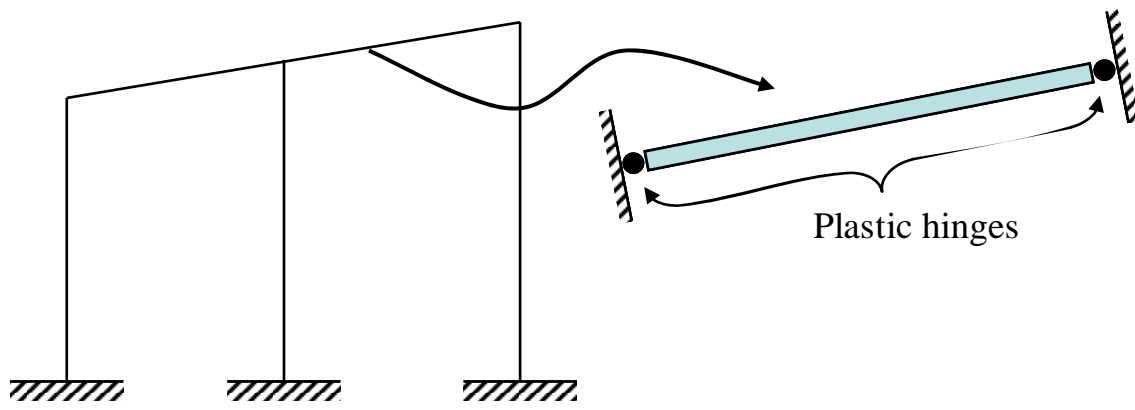


Figure 4.3 – Lumped plastic model for Frames.

Since we assume that the plasticity is “concentrated” at the end of the beam-element, we can admit that at each node we have one plastic rotation, ϕ_i^p at the node i , and ϕ_j^p at the node j , in such a way that these variable can be grouped into a new vector proposed by Flórez-López (1999): the generalized plastic deformations $\{\Phi^p\}$:

$$\{\Phi^p\}^T = \{\phi_i^p \quad \phi_j^p \quad 0\} \quad (4.3)$$

Therefore, the generalized deformations of a member $\{\Phi_b\}$ can be decomposed into elastic deformations of the beam-column $\{\Phi_b^e\}$, and the generalized plastic deformations $\{\Phi_b^p\}$ as:

$$\{\Phi\} = \{\Phi^e\} + \{\Phi^p\} \quad (4.4)$$

Once the beam-column behaviour is elastic by definition, the elastic deformations are related with the generalized stress vector, $\{\mathbf{M}\} = [\mathbf{S}]\{\Phi^e\} + \{\mathbf{M}^0\}$, in ac-

cordance with to the definitions made in Appendix 1. Adjusting in terms of the equation (4.4) we can obtain the elastoplastic equation for a beam-column:

$$\{\mathbf{M}_b\} = [\mathbf{S}_b] : (\{\Phi_b\} - \{\Phi_b^p\}) + \{\mathbf{M}_b^0\} \quad (4.5)$$

where $[\mathbf{S}_b]$ is the stiffness matrix for a beam-column, and $\{\mathbf{M}_b^0\}$ the distributed loads along the member.

4.3.1 Perfect Elastoplastic Frames

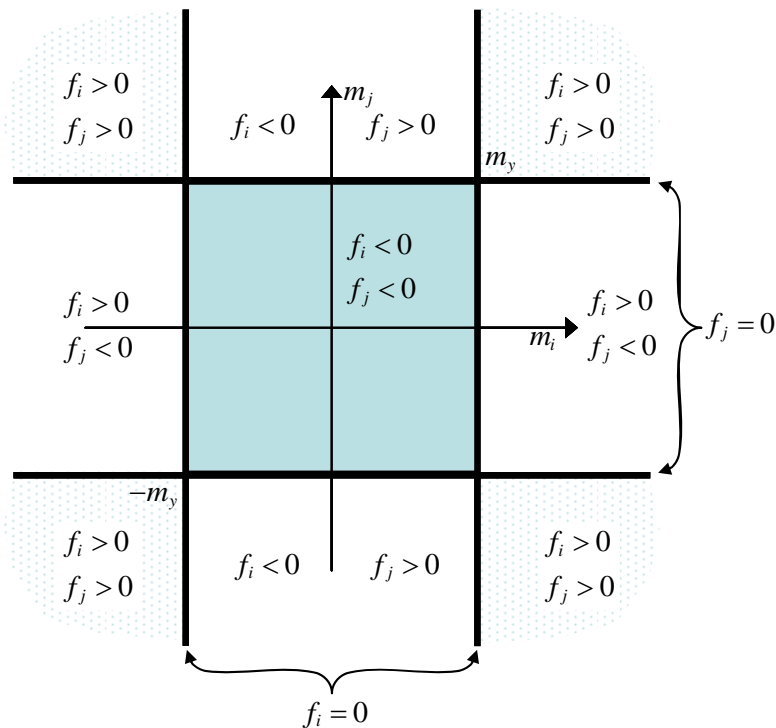


Figure 4.4 – Moment-moment diagram of the elastic domain and admissible states

Similarly to the yield function for plastic described in 4.2, the elements of the generalized plastic deformations vector $\{\Phi^p\}$ are ruled by a yield function, one for each plastic hinge, i.e., for perfect plastic hinge we have:

$$f_i(m_i) = |m_i| - m_y \quad f_j(m_j) = |m_j| - m_y \quad (4.6)$$

where $f_i = f_i(m_i)$ is the yield function of the plastic hinge i , and $f_j = f_j(m_j)$ is the yield function of the plastic hinge j .

The evolution of the plastic rotation can be expressed as:

$$\begin{cases} d\phi_i^p = 0 & \Rightarrow f_i < 0 \vee df_i < 0 \\ d\phi_i^p \neq 0 & \Rightarrow f_i = 0 \wedge df_i = 0 \end{cases} \quad (4.7)$$

$$\begin{cases} d\phi_j^p = 0 & \Rightarrow f_j < 0 \vee df_j < 0 \\ d\phi_j^p \neq 0 & \Rightarrow f_j = 0 \wedge df_j = 0 \end{cases}$$

And the plastic rotations can be expressed as a function of the plastic multipliers, λ_i^p and λ_j^p , as proposed by Cipolina *et al.* (1995):

$$d\phi_i^p = \Delta\lambda_i^p \frac{\partial f_i}{\partial m_i} \quad ; \quad d\phi_j^p = \Delta\lambda_j^p \frac{\partial f_j}{\partial m_j} \quad (4.8)$$

The plastic multipliers are a scalar factor that controls the magnitude of the plastic rotations. The equation (4.8) is similar to the flow rule defined in Appendix 2 for the uniaxial stress. Using the Kuhn-Tucker conditions for both plastic hinges, we have:

$$\begin{aligned} \Delta\lambda_i^p &\geq 0 \quad ; \quad f_i \leq 0 \quad ; \quad d\lambda_i^p f_i = 0 \\ \Delta\lambda_j^p &\geq 0 \quad ; \quad f_j \leq 0 \quad ; \quad d\lambda_j^p f_j = 0 \end{aligned} \quad (4.9)$$

and the consistency condition is given as

$$\Delta\lambda_i^p df_i = 0 \quad ; \quad \Delta\lambda_j^p df_j = 0 \quad (4.10)$$

It is important to point out that the evolutions of the plastic rotations are independent between them, despite the fact that the yield functions are the same for both the plastic hinges. However, in the beam-column element, the moment equilibrium has to be maintained. This results in the requirement of interactive methods, i.e. Newton-Raphson, to enable the final solution to be found during the integration of constitutive equations (4.7).

4.3.1.1 Return Mapping

During the solution of the constitutive equation, we could have at least one of bending moments outside the yield, $f_i(m_i) > 0$ or $f_j(m_j) > 0$, any region outside the elastic domain, represented by the blue area shown in Figure 4.4 . Therefore, we are obliged to use the return-mapping algorithm, describe in Appendix 2, to

bring to the yield surface the bending moment, or the bending moments, which are out of the surface. Therefore, similar to the procedure described in Appendix 1, we can define the generalized "trial" stress vector $\{\mathbf{M}_b\}_{trial}^T = \{m_i^{trial} \quad m_j^{trial} \quad n^{trial}\}$ for a b element as

$$\{\mathbf{M}_b\}_{trial}^{n+1} = [\mathbf{S}_b] : \left(\{\Phi_b\}^{n+1} - \{\Phi_b^p\}^n \right) \quad (4.11)$$

here $\{\Phi_b\}^{n+1} = \{\Phi_b\}^n + \{\Delta\Phi_b\}^{n+1}$ is the generalized deformations at the step $n+1$, and $\{\Phi_b^p\}^n$ is generalized plastic deformations obtained in the previous step. For the case of perfect plasticity, (4.6), the bending moments are obtained by the solution of

$$\begin{aligned} m_i^{n+1} &= m_i^{trial} - \Delta\lambda_i^p [\mathbf{S}_b] : \frac{\partial f_i^{trial}}{\partial m_i^{trial}} \\ m_j^{n+1} &= m_j^{trial} - \Delta\lambda_j^p [\mathbf{S}_b] : \frac{\partial f_j^{trial}}{\partial m_j^{trial}} \end{aligned} \quad (4.12)$$

$$\begin{aligned} (\phi_i^p)^{n+1} &= (\phi_i^p)^n + \Delta\lambda_i^p \frac{\partial f_i^{trial}}{\partial m_i^{trial}} \\ (\phi_j^p)^{n+1} &= (\phi_j^p)^n + \Delta\lambda_j^p \frac{\partial f_j^{trial}}{\partial m_j^{trial}} \end{aligned} \quad (4.13)$$

$$\begin{aligned} f_i^{trial} &= |m_i^{trial}| - m_y \\ f_j^{trial} &= |m_j^{trial}| - m_y \end{aligned} \quad (4.14)$$

The plastic multipliers can be obtained by the expression:

$$\Delta\lambda_i^p = \frac{f_i^{trial}}{\frac{\partial f_i^{trial}}{\partial m_i^{trial}} : [\mathbf{S}_b] : \frac{\partial f_i^{trial}}{\partial m_i^{trial}}} \quad ; \quad \Delta\lambda_j^p = \frac{f_j^{trial}}{\frac{\partial f_j^{trial}}{\partial m_j^{trial}} : [\mathbf{S}_b] : \frac{\partial f_j^{trial}}{\partial m_j^{trial}}} \quad (4.15)$$

As commented before, the plastic multipliers are independents among them. This affirmation can hold if only one of the two bending moment are out of the yield surface, $f_i^{trial} > 0$ or $f_j^{trial} > 0$. When both bending moments are out of the yield surface, $f_i^{trial} > 0$ and $f_j^{trial} > 0$, it will be necessary to solve the plastic multiplier at the same time, to bring back both bending moments to the yield surface.

Consequently, the plastic multipliers will be obtained through the solution of a linear problem:

$$\begin{bmatrix} \frac{\partial f_i^{trial}}{\partial m_i^{trial}} : [\mathbf{S}_b] : \frac{\partial f_i^{trial}}{\partial m_i^{trial}} & 0 \\ 0 & \frac{\partial f_j^{trial}}{\partial m_j^{trial}} : [\mathbf{S}_b] : \frac{\partial f_j^{trial}}{\partial m_j^{trial}} \end{bmatrix} \begin{Bmatrix} \Delta \lambda_i^p \\ \Delta \lambda_j^p \end{Bmatrix} = \begin{Bmatrix} f_i^{trial} \\ f_j^{trial} \end{Bmatrix} \quad (4.16)$$

The equation (4.16) guarantees the independence of the plastic multipliers, and this will be obtained at the same instant in the step $n+1$.

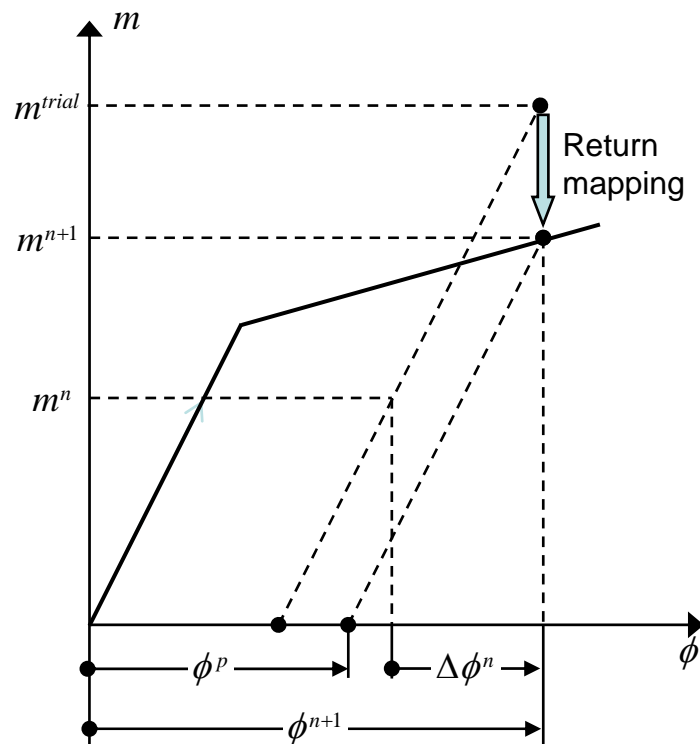


Figure 4.5 – The final moment obtained through the Return-Mapping procedure

The expressions defined above can be solved through the Newton-Raphson procedure as shown in Table 4.1

Table 4.1 – Return-Mapping Algorithm for Perfect Elastoplastic Frames.

-
- For each b elements at n th+1 iteration at the time t :
- 1) Generalized deformations at the step: $\{\Phi_b\}_t^{(n+1)} = \{\Phi_b\}_t^{(n)} + \{\Delta\Phi_b\}_t^{(n+1)}$
 - 2) Determination of generalized effective 'trial' ${}^k\{\mathbf{M}_b\}_{trial}^{(n+1)T} = \{ {}^k m_i^{trial} \quad {}^k m_j^{trial} \quad n^{trial} \}$ stress and update of internal variables ${}^k\{\Delta\Phi_b^p\}^T = \{ {}^k \phi_i^p \quad {}^k \phi_j^p \quad 0 \}$ at $k = 1$:
 - a) ${}^k\{\mathbf{M}_b\}_{trial}^{(n+1)} = [\mathbf{S}_b] : \left(\{\Phi_b\}_t^{(n+1)} - {}^k\{\Delta\Phi_b^p\} \right) ; \quad {}^k\{\Delta\Phi_b^p\} = \{\Phi_b^p\}_t^{(n)}$
 - 3) Plastic evolution:
 - a) $f_i^{trial} = |{}^k m_i^{trial}| - m_y ; \quad f_j^{trial} = |{}^k m_j^{trial}| - m_y$
 - b) ${}^k f_i^{trial} \leq TOL$ and ${}^k f_j^{trial} \leq TOL$, no plasticity evolution or unload, go to 6)
 - c) ${}^k f_i^{trial} > TOL$ or ${}^k f_j^{trial} > TOL$, plasticity step: proceed to step 4)
 - 4) Determination of plastic multiplier:
 - a) ${}^k f_i^{trial} > 0 \quad \begin{cases} {}^{k+1}\Delta\lambda_i^p = \frac{{}^k f_i^{trial}}{\frac{\partial {}^k f_i^{trial}}{\partial {}^k m_i^{trial}} : [\mathbf{S}_b] : \frac{\partial {}^k f_i^{trial}}{\partial {}^k m_i^{trial}}} \\ {}^{k+1}\Delta\lambda_j^p = 0 \end{cases} ; \quad {}^k f_i^{trial} \leq 0 \quad \begin{cases} {}^{k+1}\Delta\lambda_i^p = 0 \\ {}^{k+1}\Delta\lambda_j^p = \frac{{}^k f_j^{trial}}{\frac{\partial {}^k f_j^{trial}}{\partial {}^k m_j^{trial}} : [\mathbf{S}_b] : \frac{\partial {}^k f_j^{trial}}{\partial {}^k m_j^{trial}}} \end{cases}$
 - or
 - b) ${}^k f_i^{trial} > 0 \quad \begin{bmatrix} \frac{\partial {}^k f_i^{trial}}{\partial {}^k m_i^{trial}} : [\mathbf{S}_b] : \frac{\partial {}^k f_i^{trial}}{\partial {}^k m_i^{trial}} & 0 \\ 0 & \frac{\partial {}^k f_j^{trial}}{\partial {}^k m_j^{trial}} : [\mathbf{S}_b] : \frac{\partial {}^k f_j^{trial}}{\partial {}^k m_j^{trial}} \end{bmatrix} : \begin{Bmatrix} {}^{k+1}\Delta\lambda_i^p \\ {}^{k+1}\Delta\lambda_j^p \end{Bmatrix} = \begin{Bmatrix} {}^k f_i^{trial} \\ {}^k f_j^{trial} \end{Bmatrix}$
 - 5) Update of plastic variables and of the generalized effective 'trial' stress:
 - a) ${}^{k+1}\phi_i^p = {}^k\phi_i^p + {}^{k+1}\Delta\lambda_i^p \frac{\partial {}^k f_i^{trial}}{\partial {}^k m_i^{trial}} ; \quad {}^{k+1}\phi_j^p = {}^k\phi_j^p + {}^{k+1}\Delta\lambda_j^p \frac{\partial {}^k f_j^{trial}}{\partial {}^k m_j^{trial}}$
 - b) ${}^{k+1}m_i^{trial} = {}^k m_i^{trial} + {}^{k+1}\Delta\lambda_i^p [\mathbf{S}_b] : \frac{\partial {}^k f_i^{trial}}{\partial {}^k m_i^{trial}} ; \quad {}^{k+1}m_j^{trial} = {}^k m_j^{trial} + {}^{k+1}\Delta\lambda_j^p [\mathbf{S}_b] : \frac{\partial {}^k f_j^{trial}}{\partial {}^k m_j^{trial}}$
 - c) Update $k = k + 1$ and back to 3)
 - 6) End of the process of plastic correction
 - a) $\{\mathbf{M}_b\}_t^{(n+1)} = {}^k\{\mathbf{M}_b\}_{trial}^{(n+1)} ; \quad \{\Phi_b\}_t^{(n+1)} = {}^k\{\Delta\Phi_b^p\}$
 - 7) End of integration process of the constitutive equation.
-

The term TOL is a variable so that its value depends on the precision required in the analysis. Usually this variable can be defined with values between 1×10^{-6} and 1×10^{-15} .

4.3.2 Elastoplastic Frames with Kinematic Hardening

As for the uniaxial stress, we can define one yield function which includes the kinematic hardening effect.

So, the yield function with kinematic hardening can be expressed as

$$f(\phi_i) = |\phi_i| - m_y ; \quad f(\phi_j) = |\phi_j| - m_y \quad (4.17)$$

$$\varphi_i = m_i - q_i \quad ; \quad \varphi_j = m_j - q_j \quad (4.18)$$

where q_i and q_j are called the back stresses, and can be defined as

$$dq_i = H d\phi_i^p \quad ; \quad dq_j = H d\phi_j^p \quad (4.19)$$

where H , kinematic hardening modulus, and is a propriety of the material of which the beam-column is made. The plastic rotations are defined as:

$$d\phi_i^p = \Delta\lambda_i^p \frac{\partial f_i}{\partial \varphi_i} \quad ; \quad d\phi_j^p = \Delta\lambda_j^p \frac{\partial f_j}{\partial \varphi_j} \quad (4.20)$$

we can observe that the only difference (4.20) with respect to (4.8) is that the differential is now in terms of the variable φ , defined in (4.18). The plastic multipliers can now be defined as:

$$\Delta\lambda_i^p = \frac{f_i}{\frac{\partial f_i}{\partial \varphi_i} : [\mathbf{S}_b] : \frac{\partial f_i}{\partial \varphi_i} + \frac{\partial f_i}{\partial \varphi_i} H \frac{\partial f_i}{\partial \varphi_i}} \geq 0 \quad ; \quad \Delta\lambda_j^p = \frac{f_j}{\frac{\partial f_j}{\partial \varphi_j} : [\mathbf{S}_b] : \frac{\partial f_j}{\partial \varphi_j} + \frac{\partial f_j}{\partial \varphi_j} H \frac{\partial f_j}{\partial \varphi_j}} \geq 0 \quad (4.21)$$

once, in this specific case, $\frac{\partial f}{\partial \varphi} = \text{sign}(\varphi)$, the term $\frac{\partial f}{\partial \varphi} H \frac{\partial f}{\partial \varphi}$ can be reduced to $\text{sign}(\varphi) H \text{sign}(\varphi) = H$.

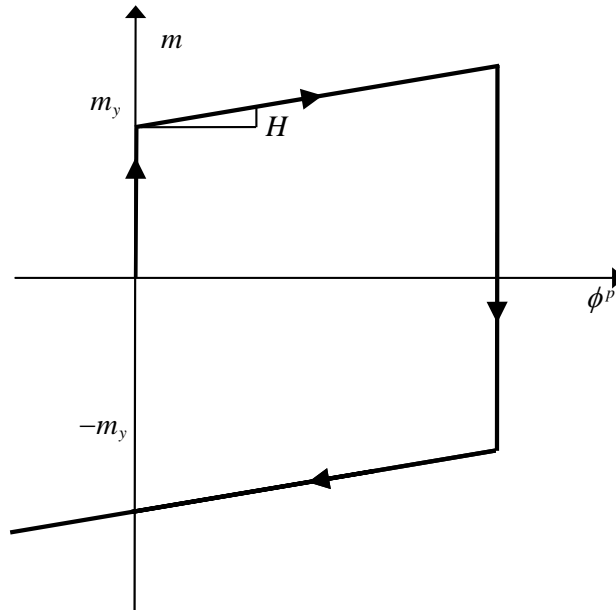


Figure 4.6 – Plastic hinge with kinematic hardening.

Table 4.2 shows the procedure to solve the return-mapping problem for elastoplastic frames with kinematic hardening. The only difference with respect to the procedure described in Table 4.2 is the inclusion of the back stress vector $\{\mathbf{q}_b\}^T = \{q_i \quad q_j \quad 0\}$ due to the kinematic hardening.

Table 4.2 – Return-Mapping algorithm for Elastoplastic Frames with Kinematic Hardening.

-
- For each b elements at n th+1 iteration at the time t :
- 1) Generalized deformations at the step: $\{\Phi_b\}_t^{(n+1)} = \{\Phi_b\}_t^{(n)} + \{\Delta\Phi_b\}_t^{(n+1)}$
 - 2) Determination of generalized effective ‘trial’ ${}^k\{\mathbf{M}_b\}_{trial}^{(n+1)T} = \left\{ {}^k m_i^{trial} \quad {}^k m_j^{trial} \quad n^{trial} \right\}$ stress and update of internal variables ${}^k\{\Delta\Phi_b^p\}^T = \left\{ {}^k \phi_i^p \quad {}^k \phi_j^p \quad 0 \right\}$, and ${}^k\{\Delta\mathbf{q}\}^T = \left\{ {}^k q_i \quad {}^k q_j \quad 0 \right\}$ at $k = 1$:
 - a) ${}^k\{\mathbf{M}_b\}_{trial}^{(n+1)} = [\mathbf{S}_b] : \left(\{\Phi_b\}_t^{(n+1)} - {}^k\{\Delta\Phi_b^p\} \right)$; ${}^k\{\Delta\Phi_b^p\} = \{\Phi_b^p\}_t^{(n)}$; ${}^k\{\Delta\mathbf{q}_b\} = \{\mathbf{q}_b\}_t^{(n)}$
 - 3) Plastic evolution:
 - a) ${}^k \phi_i^{trial} = {}^k m_i^{trial} - {}^k q_i$; ${}^k \phi_j^{trial} = {}^k m_j^{trial} - {}^k q_j$
 - b) $f_i^{trial} = \left| {}^k \phi_i^{trial} \right| - m_y$; $f_j^{trial} = \left| {}^k \phi_j^{trial} \right| - m_y$
 - c) ${}^k f_i^{trial} \leq TOL$ and ${}^k f_j^{trial} \leq TOL$, no plasticity evolution or unload, go to 6)
 - d) ${}^k f_i^{trial} > TOL$ or ${}^k f_j^{trial} > TOL$, plasticity step: proceed to step 4)
 - 4) Determination of plastic multiplier:
 - a) ${}^k f_i^{trial} > 0$ $\left\{ \begin{array}{l} {}^{k+1}\Delta\lambda_i^p = \frac{{}^k f_i^{trial}}{\frac{\partial {}^k f_i^{trial}}{\partial {}^k \phi_i^{trial}} : [\mathbf{S}_b] : \frac{\partial {}^k f_i^{trial}}{\partial {}^k \phi_i^{trial}} + H} \end{array} \right.$; ${}^k f_i^{trial} \leq 0$ $\left\{ \begin{array}{l} {}^{k+1}\Delta\lambda_i^p = 0 \\ {}^{k+1}\Delta\lambda_j^p = \frac{{}^k f_j^{trial}}{\frac{\partial {}^k f_j^{trial}}{\partial {}^k \phi_j^{trial}} : [\mathbf{S}_b] : \frac{\partial {}^k f_j^{trial}}{\partial {}^k \phi_j^{trial}} + H} \end{array} \right.$
 - or
 - b) ${}^k f_i^{trial} > 0$ $\left[\begin{array}{cc} \frac{\partial {}^k f_i^{trial}}{\partial {}^k \phi_i^{trial}} : [\mathbf{S}_b] : \frac{\partial {}^k f_i^{trial}}{\partial {}^k \phi_i^{trial}} + H & 0 \\ 0 & \frac{\partial {}^k f_j^{trial}}{\partial {}^k \phi_j^{trial}} : [\mathbf{S}_b] : \frac{\partial {}^k f_j^{trial}}{\partial {}^k \phi_j^{trial}} + H \end{array} \right] : \left\{ \begin{array}{l} {}^{k+1}\Delta\lambda_i^p \\ {}^{k+1}\Delta\lambda_j^p \end{array} \right\} = \left\{ \begin{array}{l} {}^k f_i^{trial} \\ {}^k f_j^{trial} \end{array} \right\}$
 - 5) Update of plastic variables and of the generalized effective ‘trial’ stress:
 - a) ${}^{k+1}\phi_i^p = {}^k \phi_i^p + {}^{k+1}\Delta\lambda_i^p \frac{\partial {}^k f_i^{trial}}{\partial {}^k \phi_i^{trial}}$; ${}^{k+1}\phi_j^p = {}^k \phi_j^p + {}^{k+1}\Delta\lambda_j^p \frac{\partial {}^k f_j^{trial}}{\partial {}^k \phi_j^{trial}}$
 - b) ${}^{k+1}q_i = {}^k q_i + {}^{k+1}\Delta\lambda_i^p H \frac{\partial {}^k f_i^{trial}}{\partial {}^k \phi_i^{trial}}$; ${}^{k+1}q_j = {}^k q_j + {}^{k+1}\Delta\lambda_j^p H \frac{\partial {}^k f_j^{trial}}{\partial {}^k \phi_j^{trial}}$
 - c) ${}^{k+1}m_i^{trial} = {}^k m_i^{trial} + {}^{k+1}\Delta\lambda_i^p [\mathbf{S}_b] : \frac{\partial {}^k f_i^{trial}}{\partial {}^k m_i^{trial}}$; ${}^{k+1}m_j^{trial} = {}^k m_j^{trial} + {}^{k+1}\Delta\lambda_j^p [\mathbf{S}_b] : \frac{\partial {}^k f_j^{trial}}{\partial {}^k m_j^{trial}}$
 - d) Update $k = k + 1$ and back to 3)
 - 6) End of the process of plastic correction
 - a) $\{\mathbf{M}_b\}_t^{(n+1)} = {}^k\{\mathbf{M}_b\}_{trial}^{(n+1)}$; $\{\Phi_b^p\}_t^{(n+1)} = {}^k\{\Delta\Phi_b^p\}$; $\{\mathbf{q}_b\}_t^{(n+1)} = {}^k\{\Delta\mathbf{q}_b\}$
 - 7) End of integration process of the constitutive equation.
-

4.3.3 Elastoplastic Frames with axial force

So far, we have assumed that a plastic hinge forms if the bending moments in a critical cross section reach the plastic limit value, m_y . In the models presented above, we have neglected the effect of the other internal forces on the formation of

the yield hinge. This effect, however, can be appreciable, for example in multi-story frames or frames with a large horizontal thrust where the axial force are large. Therefore, we have to assume that the stress can be caused due to the axial force n in the member as well as the bending moment m in the member.

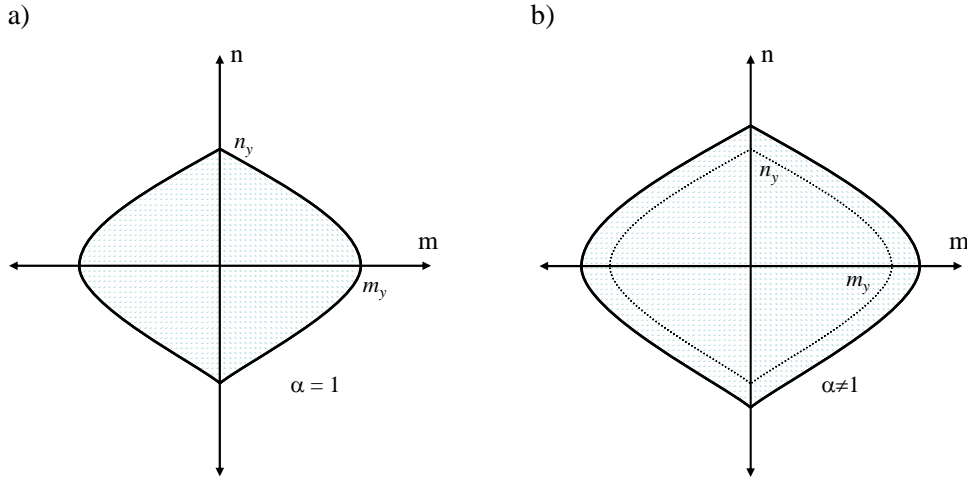


Figure 4.7 – Yield Surface in $m-n$ space: a) without hardening effect; b) with hardening.

Thus, we will now redefine our yield function, at any end, as a function of the axial and of the bending moment at the end cross section. Various such yield functions can be proposed and used. We can define at the end of the beam-column element the yield function as proposed by Argyris *et al.* (1982) and Jirásek and Bazant (2002):

$$f_j(m_i, n) = \left| \frac{m_i}{m_y} \right| + \left(\frac{n}{n_y} \right)^2 \leq 1 \quad ; \quad f_j(m_j, n) = \left| \frac{m_j}{m_y} \right| + \left(\frac{n}{n_y} \right)^2 \leq 1 \quad (4.22)$$

where m_y , and n_y are the yield moment and force respectively, Figure 4.7.a plot the yield function. The plastic evolution laws are defined as:

$$d\phi_i^p = \Delta\lambda_i^p \frac{\partial f_i}{\partial m_i} \quad ; \quad d\phi_j^p = \Delta\lambda_j^p \frac{\partial f_j}{\partial m_j} \quad ; \quad d\delta^p = \Delta\lambda_i^p \frac{\partial f_i}{\partial n} + \Delta\lambda_j^p \frac{\partial f_j}{\partial n} \quad (4.23)$$

the only difference of (4.23) with respect to the usual definition of plastic evolution (equation (4.8)) is the inclusion of the plastic elongation δ^p , which depends on the plastic multipliers λ_i^p and λ_j^p . The plastic multipliers are still ruled by the Kuhn-Tucker condition

$$\begin{aligned} \Delta\lambda_i^p \geq 0 \quad ; \quad f_i \leq 0 \quad ; \quad d\lambda_i^p f_i = 0 \\ \Delta\lambda_j^p \geq 0 \quad ; \quad f_j \leq 0 \quad ; \quad d\lambda_j^p f_j = 0 \end{aligned} \quad (4.24)$$

Other, more complicated yield surfaces can be formulated to accommodate complete plastification of the cross section, residual stress effects, or different material behaviour.

The yield function (4.22) can be redefined take into account the hardening effect, as

$$f_j(m_i, n) = \left| \frac{m_i}{m_y} \right| + \left(\frac{n}{n_y} \right)^2 - \alpha \leq 0 \quad ; \quad f_j(m_j, n) = \left| \frac{m_j}{m_y} \right| + \left(\frac{n}{n_y} \right)^2 - \alpha \leq 0 \quad (4.25)$$

where α can be defined as hardening function of the material. Figure 4.7.b shows a likely yield surface.

Other yield functions can be formulated to accommodate the complete plastification of the cross section, residual stress effects, or different material behaviour, as proposed in Deierlein *et al.* (2001)

4.3.3.1 Return-mapping

Likewise for elastoplastic frames, during the solution of the constitutive equation, we could have at least one bending moment outside the yield, $f_i(m_i) > 0$ or $f_j(m_j) > 0$. Once more, it is necessary to use the return-mapping algorithm to obtain the solution of the constitutive equations.

Let us assume the existence of the generalized "trial" stress vector $\{\mathbf{M}_b\}_{trial}^T = \{m_i^{trial} \quad m_j^{trial} \quad n^{trial}\}$ for a b element in such a way that the bending moments and axial force are obtained as:

$$\begin{aligned} m_i^{n+1} &= m_i^{trial} - [\mathbf{S}_b] : d\phi_i^p \\ m_j^{n+1} &= m_j^{trial} - [\mathbf{S}_b] : d\phi_j^p \\ n^{n+1} &= n^{trial} - [\mathbf{S}_b] : d\delta^p \end{aligned} \quad (4.26)$$

and the evolution of the plastic variables is defined as

$$d\phi_i^p = \Delta\lambda_i^p \frac{\partial f_i}{\partial m_i} \quad ; \quad d\phi_j^p = \Delta\lambda_j^p \frac{\partial f_j}{\partial m_j} \quad ; \quad d\delta^p = \Delta\lambda_i^p \frac{\partial f_i}{\partial n} + \Delta\lambda_j^p \frac{\partial f_j}{\partial n} \quad (4.27)$$

Replacing the plastic rotation evolution, defined in(4.27), into (4.26), we obtain

$$\begin{aligned} m_i^{n+1} &= m_i^{trial} - \Delta\lambda_i^p [\mathbf{S}_b] : \frac{\partial f_i^{n+1}}{\partial m_i^{n+1}} \\ m_j^{n+1} &= m_j^{trial} - \Delta\lambda_j^p [\mathbf{S}_b] : \frac{\partial f_j^{n+1}}{\partial m_j^{n+1}} \\ n^{n+1} &= n^{trial} - [\mathbf{S}_b] : d\delta^p \end{aligned} \quad (4.28)$$

Multiplying the bending moment by each derivation, the equation (4.28) becomes

$$\begin{aligned} m_i^{n+1} \frac{\partial f_i^{n+1}}{\partial m_i^{n+1}} &= m_i^{trial} \frac{\partial f_i^{trial}}{\partial m_i^{trial}} - \Delta\lambda_i^p \frac{\partial f_i^{trial}}{\partial m_i^{trial}} : [\mathbf{S}_b] : \frac{\partial f_i^{n+1}}{\partial m_j^{n+1}} \\ m_j^{n+1} \frac{\partial f_j^{n+1}}{\partial m_j^{n+1}} &= m_j^{trial} \frac{\partial f_j^{trial}}{\partial m_j^{trial}} - \Delta\lambda_j^p \frac{\partial f_j^{trial}}{\partial m_j^{trial}} : [\mathbf{S}_b] : \frac{\partial f_j^{n+1}}{\partial m_j^{n+1}} \end{aligned} \quad (4.29)$$

once $m \frac{\partial f}{\partial m} = |m / m_y|$, the equation (4.29) can be rewritten as

$$\begin{aligned} \left| \frac{m_i^{n+1}}{m_y} \right| &= \left| \frac{m_i^{trial}}{m_y} \right| - \Delta\lambda_i^p \frac{\partial f_i^{trial}}{\partial m_i^{trial}} : [\mathbf{S}_b] : \frac{\partial f_i^{n+1}}{\partial m_i^{n+1}} \\ \left| \frac{m_j^{n+1}}{m_y} \right| &= \left| \frac{m_j^{trial}}{m_y} \right| - \Delta\lambda_j^p \frac{\partial f_j^{trial}}{\partial m_j^{trial}} : [\mathbf{S}_b] : \frac{\partial f_j^{n+1}}{\partial m_j^{n+1}} \end{aligned} \quad (4.30)$$

The axial force may be defined in terms of the derivation of the yield function at the i node as well as that due to the yield function at the j node, so:

$$n^{n+1} = n^{trial} - [\mathbf{S}_b] : d\delta^p \quad \left\{ \begin{aligned} n^{n+1} \frac{\partial f_i^{n+1}}{\partial n^{n+1}} &= n^{trial} \frac{\partial f_i^{trial}}{\partial n^{trial}} - \frac{\partial f_i^{trial}}{\partial n^{trial}} : [\mathbf{S}_b] : d\delta^p \\ n^{n+1} \frac{\partial f_j^{n+1}}{\partial n^{n+1}} &= n^{trial} \frac{\partial f_j^{trial}}{\partial n^{trial}} - \frac{\partial f_j^{trial}}{\partial n^{trial}} : [\mathbf{S}_b] : d\delta^p \end{aligned} \right. \quad (4.31)$$

once $n \frac{\partial f}{\partial n} = 2(n / n_y)^2$, (4.31) becomes:

$$\begin{aligned}
2\left(\frac{n^{n+1}}{n_y}\right)_i^2 &= 2\left(\frac{n^{trial}}{n_y}\right)^2 - \frac{\partial f_i^{trial}}{\partial n^{trial}} : [\mathbf{S}_b] : d\delta^p \\
2\left(\frac{n^{n+1}}{n_y}\right)_j^2 &= 2\left(\frac{n^{trial}}{n_y}\right)^2 - \frac{\partial f_j^{trial}}{\partial n^{trial}} : [\mathbf{S}_b] : d\delta^p
\end{aligned} \tag{4.32}$$

Replacing (4.30) and (4.32) into the yield function defined in (4.22), we obtain:

$$\begin{aligned}
\underbrace{\left|\frac{m_i^{n+1}}{m_y}\right| + \left(\frac{n^{n+1}}{n_y}\right)_i^2}_{f_i^{n+1}} &= \underbrace{\left|\frac{m_i^{trial}}{m_y}\right| + \left(\frac{n^{trial}}{n_y}\right)^2}_{f_i^{trial}} - \Delta\lambda_i^p \frac{\partial f_i^{trial}}{\partial m_i^{trial}} : [\mathbf{S}_b] : \frac{\partial f_i^{n+1}}{\partial m_i^{n+1}} - \frac{1}{2} \frac{\partial f_i^{trial}}{\partial n^{trial}} : [\mathbf{S}_b] : d\delta^p \\
\underbrace{\left|\frac{m_j^{n+1}}{m_y}\right| + \left(\frac{n^{n+1}}{n_y}\right)_j^2}_{f_j^{n+1}} &= \underbrace{\left|\frac{m_j^{trial}}{m_y}\right| + \left(\frac{n^{trial}}{n_y}\right)^2}_{f_j^{trial}} - \Delta\lambda_j^p \frac{\partial f_j^{trial}}{\partial m_j^{trial}} : [\mathbf{S}_b] : \frac{\partial f_j^{n+1}}{\partial m_j^{n+1}} - \frac{1}{2} \frac{\partial f_j^{trial}}{\partial n^{trial}} : [\mathbf{S}_b] : d\delta^p
\end{aligned} \tag{4.33}$$

simplifying,

$$\begin{aligned}
f_i^{n+1} &= f_i^{trial} - \Delta\lambda_i^p \frac{\partial f_i^{trial}}{\partial m_i^{trial}} : [\mathbf{S}_b] : \frac{\partial f_i^{n+1}}{\partial m_i^{n+1}} - \frac{1}{2} \frac{\partial f_i^{trial}}{\partial n^{trial}} : [\mathbf{S}_b] : d\delta^p \\
f_j^{n+1} &= f_j^{trial} - \Delta\lambda_j^p \frac{\partial f_j^{trial}}{\partial m_j^{trial}} : [\mathbf{S}_b] : \frac{\partial f_j^{n+1}}{\partial m_j^{n+1}} - \frac{1}{2} \frac{\partial f_j^{trial}}{\partial n^{trial}} : [\mathbf{S}_b] : d\delta^p
\end{aligned} \tag{4.34}$$

Once the axial plastic multiplier $d\delta^p$ has been obtained by the expression (4.27), and assuming that $\frac{\partial f^{trial}}{\partial m^{trial}} = \frac{\partial f^{n+1}}{\partial m^{n+1}}$, when $f_i^{n+1} = 1$ and $f_j^{n+1} = 1$, the equation (4.34) can be simplified as:

$$\begin{aligned}
\Delta\lambda_i^p \left(\frac{\partial f_i^{trial}}{\partial m_i^{trial}} : [\mathbf{S}_b] : \frac{\partial f_i^{trial}}{\partial m_i^{trial}} + \frac{1}{2} \frac{\partial f_i^{trial}}{\partial n^{trial}} : [\mathbf{S}_b] : \frac{\partial f_i^{trial}}{\partial n^{trial}} \right) + \Delta\lambda_j^p \frac{1}{2} \frac{\partial f_i^{trial}}{\partial n^{trial}} : [\mathbf{S}_b] : \frac{\partial f_j^{trial}}{\partial n^{trial}} &= f_i^{trial} - 1 \\
\Delta\lambda_i^p \frac{1}{2} \frac{\partial f_j^{trial}}{\partial n^{trial}} : [\mathbf{S}_b] : \frac{\partial f_i^{trial}}{\partial n^{trial}} + \Delta\lambda_j^p \left(\frac{\partial f_j^{trial}}{\partial m_j^{trial}} : [\mathbf{S}_b] : \frac{\partial f_j^{n+1}}{\partial m_j^{n+1}} + \frac{1}{2} \frac{\partial f_j^{trial}}{\partial n^{trial}} : [\mathbf{S}_b] : \frac{\partial f_j^{trial}}{\partial n^{trial}} \right) &= f_j^{trial} - 1
\end{aligned} \tag{4.35}$$

since the plastic multipliers are defined positive, $\Delta\lambda_i^p \geq 0$ and $\Delta\lambda_j^p \geq 0$, the equation (4.35) can be expressed as a linear problem as:

$$[\mathbf{A}]:\{\Delta\lambda\} = \{\mathbf{f}^{trial}\} \quad (4.36)$$

where $\{\Delta\lambda^p\}^T = \{\Delta\lambda_i^p \quad \Delta\lambda_j^p\}$, $\{\mathbf{f}^{trial}\}^T = \{f_i^{trial} - 1 \quad f_j^{trial} - 1\}$ and

$$[\mathbf{A}] = \begin{bmatrix} \frac{\partial f_i^{trial}}{\partial m_i^{trial}} : [\mathbf{S}_b] : \frac{\partial f_i^{trial}}{\partial m_i^{trial}} + \frac{1}{2} \frac{\partial f_i^{trial}}{\partial n^{trial}} : [\mathbf{S}_b] : \frac{\partial f_i^{trial}}{\partial n^{trial}} & \frac{1}{2} \frac{\partial f_i^{trial}}{\partial n^{trial}} : [\mathbf{S}_b] : \frac{\partial f_j^{trial}}{\partial n^{trial}} \\ \frac{1}{2} \frac{\partial f_j^{trial}}{\partial n^{trial}} : [\mathbf{S}_b] : \frac{\partial f_i^{trial}}{\partial n^{trial}} & \frac{\partial f_j^{trial}}{\partial m_j^{trial}} : [\mathbf{S}_b] : \frac{\partial f_j^{trial}}{\partial m_j^{trial}} + \frac{1}{2} \frac{\partial f_j^{trial}}{\partial n^{trial}} : [\mathbf{S}_b] : \frac{\partial f_j^{trial}}{\partial n^{trial}} \end{bmatrix} \quad (4.37)$$

It is important to notice the influence of the axial force at both hinges, once the axial force is constant along the beam-column element, which results in the dependence between the plastic multipliers, Figure 4.8.b. This dependence occurs only when both hinges are yielding, $\Delta\lambda_i^p \geq 0$ and $\Delta\lambda_j^p \geq 0$, otherwise, they will remain independent between them, as show in Figure 4.8.a.

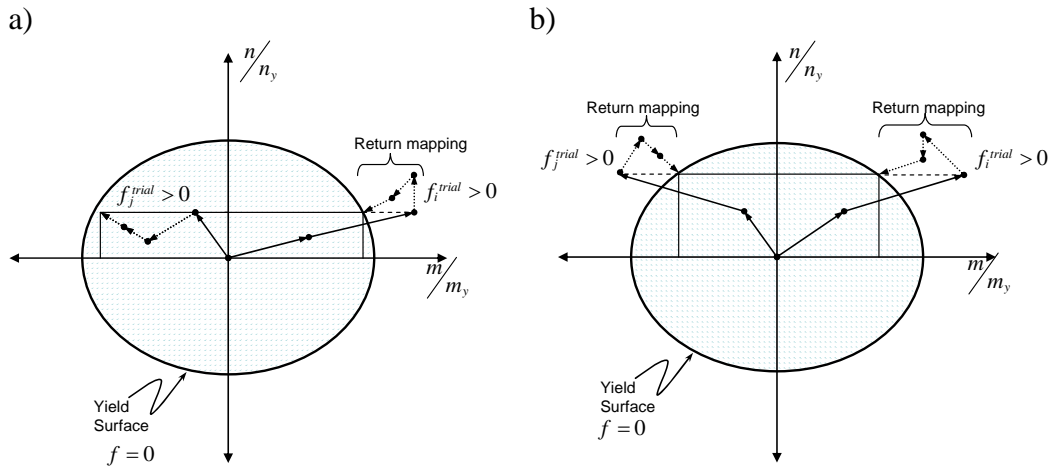


Figure 4.8 – Return-Mapping algorithm: a) one function outside the yield surface; b) both functions outside the yield surface

Table 4.3 shows the algorithm used to solve the return-mapping problem for elastoplastic frames with axial force.

Despite the fact that we have defined one axial plastic multiplier δ^p , the generalized plastic deformations $\{\Phi^p\}$ will not include this variable. This is due to the fact that the plasticity is concentrated (lumped) at the end, and all axial plasticity effect spread along the beam-column element is neglected in the analysis. However, the final axial force is influenced by the plasticity at the hinge be-

cause the axial plastic δ^p multiplier is a function of the increment of the plastic multipliers $\Delta\lambda_i^p$ and $\Delta\lambda_j^p$, as defined in the equation (4.23).

Table 4.3 – Return-Mapping algorithm for Elastoplastic Frames with Axial Force

- For each b elements at n th+1 iteration at the time t :
- 1) Generalized deformations at the step: $\{\Phi_b\}_t^{(n+1)} = \{\Phi_b\}_t^{(n)} + \{\Delta\Phi_b\}_t^{(n+1)}$
 - 2) Determination of generalized effective ‘trial’ ${}^k\{\mathbf{M}_b\}_{trial}^{(n+1)T} = \left\{ {}^k m_i^{trial} \quad {}^k m_j^{trial} \quad n^{trial} \right\}$ stress and update of internal variables ${}^k\{\Delta\Phi_b^p\}^T = \left\{ {}^k \phi_i^p \quad {}^k \phi_j^p \quad 0 \right\}$ at $k=1$:
 - a) ${}^k\{\mathbf{M}_b\}_{trial}^{(n+1)} = [\mathbf{S}_b] : \left(\{\Phi_b\}_t^{(n+1)} - {}^k\{\Delta\Phi_b^p\} \right)$; ${}^k\{\Delta\Phi_b^p\} = \{\Phi_b^p\}_t^{(n)}$
 - 3) Plastic evolution:
 - a) $f_i^{trial} = \left| \frac{{}^k m_i^{trial}}{m_y} \right| + \left(\frac{{}^k n^{trial}}{n_y} \right)^2 - 1$; $f_j^{trial} = \left| \frac{{}^k m_j^{trial}}{m_y} \right| + \left(\frac{{}^k n^{trial}}{n_y} \right)^2 - 1$
 - b) ${}^k f_i^{trial} \leq TOL$ and ${}^k f_j^{trial} \leq TOL$, no plasticity evolution or unload, go to 6)
 - c) ${}^k f_i^{trial} > TOL$ or ${}^k f_j^{trial} > TOL$, plasticity step: proceed to step 4)
 - 4) Determination of plastic multiplier:

$${}^k f_i^{trial} > 0 \left\{ \begin{array}{l} {}^{k+1}\Delta\lambda_i^p = \frac{{}^k f_i^{trial} - 1}{\frac{\partial {}^k f_i^{trial}}{\partial {}^k m_i^{trial}} : [\mathbf{S}_b] : \frac{\partial {}^k f_i^{trial}}{\partial {}^k m_i^{trial}} + \frac{1}{2} \frac{\partial {}^k f_i^{trial}}{\partial {}^k n^{trial}} : [\mathbf{S}_b] : \frac{\partial {}^k f_i^{trial}}{\partial {}^k n^{trial}}} \\ {}^{k+1}\Delta\lambda_j^p = 0 \end{array} \right.$$

$${}^k f_j^{trial} \leq 0 \left\{ \begin{array}{l} {}^{k+1}\Delta\lambda_i^p = 0 \\ {}^{k+1}\Delta\lambda_j^p = \frac{{}^k f_j^{trial} - 1}{\frac{\partial {}^k f_j^{trial}}{\partial {}^k m_j^{trial}} : [\mathbf{S}_b] : \frac{\partial {}^k f_j^{trial}}{\partial {}^k m_j^{trial}} + \frac{1}{2} \frac{\partial {}^k f_j^{trial}}{\partial {}^k n^{trial}} : [\mathbf{S}_b] : \frac{\partial {}^k f_j^{trial}}{\partial {}^k n^{trial}}} \end{array} \right.$$

or

$$\left. \begin{array}{l} {}^k f_i^{trial} > 0 \\ {}^k f_j^{trial} > 0 \end{array} \right\} [\mathbf{A}] : \{\Delta\lambda^p\} = \{\mathbf{f}^{trial}\}$$

$$[\mathbf{A}] = \begin{bmatrix} \frac{\partial {}^k f_i^{trial}}{\partial {}^k m_i^{trial}} : [\mathbf{S}_b] : \frac{\partial {}^k f_i^{trial}}{\partial {}^k m_i^{trial}} + \frac{1}{2} \frac{\partial {}^k f_i^{trial}}{\partial {}^k n^{trial}} : [\mathbf{S}_b] : \frac{\partial {}^k f_i^{trial}}{\partial {}^k n^{trial}} & \frac{1}{2} \frac{\partial {}^k f_i^{trial}}{\partial {}^k n^{trial}} : [\mathbf{S}_b] : \frac{\partial {}^k f_j^{trial}}{\partial {}^k n^{trial}} \\ \frac{1}{2} \frac{\partial {}^k f_j^{trial}}{\partial {}^k n^{trial}} : [\mathbf{S}_b] : \frac{\partial {}^k f_i^{trial}}{\partial {}^k n^{trial}} & \frac{\partial {}^k f_j^{trial}}{\partial {}^k m_j^{trial}} : [\mathbf{S}_b] : \frac{\partial {}^k f_j^{trial}}{\partial {}^k m_j^{trial}} + \frac{1}{2} \frac{\partial {}^k f_j^{trial}}{\partial {}^k n^{trial}} : [\mathbf{S}_b] : \frac{\partial {}^k f_j^{trial}}{\partial {}^k n^{trial}} \end{bmatrix}$$

$$\{\Delta\lambda^p\} = \left\{ \begin{array}{l} {}^{k+1}\Delta\lambda_i^p \\ {}^{k+1}\Delta\lambda_j^p \end{array} \right\} ; \{\mathbf{f}^{trial}\} = \left\{ \begin{array}{l} {}^k f_i^{trial} - 1 \\ {}^k f_j^{trial} - 1 \end{array} \right\}$$
 - 5) Update of plastic variables and of the generalized effective ‘trial’ stress:
 - a) ${}^{k+1}\phi_i^p = {}^k\phi_i^p + {}^{k+1}\Delta\lambda_i^p \frac{\partial {}^k f_i^{trial}}{\partial {}^k m_i^{trial}}$; ${}^{k+1}\phi_j^p = {}^k\phi_j^p + {}^{k+1}\Delta\lambda_j^p \frac{\partial {}^k f_j^{trial}}{\partial {}^k m_j^{trial}}$
 - b) ${}^{k+1}m_i^{trial} = {}^k m_i^{trial} - {}^{k+1}\Delta\lambda_i^p [\mathbf{S}_b] : \frac{\partial {}^k f_i^{trial}}{\partial {}^k m_i^{trial}}$; ${}^{k+1}m_j^{trial} = {}^k m_j^{trial} - {}^{k+1}\Delta\lambda_j^p [\mathbf{S}_b] : \frac{\partial {}^k f_j^{trial}}{\partial {}^k m_j^{trial}}$
 - c) ${}^{k+1}n^{trial} = {}^k n^{trial} - \left({}^{k+1}\Delta\lambda_i^p [\mathbf{S}_b] : \frac{\partial {}^k f_i^{trial}}{\partial {}^k n^{trial}} + {}^{k+1}\Delta\lambda_j^p [\mathbf{S}_b] : \frac{\partial {}^k f_j^{trial}}{\partial {}^k n^{trial}} \right)$
 - 6) End of the process of plastic correction
 - a) $\{\mathbf{M}_b\}_t^{(n+1)} = {}^k\{\mathbf{M}_b\}_{trial}^{(n+1)}$; $\{\Phi_b^p\}_t^{(n+1)} = {}^k\{\Delta\Phi_b^p\}$
 - 7) End of integration process of the constitutive equation.

Chapter 5

Concentrated Damage

Constitutive Model for

Frames

5.1 Introduction

The process of the load of the structure, whether cyclic or not, can frequently results in the progressive degradation of the mechanical proprieties of the structure, as well of the material of which it is made, brings about the gradual loss of its resistance. The plastic theory is not sufficient to represent the degradation of the structure, because this theory is based on the concept that the resistance of the

material is constant throughout a lifetime. Another theory to analyze the structure is necessary: Continuum Damage Mechanics. This theory is based on the concept that the damage will be measured by one variable, which assumes values between zero and one, which indicates the relative density of the microcracks and their evolution in the material.

The purpose of this chapter is to introduce the concepts of Continuum Damage Mechanics, and its application in frame structures, through the damage model applied to frame elements, concentrated damage model.

The concentrated damage model, similar to as in the lumped plasticity model, is based on the assumption that all damage is concentrated at the end of the beam,-column elements. This formulation can be considered as simplified damage mechanics for frames, because it incorporates some notions and methods of Continuum Damage Mechanics, as well as fracture mechanics, into the frame analysis.

In frame analysis, the damage can be assumed as one index, local, plastic or global, of the real damage, since the spread of the damage throughout the element is not taken into account, once the beam-column element is not discretized as layers, as is usually done in the finite element methods.

Based on method proposed by Hanganu *et al.* (2002), we will present one global damage evaluation method based on Continuum Mechanics principles in which the label "local" will be applied only to damage indices describing the state of frame member due to the concentrated damage. The label 'plastic' will be applied to damage indices describing the state of frame member due to the lumped plastic effect. The "global" damage index will refer to state of whole structure. Both damage indexes, local, plastic, and global, presented herein are independently from the chosen constitutive models for the structural material.

This feature converts the proposed local, plastic, and global damage indexes into a powerful general tool for structural assessment. Moreover, it is applicable directly to both static and dynamic analysis and to estimate the damage produced by seismic actions in reinforced concrete building structures.

The formulation of the concentrated damage model will be developed on the concepts of the isotropic strain damage, proposed by Simo and Ju (1987), in order to obtain the functions, which will describe the evolution of the all the damage parameters.

In addition, we present the unilateral damage model, which will make it possible to characterize the damage evolution under hysteretic loads, with special attention to the behaviour of reinforced concrete structures.

5.2 Elements of continuum damage mechanics

We review some basic concepts of continuum mechanics necessary for the subsequent development of the concentrated damage concepts. These concepts were introduced in the works of Simo and Ju (1987), Lemaitre and Lippmann (1996), and others.

Lemaitre and Lippmann (1996), affirmed that physically, degradation of the material properties is the result of the initiation, growth, and coalescence of microcracks or microvoids. If the bar of Figure 5.1, with section area A , is loaded by a force F , the usual uniaxial stress is

$$\sigma = \frac{F}{A} \tag{5.1}$$

it will be constant along the section.

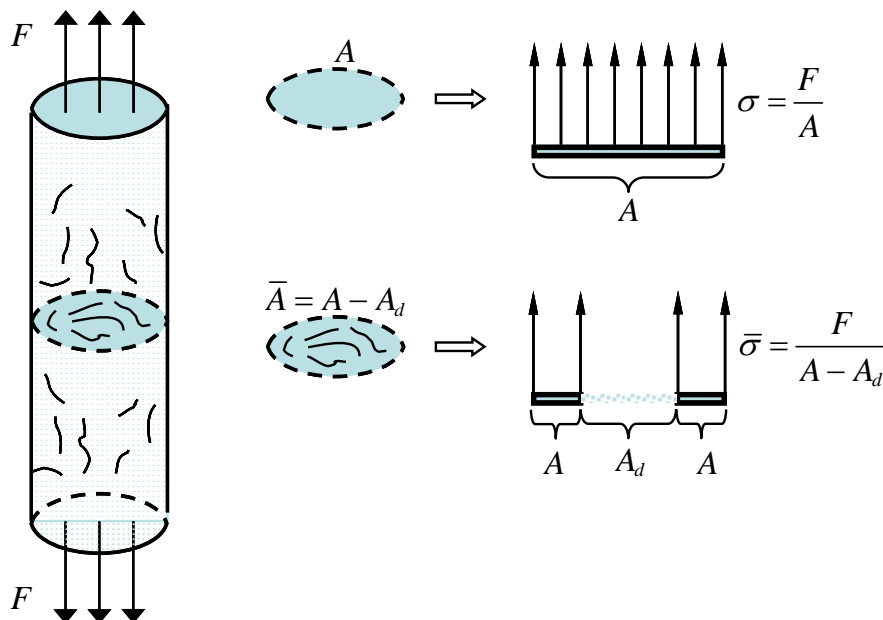


Figure 5.1 – One-dimensional damage element

If there are microcracks or microcavities within the bar, the area of the bar will be the sum of the all areas which still keep contact with each other. So, the fi-

nal area can be evaluated as the difference between section A and the microcracks area A_d . This section will be called the effective area $\bar{A} = (A - A_d)$. It is convenient to introduce the effective stress $\bar{\sigma}$ (Lemaitre and Lippmann (1996)), related to the surface that effectively resists the load:

$$\bar{\sigma} = \frac{F}{\bar{A}} = \frac{F}{A - A_d} \quad (5.2)$$

if the load remain the same, the stress σ can be obtained in terms of the effective stress $\bar{\sigma}$ by:

$$F = \sigma A = (A - A_d) \bar{\sigma} \Rightarrow \sigma = \left(1 - \frac{A_d}{A}\right) \bar{\sigma} \quad (5.3)$$

Defining that $d = \frac{A_d}{A}$, which is called the damage variable d ,

$$\sigma = (1 - d) \bar{\sigma} \text{ or } \bar{\sigma} = \frac{\sigma}{(1 - d)} \quad (5.4)$$

here, $d \in (0, 1]$ is a given constant. The coefficient $1 - d$ dividing the stress tensor in equation (5.4) is a reduction factor associated with the amount of damage in the material, initially introduced by Kachanov (1958). The value $d = 0$ corresponds to the undamaged state, whereas a value $d = 1$ corresponds to a damaged state, which also defines the complete local rupture.

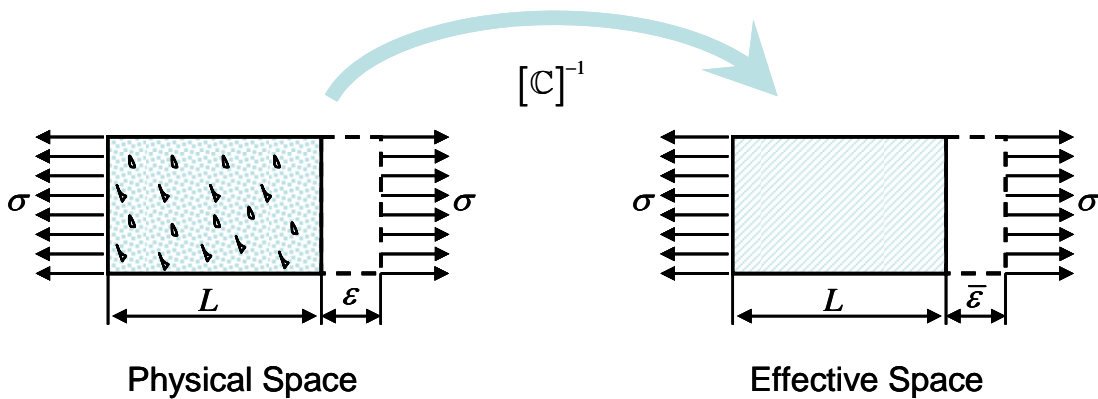


Figure 5.2 – Schematic illustration of the strain equivalence principle.

Another possible interpretation is that physically the damage parameter d is the ratio of damage surface area over total (nominal) surface area at a local material point. In addition, Lemaitre and Lippmann (1996) introduced the following principle results: “Any strain constitutive equation for a damage material may be

derived in the same way as for a virgin material except that the usual stress is replaced by the effective stress". This principle is well known as the strain equivalence principle or hypothesis of strain equivalence.

Within the context of continuum mechanics, one may model this process by introducing an internal damage variable that can be a scalar or a tensorial quantity. Let us consider $[C]$, a fourth-order tensor, which characterizes the state of damage and transforms the homogenized tensor $\{\sigma\}$ into the effective stress tensor $\{\bar{\sigma}\}$ (or vice versa), clearly:

$$\{\bar{\sigma}\} = [C]^{-1} : \{\sigma\} \quad (5.5)$$

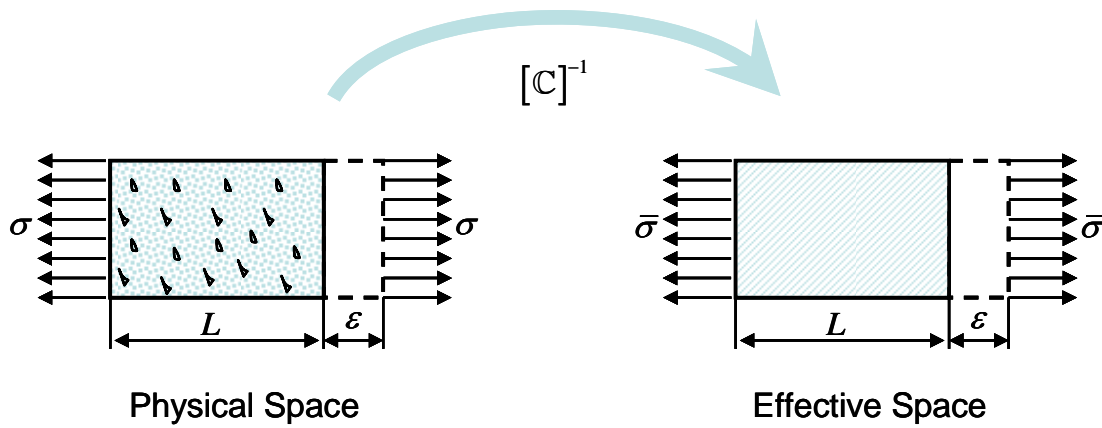


Figure 5.3 – Schematic illustration of the hypothesis of the stress equivalence proposed by (Simo and Ju, 1987).

For the isotropic damage case, the mechanical behaviour of microcracks or microvoids is independent of their orientation, and depends only on a scalar variable d . For that reason, $[C]$ will simply reduce to $[C] = (1-d)[I]$, where $[I]$ is the rank four-identity tensor, and equation (5.5) becomes:

$$\{\sigma\} = (1-d)\{\bar{\sigma}\} \quad (5.6)$$

where d is the damage parameter defined in (5.4), $\{\sigma\}$ the Cauchy stress tensor and $\{\bar{\sigma}\}$ is the effective stress tensor.

Alternatively, Simo and Ju (1987) presents the notion of effective strain:

$$\begin{aligned} \{\bar{\epsilon}\} &= [C] : \{\epsilon\} \\ \{\bar{\epsilon}\} &= (1-d)\{\epsilon\} \end{aligned} \quad (5.7)$$

where, $\{\boldsymbol{\varepsilon}\}$ is the strain tensor and $\{\bar{\boldsymbol{\varepsilon}}\}$ is the effective strain tensor. Similar to the hypothesis of strain equivalence, proposed by Lemaitre and Lippmann (1996), Simo and Ju (1987) has proposed the hypothesis of stress equivalence: "The stress associated with a damage state under the applied strain is equivalent to the stress associated with its undamaged state under the effective strain".

5.2.1 Strain-based Isotropic Continuum Damage Model

We will assume that the damage in the material is directly linked to the history of the total strain, as proposed by Simo and Ju (1987). The notion of effective stress along with the hypothesis of strain equivalence then follow from the assumed form of the free energy Ψ , as:

$$\Psi(\boldsymbol{\varepsilon}, r) = (1 - d(r)) \Psi^0(\boldsymbol{\varepsilon}) \quad (5.8)$$

where r is the internal parameter of the damage evolution, $\{\boldsymbol{\varepsilon}\}$ is the strain tensor, and $\Psi^0(\boldsymbol{\varepsilon})$ is initial elastic stored energy function of the undamaged material. For the linear case the initial elastic stored energy is defined as

$$\Psi^0(\boldsymbol{\varepsilon}) = \frac{1}{2} \{\boldsymbol{\varepsilon}\} : [\mathbf{C}^0] : \{\boldsymbol{\varepsilon}\} \quad (5.9)$$

where $[\mathbf{C}^0]$ is the linear elasticity tensor or the undamaged stiffness matrix.

The plastic flow is defined by Simo and Ju (1987) as an additive split of the stress tensor into initial and inelastic parts that follow from the assumed structure of the free energy. Therefore, using the basic principles of the mechanical theory, the dissipation can be obtained through of the Clausius-Duhem inequality:

$$\Xi = -\dot{\Psi} + \{\boldsymbol{\sigma}\} : \{\dot{\boldsymbol{\varepsilon}}\} \geq 0 \quad \forall \{\boldsymbol{\varepsilon}\} \quad (5.10)$$

this inequality is valid for any admissible process. Proceeding with the derivatives in the equation (5.10), and it is assumed that the damage and plastic unloading are elastic processes, we obtain:

$$\begin{aligned} \{\boldsymbol{\sigma}\} &= \frac{\partial \Psi}{\partial \{\boldsymbol{\varepsilon}\}} = (1 - d) \frac{\partial \Psi^0}{\partial \{\boldsymbol{\varepsilon}\}} = (1 - d) [\mathbf{C}^0] : \{\boldsymbol{\varepsilon}\} \\ [\mathbf{C}^0] &= \frac{\partial^2 \Psi^0}{\partial \{\boldsymbol{\varepsilon}\}^2} \end{aligned} \quad (5.11)$$

and the dissipative inequalities is

$$\Xi^d = \Psi^0(\boldsymbol{\varepsilon})\dot{d} \geq 0 \quad (5.12)$$

The undamaged energy norm of the strain tensor $\bar{\tau}(\boldsymbol{\varepsilon})$, defined in Simo and Ju (1987):

$$\bar{\tau}(\boldsymbol{\varepsilon}) = \sqrt{2\Psi^0(\boldsymbol{\varepsilon})} = \sqrt{\{\boldsymbol{\varepsilon}\} : [\mathbf{C}^0] : \{\boldsymbol{\varepsilon}\}} \quad (5.13)$$

The state of the damage in the material is characterized by the damage criterion

$$g(\boldsymbol{\varepsilon}_t, r_t) = \bar{\tau}(\boldsymbol{\varepsilon})_t - r_t \leq 0 \quad (5.14)$$

here, the subscript t refers to value at current time, and r_t is the damage threshold at current time t . Since must have that $r_t \geq r_0$, where r_0 is the initial damage threshold before any loading is applied, which can also represent a property characteristic of the material. In the case of the material where the yield limit is σ_y and the elastic modulus E , the parameter r_0 can be defined as proposed by Luccioni (2003):

$$r_0 = \frac{\sigma_y}{\sqrt{E}} \quad (5.15)$$

Through the equation (5.14) we can state that the damage in the material is initiated when the energy norm of the strain tensor $\bar{\tau}(\boldsymbol{\varepsilon})$ exceeds the initial damage threshold r_0 . For the isotropic case, we can define the evolution of the damage variable d as

$$d(r) = 1 - \frac{q(r)}{r} \quad (5.16)$$

$$\dot{r} = \dot{\lambda}_d(\boldsymbol{\varepsilon}, r) \quad (5.17)$$

where $\dot{\lambda}_d \geq 0$ is the damage consistency parameter that defines damage/unloading conditions according to the Kuhn-Tucker relations

$$\dot{\lambda}_d \geq 0 \quad ; \quad g(\boldsymbol{\varepsilon}, r) \leq 0 \quad ; \quad \dot{\lambda}_d g(\boldsymbol{\varepsilon}, r) = 0 \quad (5.18)$$

Conditions (5.18) are standard for problems involving unilateral constrain. The damage consistency condition is defined as:

$$g(\boldsymbol{\varepsilon}, r) = 0 \Rightarrow \lambda_d \dot{g}(\boldsymbol{\varepsilon}, r) = 0 \quad (5.19)$$

by means of the persistency condition (5.19), the evolution of the parameter r is:

$$\lambda_d \dot{g} = 0 \left\{ \begin{array}{l} \underbrace{g < 0 \Leftrightarrow \lambda_d = 0 \Rightarrow \dot{r} = 0}_{\text{ELASTIC DOMAIN}} \\ \underbrace{g = 0 \Leftrightarrow \lambda_d \dot{g} = 0}_{\text{DAMAGE DOMAIN}} \\ \underbrace{\dot{g} > 0 \Leftrightarrow g_t = 0 \Leftrightarrow g_{t+\Delta t} > 0 \Leftrightarrow \exists}_{\text{INADMISSIBLE STATE}} \end{array} \right. \quad (5.20)$$

$$\left\{ \begin{array}{l} \underbrace{\dot{g} < 0 \Leftrightarrow \lambda_d = 0 \Rightarrow \dot{r} = 0}_{\text{UNLOAD}} \\ \underbrace{\dot{g} = 0 \left\{ \begin{array}{l} \underbrace{\lambda_d = 0 \Rightarrow \dot{r} = 0 \Leftrightarrow r_{t+\Delta t} = r_t}_{g_{t+\Delta t} = g_t \text{ (NEUTRAL LOAD)}} \\ \underbrace{\lambda_d > 0 \Rightarrow \dot{r} = \lambda \Leftrightarrow r_{t+\Delta t} > r_t}_{\text{DAMAGE EVOLUTION}} \end{array} \right.}_{\dot{g} = 0} \end{array} \right.$$

Based on the damage consistency condition(5.20), the internal parameter r can be obtained by the expression

$$r_t = \max \left\{ r_0, \max_{s \in (0, t)} \bar{r}_s \right\} \quad (5.21)$$

The parameter $q(r)$ shown in (5.16) defines the damage threshold. This variable can be defined as lineal function:

$$q(r) = \begin{cases} r_0 \Rightarrow r_t \leq r_0 \\ r_0 + H(r - r_0) \Rightarrow r_t > r_0 \end{cases} \quad (5.22)$$

where H is the hardening ($H > 0$) or softening ($H < 0$) modulus, one of parameter of the material. It is also possible to use one exponential function, as proposed by Oller (2001b), to define the parameter $q(r)$:

$$q(r) = r_0 \left(e^{A \left(1 - \frac{r}{r_0} \right)} \right) \quad (5.23)$$

where A is defined by Oller (2001b) as

$$A = \frac{1}{\frac{g_f}{r_0^2} - \frac{1}{2}} \quad (5.24)$$

here, the parameter g_f represents the fracture energy of the material, parameter derived from fracture mechanics as $g_f = G_f / l_c$, where G_f is the fracture energy and l_c can be defined as the characteristic length of the fractured member or alternatively as $l_c = \sqrt{A}$ where A is the element section area, as proposed by Salamy *et al.* (2005).

5.3 Concentrated Damage Constitutive Model

Similar to the plastic analysis, we will assume that all damage is concentrated at the extremities of the beam-column elements. Cipolina *et al.* (1995) considering the existence of a concentrated damage vector $\{\mathbf{D}\}$, which represents the damage at the b frame element, which can be defined as:

$$\{\mathbf{D}\}^T = \{d_i \quad d_j \quad d_a\} \quad (5.25)$$

where d_i and d_j represent the measure flexion damage of hinges i and j , respectively, and d_a indicates the measure of axial damage of the member. These variables can take values between zero, no damage, and one, completely damaged. If the beam-column is a reinforced concrete element, the flexion damage variable represents the density of the cracking at the extremities, as shown in Figure 5.4. Unlike the damage in Continuum Mechanics, where the damage variable measures begin, and growth of the cracks until the appearance of macrocracks, the concentrated damage variables only measure the macrocracks in the material.

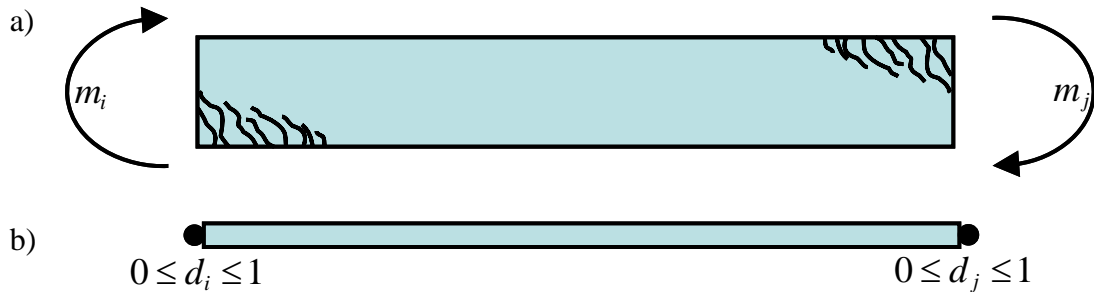


Figure 5.4 – Damage in beam-column elements: a) Cracking at the end, of one reinforced concrete beam, b) The concentrated damage model for beam-column.

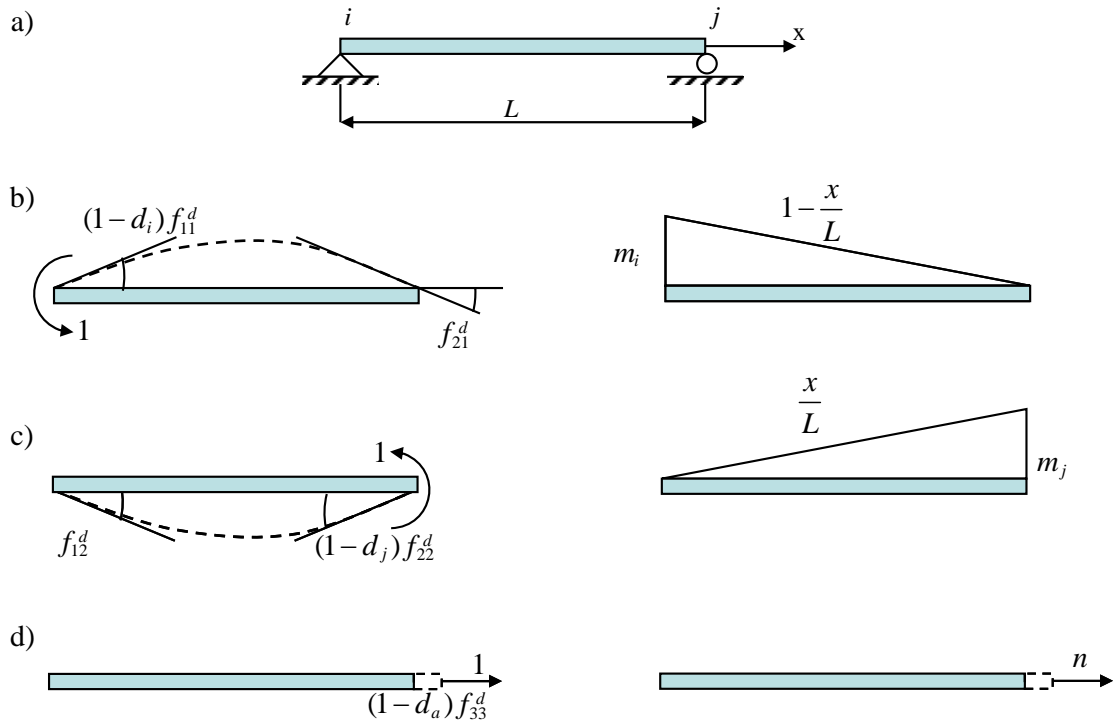


Figure 5.5 - Flexibility Damage parameters.

Now let us consider the simply supported beam shown in Figure 5.5a, using a local coordinate system, and assuming the existence of a flexibility matrix of a damaged member $[\mathbf{F}^d]$, we have

$$\begin{aligned} \{\Phi_b\} &= [\mathbf{F}_b^d] \{\mathbf{M}_b\} \\ \begin{Bmatrix} \phi_i \\ \phi_j \\ \delta \end{Bmatrix} &= \begin{bmatrix} f_{11} & f_{12} & f_{13} \\ f_{21} & f_{22} & f_{23} \\ f_{31} & f_{32} & f_{33} \end{bmatrix} \begin{Bmatrix} m_i \\ m_j \\ n \end{Bmatrix} \end{aligned} \quad (5.26)$$

If we assume the existence of one unit moment force applied at the extremities of the beam, Figure 5.5a and Figure 5.5b, the moment's influence will be decreasing along the beam. Thus, we can assume that moments are concentrated at the ends, as well the stress. We can define the stress in terms of the moment as:

$$\sigma_i = \frac{m_i y}{I} \quad \sigma_j = \frac{m_j y}{I} \quad (5.27)$$

where y , E , and I , indicate, respectively, the position of the neutral axis of the beam, the elastic modulus, and the moment of inertia. The stress due the axial force, Figure 5.5c, can be expressed as

$$\sigma_a = \frac{n}{A} \quad (5.28)$$

Once we assume that the damage due the bending moment is concentrated at the extremities of the beam, we can define that the flexibility terms at the end will be influenced by the damage, which implies that the flexibility damage matrix can be defined by one matrix with damage parameters only at the diagonal terms:

$$[\mathbf{F}^d] = \begin{bmatrix} (1-d_i) f_{11}^d & f_{12}^d & f_{13}^d \\ f_{21}^d & (1-d_j) f_{22}^d & f_{23}^d \\ f_{31}^d & f_{32}^d & (1-d_a) f_{33}^d \end{bmatrix} \quad (5.29)$$

Using the virtual work, in particular, the virtual force method to analyze this problem, and assuming that it is a nonconservative system, we obtain:

$$\left. \begin{aligned} \{\delta w\} &= \int \{\delta \bar{\sigma}\} \{\boldsymbol{\varepsilon}\} d\omega \\ \{\delta \bar{\sigma}\}^T &= \left\{ \frac{\delta m_z y}{I} \quad \frac{\delta m_z y}{I} \quad \frac{\delta n}{A} \right\} \\ \{\boldsymbol{\varepsilon}\}^T &= \left\{ \frac{m_i y}{EI} \quad \frac{m_j y}{EI} \quad \frac{n}{EA} \right\} \\ d\omega &= dA dx \\ \omega &= A dx \\ \int y^2 dA &= I \end{aligned} \right\} \{\delta w\} = \left\{ \begin{aligned} \int_0^L \delta m_z \frac{m_i}{EI} dx \\ \int_0^L \delta m_z \frac{m_j}{EI} dx \\ \int_0^L \delta n \frac{n}{EA} dx \end{aligned} \right\} \quad (5.30)$$

$$\begin{aligned} \int_0^L \delta m_z \frac{m_i}{EI} dx &= (1-d_i) \delta m_i f_{11}^d + \delta m_j f_{12}^d + \delta n f_{13}^d \\ \int_0^L \delta m_z \frac{m_j}{EI} dx &= \delta m_i f_{21}^d + (1-d_j) \delta m_j f_{22}^d + \delta n f_{23}^d \\ \int_0^L \delta n \frac{n}{EA} dx &= \delta m_i f_{31}^d + \delta m_j f_{32}^d + (1-d_a) \delta n f_{33}^d \end{aligned} \quad (5.31)$$

$$\underbrace{\{\delta w\}}_{\text{Internal Forces}} = \underbrace{[\mathbf{F}^d]}_{\text{External Forces}} \{\delta \mathbf{M}\}$$

Solving the linear system (5.31) for each unitary virtual moment, Figure 5.5a and Figure 5.5b, and for the unitary axial force, Figure 5.5c, we obtain the flexibility coefficients:

$$\begin{array}{ccc}
\delta m_z = \left(1 - \frac{x}{L}\right) & \delta m_z = \left(\frac{x}{L}\right) & \delta n = 1 \\
\underbrace{\delta m_i = 1} & \underbrace{\delta m_j = 1} & \underbrace{\hspace{10em}} \\
f_{11}^d = \int_0^L \left(1 - \frac{x}{L}\right) \frac{\left(1 - \frac{x}{L}\right)}{(1-d_i)EI} dx = \frac{L}{3(1-d_i)EI} & f_{12}^d = \int_0^L \left(\frac{x}{L}\right) \frac{\left(1 - \frac{x}{L}\right)}{EI} dx = -\frac{L}{6EI} & \begin{array}{l} f_{11}^d = 0 \\ f_{21}^d = 0 \end{array} \\
f_{21}^d = \int_0^L \left(1 - \frac{x}{L}\right) \frac{\left(\frac{x}{L}\right)}{EI} dx = -\frac{L}{6EI} & f_{22}^d = \int_0^L \left(\frac{x}{L}\right) \frac{\left(\frac{x}{L}\right)}{(1-d_j)EI} dx = \frac{L}{3(1-d_j)EI} & f_{31}^d = \int_0^L 1 \frac{1}{(1-d_a)EA} dx = \frac{L}{(1-d_a)EA} \\
f_{31}^d = 0 & f_{32}^d = 0 &
\end{array} \tag{5.32}$$

organized in matrix form, we obtain:

$$[\mathbf{F}^d] = \begin{bmatrix} \frac{1}{(1-d_i)} \frac{L}{3EI} & -\frac{L}{6EI} & 0 \\ -\frac{L}{6EI} & \frac{1}{(1-d_j)} \frac{L}{3EI} & 0 \\ 0 & 0 & \frac{1}{(1-d_a)} \frac{L}{EA} \end{bmatrix} \tag{5.33}$$

$[\mathbf{F}^d]$ represents the flexibility matrix of a damaged member. The relation between the generalized deformation $\{\Phi_b\}$ and the generalized stress vector $\{\mathbf{M}_b\}$ now can be redefined as

$$\{\Phi_b\} = [\mathbf{F}_b^d] \{\mathbf{M}_b\} \tag{5.34}$$

Since that the process is elastic, we can assume that the flexibility damage matrix is invertible. Its inverse is the stiffness matrix of a damaged member $[\mathbf{S}^d] = [\mathbf{F}^d]^{-1}$, and can be redefined as a function of concentrated damage vector $\{\mathbf{D}_b\}$ for a b element, so for small displacements, we obtain

$$\mathbf{S}_b^d(\mathbf{D}_b) = k \begin{bmatrix} 12(1-d_i) & 6(1-d_i)(1-d_j) & 0 \\ 6(1-d_i)(1-d_j) & 12(1-d_j) & 0 \\ 0 & 0 & \frac{EA(1-d_i)}{kL} \end{bmatrix}; \quad k = \frac{1}{4 - (1-d_i)(1-d_j)} \frac{EI}{L} \tag{5.35}$$

the matrix $[\mathbf{S}_b^d(\mathbf{D}_b)]$ has the same significance of the elastic-damage tangent moduli used in the finite element method.

Therefore, we can now define the generalized stress vector $\{\mathbf{M}_b\}$ in terms of the damage and the generalized deformations $\{\Phi_b\}$ of a b member

$$\{\mathbf{M}_b\} = [\mathbf{S}_b^d(\mathbf{D}_b)] \{\Phi_b\} \quad (5.36)$$

It can be observed that in the case where $\{\mathbf{D}\}$ is equal to zero, $[\mathbf{S}_b^d]$ reduces to the standard stiffness matrix defined in the Appendix 1,

$$[\mathbf{S}_b^d(\mathbf{D}_b = \mathbf{0})] = \begin{bmatrix} 4\frac{EI}{L} & 2\frac{EI}{L} & 0 \\ 2\frac{EI}{L} & 4\frac{EI}{L} & 0 \\ 0 & 0 & \frac{EA}{L} \end{bmatrix} = [\mathbf{S}_b^e] \quad (5.37)$$

If one of the bending damage variables takes value equal to one, while the other flexion damage and the axial damage are equal to zero, then $\mathbf{S}_b^d(\mathbf{D}_b)$ becomes the stiffness matrix of an elastic member with an internal hinge at the end, on the left or the right:

$$[\mathbf{S}_b^d(\mathbf{D}_b)] = \underbrace{\begin{bmatrix} 0 & 0 & 0 \\ 0 & 3\frac{EI}{L} & 0 \\ 0 & 0 & \frac{EA}{L} \end{bmatrix}}_{d_i=1 \quad d_j=0 \quad d_a=0}, \text{ or } [\mathbf{S}_b^d(\mathbf{D}_b)] = \underbrace{\begin{bmatrix} 3\frac{EI}{L} & 0 & 0 \\ 0 & 0 & 0 \\ 0 & 0 & \frac{EA}{L} \end{bmatrix}}_{d_i=0 \quad d_j=1 \quad d_a=0} \quad (5.38)$$

For the case where both flexion damage variables acquire values equal to one, while the axial damage is equal to zero, we obtain the stiffness matrix of an elastic truss bar where only the axial force remains.

$$[\mathbf{S}_b^d(\mathbf{D}_b)] = \underbrace{\begin{bmatrix} 0 & 0 & 0 \\ 0 & 0 & 0 \\ 0 & 0 & \frac{EA}{L} \end{bmatrix}}_{d_i=1 \quad d_j=1 \quad d_a=0} \quad (5.39)$$

Furthermore, the stiffness matrix of a damaged member $[\mathbf{S}_b^d]$ obtained has the same shape as presented by Cipolina *et al.* (1995) and Flórez-López (1999).

5.4 Damage evolution law of the Concentrated Damage Model

To apply Continuum Damage Mechanics concepts to frame analysis, it is necessary to adapt the theory as a function of the deformations at the hinges i

and j , as well as the deformation due to the elongation δ . In addition, another necessary condition is that the variable evolutions should be independent of each other.

5.4.1 Free energy potential

The Helmholtz Free Energy used in the equation (5.9), has been obtained using the basic concepts of Continuum Mechanics. For the frame, it will be necessary to decompose into two terms, one for flexural force and the other for axial force:

5.4.2 Free Energy for Flexural Force

Let us suppose that a frame member can be characterized by the generalized deformations $\{\Phi(\varepsilon)\}^T = \{\phi_i \ \phi_j\}$, and temperature θ . Hence, there exists a specific internal energy $u(\Phi, s)$, where s is the specific entropy. Measuring $u(\Phi, s)$ and $s(\Phi, \theta)$ would completely characterize the frame.

Given $u(\Phi, s)$ and $s(\Phi, \theta)$, we may define the Helmholtz free energy for a flexural member as:

$$\Psi_F^{not} = u_F - \theta s \quad (5.40)$$

here, the subscript F indicates that we only analysis the energy due to the bending moments. Now, recall the first law of thermodynamics:

$$\rho_0 du_F^{not} = dw_F + d\tau \quad (5.41)$$

where dw_F is the work done on the frame, ρ_0 is the density of the material in the reference configuration, and $d\tau$ is the heat flow into the frame defined in Malvern (1969).

From the power identity and the second law we can define the work done in terms of the generalized stress, without the axial force, $dw_F = [\mathbf{M}] : \{d\Phi\}$; and the heat flow as $d\tau = \rho_0 \theta ds$, now

$$d\Psi_F = du_F - \theta ds - s d\theta \quad (5.42)$$

So

$$d\Psi_F = \frac{1}{\rho_0} dw_F + \theta ds - \theta ds - sd\theta = \frac{1}{\rho_0} [\mathbf{M}] : \{d\Phi\} - sd\theta \quad (5.43)$$

Hence, we can observe that

$$[\mathbf{M}] = \rho_0 \left. \frac{\partial \Psi_F}{\partial \{\Phi\}} \right|_{\theta=\text{const}} \quad s = - \left. \frac{\partial \Psi_F}{\partial \theta} \right|_{\{\Phi\}=\text{const}} \quad (5.44)$$

If we assume that the temperature θ it is constant, the expression (5.43) reduces to:

$$\rho_0 d\Psi_F = [\mathbf{M}] : \{d\Phi\} \quad (5.45)$$

Since we can assume that the density of the material ρ_0 is constant throughout all the process,

$$\rho_0 \frac{d\Psi_F}{dt} = \frac{d\Psi_F^0}{dt} \stackrel{\text{not}}{=} \Psi_F^0 = [\mathbf{M}] : \{d\Phi\} \quad (5.46)$$

and recalling that $[\mathbf{M}] = [\mathbf{S}_F^e] \{\Phi\}$, where

$$[\mathbf{S}_F^e] = \begin{bmatrix} 4 \frac{L}{EI} & 2 \frac{L}{EI} \\ 2 \frac{L}{EI} & 4 \frac{L}{EI} \end{bmatrix} \quad (5.47)$$

is the stiffness matrix, without axial force. We can express the free energy in terms of the stiffness matrix and of the generalized deformations increment as:

$$\begin{aligned} \Psi_F^0 &= \underbrace{[\mathbf{M}]}_{[\mathbf{S}_F^e] \{\Phi\}} : \{\dot{\Phi}\} = \{\dot{\Phi}\} : [\mathbf{S}_F^e] : \{\Phi\} \\ \Psi_F^0 &= \frac{1}{2} \left(\{\dot{\Phi}\} : [\mathbf{S}_F^e] : \{\Phi\} + \{\Phi\} : [\mathbf{S}_F^e] : \{\dot{\Phi}\} \right) \\ \Psi_F^0 &= \frac{1}{2} \frac{d}{dt} \left(\{\Phi\} : [\mathbf{S}_F^e] : \{\Phi\} \right) \end{aligned} \quad (5.48)$$

Making the integration, and assuming that the free energy $\Psi_F^0(t_0)$ for the neutral state (for $t = t_0 \Rightarrow \{\Phi(t_0)\} = \mathbf{0}$) is null:

$$\underbrace{\Psi_F^0(\varepsilon, t) = \frac{1}{2} \left(\{\Phi(\varepsilon, t)\} : [\mathbf{S}^e] : \{\Phi(\varepsilon, t)\} + a(\varepsilon) \right)}_{\Psi_F^0(\varepsilon, t_0) = 0 \quad \forall \varepsilon} \quad (5.49)$$

$$\frac{1}{2} \underbrace{\{\Phi(\varepsilon, t)\} : [\mathbf{S}^e] : \{\Phi(\varepsilon, t)\}}_{=0} + a(\varepsilon) = a(\varepsilon) = 0 \quad \forall \varepsilon$$

Therefore, the initial elastic stored energy for a bending member is:

$$\Psi_F^0 = \frac{1}{2} \left(\{\Phi\} : \{\mathbf{S}^e\} : \{\Phi\} \right) = 2 \frac{EI}{L} (\phi_i^2 + \phi_i \phi_j + \phi_j^2) \quad (5.50)$$

5.4.3 Free Energy for Axial Force

Following the same procedure for the flexural terms, but in this case redefining the work done on the frame (equation (5.41)) in terms of the axial force as $dw = Q : d\delta$, equation (5.43) becomes:

$$d\Psi_A = \frac{1}{\rho_0} dw + \theta ds - \theta ds - sd\theta = \frac{1}{\rho_0} Q : d\delta - sd\theta \quad (5.51)$$

here, the subscript A indicates that we only analysis the energy due to the axial force.

Hence

$$Q = \rho_0 \left. \frac{\partial \Psi_A}{\partial \delta} \right|_{\theta = \text{const}} \quad s = - \left. \frac{\partial \Psi_A}{\partial \theta} \right|_{\delta = \text{const}} \quad (5.52)$$

Once more, we assume that the temperature θ is constant, and $Q = \frac{EA}{L} \delta$, so:

$$\rho_0 d\Psi_A = \frac{EA}{L} \delta d\delta \quad (5.53)$$

Once more, we can assume that the density of the material ρ_0 is constant the whole time:

$$\rho_0 \frac{\delta \Psi_A}{\delta t} \stackrel{\text{not}}{=} \frac{\delta \Psi_A^0}{\delta t} \quad (5.54)$$

This leads to the free energy:

$$\Psi_A^0 = \frac{EA}{L} \delta^2 \quad (5.55)$$

5.4.4 Free Energy for Frame Member

The free energy of a frame member can be considered as the sum of the free flexural energy (equation (5.50)) plus the free axial energy (5.55), so:

$$\Psi_b^0 = \Psi_F^0 + \Psi_A^0 = 2 \frac{EI}{L} (\phi_i^2 + \phi_i \phi_j + \phi_j^2) + \frac{EA}{L} \delta^2 \quad (5.56)$$

$$\Psi_b^0 = \frac{1}{2} \left(4 \frac{EI}{L} \phi_i + 2 \frac{EI}{L} \phi_j \right) \phi_i + \frac{1}{2} \left(4 \frac{EI}{L} \phi_j + 2 \frac{EI}{L} \phi_i \right) \phi_j + \frac{1}{2} \frac{EA}{L} \delta^2 \quad (5.57)$$

In equation (5.57) we may observe that the free energy potential is the sum of the energies obtained due to the rotations at the i and j nodes plus the elongation δ , in such a way that the free energy potential can be redefined as

$$\Psi_b^0 = \Psi_i^0 + \Psi_j^0 + \Psi_\delta^0, \text{ where} \\ \Psi_i^0 = \frac{1}{2} \left(4 \frac{EI}{L} \phi_i + 2 \frac{EI}{L} \phi_j \right) \phi_i, \Psi_j^0 = \frac{1}{2} \left(4 \frac{EI}{L} \phi_j + 2 \frac{EI}{L} \phi_i \right) \phi_j \text{ and } \Psi_\delta^0 = \frac{1}{2} \frac{EA}{L} \delta^2. \quad (5.58)$$

Using equation (5.44), once the density of the material ρ_0 is constant (Malvern, 1969), we can define the generalized stress of a frame member b as:

$$[\mathbf{M}_b] = \frac{\partial \Psi_b^0}{\partial \{\Phi\}} \begin{cases} m_i = \frac{\partial \Psi_b^0}{\partial \phi_i} = \left(4 \frac{EI}{L} \phi_i + 2 \frac{EI}{L} \phi_j \right) \\ m_j = \frac{\partial \Psi_b^0}{\partial \phi_j} = \left(2 \frac{EI}{L} \phi_i + 4 \frac{EI}{L} \phi_j \right) \\ n = \frac{\partial \Psi_b^0}{\partial \delta} = \frac{EA}{L} \delta \end{cases} \quad (5.59)$$

The stiffness flexural matrix can also be obtained as:

$$[\mathbf{S}_b^e] = \frac{\partial^2 \Psi_b^0}{\partial \Phi \partial \Phi} = \begin{bmatrix} \frac{\partial^2 \Psi_b^0}{\partial \phi_i \partial \phi_i} & \frac{\partial^2 \Psi_b^0}{\partial \phi_i \partial \phi_j} & \frac{\partial^2 \Psi_b^0}{\partial \phi_i \partial \delta} \\ \frac{\partial^2 \Psi_b^0}{\partial \phi_j \partial \phi_i} & \frac{\partial^2 \Psi_b^0}{\partial \phi_j \partial \phi_j} & \frac{\partial^2 \Psi_b^0}{\partial \phi_j \partial \delta} \\ \frac{\partial^2 \Psi_b^0}{\partial \delta \partial \phi_i} & \frac{\partial^2 \Psi_b^0}{\partial \delta \partial \phi_j} & \frac{\partial^2 \Psi_b^0}{\partial \delta \partial \delta} \end{bmatrix} = \begin{bmatrix} 4 \frac{EI}{L} & 2 \frac{EI}{L} & 0 \\ 2 \frac{EI}{L} & 4 \frac{EI}{L} & 0 \\ 0 & 0 & \frac{EA}{L} \end{bmatrix} \quad (5.60)$$

which is the same matrix defined in Appendix 1.

5.4.5 Undamaged energy norm and damage evolution

Now the undamaged energy norm vector τ^b is defined in the same way as the free energy; that is, as a function of the rotations ϕ_i and ϕ_j at the ends of the element and by the elongation δ , following the same definition (5.13), the energy norm vector is decomposed into three terms:

$$\begin{aligned} \tau_i^b &= \sqrt{2\Psi_i^0} = \sqrt{\left(4 \frac{EI}{L} \phi_i + 2 \frac{EI}{L} \phi_j\right)} \phi_i \\ \tau_j^b &= \sqrt{2\Psi_j^0} = \sqrt{\left(4 \frac{EI}{L} \phi_j + 2 \frac{EI}{L} \phi_i\right)} \phi_j \\ \tau_\delta^b &= \sqrt{2\Psi_\delta^0} = \sqrt{\frac{EA}{L}} \delta^2 \end{aligned} \quad (5.61)$$

It is important to observe the influence of the rotations ϕ_i and ϕ_j in each flexural energy norm vector, τ_i^b and τ_j^b .

We then characterize the state of damage in the frame element by means of a damage criterion, with the following functional form:

$$\begin{aligned} g_i(\tau_i^b, r_i^b)_t &= (\tau_i^b)_t - (r_i^b)_t \leq 0 \\ g_j(\tau_j^b, r_j^b)_t &= (\tau_j^b)_t - (r_j^b)_t \leq 0 \\ g_\delta(\tau_\delta^b, r_\delta^b)_t &= (\tau_\delta^b)_t - (r_\delta^b)_t \leq 0 \end{aligned} \quad (5.62)$$

Here, the subscript t refers to value at current time $t \in \mathbb{R}_+$, r_i^b, r_j^b and r_δ^b are the damage threshold at current time for the rotations ϕ_i and ϕ_j , and the elongation δ , respectively. We can consider the existence of one vector $\{r_0\}$, for $t=0$,

which denotes the initial damage threshold before any loading is applied, defined as:

$$\{r_0^b\} = \sqrt{\{\mathbf{M}_y\} : [\mathbf{S}_b^{-1}] : \{\mathbf{M}_y\}} = \begin{cases} (r_i^b)_0 \\ (r_j^b)_0 \\ (r_\delta^b)_0 \end{cases} \Rightarrow \begin{cases} (r_i^b)_0 = (r_j^b)_0 = \sqrt{\frac{L}{3EI}} m_y^2 \\ (r_\delta^b)_0 = \sqrt{\frac{L}{EA}} n_y^2 \end{cases} \quad (5.63)$$

here $\{\mathbf{M}_y\}^T = \{m_y \ m_y \ n_y\}$, where m_y and n_y are the bending moment and the axial force limits. The vector $\{r_0\}$ can be considered as a property characteristic of the element, in way that we must have $\|\{r_t^b\}\| \geq \|\{r_0^b\}\|$, which implies that, $(r_i^b)_t \geq (r_i^b)_0$, $(r_j^b)_t \geq (r_j^b)_0$, or $(r_\delta^b)_t \geq (r_\delta^b)_0$. Condition (equation (5.62)) states that damage in the element is initiated when the energy norm vector $\{\tau^b\}$ exceeds the initial damage threshold $\{r_0\}$. For the isotropic case, we define the evolution of the damage variables by:

$$\{\dot{\mathbf{D}}_t^b\} = \{\dot{\lambda}^d\} H(\{\tau_t^b\}, \{\mathbf{D}_t^b\}) = \begin{cases} \dot{d}_i = \dot{\lambda}_i^d \left((\tau_i^b)_t, d_i \right) \\ \dot{d}_j = \dot{\lambda}_j^d \left((\tau_j^b)_t, d_j \right) \\ \dot{d}_a = \dot{\lambda}_\delta^d H \left((\tau_\delta^b)_t, d_a \right) \end{cases} ; \{\dot{r}_t^b\} = \{\dot{\lambda}^d\} = \begin{cases} (\dot{r}_i^b)_t = \dot{\lambda}_i^d \\ (\dot{r}_j^b)_t = \dot{\lambda}_j^d \\ (\dot{r}_\delta^b)_t = \dot{\lambda}_\delta^d \end{cases} \quad (5.64)$$

where $\dot{\lambda}_i^d \geq 0$, $\dot{\lambda}_j^d \geq 0$ and $\dot{\lambda}_\delta^d \geq 0$ are damage consistency parameters that define damage loading/unloading conditions according to the Kuhn-Tucker's relations:

$$\begin{aligned} \dot{\lambda}_i^d \geq 0; \quad g_i \left((\tau_i^b)_t, (r_i^b)_t \right) \leq 0; \quad \dot{\lambda}_i^d g_i &= 0 \\ \dot{\lambda}_j^d \geq 0; \quad g_j \left((\tau_j^b)_t, (r_j^b)_t \right) \leq 0; \quad \dot{\lambda}_j^d g_j &= 0 \\ \dot{\lambda}_\delta^d \geq 0; \quad g_\delta \left((\tau_\delta^b)_t, (r_\delta^b)_t \right) \leq 0; \quad \dot{\lambda}_\delta^d g_\delta &= 0 \end{aligned} \quad (5.65)$$

Let us now analyze the damage evolution at the hinge i using the same concepts described in (5.20). Conditions (5.65) are standard for problems involving unilateral constraint. If $g_i < 0$, the damage criterion is not satisfied, and by condition (5.65)₃, $\dot{\lambda}_i = 0$. Hence, the damage rule (5.64) implies that $\dot{d}_i = 0$ and no further damage occurs. If, on the other hand, $\dot{\lambda}_i^d > 0$, further damage (loading) is taking place, condition (5.65)₃ now implies that $g_i = 0$. In this event the value of $\dot{\lambda}_i$ can be determined by the damage consistency condition, i.e.:

$$g_i\left(\left(\tau_i^b\right)_t, \left(r_i^b\right)_t\right) = \dot{g}_i\left(\left(\dot{\tau}_i^b\right)_t, \left(r_i^b\right)_t\right) = 0 \Rightarrow \dot{\lambda}_i^d = \left(\dot{\tau}_i^b\right)_t \quad (5.66)$$

Finally, $\left(r_i^b\right)_t$ can be given by the expression:

$$\left(r_i^b\right)_t = \max\left\{\left(r_i^b\right)_0, \max_{s \in (0,t)}\left(\tau_i^b\right)_s\right\} \quad (5.67)$$

By applying to the other parameters, we obtain:

$$\left\{r_i^b\right\} = \max\left\{\left\{r_0^b\right\}, \max_{s \in (0,t)}\left(\left\{\tau_\Phi^b\right\}\right)_s\right\} = \begin{cases} \max\left\{\left(r_i^b\right)_0, \max_{s \in (0,t)}\left(\tau_i^b\right)_s\right\} \\ \max\left\{\left(r_j^b\right)_0, \max_{s \in (0,t)}\left(\tau_j^b\right)_s\right\} \\ \max\left\{\left(r_\delta^b\right)_0, \max_{s \in (0,t)}\left(\tau_\delta^b\right)_s\right\} \end{cases} \quad (5.68)$$

If now we consider that $H\left(\tau_i^b, \mathbf{D}_i^b\right)$ in condition (5.64) is independent of the vector \mathbf{D}_i^b , and assuming that the existence of one function monotonic G , such that $H\left(\tau_i^b\right) = \partial G\left(\tau_i^b\right) / \partial\left(\tau_i^b\right)$, the damage criterion defined in (5.62) can now be rewritten in relation as a function of $G = 1 - \frac{q(r)}{r_0}$, i.e. at hinge i , by $g_i\left(\tau_i^b, r_i^b\right)_t = G\left(\tau_i^b\right)_t - G\left(r_i^b\right)_t \leq 0$. In this way, the flow rule (5.64) and loading/unloading conditions (5.65) then become:

$$\dot{\mathbf{D}}_i^b = \dot{\lambda}^d \frac{\partial G\left(\left\{\tau_i^b\right\}, \left\{r_i^b\right\}\right)}{\partial\left\{\tau_i^b\right\}} = \begin{cases} \dot{d}_i = \dot{\lambda}_i^d \frac{\partial G\left(\left(\tau_i^b\right)_t, \left(r_i^b\right)_t\right)}{\partial\left(\tau_i^b\right)_t} \\ \dot{d}_j = \dot{\lambda}_j^d \frac{\partial G\left(\left(\tau_j^b\right)_t, \left(r_j^b\right)_t\right)}{\partial\left(\tau_j^b\right)_t} \\ \dot{d}_a = \dot{\lambda}_\delta^d \frac{\partial G\left(\left(\tau_\delta^b\right)_t, \left(r_\delta^b\right)_t\right)}{\partial\left(\tau_\delta^b\right)_t} \end{cases} ; \dot{r}_i^b = \dot{\lambda}^d = \begin{cases} \left(\dot{r}_i^b\right)_t = \dot{\lambda}_i^d \\ \left(\dot{r}_j^b\right)_t = \dot{\lambda}_j^d \\ \left(\dot{r}_\delta^b\right)_t = \dot{\lambda}_\delta^d \end{cases} \quad (5.69)$$

Carrying through the integration in the time of the rate concentrated damage vector, the result is an expression that indicates the evolution of the damage variables as:

$$\{\mathbf{D}_i^b\} = G(\{\tau_i^b\}) = \begin{cases} d_i = G((\tau_i^b)_t) \\ d_j = G((\tau_j^b)_t) \\ d_a = G((\tau_\delta^b)_t) \end{cases} \quad (5.70)$$

In function $G = 1 - \frac{q(r)}{r}$, the parameter $q(r)$ can be expressed using the equations (5.22) or (5.23), i.e., using the exponential softening proposed by Oller (2001b):

$$G\left(\left(\tau_k^b\right)_t\right) = 1 - \frac{q\left(\left(\tau_k^b\right)_t\right)}{\left(\tau_k^b\right)_t} \left\{ \begin{array}{l} q\left(\left(\tau_k^b\right)_t\right) = \left(r_k^b\right)_0 e^{A\left(1 - \frac{\left(\tau_k^b\right)_t}{\left(r_k^b\right)_0}\right)} \\ A = \frac{1}{\frac{g_f}{\left(r_k^b\right)_0^2} - \frac{1}{2}} \end{array} \right. ; \quad (5.71)$$

where the parameter g_f represents the fracture energy, one characteristic of the material.

5.5 Local, plastic and global damage indexes

5.5.1 Local damage index

The idea for the local damage index definition stemmed from a macroscale analogy with the concentrated damage model definition. Thus, the starting point for deducing the local damage index is by the assumptions that we can express the free energy Ψ_b of a member with the non-damaged free energy Ψ_b^0 , defined in equation (5.57), as:

$$\Psi_b = (1 - D_b^L) \Psi_b^0 \quad (5.72)$$

where D_b^L is the local damage index. The free energy Ψ_b of a member can be defined in terms of the concentrated damage vector $\{\mathbf{D}_b\}$ as

$$\Psi_b(\mathbf{D}_b) = \frac{1}{2} \{\Phi_b\} : [\mathbf{S}_b^d(\mathbf{D}_b)] : \{\Phi_b\} \quad (5.73)$$

considering

$$[\mathbf{S}_b^d(\mathbf{D}_b)] : \{\Phi_b\} \cong \begin{cases} (1-d_i)m_i \\ (1-d_i)m_i \\ (1-d_i)m_i \end{cases} \quad (5.74)$$

and using (5.59) and (5.74), equation (5.73) can be rewritten as

$$\Psi_b(\mathbf{D}_b) = (1-d_i)\Psi_i^0 + (1-d_j)\Psi_j^0 + (1-d_a)\Psi_\delta^0 \quad (5.75)$$

Solving (5.72) for D_b^L , we obtain

$$D_b^L = 1 - \frac{\Psi_b(\mathbf{D}_b)}{\Psi_b^0} = 1 - \frac{(1-d_i)\Psi_i^0 + (1-d_j)\Psi_j^0 + (1-d_a)\Psi_\delta^0}{\Psi_i^0 + \Psi_j^0 + \Psi_\delta^0} \quad (5.76)$$

$$D_b^L = \frac{d_i\Psi_i^0 + d_j\Psi_j^0 + d_a\Psi_\delta^0}{\Psi_i^0 + \Psi_j^0 + \Psi_\delta^0} \quad (5.77)$$

this is the expression for local damage index for a frame member.

5.5.2 Plastic Damage index

The idea for the plastic damage index for a frame member follows the same idea of the local damage definition. However, the purpose of the plastic damage index is to indicate the plastic state in the member by means of the evolution of the plasticity in the hinges. Thus, the starting point for deducing the plastic damage index is by the assumptions that we can express the free energy due to plasticity Ψ_b^P of a member with the non-damaged free energy Ψ_b^0 , defined in equation (5.57), as:

$$\Psi_b^P = (1-D_b^P)\Psi_b^0 \quad (5.78)$$

where D_b^P is the plastic damage index. The free energy Ψ_b^P of a member can be defined in terms of the generalized plastic deformations vector $\{\Phi_b^P\}$ as

$$\Psi_b^P(\Phi_b^P) = \frac{1}{2}(\{\Phi_b\} - \{\Phi_b^P\}) : [\mathbf{S}_b^e] : (\{\Phi_b\} - \{\Phi_b^P\}) \quad (5.79)$$

Solving (5.72) for D_b^P , we obtain

$$D_b^P = 1 - \frac{\Psi_b^P(\Phi_b^P)}{\Psi_b^0} \quad (5.80)$$

which is the expression for plastic damage index for a frame member.

5.5.3 Global damage index

The global damage index can be defined as the sum of all free energy Ψ_b of a structure divided by the sum of the non-damaged free energy Ψ_b^0

$$D_G = 1 - \frac{\sum_{b=1}^{3n} \Psi_b(\mathbf{D}_b)}{\sum_{b=1}^{3n} \Psi_b^0} = 1 - \frac{\sum_{b=1}^{3n} \{\Phi_b\} : [\mathbf{S}_b^d(\mathbf{D}_b)] : \{\Phi_b\}}{\sum_{b=1}^{3n} \{\Phi_b\} : [\mathbf{S}_b^e] : \{\Phi_b\}} \quad (5.81)$$

where D_G is the global damage index. Replacing $[\mathbf{S}_b^e]\{\Phi_b\} = \{\bar{\mathbf{M}}_b\}$, as well as $[\mathbf{S}_b^d(\mathbf{D}_b)]\{\Phi_b\} = \{\mathbf{M}_b\}$, and assuming that $\{\Phi_b\}^T = \{\mathbf{U}\}^T[\mathbf{B}_b]$, equation (5.81) becomes

$$D_G = 1 - \frac{\sum_{b=1}^{3n} \{\Phi_b\} : [\mathbf{S}_b^d(\mathbf{D}_b)] : \{\Phi_b\}}{\sum_{b=1}^{3n} \{\Phi_b\} : [\mathbf{S}_b^e] : \{\Phi_b\}} = 1 - \frac{\sum_{b=1}^{3n} \{\Phi_b\}^T \{\mathbf{M}_b\}}{\sum_{b=1}^{3n} \{\Phi_b\}^T \{\bar{\mathbf{M}}_b\}} = 1 - \frac{\{\mathbf{U}\}^T \sum_{b=1}^{3n} [\mathbf{B}_b]^T \{\mathbf{M}_b\}}{\{\mathbf{U}\}^T \sum_{b=1}^{3n} [\mathbf{B}_b]^T \{\bar{\mathbf{M}}_b\}} \quad (5.82)$$

$$D_G = 1 - \frac{\{\mathbf{U}\}^T \{\mathbf{F}_{int}^D\}}{\{\mathbf{U}\}^T \{\mathbf{F}_{int}\}} \quad (5.83)$$

where $\{\mathbf{F}_{int}\}$ is the linear internal forces vector should the material preserve its original characteristics and undergo the actual deformation, and $\{\mathbf{F}_{int}^D\}$ is the nonlinear internal forces vector in the actual deformation. This global damage index is similar to that proposed by Barbat *et al.* (1998) and by Hanganu *et al.* (2002) for finite element analysis. The global damage index, as well as local and plastic damage indexes, is basically a tool for assessing the state of a structure. The local damage index refers only to the damaged state of a member, while the plastic damage index refers only to the evolution of the plasticity in the hinges. However, the global damage index gives a measure of the structural stiffness loss, since the nonlinear internal forces $\{\mathbf{F}_{int}^D\}$ can be influenced not only by the damage but also by the plasticity.

5.6 Integration of the constitutive equation

One of advantages of the model proposed above it is that the evolution of the damages parameters can be obtained in the explicit way, without the necessity of using some interactive method to arrive at the solution. Table 5.1 describes the integration algorithm implemented in our program.

Table 5.1 – Procedure to the determination of the evolution of the damage parameters.

-
- For each b elements at n th+1 iteration at the time t :
- 8) Generalized deformations at the step: $\{\Phi_b\}_t^{(n+1)} = \{\Phi_b\}_t^{(n)} + \{\Delta\Phi_b\}_t^{(n+1)}$
 - 9) Update of internal variables:
 - a) $\{\mathbf{D}_b\}_t^{n+1} = \{\mathbf{D}_b\}_t^n$
 - b) $\{\mathbf{r}_b\}_t^{n+1} = \{\mathbf{r}_b\}_t^n$
 - 10) Determination of the undamaged energy norm vector:
 - a) $\{\tau_\Phi^b\} = \sqrt{\{\Phi_b\}_t^{n+1} : [\mathbf{S}_b] : \{\Phi_b\}_t^{n+1}}$
 - 11) Verification of the evolution of the damage:
 - a) If $\underbrace{g\left(\{\tau_\Phi^b\}, \{\mathbf{r}_b\}_t^{n+1}\right)}_{\substack{g_i(\tau_i, (r_i)^{n+1}) \leq 0 \quad g_j(\tau_j, (r_j)^{n+1}) \leq 0 \quad g_\delta(\tau_\delta, (r_\delta)^{n+1}) \leq 0}} \leq 0$, no damage evolution, go to 14)
 - 12) Update of damage variable
 - a) $\underbrace{\{\mathbf{D}_b\}_t^{n+1} = G\left(\{\tau_\Phi^b\}\right)}_{\substack{d_i=G(\tau_i) \quad d_j=G(\tau_j) \quad d_\delta=G(\tau_\delta)}}$
 - 13) Update of damage threshold
 - a) $\underbrace{\{\mathbf{r}_b\}_t^{n+1} = \{\tau_\Phi^b\}}_{\substack{(r_i)^{n+1}=\tau_i \quad (r_j)^{n+1}=\tau_j \quad (r_\delta)^{n+1}=\tau_\delta}}$
 - 14) Achievement of the final generalized stress and the local damage on the step $n+1$
 - a) $\{\mathbf{M}_b\}_t^{n+1} = [\mathbf{S}_b (\mathbf{D}_b)_t^{n+1}] \{\Phi_b\}_t^{n+1}$, $(D_b^L)_t^{n+1} = 1 - \frac{\{\Phi_b\}_t^{n+1T} \{\mathbf{M}_b\}_t^{n+1}}{\{\Phi_b\}_t^{n+1} : [\mathbf{S}_b] : \{\Phi_b\}_t^{n+1}}$
 - 15) End of integration process of the constitutive equation.
-

5.7 Unilateral damage model

In some materials, especially the geomaterials, under cycling loads, parts of the microcracks may close or remain stable, while other microcracks open or remain growing. This is often the case for brittle materials, such as concrete, where the cracks due to the positive bending moments tend to close up, when there is an alteration in the sign of the bending moment, as shown in Figure 5..

With the aim of representing this behaviour in a simplified way, we use the same procedure for the unilateral damage model described in the Continuum

Damage theory (Lemaitre and Lippmann (1996)). For this reason, we now introduce two concentrated damage vectors, as proposed by Flórez-López (1999):

$$\{\mathbf{D}^+\} = \begin{Bmatrix} d_i^+ \\ d_j^+ \\ d_a^+ \end{Bmatrix} ; \quad \{\mathbf{D}^-\} = \begin{Bmatrix} d_i^- \\ d_j^- \\ d_a^- \end{Bmatrix}; \quad (5.84)$$

here the superscripts + and – indicate the damage due to the positive bending moments and positive (traction) axial force, and the damage due to the negative bending moments and negative (compression) axial force, respectively.

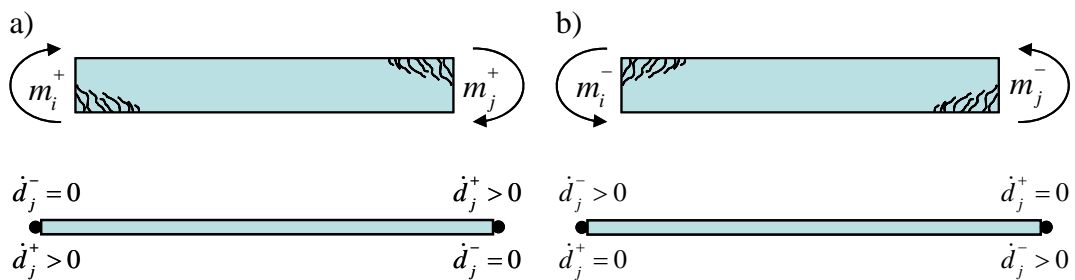


Figure 5.6 – Unilateral damage model, the damage evolution at hinges i and j : a) due to positive actions at hinges, b) due to negative actions at hinges.

Under positive loads, only the positive damage parameters can increase, Figure 5.a, while the negative damage parameters remain constant, or vice-versa. This occurs because of the assumption that the flexural damage due to positive actions has no influence on the behaviour of the member under negative actions.

This assumption can be justified by the observation that in some reinforced concrete elements, when the loading changes sign, the cracks tend to close. As in the case of Continuum Mechanics, this assumption must be considered as an idealization of the real behaviour of a reinforced concrete member.

Thus, we assume that the flexure cracks in the concrete due to a bending moment, positive or negative, will have no influence on the behaviour of the member after the closure of these cracks when the moment changes sign. Therefore, the equation (5.34) can be generalized as a function of the two concentrated damage vectors, and if the flexibility matrix can be defined as a function of the concentrated damage vector, we obtain:

$$\{\Phi\} = [\mathbf{F}(\mathbf{D}^+)] \langle [\mathbf{M}] \rangle^+ + [\mathbf{F}(\mathbf{D}^-)] \langle [\mathbf{M}] \rangle^-; \quad (5.85)$$

where $[\mathbf{F}^d]$ is the same matrix defined in (5.33), while $\langle[\mathbf{M}]\rangle^+$ and $\langle[\mathbf{M}]\rangle^-$ represent the positive and negative values of the generalized stress, respectively, in such a way that

$$\underbrace{\langle[\mathbf{M}]\rangle^+}_{\begin{Bmatrix} \langle m_i \rangle^+ \\ \langle m_j \rangle^+ \\ \langle n \rangle^+ \end{Bmatrix}} = \begin{cases} \langle m_i \rangle^+ = \begin{cases} m_i & \text{if } m_i \geq 0 \\ 0 & \text{if } m_i < 0 \end{cases} \\ \langle m_j \rangle^+ = \begin{cases} m_j & \text{if } m_j \geq 0 \\ 0 & \text{if } m_j < 0 \end{cases} \\ \langle n \rangle^+ = \begin{cases} n & \text{if } n \geq 0 \\ 0 & \text{if } n < 0 \end{cases} \end{cases} ; \quad \underbrace{\langle[\mathbf{M}]\rangle^-}_{\begin{Bmatrix} \langle m_i \rangle^- \\ \langle m_j \rangle^- \\ \langle n \rangle^- \end{Bmatrix}} = \begin{cases} \langle m_i \rangle^- = \begin{cases} m_i & \text{if } m_i \leq 0 \\ 0 & \text{if } m_i > 0 \end{cases} \\ \langle m_j \rangle^- = \begin{cases} m_j & \text{if } m_j \leq 0 \\ 0 & \text{if } m_j > 0 \end{cases} \\ \langle n \rangle^- = \begin{cases} n & \text{if } n \leq 0 \\ 0 & \text{if } n > 0 \end{cases} \end{cases} ; \quad (5.86)$$

5.7.1 Undamaged energy norm and damage evolution for unilateral damage

Before we define the evolution of the damage parameters for the unilateral damage case, it is necessary to redefine some variables in terms of the generalized effective stress $\{\bar{\mathbf{M}}\}$.

The free energy Ψ^0 , instead of that proposed in 5.4.4, can be redefined as a function of the generalized effective stress $\{\bar{\mathbf{M}}\}$ as

$$\left. \begin{aligned} \{\bar{\mathbf{M}}\} &= [\mathbf{S}^e] : \{\Phi\} \\ \{\Phi\} &= [\mathbf{F}^e] \{\mathbf{M}\} \end{aligned} \right\} \Psi_{\mathbf{M}}^0 = \frac{1}{2} \{\Phi\} : [\mathbf{S}^e] : \{\Phi\} = \frac{1}{2} \{\Phi\} : \{\bar{\mathbf{M}}\} = \frac{1}{2} \{\bar{\mathbf{M}}\} : [\mathbf{F}^e] : \{\bar{\mathbf{M}}\}; \quad (5.87)$$

$$\Psi_{\mathbf{M}}^0 = \frac{1}{2} \left(\frac{L}{3EI} m_i - \frac{L}{6EI} m_j \right) m_i + \frac{1}{2} \left(\frac{L}{3EI} m_j - \frac{L}{6EI} m_i \right) m_j + \frac{1}{2} \frac{L}{EA} n^2; \quad (5.88)$$

here the subscript \mathbf{M} indicates that the variable is defined in terms of the generalized stress vector $\{\mathbf{M}\}$, and $[\mathbf{F}^e] = [\mathbf{S}^e]^{-1}$ is the elastic flexibility matrix. The expression (5.88) can be expressed using the same idea used in (5.58), which consists in assuming that the free energy can be defined as the sum of the energies obtained due, in this case, to the bending moments m_i and m_j plus the axial force n , so

$$\Psi_{\mathbf{M}}^0 = \Psi_{m_i}^0 + \Psi_{m_j}^0 + \Psi_n^0, \text{ where} \quad (5.89)$$

$$\Psi_{m_i}^0 = \frac{1}{2} \left(\frac{L}{3EI} m_i - \frac{L}{6EI} m_j \right) m_i; \quad \Psi_{m_j}^0 = \frac{1}{2} \left(\frac{L}{3EI} m_j - \frac{L}{6EI} m_i \right) m_j; \quad \Psi_n^0 = \frac{1}{2} \frac{L}{EA} n^2$$

Therefore, undamaged energy norm vector τ^b of a b element will be redefined in the same way as the free energy; that is, as a function of the bending moments m_i and m_j by the axial force n

$$\{\tau_{\mathbf{M}}^b\} = \sqrt{2\{\Psi_{\mathbf{M}}^0\}} \begin{cases} \tau_{m_i} = \sqrt{2\Psi_{m_i}^0} = \sqrt{\left(\frac{L}{3EI}m_i - \frac{L}{6EI}m_j\right)m_i} \\ \tau_{m_j} = \sqrt{2\Psi_{m_j}^0} = \sqrt{\Psi_{m_j}^0} = \left(\frac{L}{3EI}m_j - \frac{L}{6EI}m_i\right)m_j \\ \tau_n = \sqrt{2\Psi_n^0} = \sqrt{\frac{L}{EA}n^2} \end{cases} \quad (5.90)$$

Because in unilateral damage it is necessary to take into account the sign of the efforts, the equation (5.90) must be expressed in terms of the sign of the generalized stress, as defined in (5.85), as

$$\begin{aligned} \{\tau_{\mathbf{M}}^b\}^+ &= \sqrt{\langle\{\bar{\mathbf{M}}_b\}\rangle^+ : [\mathbf{F}_b^e] : \langle\{\bar{\mathbf{M}}_b\}\rangle^+} \\ \{\tau_{\mathbf{M}}^b\}^- &= \sqrt{\langle\{\bar{\mathbf{M}}_b\}\rangle^- : [\mathbf{F}_b^e] : \langle\{\bar{\mathbf{M}}_b\}\rangle^-} \end{aligned} \quad (5.91)$$

The damage criterion must also be redefined in two terms: one due to the positive norm vector $\{\tau_{\{\mathbf{M}\}}^b\}^+$, and other in terms of the negative norm vector $\{\tau_{\{\mathbf{M}\}}^b\}^-$, at the time t is:

$$g\left(\{\tau_{\mathbf{M}}^b\}^+, \{r_t^b\}^+\right)_t \quad ; \quad g\left(\{\tau_{\mathbf{M}}^b\}^-, \{r_t^b\}^-\right)_t \quad (5.92)$$

$$\begin{aligned} g_i\left(\left(\tau_{m_i}^b\right)_t^+, \left(r_i^b\right)_t^+\right) &= \left(\tau_{m_i}^b\right)_t^+ - \left(r_i^b\right)_t^+ \leq 0 & g_i\left(\left(\tau_{m_i}^b\right)_t^-, \left(r_i^b\right)_t^-\right) &= \left(\tau_{m_i}^b\right)_t^- - \left(r_i^b\right)_t^- \leq 0 \\ g_j\left(\left(\tau_{m_j}^b\right)_t^+, \left(r_j^b\right)_t^+\right) &= \left(\tau_{m_j}^b\right)_t^+ - \left(r_j^b\right)_t^+ \leq 0; & g_j\left(\left(\tau_{m_j}^b\right)_t^-, \left(r_j^b\right)_t^-\right) &= \left(\tau_{m_j}^b\right)_t^- - \left(r_j^b\right)_t^- \leq 0 \\ g_n\left(\left(\tau_n^b\right)_t^+, \left(r_n^b\right)_t^+\right) &= \left(\tau_n^b\right)_t^+ - \left(r_n^b\right)_t^+ \leq 0 & g_n\left(\left(\tau_n^b\right)_t^-, \left(r_n^b\right)_t^-\right) &= \left(\tau_n^b\right)_t^- - \left(r_n^b\right)_t^- \leq 0 \end{aligned} \quad (5.93)$$

while the evolution of the threshold vectors $\{r_t^b\}^+$ and $\{r_t^b\}^-$ are defined using the same proposition (5.68):

$$\left\{ r_t^b \right\}^+ = \max \left\{ \left\{ r_0^b \right\}^+, \max_{s \in (0,t)} \left(\left\{ \tau_M^b \right\}^+ \right)_s \right\}; \left\{ r_t^b \right\}^- = \max \left\{ \left\{ r_0^b \right\}^-, \max_{s \in (0,t)} \left(\left\{ \tau_M^b \right\}^- \right)_s \right\}$$

$$\begin{aligned} & \max \left\{ \left(r_t^b \right)_0^+, \max_{s \in (0,t)} \left(r_t^b \right)_s^+ \right\} & \max \left\{ \left(r_t^b \right)_0^-, \max_{s \in (0,t)} \left(r_t^b \right)_s^- \right\} \\ & \max \left\{ \left(r_j^b \right)_0^+, \max_{s \in (0,t)} \left(r_j^b \right)_s^+ \right\} & \max \left\{ \left(r_j^b \right)_0^-, \max_{s \in (0,t)} \left(r_j^b \right)_s^- \right\} \\ & \max \left\{ \left(r_n^b \right)_0^+, \max_{s \in (0,t)} \left(r_n^b \right)_s^+ \right\} & \max \left\{ \left(r_n^b \right)_0^-, \max_{s \in (0,t)} \left(r_n^b \right)_s^- \right\} \end{aligned} \quad (5.94)$$

and the initial threshold vectors $\{r_0^b\}^+$ and $\{r_0^b\}^-$ can be obtained as

$$\begin{aligned} \left\{ r_0^b \right\}^+ &= \sqrt{\left\{ \mathbf{M}_y^+ \right\} : \left[\mathbf{F}_b^e \right] : \left\{ \mathbf{M}_y^+ \right\}} \\ \left\{ r_0^b \right\}^- &= \sqrt{\left\{ \mathbf{M}_y^- \right\} : \left[\mathbf{F}_b^e \right] : \left\{ \mathbf{M}_y^- \right\}} \end{aligned} \quad (5.95)$$

where the vectors $\{\mathbf{M}_y^+\}^T = \{m_y^+ \quad m_y^+ \quad n_y^+\}$, and $\{\mathbf{M}_y^-\}^T = \{m_y^- \quad m_y^- \quad n_y^-\}$ represent the yield limits positive and negative, respectively, of a beam-column element. In some materials the bending moments yield limits positive and negative, in absolute terms, can be the same, $|m_y^+| = |m_y^-|$. This often occurs in reinforced concrete structures.

At this moment, the evolution of the damage can be obtained by:

$$\left\{ \mathbf{D}_b^+ \right\} = G \left(\left\{ r_t^b \right\}^+ \right) = 1 - \frac{q \left(\left\{ r_t^b \right\}^+ \right)}{\left\{ r_t^b \right\}^+} ; \quad \left\{ \mathbf{D}_b^- \right\} = G \left(\left\{ r_t^b \right\}^- \right) = 1 - \frac{q \left(\left\{ r_t^b \right\}^- \right)}{\left\{ r_t^b \right\}^-} \quad (5.96)$$

$$\begin{aligned} d_i^- = 1 - \frac{q \left(\left\{ r_t^b \right\}_t^+ \right)}{\left\{ r_t^b \right\}_t^+} ; & d_j^- = 1 - \frac{q \left(\left\{ r_j^b \right\}_t^+ \right)}{\left\{ r_j^b \right\}_t^+} ; & d_a^- = 1 - \frac{q \left(\left\{ r_n^b \right\}_t^+ \right)}{\left\{ r_n^b \right\}_t^+} & d_i^- = 1 - \frac{q \left(\left\{ r_t^b \right\}_t^- \right)}{\left\{ r_t^b \right\}_t^-} ; & d_j^- = 1 - \frac{q \left(\left\{ r_j^b \right\}_t^- \right)}{\left\{ r_j^b \right\}_t^-} ; & d_a^- = 1 - \frac{q \left(\left\{ r_n^b \right\}_t^- \right)}{\left\{ r_n^b \right\}_t^-} \end{aligned}$$

where the function $G(r) = 1 - \frac{q(r)}{r}$ can be the same damage function defined in (5.71), or by another damage function, as proposed in (Luccioni, 2003). Usually, the positive and negative damage evolutions can be obtained by the same function.

5.7.2 Integration of the constitutive equation for unilateral damage

Following the same procedure presented in 5.6 for the isotropic damage, Table 5.2 describes the integration algorithm implemented in our program. The only difference between the procedures described in 5.6 is the inclusion of the negative damage evolution in the analysis.

Table 5.2 – Procedure to determine of the evolution of the damage parameters for the unilateral damage.

-
- For each b elements at n th+1 iteration at the time t :
- 1) Generalized deformations at the step: $\{\Phi_b\}_t^{(n+1)} = \{\Phi_b\}_t^{(n)} + \{\Delta\Phi_b\}_t^{(n+1)}$
 - 2) Calculation of the effective stress vector $\{\bar{\mathbf{M}}_b\}_t^{(n+1)} = [\mathbf{S}_b^e] \{\Phi_b\}_t^{(n+1)}$
 - 3) Update of internal variables:
 - a) $\{\mathbf{D}_b^+\}_t^{n+1} = \{\mathbf{D}_b^+\}_t^n ; \{\mathbf{D}_b^-\}_t^{n+1} = \{\mathbf{D}_b^-\}_t^n$
 - b) $\{\mathbf{r}_b^+\}_t^{n+1} = \{\mathbf{r}_b^+\}_t^n ; \{\mathbf{r}_b^-\}_t^{n+1} = \{\mathbf{r}_b^-\}_t^n$
 - 4) Determination of the undamaged energy norm vector:
 - a) $\{\tau_M^b\}^+ = \sqrt{\langle \{\bar{\mathbf{M}}_b\}^+ : [\mathbf{F}_b^e] : \{\bar{\mathbf{M}}_b\}^+ \rangle} ; \{\tau_M^b\}^- = \sqrt{\langle \{\bar{\mathbf{M}}_b\}^- : [\mathbf{F}_b^e] : \{\bar{\mathbf{M}}_b\}^- \rangle}$
 - 5) Verification of the evolution of the damage:
 - a) If $\underbrace{g\left(\{\tau_M^b\}^+, \{\mathbf{r}_b^+\}_t^{n+1}\right) \leq 0}_{g_i(\tau_i^+, r_i^+)_t^{n+1} \leq 0 \quad g_j(\tau_j^+, r_j^+)_t^{n+1} \leq 0 \quad g_n(\tau_n^+, r_n^+)_t^{n+1} \leq 0}$ and $\underbrace{g\left(\{\tau_M^b\}^-, \{\mathbf{r}_b^-\}_t^{n+1}\right) \leq 0}_{g_i(\tau_i^-, r_i^-)_t^{n+1} \leq 0 \quad g_j(\tau_j^-, r_j^-)_t^{n+1} \leq 0 \quad g_n(\tau_n^-, r_n^-)_t^{n+1} \leq 0}$, no damage evolution, go to 8)
 - 6) Update of damage variable
 - a) $\underbrace{\{\mathbf{D}_b^+\}_t^{n+1} = G\left(\{\tau_M^b\}^+\right)}_{d_i^+ = G(\tau_i^+) \quad d_j^+ = G(\tau_j^+) \quad d_n^+ = G(\tau_n^+)} ; \underbrace{\{\mathbf{D}_b^-\}_t^{n+1} = G\left(\{\tau_M^b\}^-\right)}_{d_i^- = G(\tau_i^-) \quad d_j^- = G(\tau_j^-) \quad d_n^- = G(\tau_n^-)}$
 - 7) Update of damage threshold
 - a) $\underbrace{\{\mathbf{r}_b^+\}_t^{n+1} = \{\tau_\Phi^b\}^+}_{(r_i^+)_t^{n+1} = \tau_i^+ \quad (r_j^+)_t^{n+1} = \tau_j^+ \quad (r_n^+)_t^{n+1} = \tau_n^+} ; \underbrace{\{\mathbf{r}_b^-\}_t^{n+1} = \{\tau_\Phi^b\}^-}_{(r_i^-)_t^{n+1} = \tau_i^- \quad (r_j^-)_t^{n+1} = \tau_j^- \quad (r_n^-)_t^{n+1} = \tau_n^-}$
 - 8) Achievement of the final generalized stress and the local damage on the step $n+1$
 - a) $\{\mathbf{M}_b\}_t^{n+1} = [\mathbf{S}_b(\mathbf{D}_b^+)_t^{n+1}] \langle \{\Phi_b\}_t^{n+1} \rangle^+ + [\mathbf{S}_b(\mathbf{D}_b^-)_t^{n+1}] \langle \{\Phi_b\}_t^{n+1} \rangle^- ; (D_b^L)_t^{n+1} = 1 - \frac{\{\Phi_b\}_t^{n+1T} \{\mathbf{M}_b\}_t^{n+1}}{\{\Phi_b\}_t^{n+1} : [\mathbf{S}_b] : \{\Phi_b\}_t^{n+1}}$
 - 9) End of integration process of the constitutive equation.
-

Chapter 6

Elastoplastic-Damage

Model for Frames

6.1 Introduction

Plasticity theory and damage theory can be used separately to represent the behaviour of the structure, especially if the structure is made of only one material, such as steel. However, there are some cases where the elements are made of reinforced concrete, where either the plasticity theory or damage theory are sufficient to represent the real behaviour.

They indeed fail to reproduce the unloading slopes during cyclic loads, which define experimentally the value of the damage in the material. This occurs because plasticity theory does not take into account the degradation of the stiffness of the element, while the damage theory does not take into account the residual deformations. In reinforced concrete, the plasticity usually is physically re-

lated with the steel yielding, while the damage is the measure of the cracking in the concrete, only at very high loads, when the concrete crushing, the damage in steel began.

In this chapter, we discuss the behaviour of reinforced concrete structures, followed by the description of one plastic-damage model for reinforced concrete frame structure, based on the isotropic damage model of Simo and Ju (1987). Our assumption is that the damage will rule the behaviour of the concrete, while the plasticity will control the steel yielding, and the beam-columns will be designed using the ultimate load conditions.

6.2 Characteristics of Reinforced Concrete Behaviour

Reinforced concrete elements are designed to carry three types of loads, namely, axial force, bending moment, and shearing force. Axial compressive loads are associated with columns, piles, and foundation walls, and tensile forces may be introduced into members because of restrained shrinkage. Bending moments occur in a member supported at discrete points and subjected to loads that are transverse to the longitudinal axis of the member. Shearing forces arise from transverse loads or from torsional moments. In designing a member to assure adequate safety, the engineer considers all the foreseeable loads that may occur during the service life of the structure.

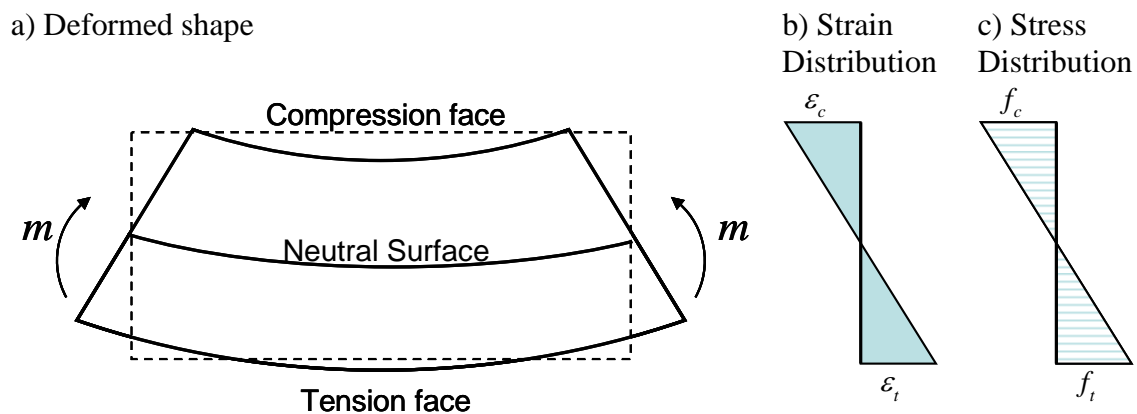


Figure 6.1 – Pure bending of a beam.

To gain an understanding of the cracking expected under service loads, the flexural behaviour of a reinforced concrete member is discussed. Figure 6.1.a is a side view of a segment of a beam subjected to a constant bending moment (pure bending). For the direction of the bending moment shown in the figure, the top half of the beam is subjected to compression and the bottom half is subjected to

tension. There is a plane in the beam, which is not strained, and this is known as the neutral surface. The intersection of the neutral surface with a cross section defines the neutral axis. A fundamental assumption of Timoshenko's bending theory is that plane sections remain plane. Thus, the ends of the beam remain plane under the action of the bending moment, and this results in a linear variation of strain with distance from the neutral axis, Figure 6.1.b. The maximum compressive strain, ε_c , occurs at the top surface of the beam, and the maximum tensile strain, ε_t , occurs at the bottom surface. If the beam is made of a linear-elastic material, that is, a material for which stress is proportional to strain, there is also a linear stress distribution over the depth of the beam, as shown in Figure 6.1.c.

The assumption of a linear strain distribution is fundamental in analyzing the behaviour of a reinforced concrete beam as the bending moment is increased up to the ultimate strength of the beam. This assumption, along with the stress-strain curves of the concrete (Figure 6.2.a) and steel (Figure 6.2.b), permit determination of the stress distribution in the beam.

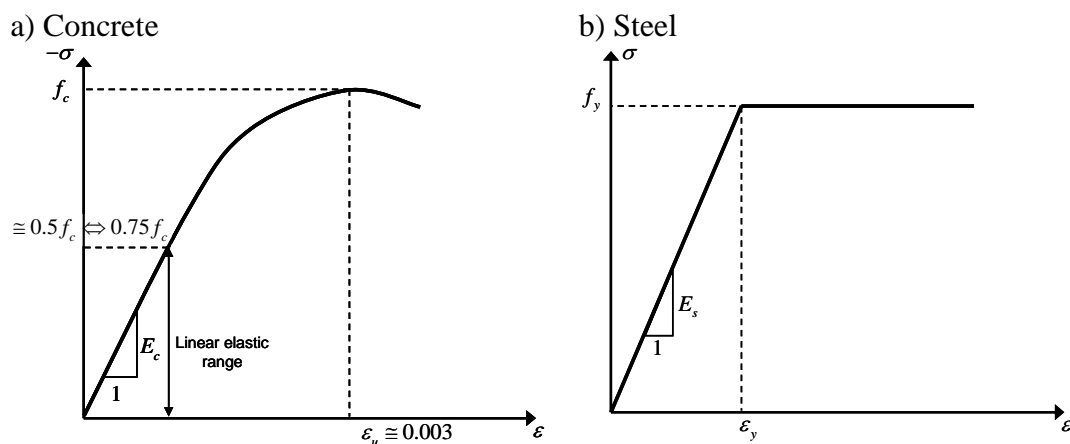


Figure 6.2 – Schematic stress-strain curves of concrete and steel.

We can illustrate the characteristics of reinforced concrete behaviour by a typical load-displacement relationship, as shown in Figure 6.3. This relationship can be the result of a beam test, for example. Similar diagrams can be obtained for load-deformation relations of any other reinforced concrete structures, although that is not unique because it depends on the test conditions and the nature of the materials that make up the concrete.

As proposed by Chen (1982), this highly nonlinear relationship can be roughly divided into three intervals: the uncracked elastic stage (phase *I* at Figure 6.3), crack propagation (the stress is within the elastic range, phase *II*) and plastic stage (the beam reaches its ultimate strength, phase *III*). The nonlinear re-

sponse is caused by the two major material effects, cracking of the concrete and plasticity of the reinforcement and of the compression concrete.

In design, it is often assumed that concrete fails in compression when it reaches a compressive strain of $\varepsilon_c = 0.003$. Compressive failure occurs by formation of cracks parallel to the loading direction, and is referred to as “splitting failure” (CEB (1998)). The steel is assumed to have a linear stress-strain relation until the yield stress, f_y , is attained. After the yield stress is attained, it is assumed that the stress in the steel remains constant as the strain increases, that is, strain hardening is neglected. The steel tensile strain corresponding to the onset of yielding is ε_y .

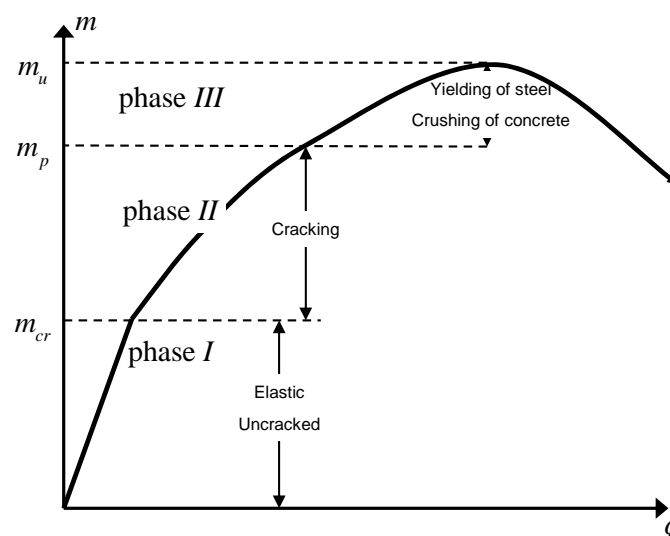


Figure 6.3 – Typical moment-deformation of reinforced concrete structure: phase I and II define the serviceability limit states; phase III defines the ultimate state.

Let us now analyze separately the three principal stages of the flexural behaviour.

6.2.1 Uncracked section

Figure 6.4 shows a rectangular reinforced concrete beam subjected to a bending moment. The total area of reinforcing bars at a distance d from the compression face is A_s . It is assumed that there is complete bond between the concrete and steel, which means that the steel and concrete experience the same strain. Provided the maximum tensile stress in the concrete is less than the modulus of rupture (the maximum tensile stress at cracking of an unreinforced concrete beam), the entire section of the beam acts to resist the bending moment. The tensile stress in the steel bars is greater than the tensile stress in the concrete at the same depth because the steel has a larger modulus of elasticity (ratio of stress to

strain in the elastic range). Since the steel and concrete experience the same strain, the ratio of stresses equals the modular ratio, $n = \frac{E_s}{E_c}$, which is the ratio of the modulus of elasticity of the steel E_s to that of the concrete E_c . For ordinary strength concrete, this ratio is approximately eight. For the purpose of analysis, Park and Paulay (1975) assumes that the steel bars can be replaced by an area of concrete equal to nA_s , which allows the composite beam to be represented as an equivalent beam made entirely of concrete. The elastic bending formula can be used to calculate the maximum compression and tensile stresses, f in the concrete:

$$f = \frac{My}{I_{uc}} \quad (6.1)$$

In equation (6.1), y is the distance from the neutral axis to the extreme face of the beam, and $I_{uc} = \int y^2 dA$, is the moment of inertia of the uncracked transformed cross section about the neutral axis. Figure 6.4 shows the strain and stress distribution in the beam during this stage. The stress in the steel is n times the stress computed using the bending formula, with a value of y equal to the distance from the neutral axis to the depth of the steel.

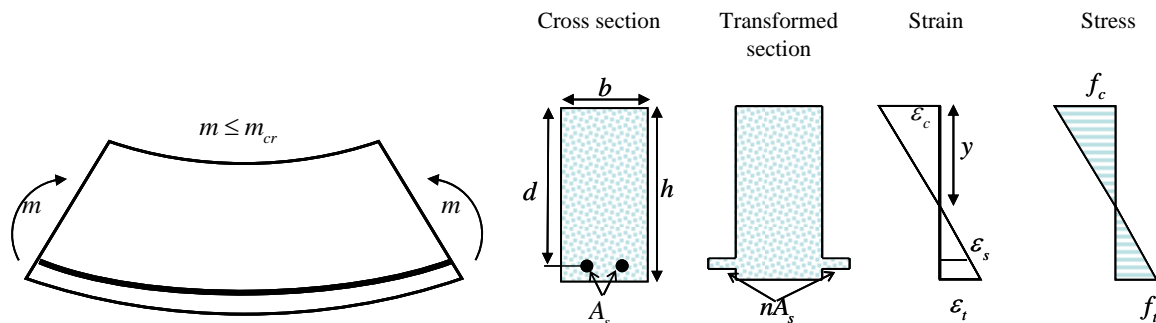


Figure 6.4 – Uncracked behaviour of reinforced concrete.

We can assume that the existence of one limit moment, the cracking moment $m_{cr} = \frac{f_c I_{uc}}{y}$, which indicates the beginning of the cracking at the tensile face usually $\frac{1}{6}$ to $\frac{1}{4}$ of the maximum service load. This moment can be calculated from the elastic bending formula, by setting the stress at tensile face f_c equal to the so-called modulus of rupture (flexural strength) of concrete f_r (Jirásek and Bazant (2002)) or f_t (using 'Comité Euro-International du Béton' (FIB) notation)

6.2.2 Crack propagation in the elastic section

The concrete cracks when the maximum tensile stress in the uncracked beam reaches the modulus of rupture. Cracks are assumed to extend from the tension face to the neutral surface, which is the same as assuming that the concrete below the neutral surface has zero tensile strength. After cracking, it is still assumed that plane sections remain plane, so that there is still a linear strain distribution through the depth of the beam. For analysis, the steel is replaced by an equivalent area of concrete equal to nA_s , so that the cracked transformed section is as shown in Figure 6.5.

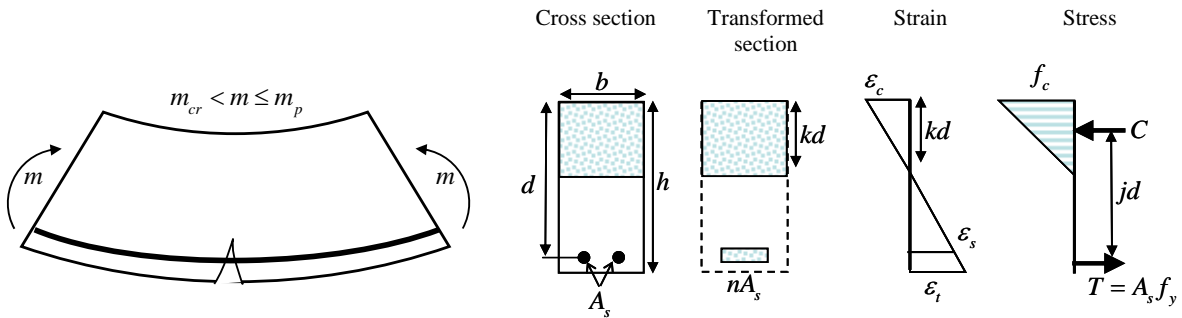


Figure 6.5 – Crack propagation within the elastic range.

When the crack develops, there is a sudden increase in the maximum stresses in the concrete and steel. However, for a properly designed beam these stresses will remain within the elastic ranges. The stress distribution in the concrete is as shown in Figure 6.5. The compressive stresses in the concrete can be replaced by an equivalent compressive force, C , passing through the centroid of the triangular stress distribution. The stresses in the steel can be replaced by a tensile force, $T = A_s f_y$, acting at the centre of the steel, where f_y (in American Concrete Institute (ACI) notation) is the uniaxial yield strength of the bars, and A_s the combined cross section area of all tensile steel bars. Equilibrium of forces requires that $C = T$, which establishes the depth of the neutral axis, kd , and the depth of the crack.

Another equilibrium condition, $m = jdT = jdC$, establishes the relationship between the bending moment and the maximum stresses in the steel and concrete. Under service loads, normally designed flexural members will be in this cracked, elastic condition. The maximum stresses in the concrete and steel at a particular cross section will depend on the bending moment produced by the applied loads. In actual structures, the bending moment varies along the length of a beam, and so the maximum stresses in the concrete and steel will also vary along the length. In addition, for beams (or slabs) that is continuous over one or more

supports, the direction of the bending moment changes in the vicinity of the support. As a result, cracking can also exist on the top face of a continuous beam.

As the bending moment increases above the cracking moment, the neutral axis remains at the same location, kd , provided that the maximum compressive stress in the concrete is within the linear elastic range and the steel stress is less than f_y , which results in the plastic moment limit, defined as

$$m_p = Tjd = A_s f_y jd \quad (6.2)$$

where jd is the distance from centroid of compressive forces in the steel and concrete to the centroid of tension.

The neutral axis moves toward to the compression face when the concrete stress goes beyond the linear elastic range. However, the strain distribution through the depth is still assumed to be linear. Consequently, the stress distributions in the concrete looks like the portion of the stress-strain curve up to the strain corresponding to the maximum strain on the compression face.

The design requirement is that $m_p \leq \phi_s m_u$, where is m_p the plastic moment defined in (6.2), $m_u = m_y$ is the ultimate (maximum) bending moment, and ϕ_s is the capacity reduction factor (or under strength factor), which can be assumed as $\phi_s = 0.9$ for the case of the bending (Jirásek and Bazant (2002))

6.2.3 Ultimate strength

As the bending moment is increased further, the neutral axis moves further toward the compressive face. In a properly designed member, the next key stage is yielding of the steel. This occurs when the strain at the level of the steel reaches ε_y . The bending moment can be increased further until the maximum compressive strain in the concrete reaches the assumed limiting value of $\varepsilon_c = 0.003$. The strain distribution at failure is shown in Figure 6.6. Because the steel has yielded, the steel stress is f_y and the steel provides a tensile force equal to $A_s f_y$. The tensile force is balanced by an equivalent compressive force in the concrete, which acts through the centroid of the concrete stress distribution. The balance of forces establishes the location of the neutral axis, c , and the ultimate moment equals $m_u = A_s f_y z$, where z is the distance between the tensile and compressive forces. At this stage, the concrete undergoes compressive failure and the beam is no longer able to support the applied moment.

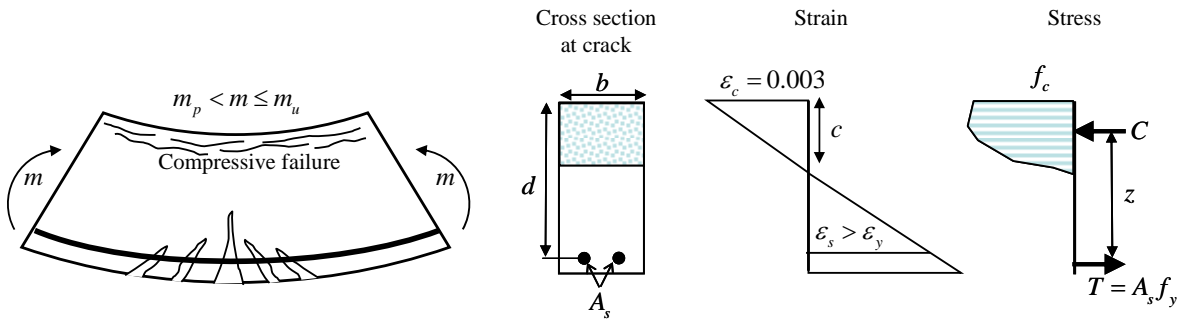


Figure 6.6 – Ultimate strength condition.

For example, analyzing a singly reinforced rectangular cross section of width b and depth d measured from the compression face to the centroid to steel bars, as shown in the Figure 6.7.

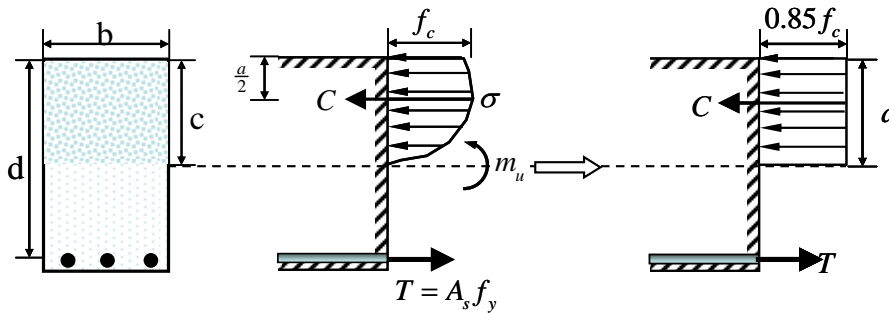


Figure 6.7 – Singly reinforced rectangular beam

Equilibrium of the horizontal forces requires that

$$\underbrace{0.85 f_c b a}_C = \underbrace{A_s f_y}_T \tag{6.3}$$

where, C is the compressive stresses in the concrete, replaced by an equivalent rectangular stress block having uniform stress magnitude and depth a , T is the tensile steel resultant, f_y is the uniaxial yield strength of the bars, and A_s the combined cross section area of all tensile steel bars. Thus (Jirásek and Bazant (2002)),

$$a = \frac{A_s f_y}{0.85 f_c b} \tag{6.4}$$

Since the distance of the resultant C of the compressive stresses in concrete from the tensile resultant T is $z = d - \frac{1}{2}a$, the ultimate plastic moment is

$$m_u = A_s f_y z = A_s f_y \left(d - \frac{1}{2} a \right) = A_s f_y \left(d - \frac{1}{2} \frac{A_s f_y}{0.85 f_c b} \right) \quad (6.5)$$

Equation (6.5) is valid only if the tensile steel yields before compressed concrete can be crushed. For those cases where the longitudinal reinforcing steel bars are placed near the compressed face of the beams (see Figure 6.8). If this compression steel, of combined cross section area A'_s , yields, the cross section can be analyzed as if the axial force from the yielding tensile steel, $A_s f_y$, is subdivided into two parts: $(A_s - A'_s) f_y$ that must balance the axial force in concrete, and part $A'_s f_y$ that balances the axial force in the yielding compression steel. So, to obtain the ultimate plastic moment, the equation (6.5) can be rewritten as:

$$m_u = 0.85 f_c b a \left(d - \frac{1}{2} a \right) + A'_s f_y (d - d') \quad (6.6)$$

where d' is the distance of the compression steel centroid from the tensile face, A'_s is the compression steel cross section area, and

$$a = \frac{(A_s - A'_s) f_y}{0.85 f_c b} \quad (6.7)$$

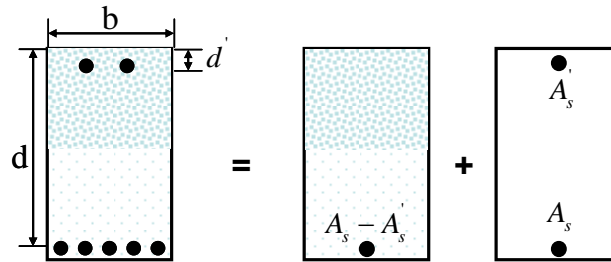


Figure 6.8 - Doubly reinforced rectangular cross section.

From now on, the ultimate plastic moment m_u (the maximum bending moment) will be used to determine the plastic limit behaviour of the column-beam element, while the critical bending moment m_{cr} will refer to the begins of the damage in the concrete.

Furthermore, the elastic modulus E can be calculated by using the Voigt homogenization hypothesis (Álvares (2004)), which supposes that all materials have a perfect adherence to each other, leading to the equivalent elastic modulus:

$$E = (1 - \rho)E_c + \rho E_s \quad (6.8)$$

where E_c and E_s are the elastic modulus of the concrete and steel, respectively, while $\rho = A_s/bd$ is the value of the steel ratio.

6.3 Plastic-Damage model

In the previous section, we demonstrated that the elastic damage models or elastic plastic laws are not sufficient to represent the constitutive behaviour of reinforced concrete. In some damage models, during the loading-unloading process, a zero stress corresponds to a zero strain and the value of the damage is thus overestimated (Figure 2.4b). An elastic plastic relation is not valid either, even with softening, (Figure 2.4a), as the unloading curve follows the elastic slope. A correct plastic-damage model should be one capable of representing the softening behaviour; the damage law reproduces the decreasing of the elastic modulus, while the plasticity effect accounts for the irreversible strains (Figure 2.4c).

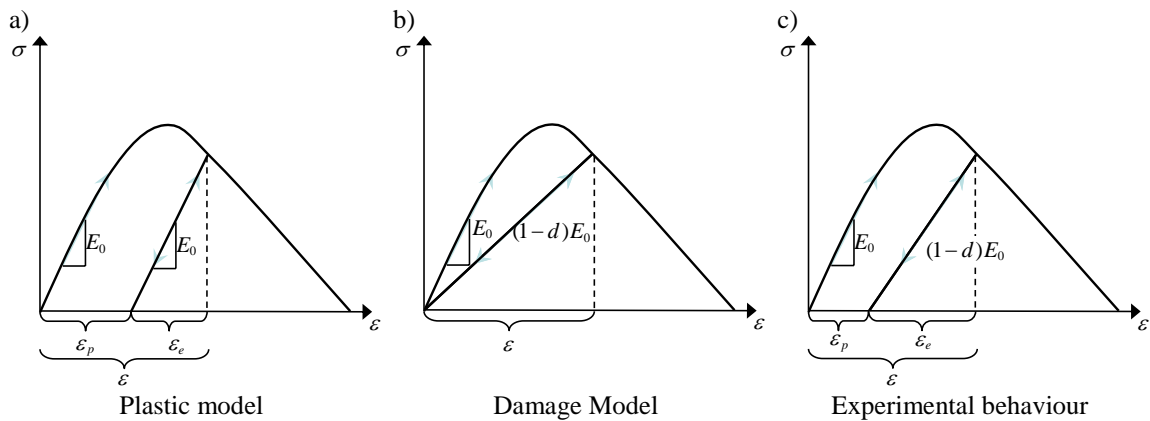


Figure 6.9 - Loading-unloading behaviour – Simulated behaviours and Experimental behaviour

Luccioni (2003) comment that there are three ways to represent this behaviour:

- In one of these ways, called a plastic-damage coupled model, the damage and the plastic are evaluated at the same time. In this case, the free energy can be expressed as the sum of elastic energy plus plastic energy, both of them influenced by the damage parameter.

$$\Psi = \Psi_e(\varepsilon, d) + \Psi_p(\lambda^p, d) \quad (6.9)$$

- Another option is that the free energy is now assumed as the sum of the elastic energy, plastic energy and one term dependent on the damage. The result is that the dissipation energy is influenced by the damage parameter as the plasticity parameter.

$$\begin{aligned}\Psi &= \Psi_e(\varepsilon, d) + \Psi_p(\lambda^p) + \Psi_d(\lambda^d) \\ \Xi_d &= \Psi \dot{d} - \lambda^p \lambda^d\end{aligned}\quad (6.10)$$

- The last option is to consider that the damage and plasticity are uncoupled and follow their own laws independently;

$$\Psi = \Psi_e(\varepsilon, d) + \Psi_p(\lambda^p) \quad (6.11)$$

This theory can be used when there are permanent deformations and have the advantage of allowing independent laws of plasticity and damage, but coupled through the effective tension concept.

6.3.1 Thermodynamic references

As commented before, in the concrete at reinforced concrete elements the damage effect modifies the constitutive plastic equation by the degradation of the stiffness, for small deformations. To determinate this brand new constitutive equation, formulated with no temperature time variation for thermodynamically stable problems, the following mathematical form for the free energy is assumed, constituted by one elastic term and by another plastic (Oller (2001b)):

$$\Psi(\Phi^e, \mathbf{D}, q^p, q^d) = \Psi^e(\Phi^e, \mathbf{D}, q^d) + \Psi^p(q^p) \quad (6.12)$$

where Ψ^p denotes a plastic potential function and $\Psi^e(\Phi^e, \mathbf{D}, q^d)$ is the initial elastic stored energy. Additionally, q^p and q^d indicate the suitable set of internal (plastic and damage, respectively) variables and the elastic deformations Φ^e is the free variable in the process.

For stable thermal state problems, the Clausius-Duhem dissipation inequality is valid, and takes the form:

$$\dot{\Xi} = \{\mathbf{M}\} : \{\dot{\Phi}^e\} - \dot{\Psi} \geq 0 \quad (6.13)$$

This inequality is valid for any loading-unloading stage. Taking the time derivative of equation (6.12) and substituting into (6.13) gives the following equation for dissipation:

$$\dot{\Xi} = \left(\{\mathbf{M}\} - \frac{\partial \Psi}{\partial \{\Phi^e\}} \right) : \{\dot{\Phi}\} + \frac{\partial \Psi}{\partial \{\Phi^e\}} : \{\dot{\Phi}^p\} - \frac{\partial \Psi}{\partial q^d} \dot{q}^d - \frac{\partial \Psi}{\partial q^p} \dot{q}^p \geq 0 \quad (6.14)$$

In order to guarantee the unconditional fulfilment of the Clausius-Duhem inequality, the multiplier of $\{\dot{\Phi}\}$ representing an arbitrary temporal variation of the free variable must be null. This condition provides the constitutive law of the damage problem:

$$\left(\{\mathbf{M}\} - \frac{\partial \Psi}{\partial \{\Phi^e\}} \right) \geq 0 \quad \forall \{\dot{\Phi}\} \quad (6.15)$$

from where the final generalized stress of member can be defined as:

$$\{\mathbf{M}_b\} = \frac{\partial \Psi_b}{\partial \{\Phi_b^e\}} \quad (6.16)$$

Once $\{\Phi_b^e\} = (\{\Phi_b\} - \{\Phi_b^p\})$, the free energy for an elastic-plastic frame element with stiffness degradation can be written for small deformations as

$$\Psi_b(\Phi_b^e, \mathbf{D}_b, q^p, q^d) = \frac{1}{2} (\{\Phi_b\} - \{\Phi_b^p\}) : [\mathbf{S}_b^d(\mathbf{D}_b)] : (\{\Phi_b\} - \{\Phi_b^p\}) + \Psi_b^p(q^p) \quad (6.17)$$

where the stiffness matrix of the damaged member $[\mathbf{S}_b^d(\mathbf{D}_b)]$ is the same matrix defined in (5.35). By replacing this last equation in (6.16) one arrives at the expression for plastic-damage analysis

$$\{\mathbf{M}_b\} = [\mathbf{S}_b^d(\mathbf{D}_b)] : (\{\Phi_b\} - \{\Phi_b^p\}) \quad (6.18)$$

6.3.2 Internal variable evolution laws

Once we assume that the plastic multipliers and the damage parameter are independent, the evolution of the damage parameter can be obtained by:

$$\{\mathbf{D}_i^b\} = G(\{\tau_i^b\}) = \begin{cases} d_i = G((\tau_i^b)_i) \\ d_j = G((\tau_j^b)_i) \\ d_a = G((\tau_\delta^b)_i) \end{cases} \quad (6.19)$$

which follow the same principles defined in Chapter 5.

The characterization of the plastic response will be formulated in terms of the effective generalized stress $\{\bar{\mathbf{M}}_b\} = [\mathbf{S}_b^e] : (\{\Phi_b\} - \{\Phi_b^p\})$. Consequently, the yield function is defined as:

$$f(\{\bar{\mathbf{M}}_b\}, q_b) \leq 0 \begin{cases} f_i(\bar{m}_i, q_i) \leq 0 \\ f_j(\bar{m}_j, q_j) \leq 0 \end{cases} \quad (6.20)$$

where q_i and q_j are the back stresses defined in Chapter 4. The plastic response can be characterized in terms of the generalized deformations $\{\Phi_b\}^T = \{\phi_i \ \phi_j \ 0\}$ as:

$$\begin{aligned} \dot{\bar{m}}_i^p &= \dot{\lambda}_i^p \frac{\partial f_i \left(\frac{\partial \Psi_i^0}{\partial \phi_i} - \bar{m}_i^p, q_i \right)}{\partial \phi_i} & \dot{\bar{m}}_j^p &= \dot{\lambda}_j^p \frac{\partial f_j \left(\frac{\partial \Psi_j^0}{\partial \phi_j} - \bar{m}_j^p, q_j \right)}{\partial \phi_j} \\ \dot{\bar{m}}_i^p &= \dot{\lambda}_i^p \frac{\partial f_i}{\partial \bar{m}_i} \frac{\partial \bar{m}_i}{\partial \phi_i} = \dot{\lambda}_i^p \frac{\partial f_i}{\partial \bar{m}_i} \frac{\partial^2 \Psi_i^0}{\partial \phi_i \partial \phi_i}; & \dot{\bar{m}}_j^p &= \dot{\lambda}_j^p \frac{\partial f_j}{\partial \bar{m}_j} \frac{\partial \bar{m}_j}{\partial \phi_j} = \dot{\lambda}_j^p \frac{\partial f_j}{\partial \bar{m}_j} \frac{\partial^2 \Psi_j^0}{\partial \phi_j \partial \phi_j} \\ \dot{q}_i &= \dot{\lambda}_i^p h_i \left(\frac{\partial \Psi_i^0}{\partial \phi_i} - \bar{m}_i, q_i \right) & \dot{q}_j &= \dot{\lambda}_j^p h_j \left(\frac{\partial \Psi_j^0}{\partial \phi_j} - \bar{m}_j, q_j \right) \end{aligned} \quad (6.21)$$

Where Ψ_i^0 and Ψ_j^0 are the free energy defined in Chapter 5, λ_i^p and λ_j^p are the plastic multipliers, and $h_i = h_j$ are the kinematic hardening. The effective bending moments can be expressed as

$$\bar{m}_i = \frac{\partial \Psi_i^0}{\partial \phi_i} - \bar{m}_i^p; \quad \bar{m}_j = \frac{\partial \Psi_j^0}{\partial \phi_j} - \bar{m}_j^p \quad (6.22)$$

The plastic load-unload conditions is given as:

$$\begin{aligned}
f_i(\bar{m}_i, q_i) \leq 0 \quad \dot{\lambda}_i^p \geq 0 \quad \dot{\lambda}_i^p f_i(\bar{m}_i, q_i) &= 0 \\
f_j(\bar{m}_j, q_j) \leq 0 \quad \dot{\lambda}_j^p \geq 0 \quad \dot{\lambda}_j^p f_j(\bar{m}_j, q_j) &= 0
\end{aligned} \tag{6.23}$$

with the consistency condition $\dot{f}_i = 0$ and $\dot{f}_j = 0$, it results:

$$\begin{aligned}
\frac{\partial f_i}{\partial \bar{m}_i} \dot{\bar{m}}_i + \frac{\partial f_i}{\partial q_i} \dot{q}_i &= 0 & \frac{\partial f_j}{\partial \bar{m}_j} \dot{\bar{m}}_j + \frac{\partial f_j}{\partial q_j} \dot{q}_j &= 0 \\
\dot{\bar{m}}_i &= \frac{\partial^2 \Psi_i^0}{\partial \phi_i \partial \phi_i} \dot{\phi}_i - \dot{\bar{m}}_i^p & \dot{\bar{m}}_j &= \frac{\partial^2 \Psi_j^0}{\partial \phi_j \partial \phi_j} \dot{\phi}_j - \dot{\bar{m}}_j^p \\
\dot{\bar{m}}_i^p &= \lambda_i^p \frac{\partial f_i}{\partial \bar{m}_i} \frac{\partial^2 \Psi_i^0}{\partial \phi_i \partial \phi_i} & \dot{\bar{m}}_j^p &= \lambda_j^p \frac{\partial f_j}{\partial \bar{m}_j} \frac{\partial^2 \Psi_j^0}{\partial \phi_j \partial \phi_j} \\
\dot{\bar{m}}_i &= \frac{\partial^2 \Psi_i^0}{\partial \phi_i \partial \phi_i} \left(\dot{\phi}_i - \lambda_i^p \frac{\partial f_i}{\partial \bar{m}_i} \right) & \dot{\bar{m}}_j &= \frac{\partial^2 \Psi_j^0}{\partial \phi_j \partial \phi_j} \left(\dot{\phi}_j - \lambda_j^p \frac{\partial f_j}{\partial \bar{m}_j} \right) \\
\dot{q}_i &= \dot{\lambda}_i^p h_i & \dot{q}_j &= \dot{\lambda}_j^p h_j
\end{aligned} \tag{6.24}$$

Finally, through equation (6.24), the plastic multipliers can be expressed as:

$$\lambda_i^p = \frac{\frac{\partial f_i}{\partial \bar{m}_i} \frac{\partial^2 \Psi_i^0}{\partial \phi_i \partial \phi_i} \left(\dot{\phi}_i - \lambda_i^p \frac{\partial f_i}{\partial \bar{m}_i} \right) + \frac{\partial f_i}{\partial q_i} \dot{\lambda}_i^p h_i = 0}{\frac{\partial f_i}{\partial \bar{m}_i} \frac{\partial^2 \Psi_i^0}{\partial \phi_i \partial \phi_i} \dot{\phi}_i} ; \lambda_j^p = \frac{\frac{\partial f_j}{\partial \bar{m}_j} \frac{\partial^2 \Psi_j^0}{\partial \phi_j \partial \phi_j} \left(\dot{\phi}_j - \lambda_j^p \frac{\partial f_j}{\partial \bar{m}_j} \right) + \frac{\partial f_j}{\partial q_j} \dot{\lambda}_j^p h_j = 0}{\frac{\partial f_j}{\partial \bar{m}_j} \frac{\partial^2 \Psi_j^0}{\partial \phi_j \partial \phi_j} \dot{\phi}_j} \tag{6.25}$$

6.3.3 Integration of the constitutive equation for plastic-damage model

The solution of the plastic-damage model is obtained by an uncoupled solver, which first the damage evolution will be obtained, and after that, we will determine the plastic constitutive solution, which is obtained using the return-mapping algorithm (Chapter 4), as shown in Table 6.1. With this assumption, the damage evolution and the plastic rotation are independent, being coupled only at the end of the numerical solution through the generalized effective stress, equation (6.20).

Once we have assumed that damage is linked with the concrete behaviour, the initial damage threshold vector $\{r_0\}$, will now be defined in terms of the cracking moment m_{cr} , as:

$$\{r_0^b\} = \sqrt{\{\mathbf{M}_{cr}\} : [\mathbf{S}_b^{-1}] : \{\mathbf{M}_{cr}\}} = \begin{cases} (r_i^b)_0 \\ (r_j^b)_0 \\ (r_\delta^b)_0 \end{cases} \Rightarrow \begin{cases} (r_i^b)_0 = (r_j^b)_0 = \sqrt{\frac{L}{3EI} m_{cr}^2} \\ (r_\delta^b)_0 = \sqrt{\frac{L}{EA} n_{cr}^2} \end{cases} \quad (6.26)$$

while the plastic limits will be defined in terms of the ultimate moment m_u , once we assume that the plastification is related with the yielding of the steel.

Table 6.1 - Procedure to determine of the damage and plastic parameters

-
- For each b elements at n th+1 iteration at the time t :
- 1) Generalized deformations at the step: $\{\Phi_b\}_t^{(n+1)} = \{\Phi_b\}_t^{(n)} + \{\Delta\Phi_b\}_t^{(n+1)}$
 - 2) Verification of the evolution of the damage:
 - i) Update of the internal variables: $\{\mathbf{D}_b\}_t^{(n+1)} = \{\mathbf{D}_b\}_t^{(n)}$; $\{\mathbf{r}_b\}_t^{(n+1)} = \{\mathbf{r}_b\}_t^{(n)}$
 - ii) Determination of the free energy and the undamaged energy norm vector:

$$\{\Psi_b^0\} = \frac{1}{2} \{\Phi_b\}_t^{(n+1)} : [\mathbf{S}_b] : \{\Phi_b\}_t^{(n+1)} ; \{\tau_\Phi^b\} = \sqrt{2\{\Psi_b^0\}}$$
 - iii) Verification of the evolution of the damage:

If $g(\{\tau_\Phi^b\}, \{\mathbf{r}_b\}_t^{(n+1)}) \leq 0$ No damage evolution $\rightarrow 3$
 - iv) Update of damage variable: $\{\mathbf{D}_b\}_t^{(n+1)} = G(\{\tau_\Phi^b\})$
 - v) Update of damage threshold: $\{\mathbf{r}_b\}_t^{(n+1)} = \{\tau_\Phi^b\}$
 - 3) Verification of the evolution of the plastic variable:
 - i) Determination of generalized effective 'trial' stress and update of internal variables for $k=0$:

$${}^{k=0}\{\Delta\Phi_b^p\} = \{\Phi_b^p\}_t^{(n)} ; {}^{k=0}\{\Delta q^p\} = \{q^p\}_t^{(n)}$$
 - ii) Plastic evolution k th iteration: ${}^k\{\bar{\mathbf{M}}_b^{trial}\} = [\mathbf{S}_b] : (\{\Phi_b\}_t^{(n+1)} - {}^k\{\Delta\Phi_b^p\})$
 - iii) Verification of flow conditions $f(m, q) = |m - q| - m_u$ and determination of plastic multiplier

$${}^k\Delta\lambda_i^p = 0 \quad \text{if} \quad {}^k f_i^{trial}({}^k\bar{m}_i^{trial}, {}^k\Delta q_i^p) < 0 \quad \text{or} \quad (\lambda_i^p)_k ({}^k d f_i^{trial})_k < 0$$

No plasticity evolution $\rightarrow 4$)

$${}^k\Delta\lambda_j^p = 0 \quad \text{if} \quad {}^k f_j^{trial}({}^k\bar{m}_j^{trial}, {}^k\Delta q_j^p) < 0 \quad \text{or} \quad (\lambda_j^p)_k ({}^k d f_j^{trial})_k < 0$$
 - iv) Determination of plastic multipliers

$$\begin{cases} {}^k f_i^{trial} > 0 \\ {}^k f_j^{trial} \leq 0 \end{cases} \left\{ \begin{array}{l} {}^{k+1}\Delta\lambda_i^p = \frac{{}^k f_i^{trial}}{\left(\frac{\partial f_i^{trial}}{\partial \bar{m}_i^{trial}} \frac{\partial^2 \Psi_i^0}{\partial \phi_i \partial \phi_i} \frac{\partial f_i^{trial}}{\partial \bar{m}_i^{trial}} - \frac{\partial f_i^{trial}}{\partial q_i} h_i \right)} ; \\ {}^{k+1}\Delta\lambda_j^p = 0 \end{array} \right.$$

$$\begin{cases} {}^k f_i^{trial} \leq 0 \\ {}^k f_j^{trial} > 0 \end{cases} \left\{ \begin{array}{l} {}^{k+1}\Delta\lambda_i^p = 0 \\ {}^{k+1}\Delta\lambda_j^p = \frac{{}^k f_j^{trial}}{\left(\frac{\partial f_j^{trial}}{\partial \bar{m}_j^{trial}} \frac{\partial^2 \Psi_j^0}{\partial \phi_j \partial \phi_j} \frac{\partial f_j^{trial}}{\partial \bar{m}_j^{trial}} - \frac{\partial f_j^{trial}}{\partial q_j} h_j \right)} \end{array} \right.$$
-
- or
-

$$\begin{matrix}
{}^k f_i^{trial} > 0 \\
{}^k f_j^{trial} > 0
\end{matrix}
\left[\begin{array}{cc}
\left(\frac{\partial f_i^{trial}}{\partial \bar{m}_i^{trial}} \frac{\partial^2 \Psi_i^0}{\partial \phi_i \partial \phi_i} \frac{\partial f_i^{trial}}{\partial \bar{m}_i^{trial}} - \frac{\partial f_i^{trial}}{\partial q_i} h_i \right) & 0 \\
0 & \left(\frac{\partial f_j^{trial}}{\partial \bar{m}_j^{trial}} \frac{\partial^2 \Psi_j^0}{\partial \phi_j \partial \phi_j} \frac{\partial f_j^{trial}}{\partial \bar{m}_j^{trial}} - \frac{\partial f_j^{trial}}{\partial q_j} h_j \right)
\end{array} \right] : \begin{Bmatrix} {}^{k+1} \Delta \lambda_i^p \\ {}^{k+1} \Delta \lambda_j^p \end{Bmatrix} = \begin{Bmatrix} {}^k f_i^{trial} \\ {}^k f_j^{trial} \end{Bmatrix}$$

v) Update of plastic variables and of the generalized effective 'trial' stress:

$$\begin{aligned}
{}^{k+1} \phi_i^p &= {}^k \phi_i^p + {}^{k+1} \Delta \lambda_i^p \frac{\partial {}^k f_i^{trial}}{\partial \bar{m}_i^{trial}} ; & {}^{k+1} \phi_j^p &= {}^k \phi_j^p + {}^{k+1} \Delta \lambda_j^p \frac{\partial {}^k f_j^{trial}}{\partial \bar{m}_j^{trial}} \\
{}^{k+1} q_i &= {}^k q_i + {}^{k+1} \Delta \lambda_i^p h_i \frac{\partial {}^k f_i^{trial}}{\partial \phi_i^{trial}} ; & {}^{k+1} q_j &= {}^k q_j + {}^{k+1} \Delta \lambda_j^p h_j \frac{\partial {}^k f_j^{trial}}{\partial \phi_j^{trial}} \\
{}^{k+1} m_i^{trial} &= {}^k m_i^{trial} + {}^{k+1} \Delta \lambda_i^p [\mathbf{S}_b] : \frac{\partial {}^k f_i^{trial}}{\partial \bar{m}_i^{trial}} ; & {}^{k+1} m_j^{trial} &= {}^k m_j^{trial} + {}^{k+1} \Delta \lambda_j^p [\mathbf{S}_b] : \frac{\partial {}^k f_j^{trial}}{\partial \bar{m}_j^{trial}}
\end{aligned}$$

vi) Update $k = k + 1$ and Back to iii)

4) End of the process of plastic correction

$$(\Phi_b^p)_t^{(n+1)} = (\Delta \Phi_b^p)_k ; \quad (q^p)_t^{(n+1)} = (\Delta q^p)_k$$

5) Achievement of the final generalized stress on the step n :

$$\{\mathbf{M}_b\}_t^{(n+1)} = [\mathbf{S}(\{\mathbf{D}_b\}_t^{(n+1)})_b] : (\{\Phi_b\}_t^{(n+1)} - \{\Phi_b^p\}_t^{(n+1)})$$

6) End of integration process of the constitutive equation.

It is important observe that the plastic yield functions f_i and f_j can be expressed by a different yield function, such as the one proposed in Chapter 4. Similarly, the damage evolution can also be replaced by the unilateral damage model described in Chapter 5.

6.4 Member damage index

Although the local and plastic damage indexes proposed in the section 5.5 of Chapter 5 are useful, both damage indexes are limited. Their limitation is due the fact that evolutions of the damage, by means of the local damage index, or the plasticity, by means of the plastic damage index, are measured separately. As result, it is not possible measure the evolution of the total deformation at a beam-column member. In opposite, the proposed global damage can measure all nonlinear effects, damage or plasticity, for the entire structure.

Thus, the starting point for deducing the member damage index is by the assumptions that we can express the plastic-damage free energy $\Psi_b(\Phi_b^e, \mathbf{D}_b)$ (equation (6.12)) of a member with the non-damaged free energy Ψ_b^0 , defined in equation (5.57), as:

$$\Psi_b(\Phi_b^e, \mathbf{D}_b) = (1 - D_b^M) \Psi_b^0 \quad (6.27)$$

where D_b^M is the member damage index. The free energy $\Psi_b(\Phi_b^e, \mathbf{D}_b)$ of a member can be defined as

$$\Psi_b(\Phi_b^e, \mathbf{D}_b) = \frac{1}{2} \{\Phi_b - \Phi_b^e\} : [\mathbf{S}_b^d(\mathbf{D}_b)] : \{\Phi_b - \Phi_b^e\} \quad (6.28)$$

Solving (6.27) for D_b^M , we obtain

$$D_b^M = 1 - \frac{\Psi_b(\Phi_b^e, \mathbf{D}_b)}{\Psi_b^0} \quad (6.29)$$

which is the expression for member damage index for a frame member.

In the equation (6.29), we can notice that for those cases where only damage is measured, $\{\Phi_b^e\} = \{0\}$, we obtain that D_b^M is numerically equal to the local damage index D_b^L proposed in the equation (5.77). Otherwise, when we have only plasticity, $\{\mathbf{D}_b\} = \{0\}$, D_b^M is numerically equal to the plastic damage index D_b^P proposed in the equation (5.80).

Chapter 7

Numerical examples

7.1 Introduction

In this chapter, we present the numerical results obtained by means of the proposed model described in Chapter 6. This model has been implemented into a frame analysis program, based on the matrixial methods. The program was developed exclusively for this thesis.

The program allows the calculus of the planar frame structures under pushover loads, loads with cyclic of load-unload and under dynamic loads. The results obtained in the program can be visualized in the postprocessor of GiD, the finite element program developed in CIMNE (International Center for Numeric Methods in Engineering).

7.2 Example 1: Model validation using a simple framed structure

The objective of this first example is to validate the proposed model and to evaluate the related concentrated damage and the global damage index of a structure. For this reason, we will analyze the results obtained by means of the proposal nonlinear frame analysis method in comparison with results obtained by means of a more refined finite element (FE) model.

The analyzed frame is 4 m high and 4 m wide loaded with two point forces (Figure 7.1a). The columns have a 8,43 cm x 5,62 cm cross section, the horizontal

beam is 5,62 cm thick and 12,65 cm wide. Two FE models have been considered by Oller *et al.* (1996), the first one was modeled using the Timoshenko 3-noded beams elements to represent the structure (see Figure 7.1d) and the second was modeled using 75 2D 8-noded quadrilateral elements (see Figure 7.1e). Three frames models have been considered, the first one the frame was discretized by only 3 frame elements: one to defines the column and two to defines the beam (see Figure 7.1a). The second frame the column and the beam are represented by 10 frame elements (see Figure 7.1c) and in the last frame, it was adopted the same division of the 3-noded beams elements described in Figure 7.1d.

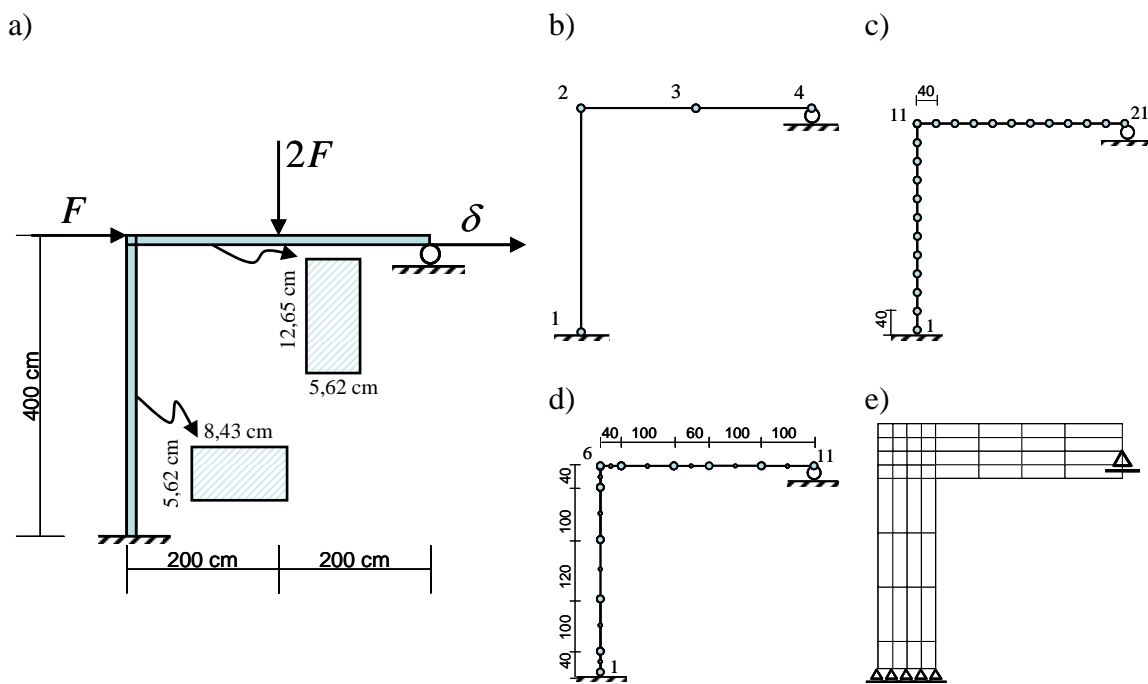


Figure 7.1 - Geometry of the studied frame. a) Geometry and cross section b) numeration of the nodes of for frame with 3 elements , c) numeration of the nodes of for frame with 20 elements; d) FE mesh using Timoshenko 3-noded beams elements, e) FE mesh using 2D 8-noded quadrilateral elements.

In all cases, elastic modulus was $E = 2.1 \times 10^5 \text{ MPa}$ while for the frame analysis it was assumed that the ultimate moment were $m_u = 45 \text{ kN} \times \text{m}$, for the beam, and $m_u = 20 \text{ kN} \times \text{m}$ for the column. The material was assumed a perfect elastoplastic law, such that, once reaches the elastic limit $\sigma_y = 200 \text{ MPa}$, it yields indefinitely at constant stress. Figure 7.2 shows the results of the evolution of the force versus the displacement in the left upper corner of the frame obtained by each model, where we can notice that the results obtained with the proposed frame analysis model are in a good agreement with the results obtained by using the FE model.

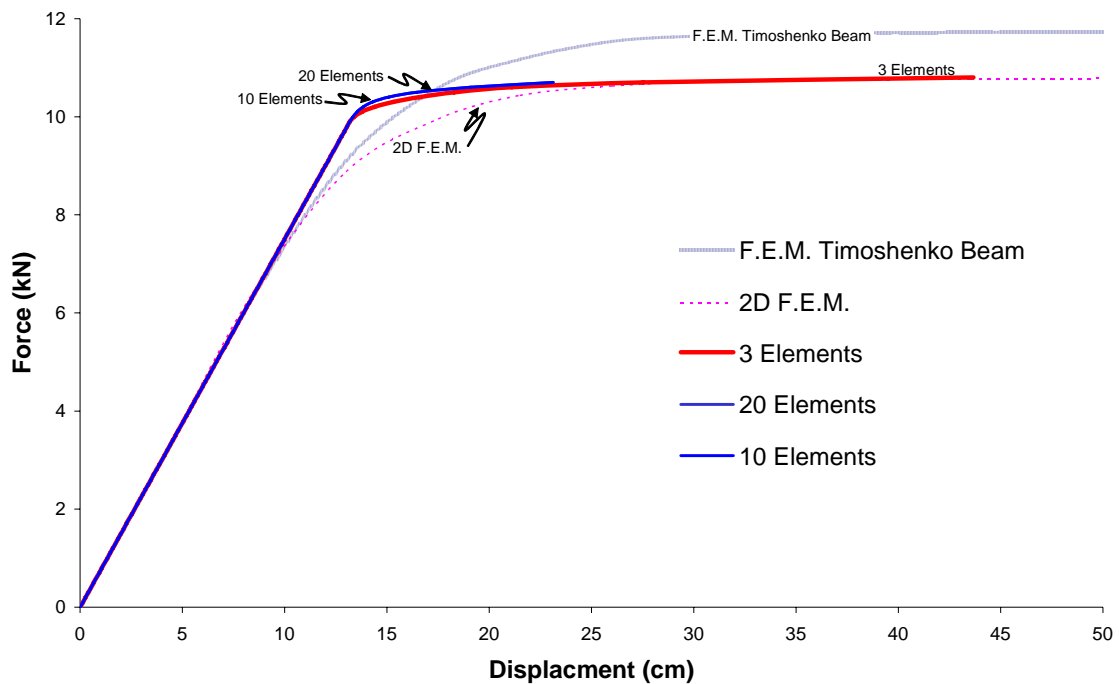


Figure 7.2 - Comparison of the force-displacement curve for FEM results with results obtained by using the proposed plastic-damage model.

The evolution of the moment at the column base is shown in Figure 7.3, where a comparison is made among the results obtained with the proposed method for different frame models. The evolution of global damage index for each frame is shown in Figure 7.4. We also monitored the concentrated damage at the base and the top of the columns for each frame, once it is clearly expected that the structure will fail due to the weakening of the column. Studying together these three graphs, we can analyze the behaviour of each frame.

Observing the results in Figures 8.2 and 8.3 we can conclude that, although the concentrated damage effect in the frame analysis influences on the deformation and load capacity, it is the plasticity by means of the plastic hinges, and not the damage, what conditions the numerical stability of the structural analysis. This behaviour is in agreement with the assumptions that the structure continues to deform until the final instability is detected by the singularity of the global stiffness matrix, caused basically by the increment of the number of the plastic hinges in the frame than by the evolution of the damage. When the analysis stops, at $\delta \cong 80$ cm for the 3 elements frame and at $\delta \cong 32$ cm for the others frames, the stiffness matrix becomes singular due to the presence of hinges (i.e., the nodes 3 and 1 in the first frame), and we can no longer perform the structural analysis.

This statement also can be confirmed by the fact that the damage at the column base is less than the global damage index for all cases (see Figure 7.4). The

same curves are obtained for the frames modeled with 10 and 20 elements for both force-displacement relation (Figure 7.2), moment-displacement relation (Figure 7.3), global damage index evolutions and evolutions of the damage for the columns (see Figure 7.4).

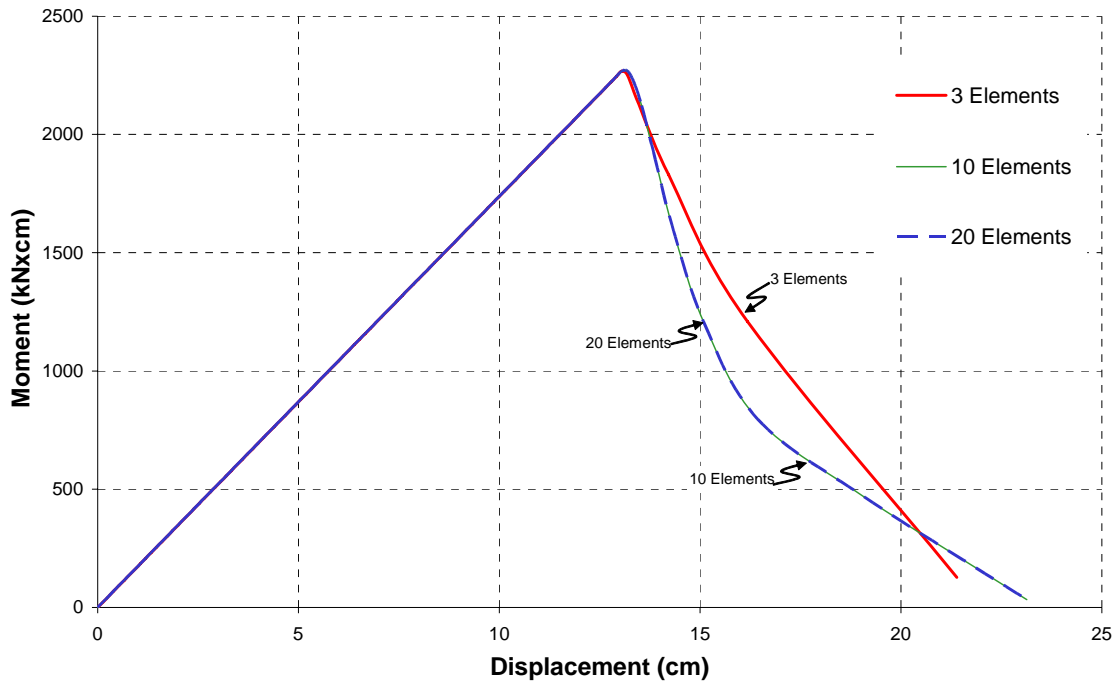


Figure 7.3 – Moment on the column base versus displacement at the left upper corner.

Analyzing the damage in the frame modeled with 3 elements, the beginning of the concentrated damage at the top of the column is closer to the beginning of the concentrated damage at its base, and both have almost the same final value. Meanwhile, for the frame with 10 elements and with 20 elements, the damage at the top begins at very high loads while the damage at the base begins almost at the same instant when plasticity begins. In both frames, the final value obtained for the concentrated damage at the base is higher than the value obtained at the top of the column.

For the frame modeled with three elements, it can be seen clearly that the evolution of the global damage index is not related only due to the concentrated damage evolution but also to the plasticity evolution at the hinges. We can also notice that for both the frames modeled with 10 elements and with 20 elements, the global damage index rapidly reaches high values for low deformations, what implies that the concentrated damage has more influence on the structural collapse than the plastic hinges, that is, the structure has little tendency to deform. This can be because the column and the beams are composed by several elements,

dispersing the effect of the plasticity, while the damage is more concentrated at the base of the column. In conclusion, the behaviour of the structure can be influenced by the number of elements and, therefore, the results obtained are smaller than it is expected.

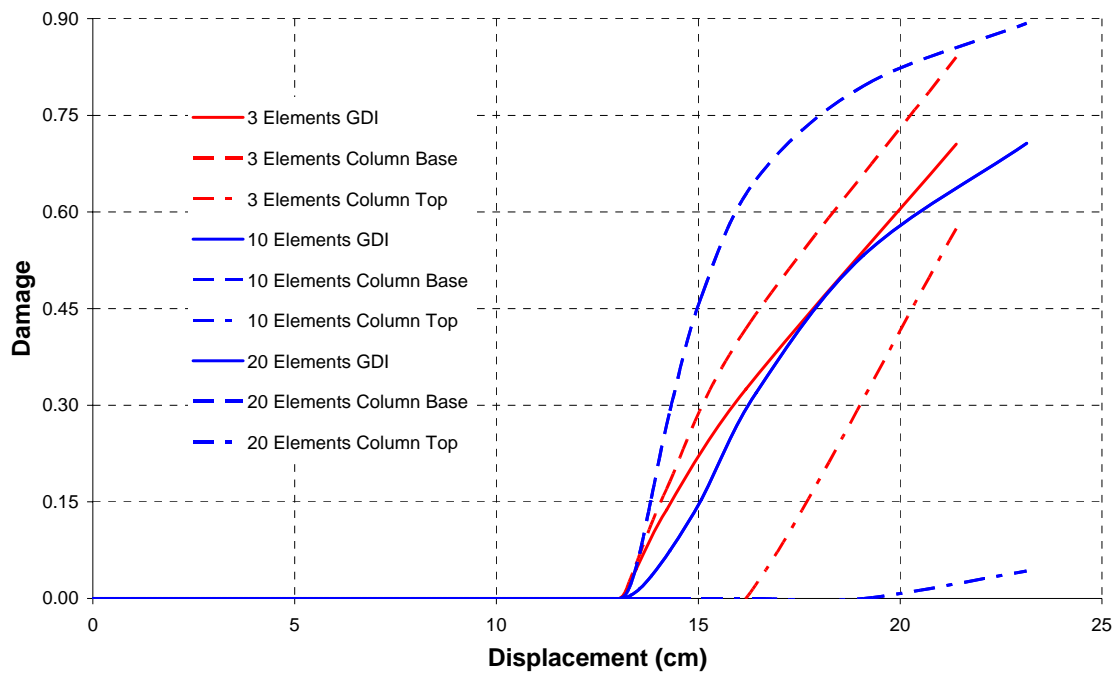


Figure 7.4 – Evolution of the global damage index (GDI) and the concentrated damage at the base and at the top of the column.

Using the plastic and local damage indexes proposed in Chapter 5, in Figure 7.5 we can observe that the evolution of the plasticity and damage begins simultaneous at the same time in the frame modeled with 3 elements. However, the values obtained for plastic damage index are high than the values obtained to the local damage index. This can be understood as that the plasticity is active and has influence in the behaviour of the structure.

Analyzing the local and plastic damage index in the frames modeled with 10 elements and 20 elements, we can notice that, even the local as the plastic damage index are identical in both cases. Similarly as observed to frame with 3 elements, the values of plastic damage index are high than the values obtained for the local damage index.

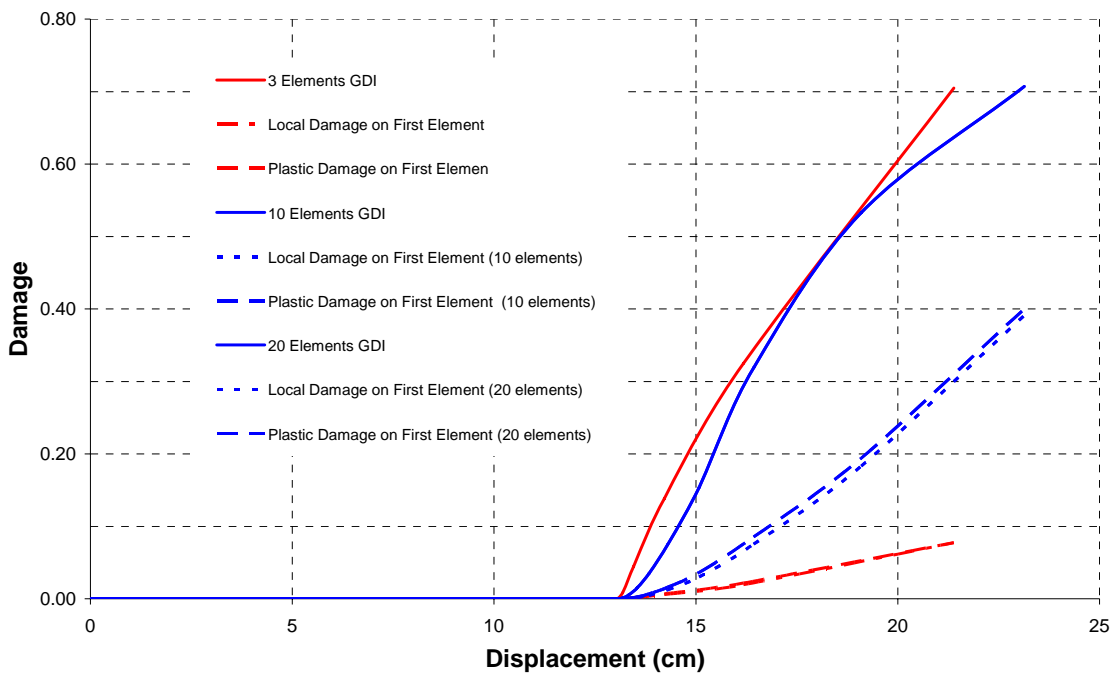


Figure 7.5 - Evolution of the global damage index (GDI), local and plastic damage on the first element.

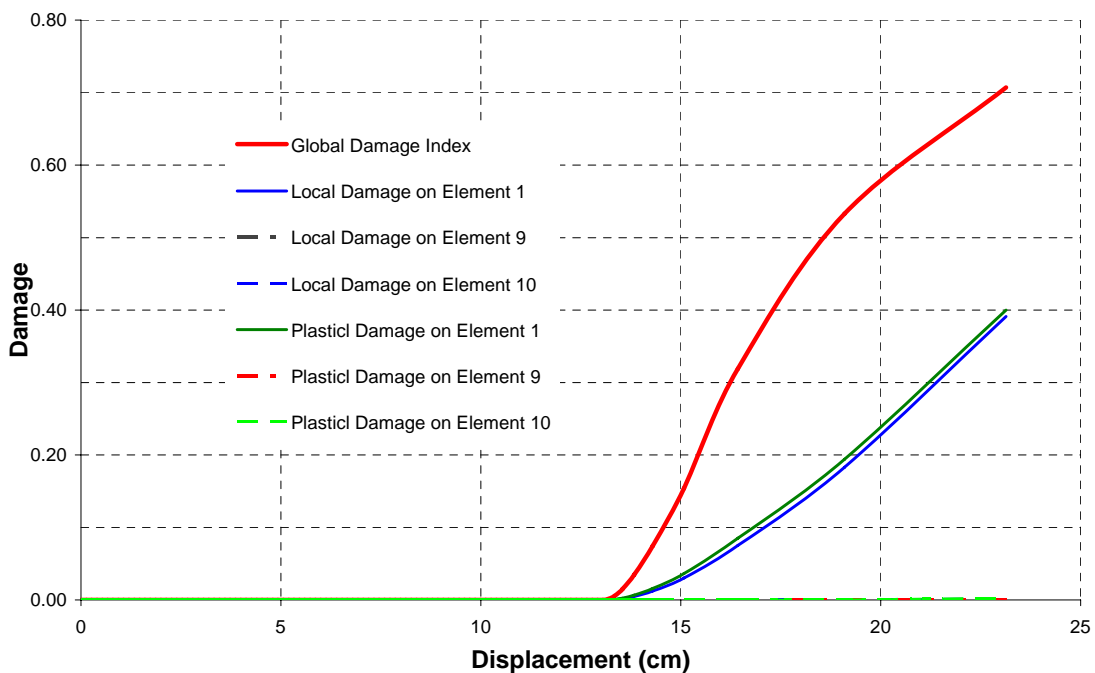


Figure 7.6 – Plastic and local damage evolution on the elements of the frame modeled with 20 elements.

Analyzing separately the frame modeled with 20 elements, Figure 7.6, we can observe the evolution of the local and damage indexes. As expected, the high

value to plastic and local damage are obtained in the first element, located on the base of the column, while the 9th and the 10th elements, on the top of the column, presents low values for plastic and local damage indexes. The plastic damage index at 9th element is an indicative that the plasticity occurs at both extremities of the 10th element, which concurs for the singularity of the stiffness matrix.

Apparently, the evolution of the global damage index describes only the evolution of the plasticity and the damage at the base of the column. This occurs because, in the frame modeled with 20 elements, we only have damage and plasticity at the base, and the structural stiffness is influenced by them. It is important remember that the global damage index give a measure of loss structural stiffness, independent of how many members are plastify or damaged.

7.3 Example 2: Model validation using a simply reinforced concrete beam.

In this example a validation test is include in which are compared the results of an experimental test with those obtained with the proposed model for a simply supported beam of 240 cm length, 30 cm height, and 12 cm width, with two symmetrical loads (Figure 7.7); the beam bearings are assumed to be perfectly rigid. Álvares (1993) tested in the laboratory two similar beams (Figure 7.7a) and also performed their computational simulation using a finite element model (Álvares (2004)) with the plastic-damage model proposed by Cipolina *et al.* (1995).

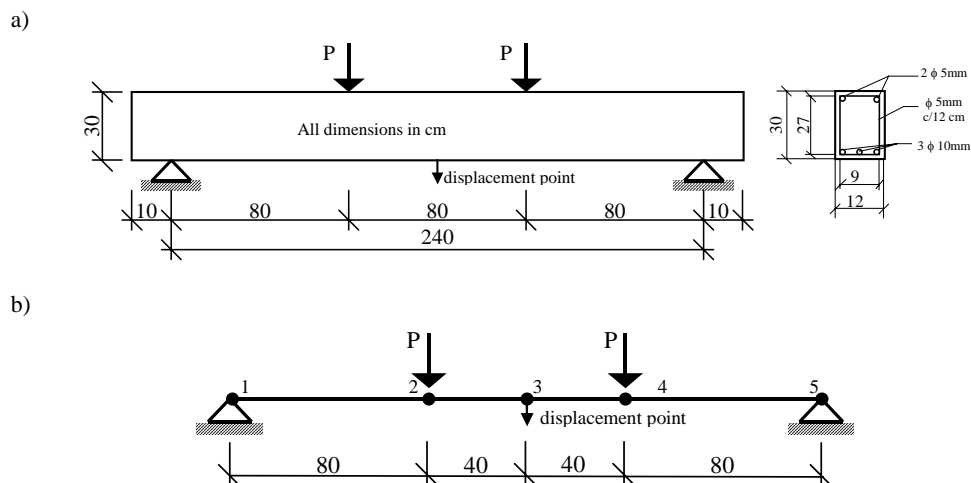


Figure 7.7 - Simply supported beam: a) Description of the geometrical and section of the beam; b) the beam modeled by means of beams elements

In the numerical analysis carried out by Álvares (2004), only the half of the beam was considered in the analysis. The beam was also divided into two sec-

tions, where each one has its own damage parameter and the analysis was made using two different functions for the damage, g_1 and g_2 .

Conversely, in this study, the beam was modeled by means of beam elements, as shown in Figure 7.7b, and the displacement reference point adopted was the node 3. Assuming a characteristic material parameter, the critical moment and ultimate moment were, $m_{cr} = 8$ kNm and $m_u = 32$ kNm respectively, while the elastic modulus was $E = 3,9$ GPa and the fracture energy $G_f = 250$ N/m.

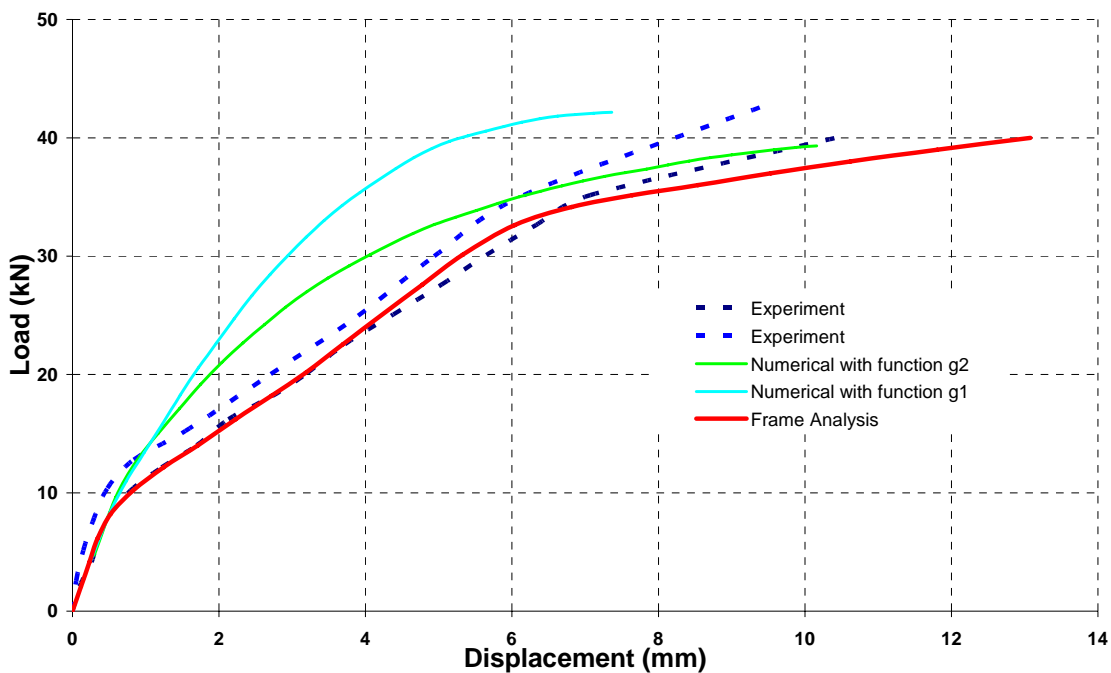


Figure 7.8 - Comparison of the numerical and experimental results

Figure 7.8 shows the comparison among the results obtained using the proposed model, the experimental results and the numerical results obtained by Álvares (1993 and 2004). It can be observed that the beam elements analyses have a good accuracy with respect to the experimental results, being better than the results obtained by means of finite elements model. It can be observed in Figure 7.9 the evolution of the global and local damage indexes for each beam.

In the analysis of the results obtained by using beam elements, it can be observed that there are three different phases. The first one is the elastic phase, which is indicate in Figure 7.8 by means of the straight line while, in Figure 7.9, all damage indexes, local, plastic or global, are null. In the second phase, the damage begins and modifies slope of the curve in Figure 7.8. In the third phase, the damage increases slowly, while the plasticity increases until the structure reaches its load capacity. This can be observed in Figure 7.9 by the tendency of all local damage curves to become constant, while the plastic damage index increases, and

consequently the global damage index increases too. At this phase, the beams reach the ultimate strength, what in the laboratory test corresponds to the crushing of concrete and the yielding of the reinforcement. The phases are similar to those of typical moment-deformation tests performed on reinforced concrete structures described by Chen (1982).

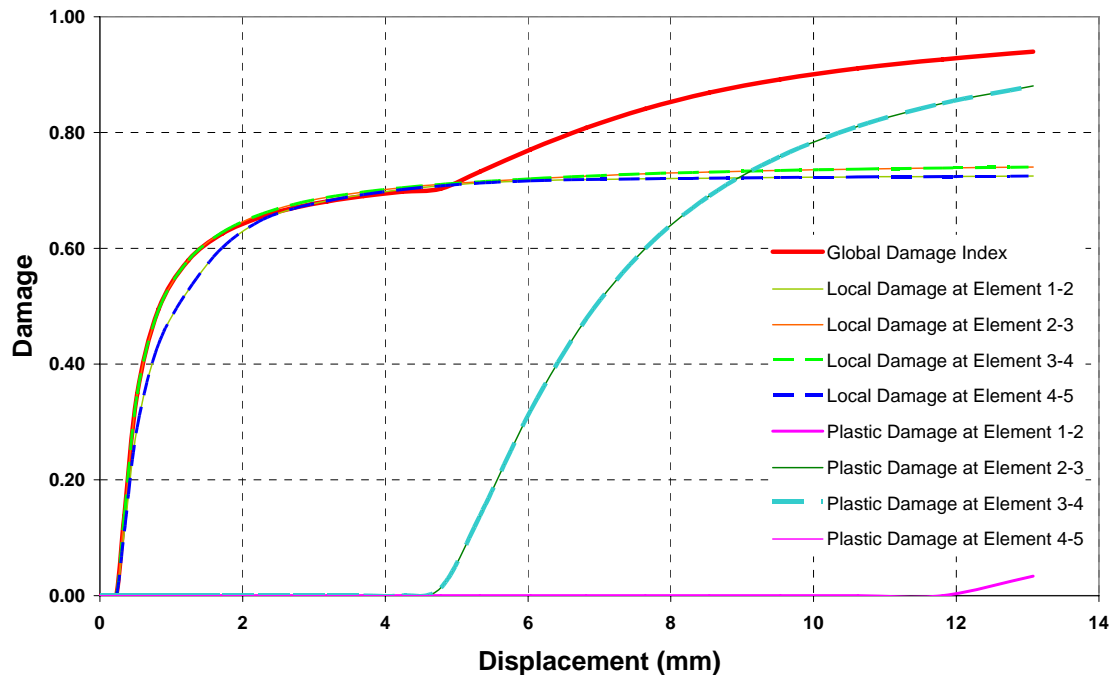


Figure 7.9 - Evolution of the global, local and plastic damage indexes in the beams elements.

In Figure 7.9, the evolution of the local damage indexes for all beams is independent of the evolution of the plastic damage indexes. We can notice that the damage begins almost at the same time in all members, having almost the same values. The value of damage in the elements 2-3 and 3-4 is a little high than at the rest of the elements. Meanwhile, the plasticity begins only when the bending moment at elements 2-3 and 3-4 reaches the ultimate moment value, which it is indicated by the beginning and increasing on the plastic damage indexes. The plasticity, and consequently the plastic damage index, at elements 1-2 and 4-5 begin almost at the time when the beam reaches its limit load.

The observed independence between the evolution of plasticity and damage is in conformity with the definition about the behaviour of reinforced concrete structures, presented in Chapter 6.

7.4 Example 3: Model validation using a reinforced concrete framed structure

The objective of this example is to compare the results obtained by using the plastic-damage model described in Chapter 6 with the results of a quasi-static laboratory test performed by Vecchio and Emara (1992) on a reinforced concrete frame. Barbat *et al.* (1997) have already performed a numerical simulation of the behaviour of the tested frame, but using a viscous damage model, implemented in a finite element program. A complete description of the geometrical and mechanical characteristics of the frame, as well as of the loads, is given in Figure 7.10.

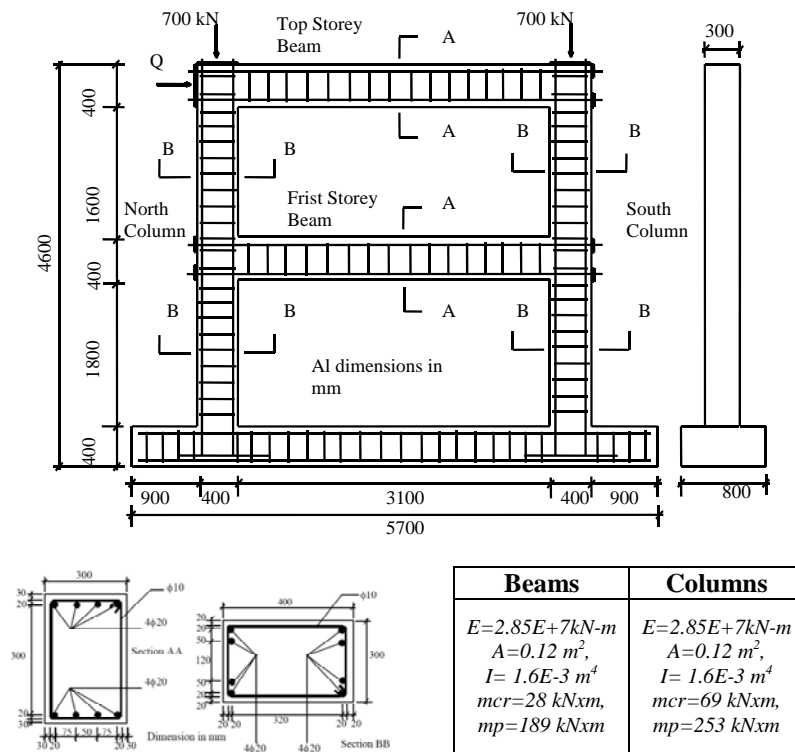


Figure 7.10 - Description of the geometrical and mechanical characteristics of the frame of Example 3

The laboratory test consisted in applying a total axial load of 700 kN to each column and in maintaining this load in a force-controlled mode throughout the test, which thus produced their pre-compression. A horizontal force was afterwards applied on the beam of the second floor, in a displacement-controlled mode, until the ultimate capacity of the frame was achieved (Vecchio and Emara (1992)). In the numerical analysis of the frame the plastic constitutive equation used only takes into account the bending moments (see Chapter 4), while the linear damage equation proposed by Oller (2001b) has been considered for determin-

ing the damage variable evolution, using in this case a fracture energy G_f equal to 250N/m.

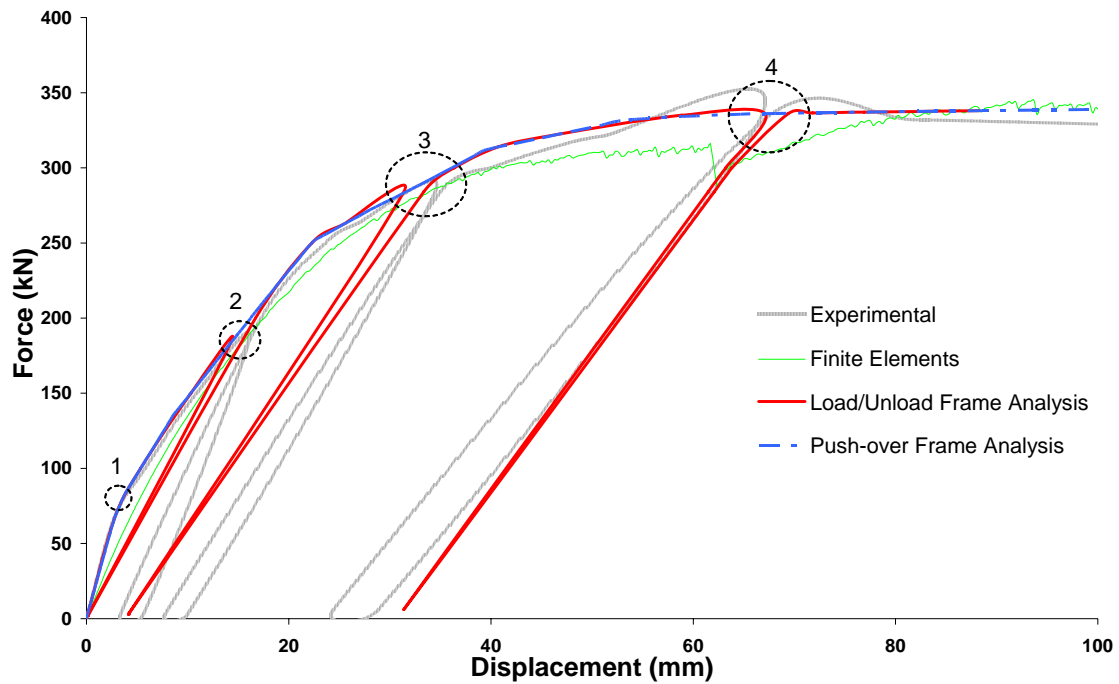


Figure 7.11 - Comparison of the experimental results with results obtained by using the frame analysis with the proposed plastic-damage model and a finite element model.

The curves in Figure 7.11 relate the horizontal forces and the displacements of the second floor beam and correspond to the load-unload laboratory test case and to the computer simulation using a viscous damage model, proposed by Barbat *et al.* (1997), and the plastic-damage model proposed in the present work. The results are reasonably in agreement, taking into account the little computational effort required by the calculation of the model. In the first load-unload cycle, marked by point number two in Figure 7.11, the presence of residual deformations can be observed in the experimental curve, while in the numerical curve this does not occur. This is because the plastic-damage model still not reaches the plastic limit and the plastic deformations are assumed to occur only after the yielding of the reinforcement. Nevertheless, when one of the elements reaches the plastic limit, it is possible to observe the influence of the plastic hinge on the curve. This situation is noticeable by the residual deformations represented in the subsequently unload-load cycles, at points three and four in Figure 7.11. However, in the laboratory test, non-negligible permanent deformations occurred before this, probably because of the inelastic strains and cracking of the concrete.

Analysing the damage evolution at the first floor, shown in Figure 7.12, and at the second floor, Figure 7.13, we can notice that the local damage begins in the first storey beam, followed almost simultaneously by damage of the second-storey beam, and after that, the damage in the first floor columns occurs. Only after a considerable increase of the deformation, the damage begins in the second floor columns. This behaviour is in agreement with the evolution of the damage observed in the laboratory test.

The effect of the damage in the first storey beam can also be detected in the force-displacement curve by the point 1 in Figure 7.11), which indicates the end of the elastic phase of the structure. However, in the first unload process of the frame, (point 2 in Figure 7.11) indicates that, at this moment, there is only damage in the frame model, aspect which is confirmed by the fact that the unload line returns to zero and all plastic damage indexes are null. At this point, as it was observed in the laboratory test, the damage occurs only at the first-storey beam, at the second-storey beam and at the columns of the first floor.

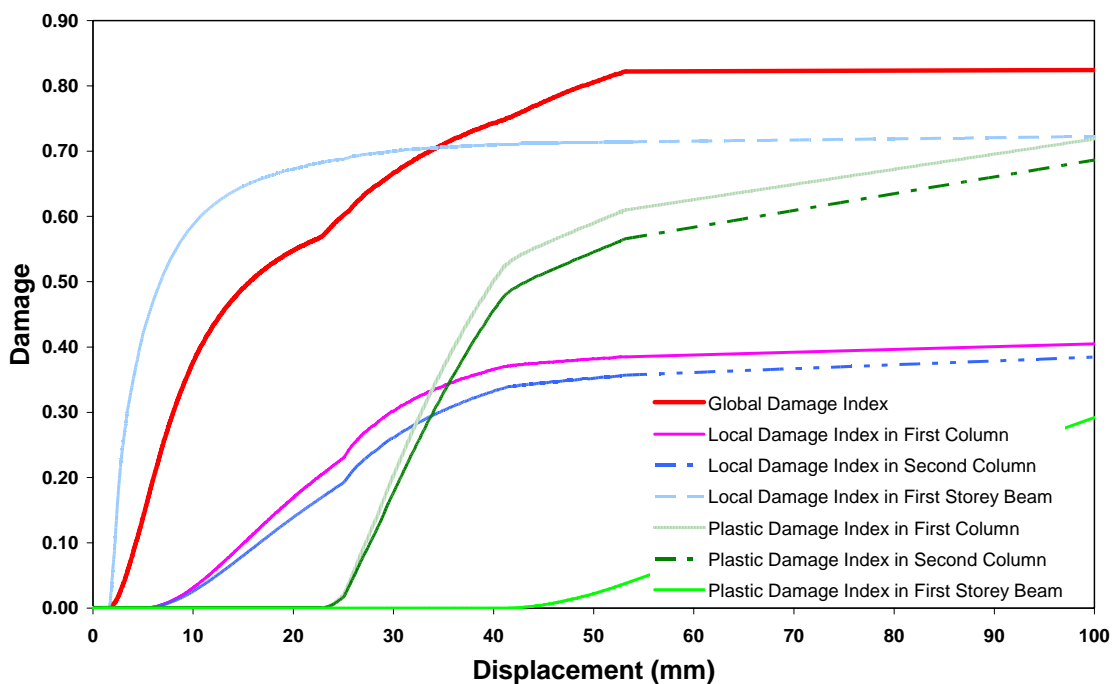


Figure 7.12 – Evolution of the global, local and plastic damage indexes in the first floor.

In the laboratory test, the structure loses stiffness because the propagation of the cracks throughout all the members at the point 2. However, in the frame analysis, the structure loses stiffness only when the plastic effect begins, for loads closer to point 3, when yielding begins in the first floor at the base of both

columns, indicated by the increase of the plastic damage indexes for the first and second column at the first floor in Figure 7.12.

In the laboratory test, the first yielding was detected at the bottom of the longitudinal reinforcement at the end of the first-story beam, followed by the yielding at the base of both columns of the first floor. In contrast, as can be observed in the plastic damage increases in Figure 7.12, in the frame analysis the first yielding is detected at the base of both columns of the first floor, followed by the yielding of the first-story beam. These differences in the sequence of the yielding can be explained by the fact that in frame analysis the plastification of the end cross section of the members is sudden, and not gradual, or fiber-by-fiber, as observed in the first-story beam in the laboratory test.

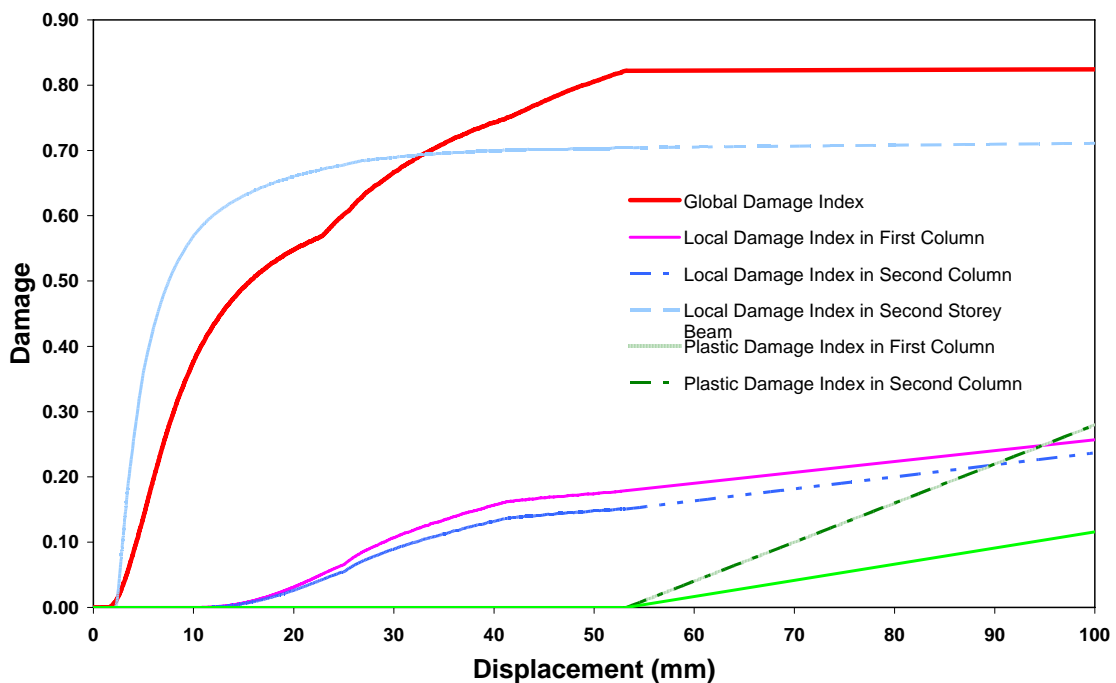


Figure 7.13 - Evolution of the global, local and plastic damage indexes in the second floor

The occurrence of the perfect plastic hinge at the first-storey beam and at the base of the first and second columns of the first floor implies a change of the static configuration for the whole structure, resulting in a slight change of the local damage indexes. This behaviour can also be observed by the change in curvature of the global damage index curve. Physically, this can be interpreted as the failure of the concrete in compression of the first floor columns and of the beams and the ensuing redistribution of the stresses towards the steel.

Meanwhile, in the frame analysis the plasticity in the second floor occurs only at the second storey beam, as can be seen in Figure 7.13. In this case, we can observe by the plastic damage index that the plasticity in the second story beam is sudden. At this point, the structure becomes unstable due to the development of many plastic hinges, increasing its deformation without an increase in load. Due to the increase of the deformation, we can observe that all plastic and damage indexes, as well as the global damage, increases faster, generating a gap between the points where the plasticity in the second story beam begins and the previous points.

Anyway, in frame analysis, the plasticity in the first and second column of the second floor occurs only after a considerable increase in the deformations, by means of the formation of the plastic hinges at the top of both columns.

Figure 7.14 shows the sequence of formation of the plastic hinges in the frame analysis. Although it is different from the sequence observed in the laboratory test, the final result is the same. Nevertheless, the final deformation obtained in the frame analysis is less than in the laboratory tests because the structural analysis can no longer be performed due to the presence of various plastic hinges.

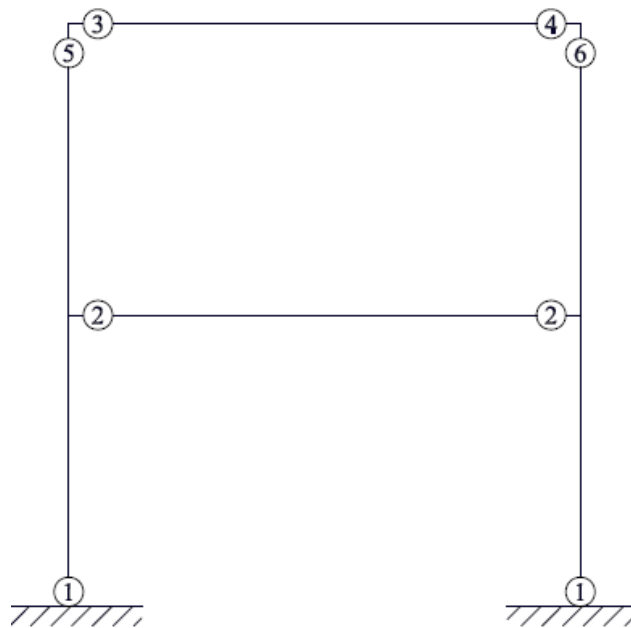


Figure 7.14 – Sequence of formation of the plastic hinges within the frame.

7.4.1 Comparison between local, plastic and member damage indexes

Although the results obtained by means of the local and plastic damage indexes proposed in Chapter 5 are useful, these results express only the evolution of

the concentrated damage indexes, in the case of the local damage index, or the plasticity hinge evolution, in the case of the plastic damage index. These limitations it can be observed in Figure 7.15, where we can notice that the evolution of local damage index begins when the damage at the node i begins and when both concentrated damage stabilize, the local damage index also stabilizes. Meanwhile, the first nonzero value of the plastic damage index is an indication that the plasticity begins in the column. However, the plasticity has no effect on the evolution of the local damage index.

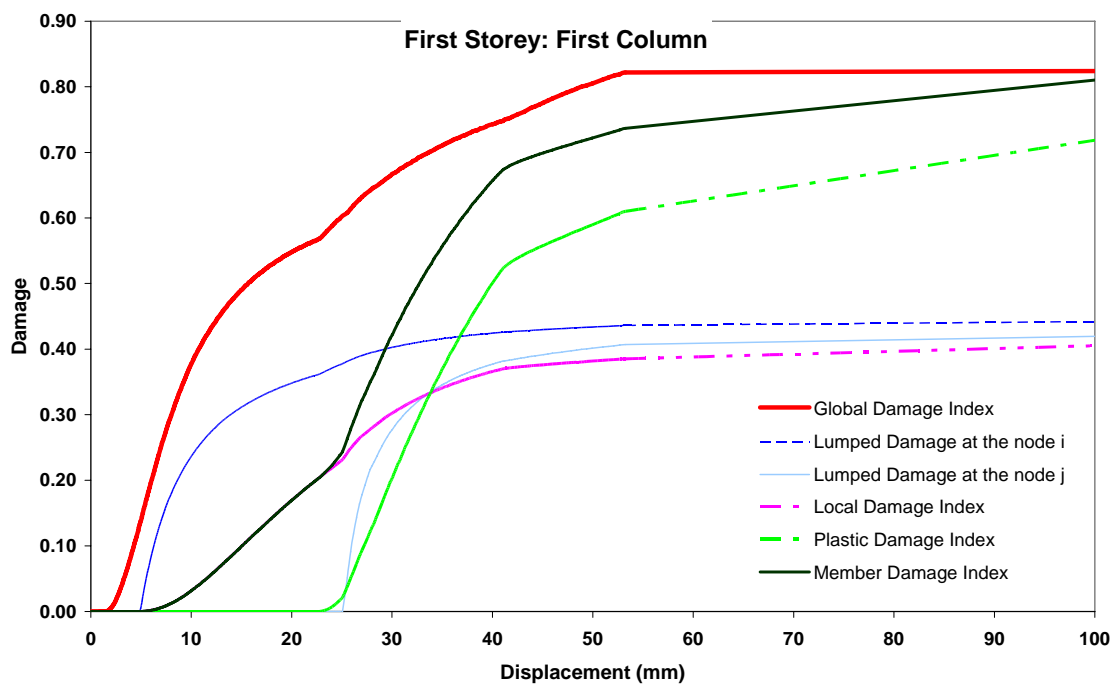


Figure 7.15 – Evolution of the damage indexes at first column of the first storey.

Let us now use the member damage index proposed in the Chapter 6. Analyzing its evolution (see Figure 7.15), we can notice that initially, both local and member damage indexes have the same value, but when the plasticity begins, the member damage begins increasing more than the local damage index. The point where the member damage index separates from the local damage index is also coincident with the point where the global damage also changes its slope. The same behaviour can be observed in the evolution of the damage indexes for the beam of the first storey, Figure 7.16 .

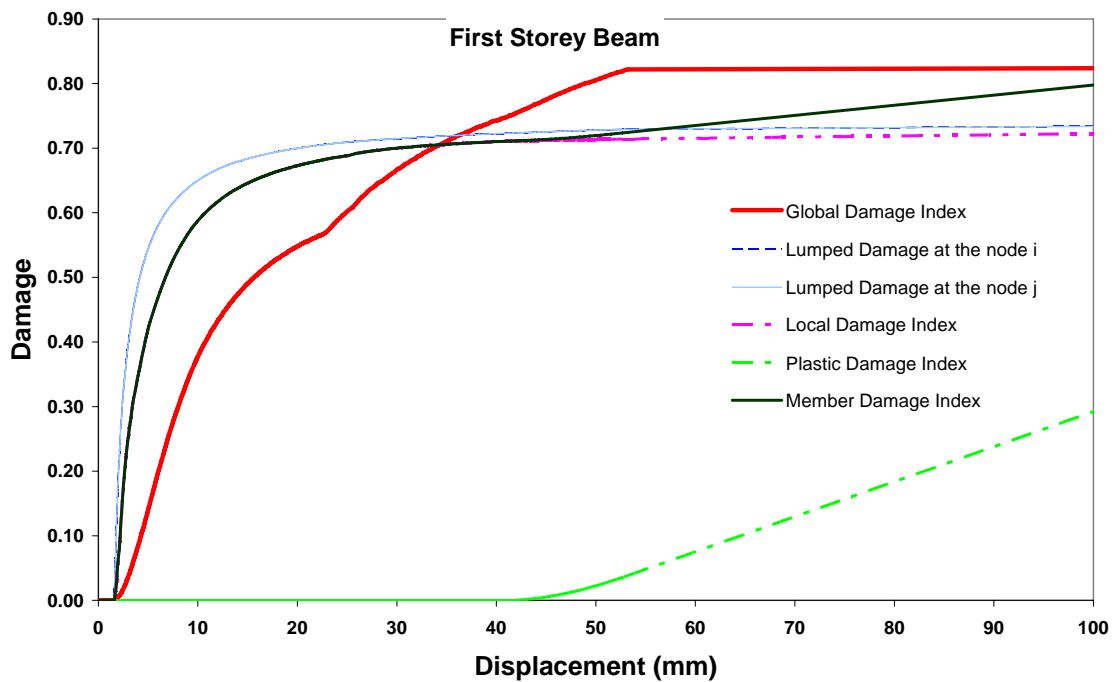


Figure 7.16 - Evolution of the damage indexes in the beam of the first storey.

7.5 Example 4: Model validation using dynamic analysis of a reinforced concrete framed structure

This example analyzes the simulation of the evolutions of the damage and plasticity process in a reinforced concrete plane frame (see Figure 7.17) subjected to dynamic loading.

The frame is 7,5 m high and 10 m wide and has three levels. The columns have a 0,40 m×0,40 cm cross-section of reinforced concrete with 1,9 % steel ratio with critical moment and ultimate moment $m_{cr} = 30$ kNm and $m_u = 182$ kNm respectively. All horizontal beams are 0,40 m thick and 0,30 m wide, with a steel ratio of 0,75 % on the bottom and 0,42 % on the top, as shown in Figure 7.17. For beams, the critical moment and ultimate moment adopted were $m_{cr} = 18$ kNm and $m_u = 111$ kNm respectively. The proposed reinforced concrete has the following properties: the compressive strength of concrete is $\sigma = 21$ MPa, its elastic modulus $E = 3,1 \times 10^4$ MPa, density $\rho_0 = 2,5$ kN/m³, and using in this case a fracture energy G_f equal to 250 kN/m. It is also considered that the steel has a hardening plastic modulus equal to 10^8 . Each frame element is formed by two beam-column elements.

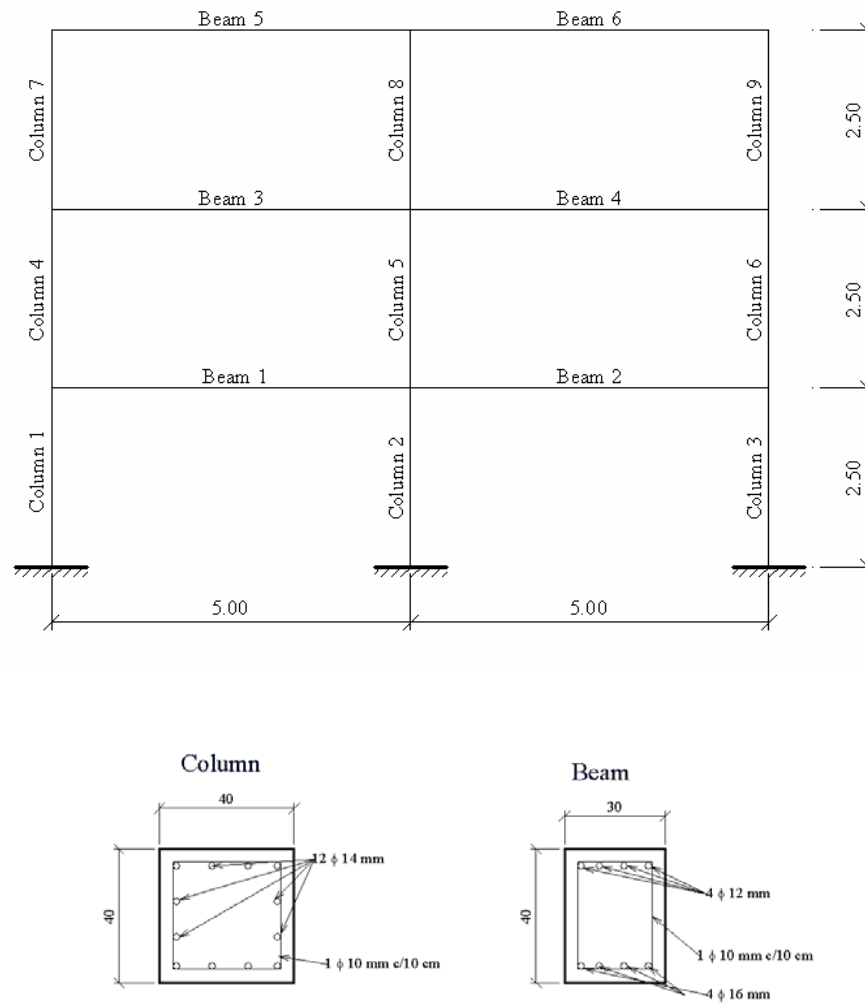


Figure 7.17 - Geometry and sections of the studied frame.

The equation of motion governing the dynamic behaviour of the structure has been solved using the Newmark algorithm proposed in 3.8 with $\beta = 0,25$ and $\gamma = 0,5$ while the time step used was $\Delta t = 0,01$ s. The structure was subjected to a harmonically acceleration function $a(t) = g \sin(10t)$, where $g = 9.81 \text{ m/s}^2$ is the gravitational acceleration.

With the aim of comparing the models proposed in this work, the structure has been analyzed under three situations: using the plastic model proposed in Chapter 4, using the damage model proposed in Chapter 5 and using the plastic-damage model proposed in Chapter 6. Figure 7.18 shows the comparison between the elastic response of structure and the nonlinear response considering the proposed plastic, damage plastic-damage models.

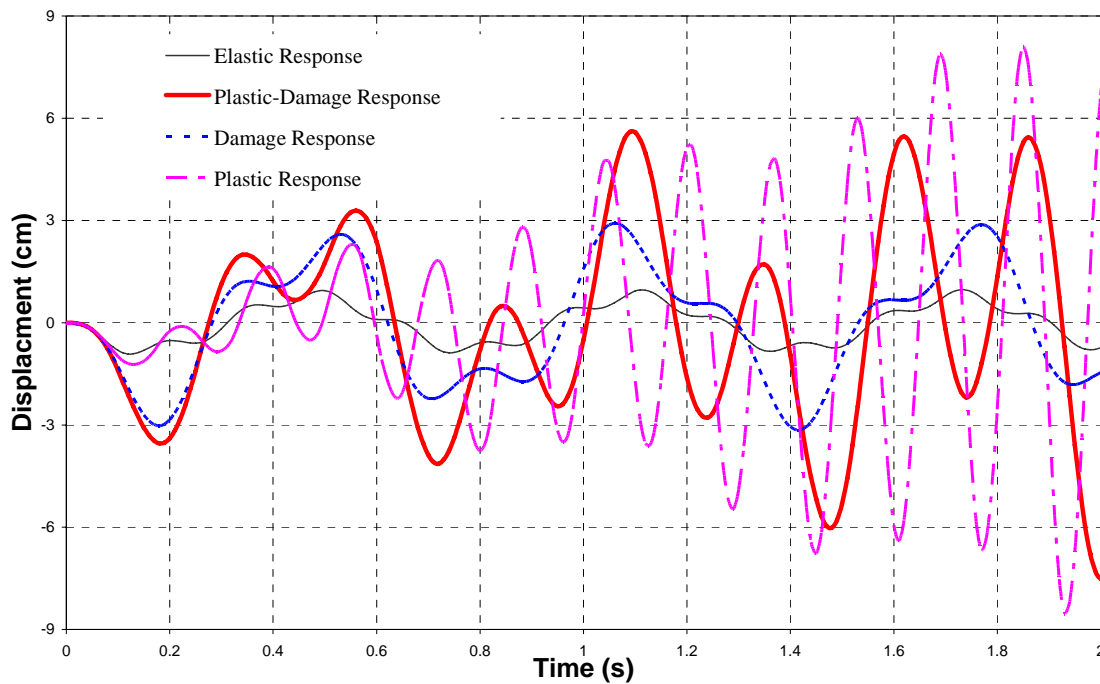


Figure 7.18 – Third floor displacement, in elastic, plastic, damage and plastic-damage behaviour.

The displacement has been measured at the third floor, and we can observe that for all cases the response builds up gradually. Nevertheless, in the plastic model, the response continues to grow by the amount of a constant period for each cycle. This period is shorter than in the damage and plastic-damage response. However, the displacements obtained in the plastic response are higher than the others are. This occurs because, in the damage or plastic-damage model, the damage works as a damping force, and consequently the response of the structure looks like a damped system, while in the plastic model we obtain a resonant undamped system response.

Using the global damage equation proposed in the Chapter 6, Figure 7.19 shows the evolution of the global damage indexes for each model. We can observe that both damage and plastic-damage indexes begin at same time and their have identical values. They kept the same values until the instant when the plasticity begins, causing the global damage index in the plastic-damage response to increase more than in the damage response. The effect of plasticity in the plastic-damage response is coincident with the increasing of the global damage index in the plastic response.

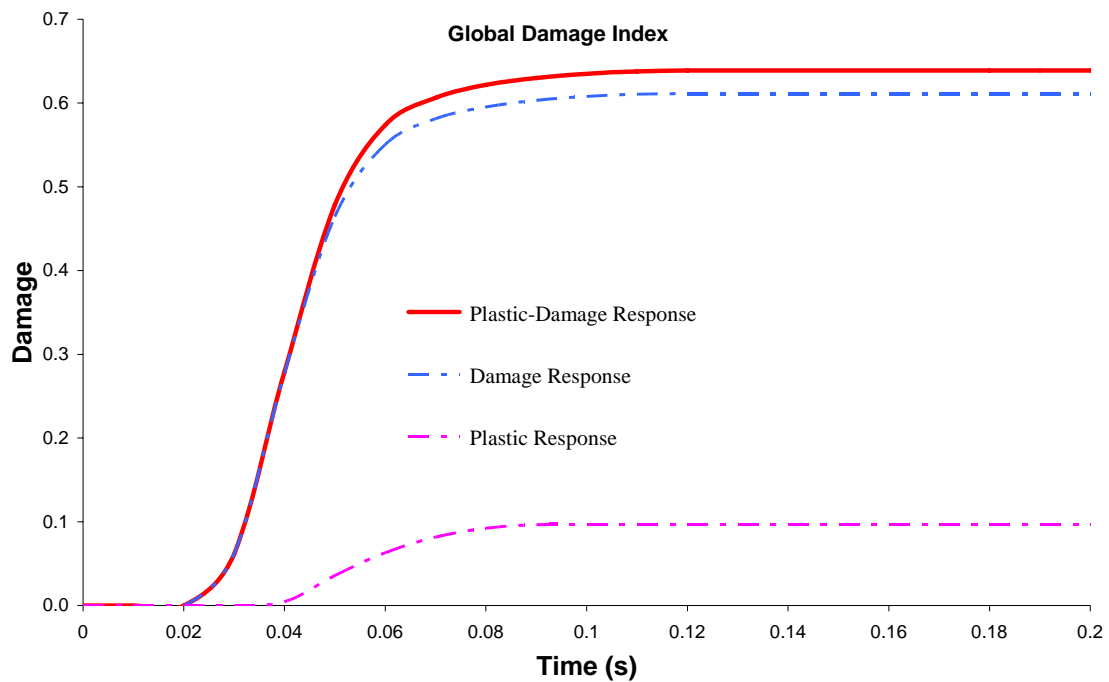


Figure 7.19 –Comparison of the global damage indexes evolution.

The same behaviour is observed in the evolution of the member damage index, i.e., Figure 7.20 shows the evolution of the member damage evolution at the second column and at the first column of the first floor. In both cases, the member damage index was obtained by means of the equation proposed in Chapter 6.

Comparing the evolution of the plastic hinge in the plastic response and in the plastic-damage response (Figure 7.20), as expected, the results at plastic response are higher than the results obtained at plastic-damage response. In the plastic-damage response, the influences of the damage can be observed through the slope of the curve, which is more than in the plastic response (see Figure 7.20.a), and by the values of the bending moment obtained, which are smaller than the values obtained in the plastic response.

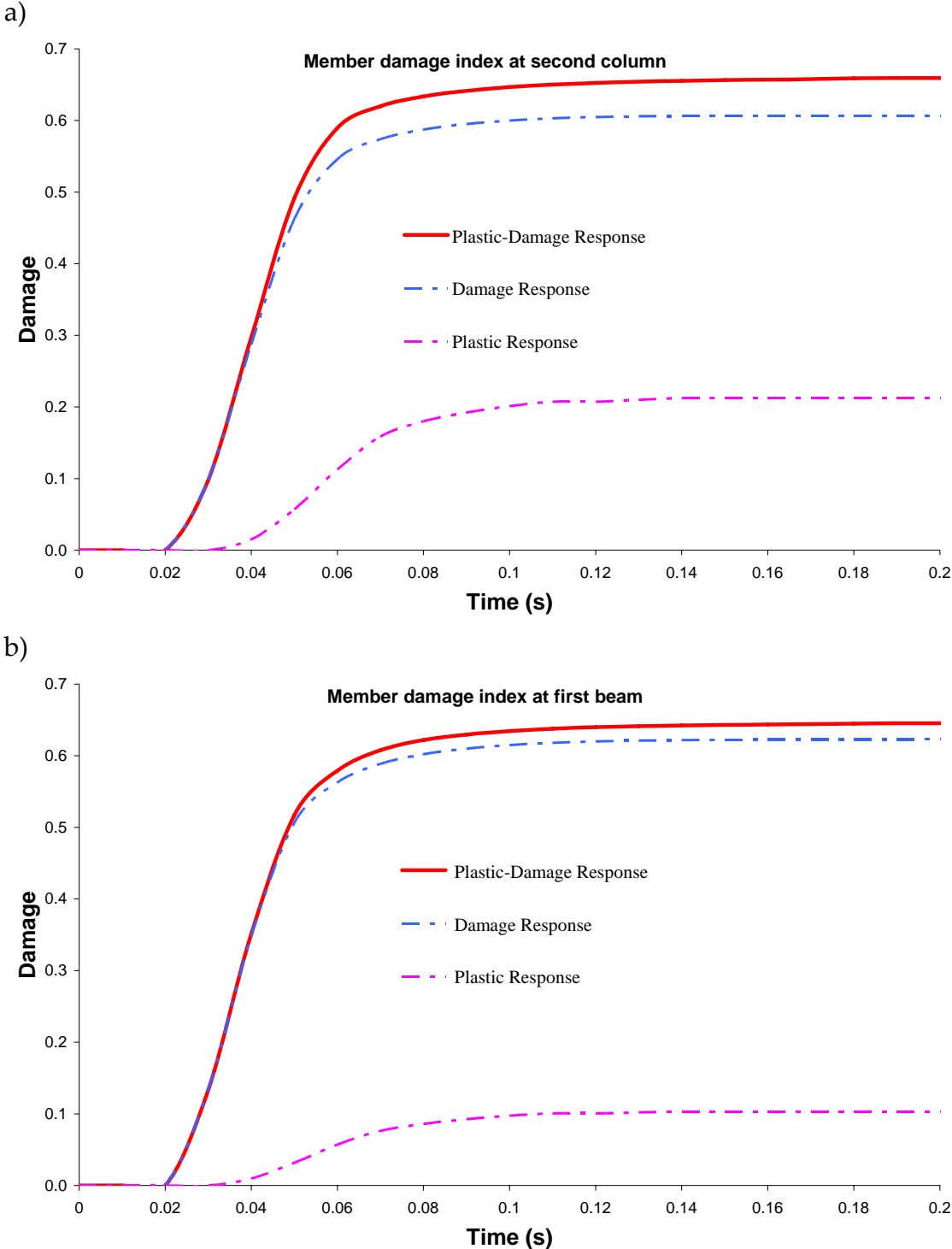


Figure 7.20- Evolution of the member damage indexes a) at the second column and b) at the first beam of the first floor

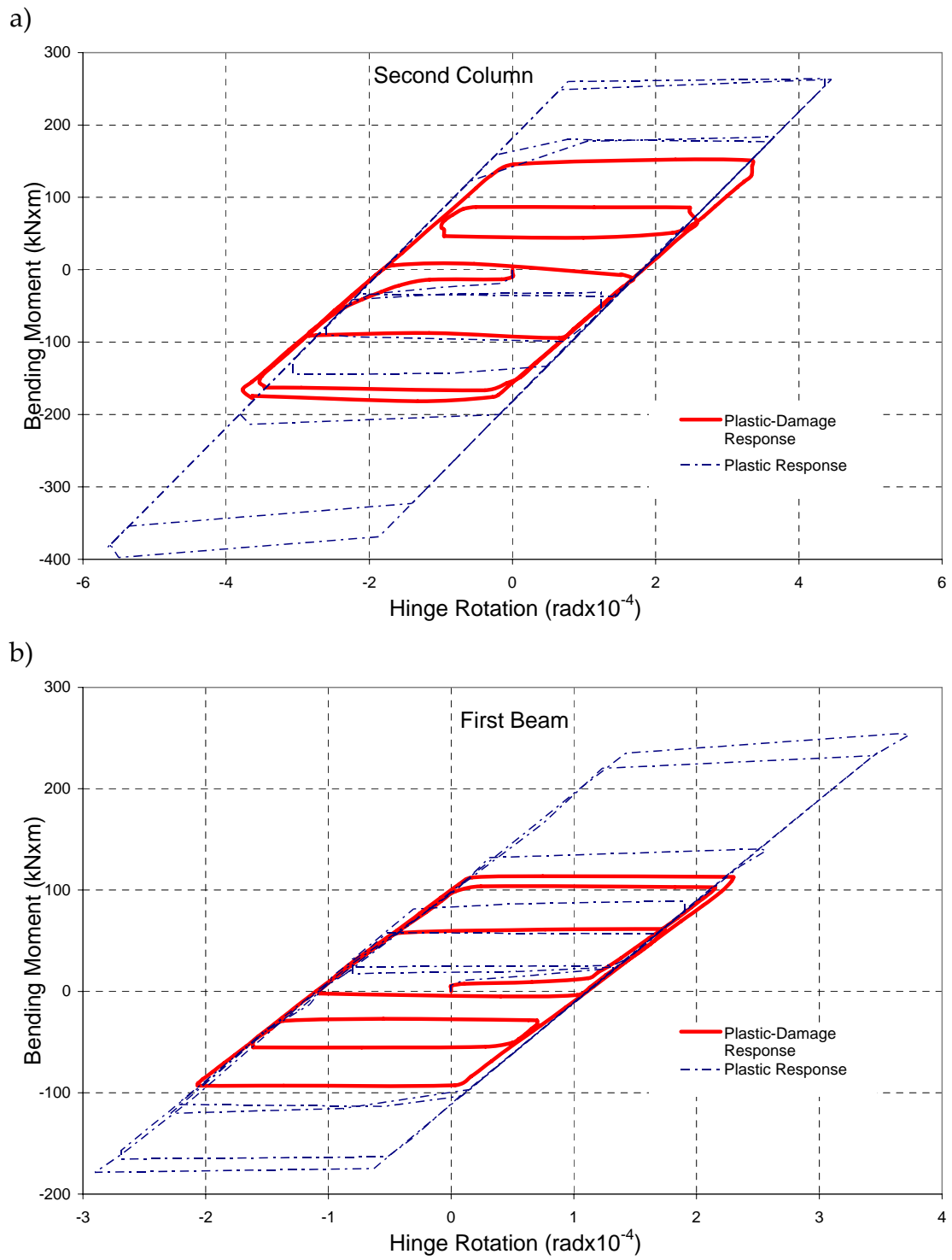


Figure 7.21 - Moment-rotation a) in the second column and b) in the first beam of the first floor

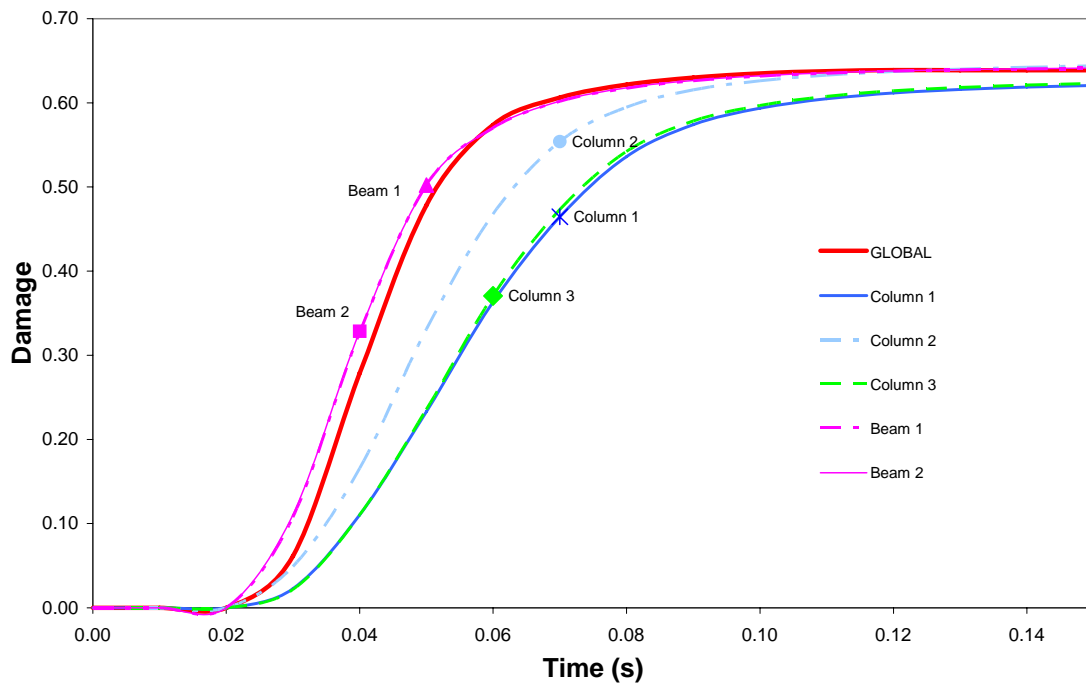


Figure 7.22 - Evolution of the global and member damage indexes for beams and columns at the first floor.

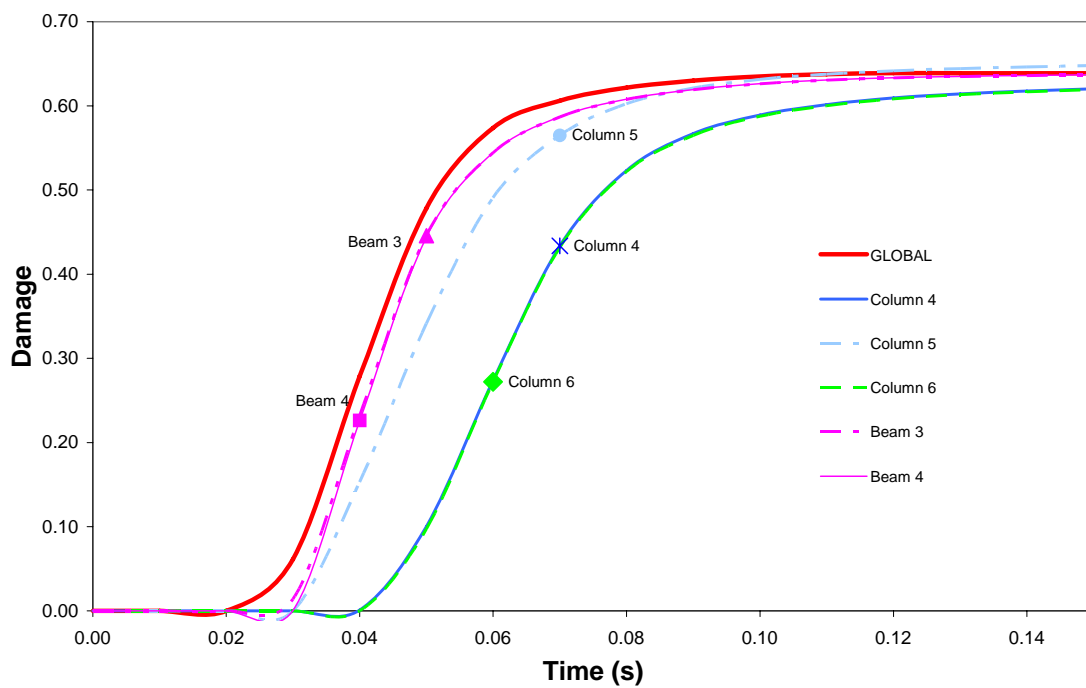


Figure 7.23 - Evolution of the global and member damage indexes for beams and columns at the second floor.

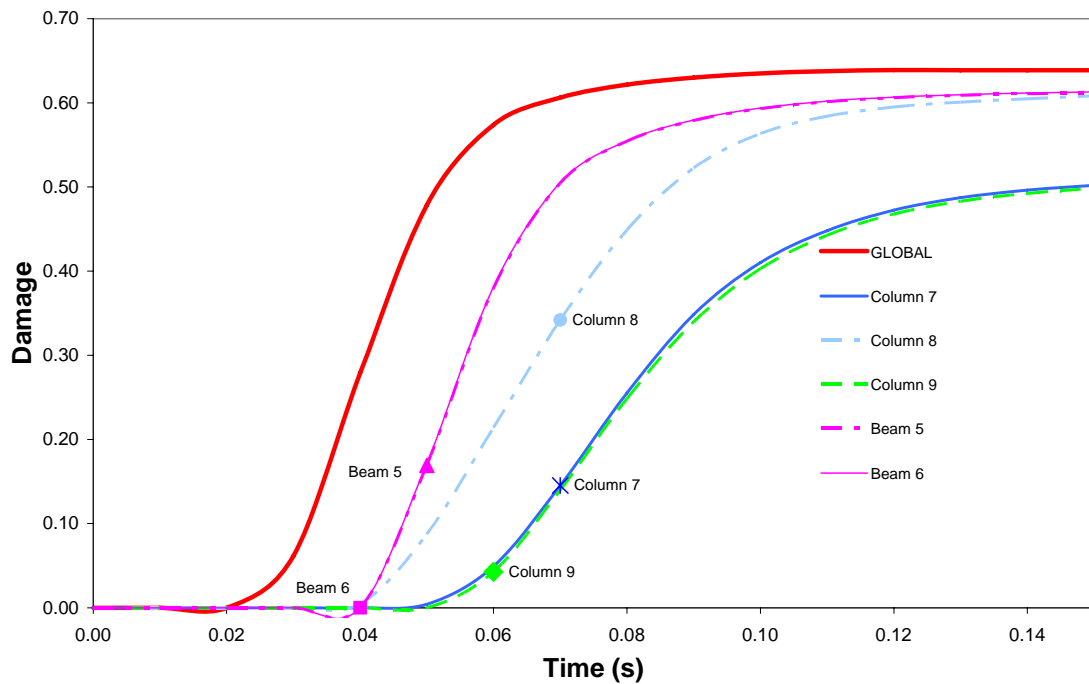


Figure 7.24 - Evolution of the global and member damage indexes for beams and columns at the third floor.

Analyzing the evolution of member damage indexes in figures 7.22 -7.24, it can be observed that the damage decreases with the height. In the first floor (see Figure 7.22), the second column and the both beams are the only elements where the member damage indexes are slightly greater than the global damage. In the case of the second column, the member damage index is slightly greater than the global damage only when the plastic hinge appears at the top of the column. Likewise, the same response can be observed in the elements of the second and third floor. This behaviour is in agreement with the evolution of the plastic hinge described in Figure 7.25, where beams of the first floor are the first elements at which the plasticity appears at both extremities, detected by means of the formation of the plastic hinges, followed by the beams of the second and of the third floor.

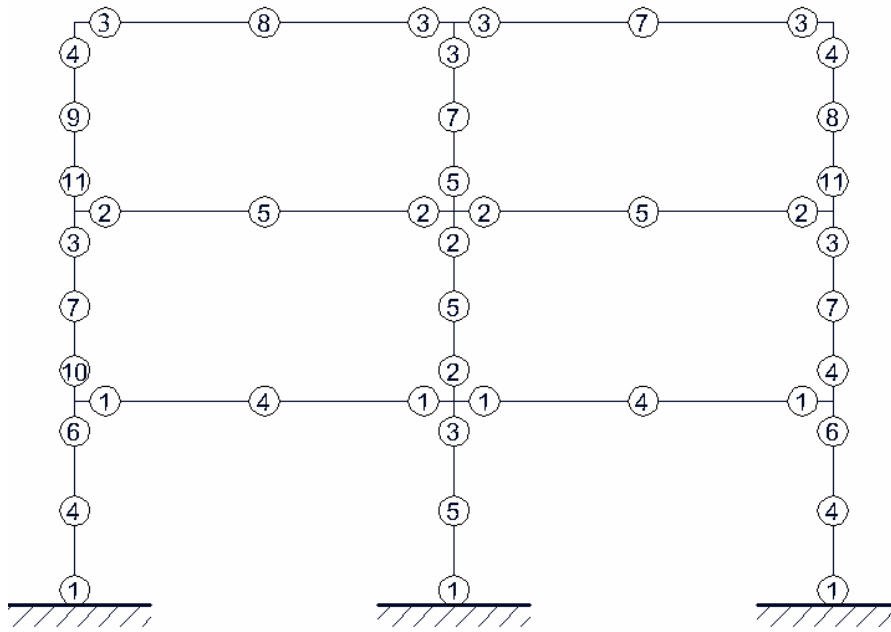


Figure 7.25 – Sequence of plastic hinges developments within the frame.

7.6 Example 5: Pushover and dynamic analysis of a reinforced concrete frame

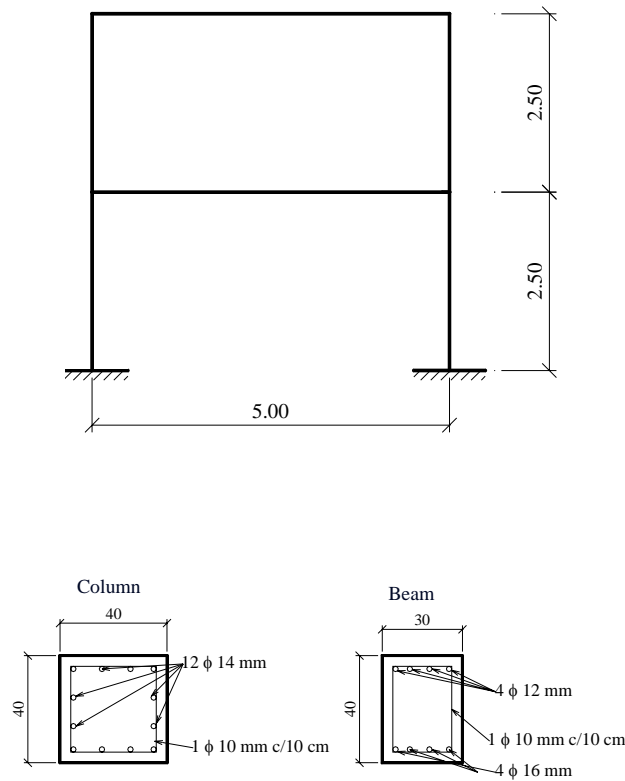


Figure 7.26 - Geometry and sections of the studied frame.

This example compares of the evolutions of the global damage index in the reinforced concrete plane frame of Figure 7.17 subjected to a pushover load and a dynamic load.

The frame is 5 m high and 5 m wide and has two levels. The columns have a 0,40 m×0,40 cm cross-section with a steel ratio of 1,9 % . The critical and ultimate moments are $m_{cr} = 30$ kNm and $m_u = 182$ kNm, respectively. All the horizontal beams are 0,40 m thick and 0,30 m wide, with a steel ratio of 0,75 % on the bottom and 0,42 % on the top, as shown in Figure 7.17. For the beams, the adopted critical and ultimate moments are $m_{cr} = 18$ kNm and $m_u = 111$ kNm, respectively. The reinforced concrete is assumed to have the following properties: compressive strength is $\sigma = 21$ MPa, elastic modulus $E = 3,1 \times 10^4$ MPa, density $\rho_0 = 2,5$ kN/m³, and a fracture energy G_f equal to 250 kN/m. The steel has a hardening plastic modulus equal to 10^2 . The time history of the dynamic load is given in Figure 7.27 while the pushover-loading pattern can be seen in Figure 7.28.

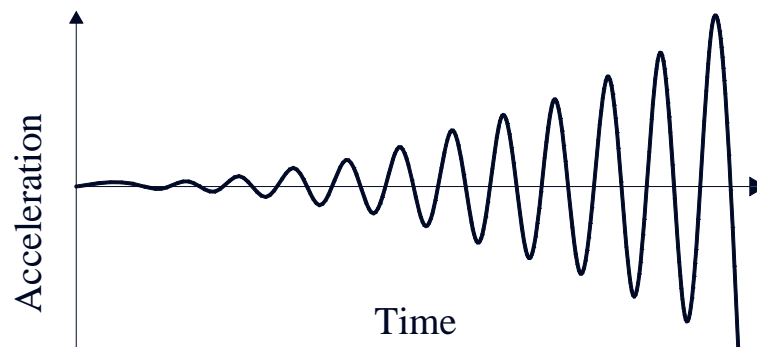


Figure 7.27 – Dynamic Load.

The conventional pushover analysis searches the nonlinear incremental-iterative solution of the equilibrium equation $[\mathbf{K}]\{\mathbf{U}\} = \{\mathbf{F}\}$, where $\{\mathbf{U}\}$ is the displacement vector, $[\mathbf{K}] = \sum [\mathbf{B}_b^t] : [\mathbf{S}_b^d(\mathbf{D}_b)] : [\mathbf{B}_b]$ is the nonlinear stiffness matrix and $\{\mathbf{F}\}$ is a predefined load vector applied laterally along the height of the structure in relatively small load increments (see Figure 7.28). This lateral load can be a set of forces or displacements that have necessarily a fixed pattern, which, in this example, correspond to the first mode of vibration of the structure.

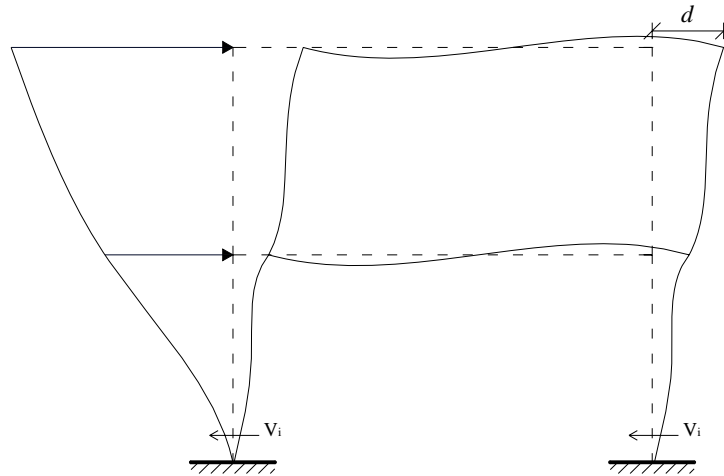


Figure 7.28 – Pushover loading pattern.

The pushover analysis allows computing the sequence of yielding and failure at member and structural level, as well as the progress of the overall strength capacity of the structure, as shown in Figure 7.29. The horizontal forces (V_i) of the base nodes were plotted against the horizontal displacement of the top floor d in Figure 7.28. In dynamic analysis, the support displacement is rested from the top displacement in order to establish the global drift of the structure. It can be observed in Figure 7.29 that the pushover curve enveloping the absolute values of the dynamic response.

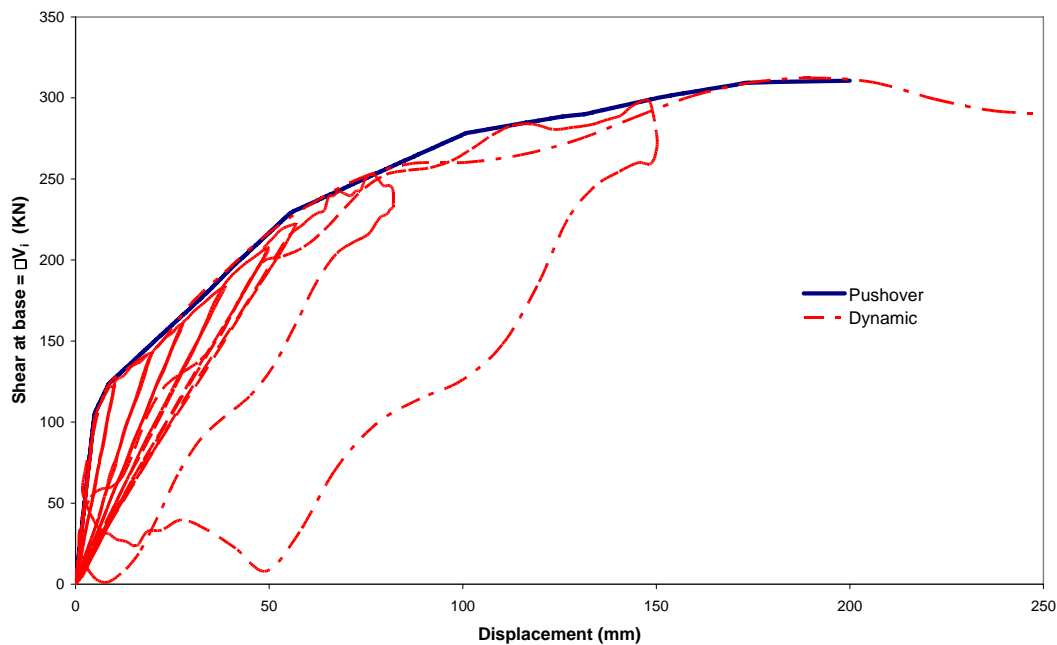


Figure 7.29 – Base shear versus global structural drift.

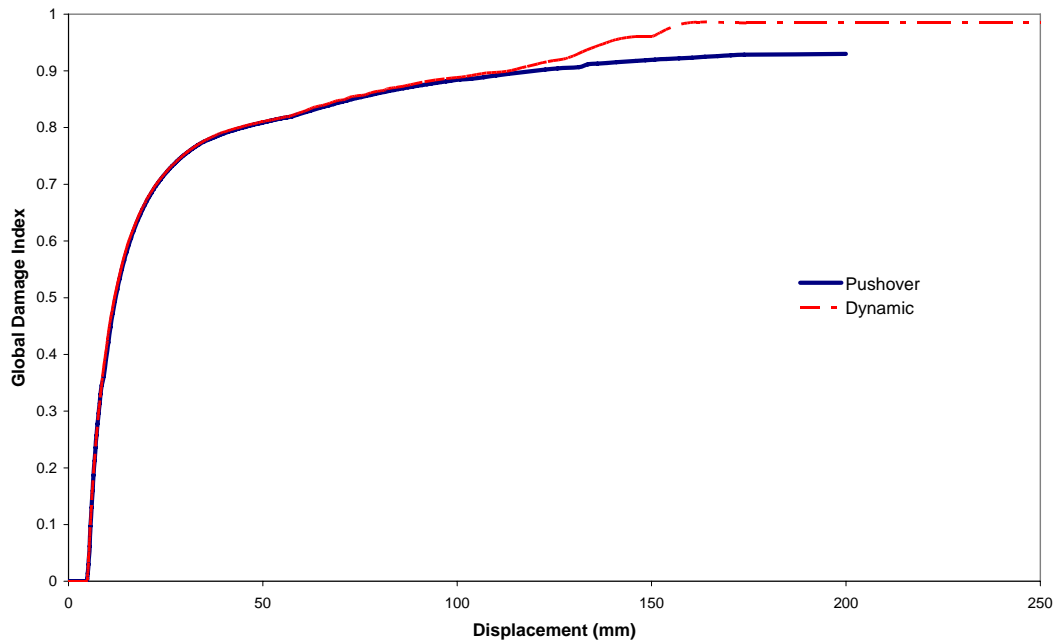


Figure 7.30 – Global damage evolution.

Analyzing the evolution of the global damage index of Figure 7.30, we can perceive that during the phase where the plasticity is null or irrelevant, both global damage curves, dynamic and pushover response, are similar. However, the final value of the global damage obtained by means of dynamic analysis is higher than the value of the global damage obtained by pushover analysis. This occurs because in the dynamic analysis, when the plasticity appears suddenly, while in the pushover analysis the influence of the plasticity is gradual. The static pushover analysis neglects dynamic effects, since that the conventional pushover analysis procedure does not account for the progressive changes in the modal properties during nonlinear yielding and cracking in the structure.

This is due to the constant lateral load pattern used ignores the potential redistribution of inertia forces and higher mode effects, as cracking and yielding which governs the inelastic structural behaviour. Consequently, the energy dissipated by the plasticity during a dynamic action is higher than in the pushover response, affecting directly the global damage index.

7.7 Example 6: Model validation using a reinforced concrete framed structure subjected to a synthetic earthquake accelerogram.

This example analyzes the simulation of the evolutions of the damage and plasticity process in a reinforced concrete plane frame (see Figure 7.31) subjected to dynamic loading.

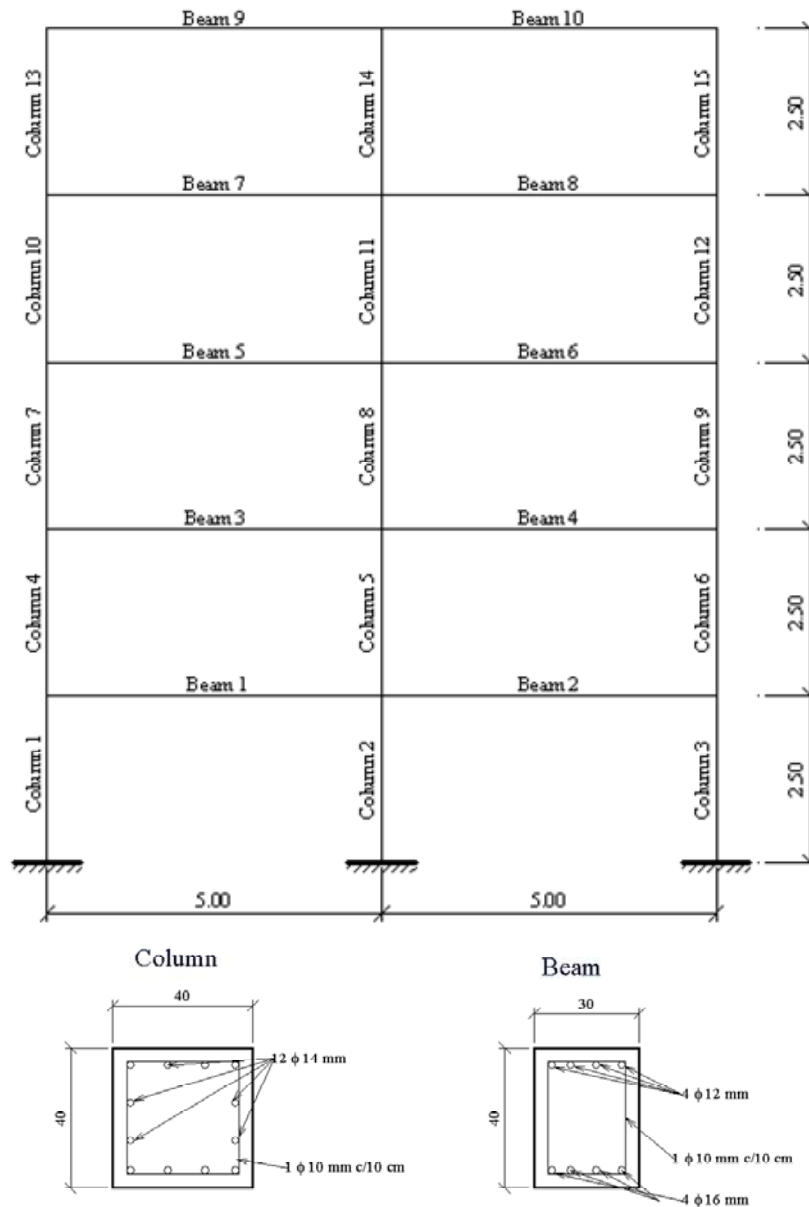


Figure 7.31 – Geometry and sections of the studied frame.

The frame is 12,5 m high and 10 m wide and has five levels. The columns have a 0,40 m×0,40 cm cross-section of reinforced concrete with 1,9 % steel ratio

with critical moment and ultimate moment $m_{cr} = 30$ kNm and $m_u = 182$ kNm respectively. All horizontal beams are 0,40 m thick and 0,30 m wide, with a steel ratio of 0,75 % on the bottom and 0,42 % on the top, as shown in Figure 7.31. For beams, the critical moment and ultimate moment adopted were $m_{cr} = 18$ kNm and $m_u = 111$ kNm respectively. The reinforced concrete has the following properties: the compressive strength of concrete is $\sigma = 21$ MPa, its elastic modulus $E = 3,1 \times 10^4$ MPa, density $\rho_0 = 2,5$ kN/m³, and using in this case a fracture energy G_f equal to 250 kN/m. It is also considered that the steel has a hardening plastic modulus equal to 10^8

This example studies the evolutions of the damage and plasticity process in the five floors of a reinforced concrete plane frame (see Figure 7.31) subjected to dynamic loading.

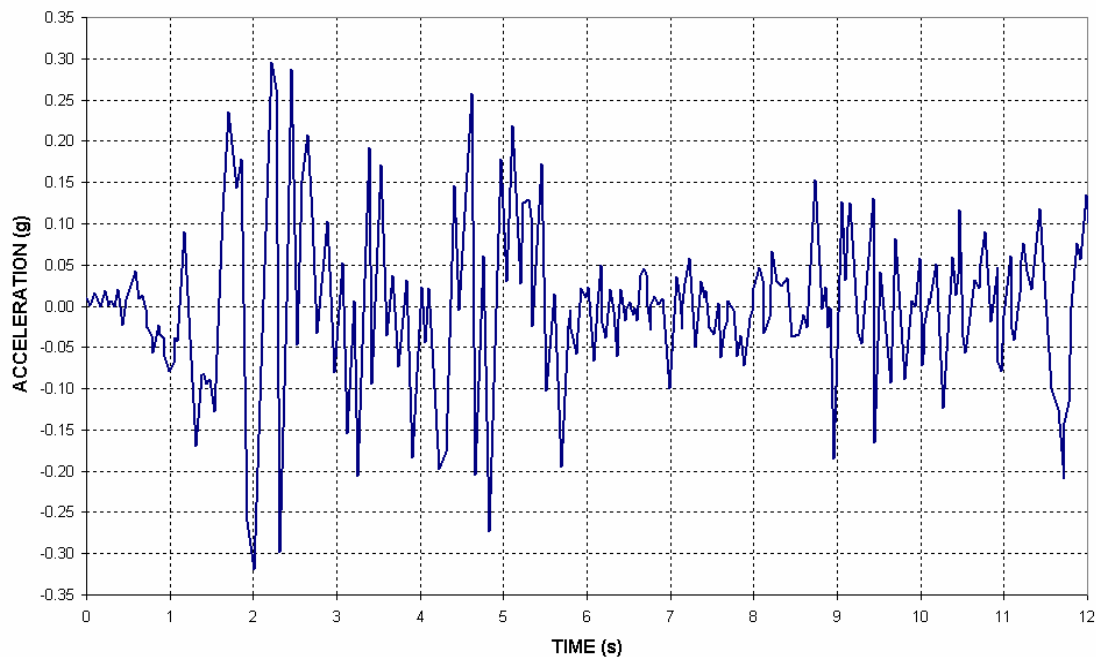


Figure 7.32 – Synthetic seismic accelerogram.

The frame is 12,5 m high and 10 m wide and has five levels. The columns have a 0,40 m \times 0,40 m cross-section with a 1,9 % steel ratio. The critical and ultimate bending moments are $m_{cr} = 30$ kNm and $m_u = 182$ kNm, respectively. All the horizontal beams have 0,40 m thick and 0,30 m wide, with a steel ratio of 0,75 % on the bottom and 0,42 % on the top, as shown in Figure 7.31. The critical and ultimate moments of the beams are $m_{cr} = 18$ kNm and $m_u = 111$ kNm, respectively. Just for this studies, we assume that the reinforced concrete has the following

properties: compressive strength $\sigma = 21 \text{ MPa}$, elastic modulus $E = 3,1 \times 10^4 \text{ MPa}$, density $\rho_0 = 2,5 \text{ kN/m}^3$, and a fracture energy $G_f = 250 \text{ kN/m}$. The steel has a hardening plastic modulus equal to 10^8 .

The equation of motion that governs the dynamic behaviour of the structure has been solved using Newmark's algorithm proposed in 3.9.2 with $\beta = 0,25$, $\gamma = 0,5$ and a time step $\Delta t = 0,01 \text{ s}$. The structure was subjected to a synthetic earthquake accelerogram of Figure 7.32 having a maximum amplitude of $0,295 \text{ g}$.

Figure 7.33 shows the comparison among the responses of the structure considering elastic, damage, plastic and plastic-damage behaviour of the material. The displacements correspond to the fifth floor.

Using a plastic model, the response continues to grow by a constant period for each cycle. This period is shorter than in the damage and plastic-damage response. However, the displacements obtained in the damage response are higher than the others are. This occurs because in the damage response, the damage works as a damping force and, consequently, the response of the structure looks like a damped one, while in the plastic-damage model, the combination of plasticity and damage makes that the structures behaves as a undamped system.

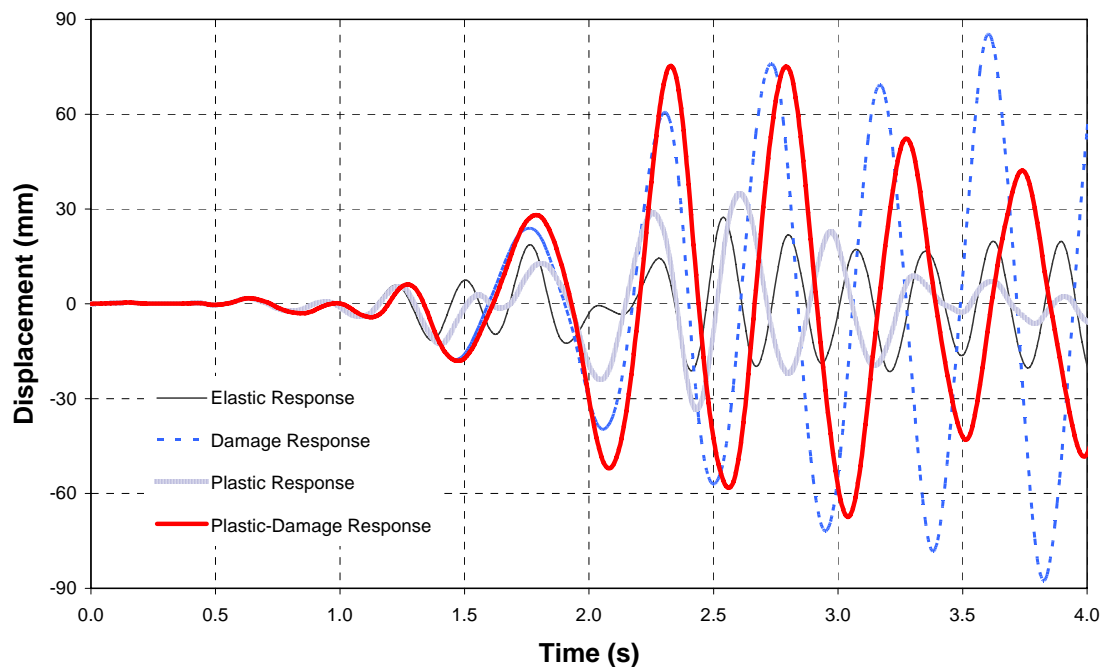


Figure 7.33 – Fifth floor displacement, in elastic, damage, plastic and plastic-damage behaviour.

Figure 7.34 shows the evolution of the concentrated damage in the first, second and third columns of the first floor, while Figures 7.36 and 7.37 shows the evolution of the global, local and plastic damage indexes for the first and the fifth floor, respectively. As expected, the frame fails mainly due to the damage of the columns at its base; this behaviour is confirmed by the evolution of the local damage indexes.

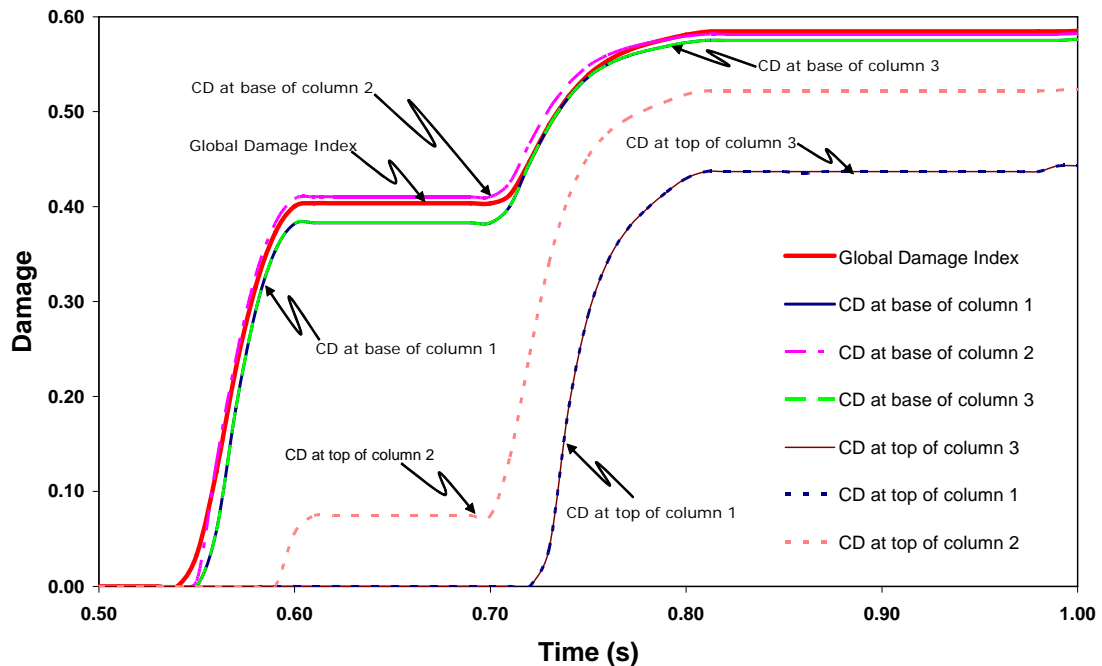


Figure 7.34 – Evolution of the global damage index and of the concentrated damage at the base and top of columns of the first floor.

By analyzing the evolution of the concentrated damage of the first floor columns, shown in Figure 7.34, we can observe that the damage at the base of all the columns is practically the same as the global damage and constantly increase in time. However, for the member damage indexes of the first floor columns (see Figure 7.35) we can observe that the trend is practically the same as the global damage curve of the entire structure, similarly as observed in the concentrated damage case of Figure 7.34. It can be observed that the damage of the columns decreases with the height.

With respect to the beams, we can observe that in the first (Figure 7.35), their member damage is slightly higher than the global damage index, while in the fifth floor it decreases (Figure 7.36). This occurs because damage decreases with the height. Furthermore, in the first, second and third floors, the damage in all beams begin at the same time as the damage of the first floor columns.

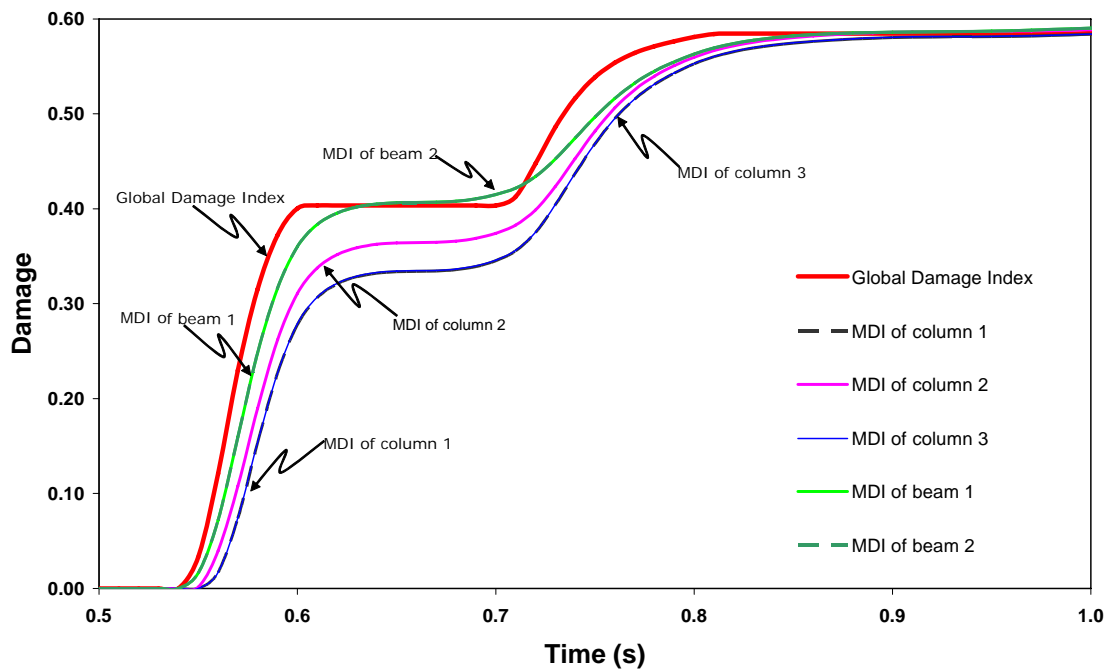


Figure 7.35 – Evolution of the global and member damage (MDI) indexes for the first floor: a) columns; b) beams.

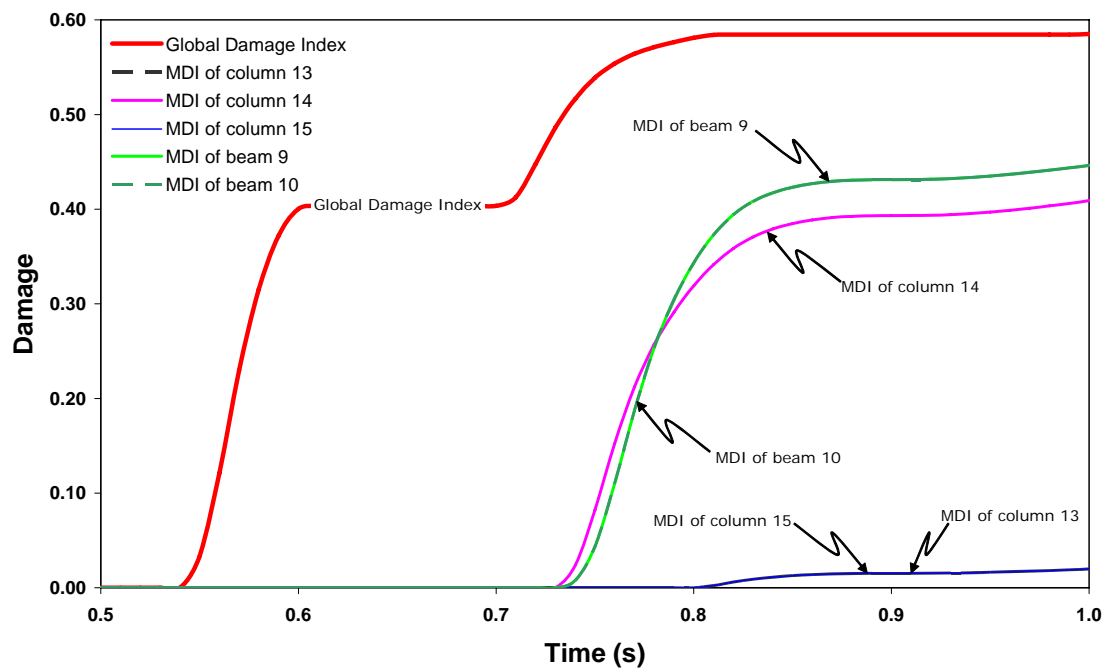


Figure 7.36 – Evolution of the global and member damage (MDI) indexes for the fifth floor: a) columns; b) beams.

Unlike the non-decreasing nature of the concentrated damage, the plastic rotations under cyclic loads have an increasing-decreasing nature. Once the plas-

tic rotations are active, their value can be higher, equal, or lower than in the previous time step (see Figure 7.38). This occurs because the plastic hinge rotations are functions of the evolution of the bending moment. The hardening of the material can influence the member damage index and might not allow maximum plastic dissipation.

Due to the hardening adopted in this case, the global behaviour of the structure is not influenced by the plasticity, because even if all the members are yielding, member damage indexes are not higher than the global damage index. Observing the member damage indexes, it can be seen that the maximum plastic dissipation in the beams is greater than in the columns. This is in agreement with the well-known real behaviour of the structures under a seismic load, because in seismic design, for safety, the beam should develop plastic hinges before the columns. Furthermore, in this example the parameters were defined with the aim of analyzing the structure before its collapse.

Figure 7.38 shows the plot of the moment- plastic rotation at the base and at the top of the column of the first floor. Figure 7.39 shows the sequence of the evolution of the plastic hinges in the frame and Figure 7.40 shows the sequence of the deformations of the structure

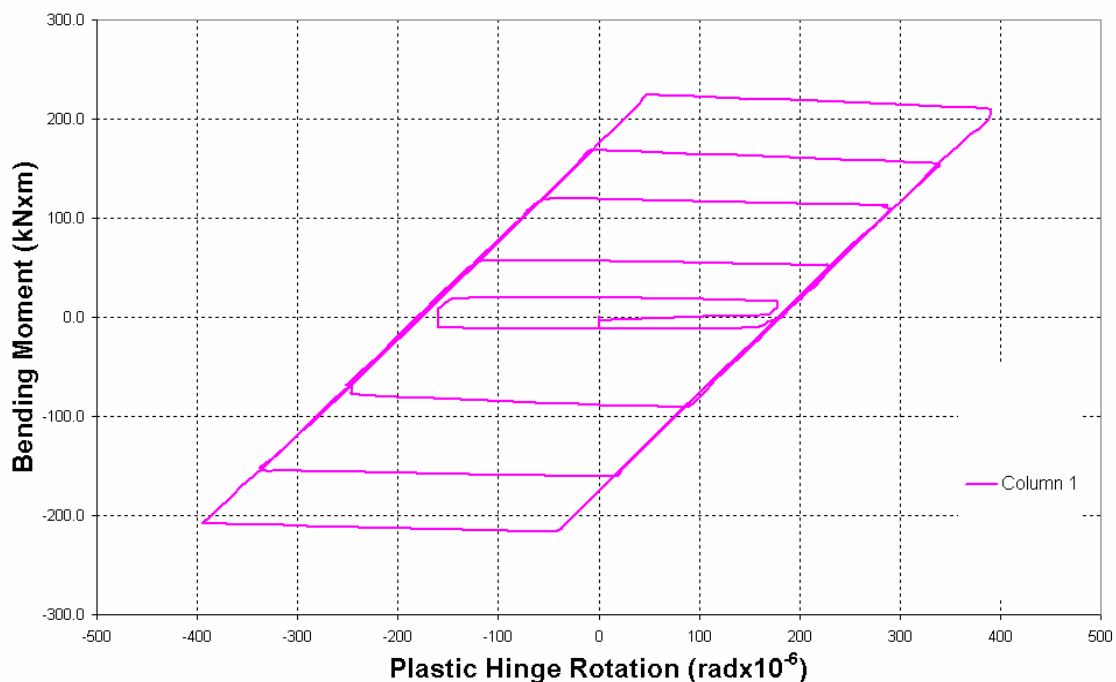


Figure 7.37 - Moment-rotation at the base of the first column of the first floor

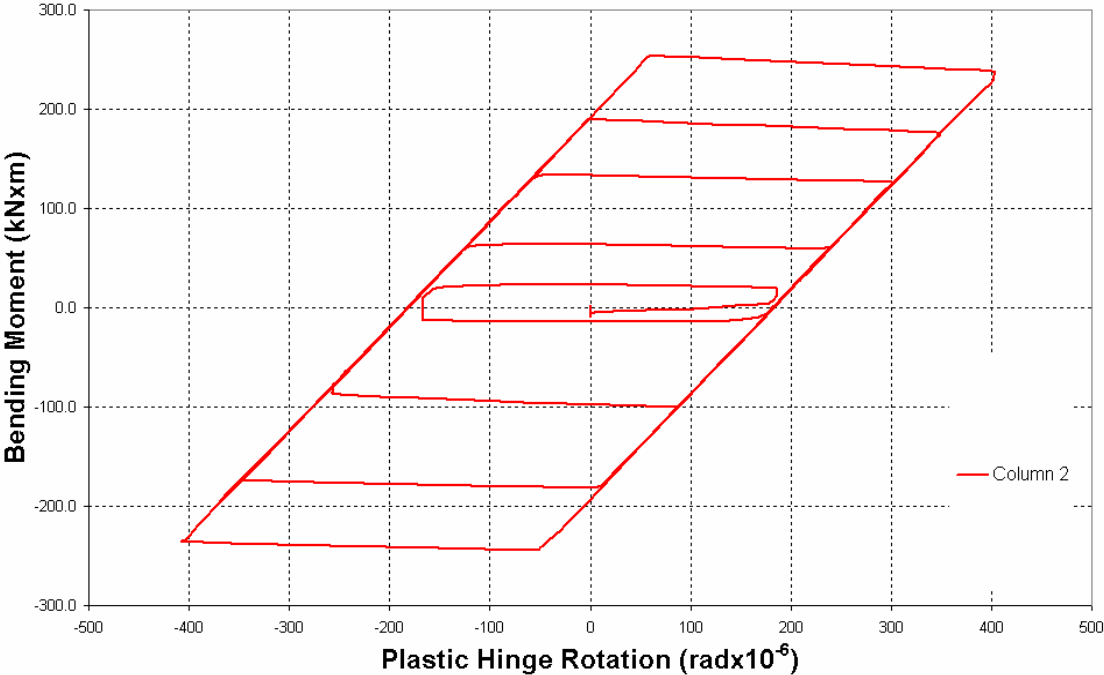


Figure 7.38 - Moment-plastic rotation at the base of the second column of the first floor

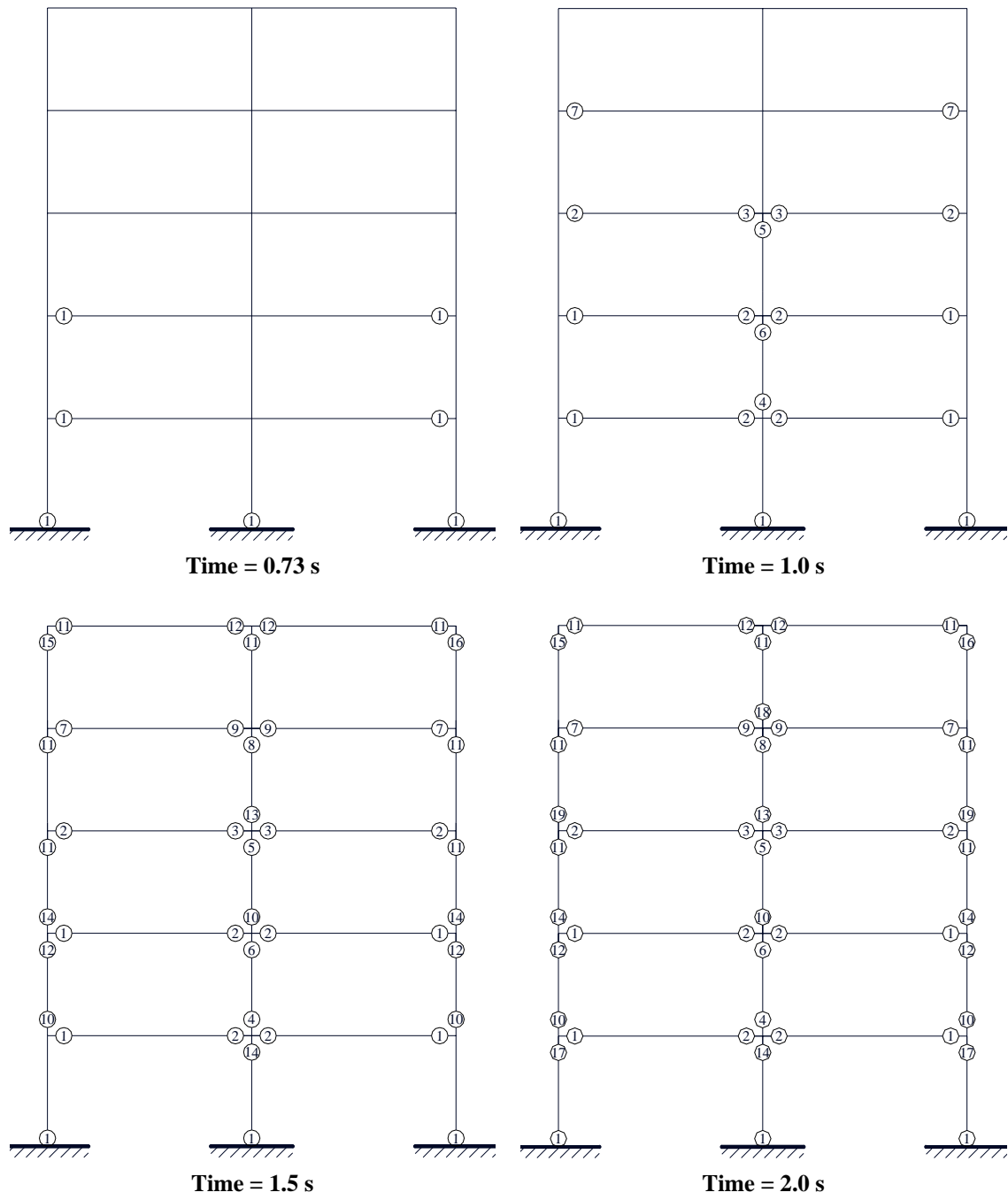


Figure 7.39 - Sequence of formation of the plastic hinges within the frame.

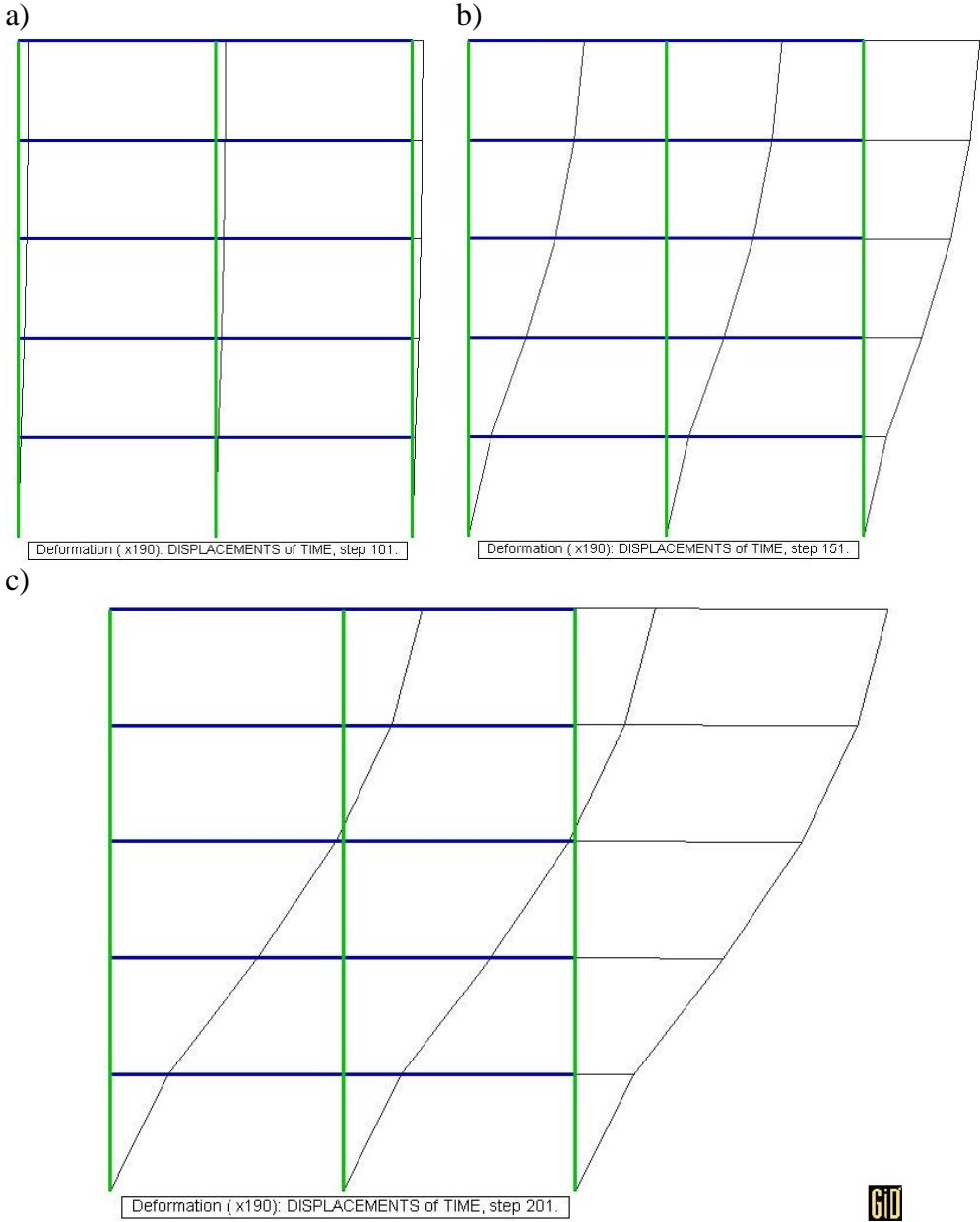


Figure 7.40 – Deformed configuration at: a) 1.0 seconds; b) 1.5 seconds; and c) 2.0 seconds.

Chapter 8

Conclusions and Recommendations for Further Work

8.1 Conclusions of the research

A general framework for the nonlinear analysis of frames based on the Continuum Damage Mechanics and Plasticity Theory has been developed. The plastic-damage model developed in this thesis assumes that plasticity and damage are uncoupled, have their own laws and that both are concentrated at the ends of the frame members. Within this framework, many kinds of materials and loading conditions have been considered. Even the loading-unloading process has been simulated, and the values obtained provide satisfactory results when compared with laboratory tests, especially for reinforced concrete building. Additionally, the dynamic response has been simulated.

We can make the following considerations:

- The elastoplastic behaviour of frames is described by means of the plastic hinge concept. The plasticity is assumed concentrated at the

end of the cross section, leading to a sudden, and not gradual, plastification of the hinges. For convenience in computation, we will assume that the inelastic behaviour is concentrated at the ends, the plastic hinges, instead of being spread along the length of the beam-column element. Further, the beam-column element is assumed to remain elastic between the plastic hinges.

- The evolution of plastic hinges is given by yield functions for the bending moment evolution of the beam-column. In the thesis, we discussed three yield function options. The first yield function proposed is for those cases where the material is assumed to have a perfect plastic behaviour. The second yield function is when the kinematic hardening effect in the bending moment is taken into account. Moreover, as the last option, we introduced a yield function as a function of the axial and of the bending moment at the end cross section, at any end.
 - The evolutions of the plastic rotations, as well as the yield function, at the end of the beam-column are independent between them. However, in the beam-column element, the moment equilibrium has to be maintained. For this reason, a return-mapping algorithm for frame elements is proposed and implemented. This procedure is necessary to maintain the evolution of the plastic within the surface of the yield function chosen and to control the loading/unloading conditions, in agreement with the Kuhn-Tucker inequality constraints.
 - The damage at the hinges is obtained through a new variable called concentrated damage parameter. The formulation and evolution of this parameter is developed by means of the Continuum Damage Mechanics. This formulation can be considered as simplified damage mechanics for frames, because it incorporates notions and methods of Continuum Damage Mechanics, as well as of fracture mechanics, into the frame analysis. Its evolution is based on the Strain Isotropic Continuum Damage Model proposed by Simo and Ju (1987). Using this theory, we assume that the damage will be measured by one variable, located at the hinge of the beam-column, which assumes values between zero and one, which indicates the relative density of the microcracks and their evolution in the material.
-

- The behaviour of the reinforced concrete is described throughout by means of continuum constitutive equations rates. We assume that the reinforced concrete presents two distinguished phases: the cracking of the concrete and the yielding of the reinforcement. The cracking phase of the concrete is described by means of Continuum Damage Mechanics, while the yielding of the reinforced steel is described by means of the Plasticity theory. Both, damage and plasticity are solved simultaneous by means of an uncoupled Plastic-Damage model proposed for frame structures. With this model, we can describe adequately the behaviour of the reinforced concrete elements.
- Member and global damage indexes has been developed to describe the actual state of deformation of a frame element as well as the entire structure, respectively. Although the use of the term “damage”, both variables are obtained by the ratio between the potential energy of the actual field the structure, or member, undertake because of the damage and plasticity (also called as the actual free energy) and the hypothetic potential energy the structure would store if it were composed by an elastic material under the same strain field, also called as the elastic free energy. Furthermore, both indexes, global and member, gives a measure of the structural stiffness loss.

8.2 Main contributions

Based on the above-mentioned concepts, the main contribution made in the present work are:

- √ The proposed plastic-damage model proves to be an effective tool for the numerical simulation of the collapse of frames. Its implementation under a matricial analysis program gives an efficient tool, being computationally economic and faster in the input as well as in the output than another programs based on finite element methods. It is a valuable alternative when other types of analyses, such as those based on multi-layer models; appears to be too expensive or impractical due to the size and complexity of the structure.
- √ As exposed in the numerical examples, the proposed model for reinforced concrete frames exhibited a very good precision. It can be observed that the results obtained by means of the matricial analysis program presents a good exactness in comparison with results obtained by means of finite elements. When compared with the results

obtained by means of experimental tests, the results obtained through the proposed plastic-damage model are better than those obtained by means of finite elements. Under cyclic or dynamic loads, the proposed model has been demonstrated that can represent with sufficient accuracy the real behaviour of reinforced concrete structures.

- √ The global damage index, together with the member damage index, has proved to be a powerful and precise tool for identifying the failure load and the structural mechanism leading to failure of reinforced concrete frame structures.
- √ The global damage index, together with the member and the concentrated damage indexes, provide accurate quantitative measures for evaluating the state of any component of a damaged structure and of the overall structural behaviour. It is an excellent tool for the seismic damage evaluation, reliability, and safety assessment of existing structures and can also be used in the evaluation of the repair or retrofitting strategies.

8.3 Future research lines

Starting from the studies carried out in this work, we propose the following future developments aimed at the extension and deepening of some aspects that still remain open:

- Extension to determine the influence of the shear reinforcement in the analysis. The design of beam-column connections is an important part of earthquake resistant design for reinforced concrete moment-resisting frames; therefore, the proposed model should be extended to other constitutive equations able to describe the influence of joint shear failure on the structural members. Joint shear failure is a set of phenomena characterized with combination of diagonal cracking, yielding of joint hoops and concrete crushing in beam-column joint as well as story shear degradation.
 - Extension to calculate the P-Delta effects on columns. P-Delta is a non-linear (second order) effect that occurs in every structure where elements are subject to axial load. It is a genuine "effect" that is associated with the magnitude of the applied axial load (P) and a displacement (Delta).
-

- Extension to determine the length of influence of the damage and plasticity on the beams elements. For accurately represent the hysteretic behaviour of the plastic zone, requires tracing the response of each section during the entire response time history. The first option could be divided the beam into various segments. However, this is undesirable form the standpoint of computational efficiency. Therefore, the model should take accounts for the gradual spread of inelastic deformations into the beam and the shift of the inflection point during the response time history, since the length of the plastic zone varies during the response history as a function of the moment distribution in the beam.
 - Extension to 3 D analysis, including slabs or another structural element. The slabs could be defined by means of finite elements through a shell element with six degrees of freedom for each node, while for beams and columns are defined by a bar element with six degrees of freedom for each node. This could make it possible to analyze composite structures.
-

Appendix 1

Element Flexibility and Stiffness Matrix

A1.1 Introduction

In the Chapter 3, we obtained the dynamic equilibrium equation for a frame structure. However, the equation (3.42) itself is not sufficient to analyze the structure, since no physical characteristic of the frame was considered in the equation, such as the area, inertia, elastic behaviour, etc. For this reason, the implementation of a new variable will be necessary, enabling us to describe the physical behaviour of the frame, as well the relationship between the forces and displacements acting on the structure.

Force and displacement are two categories of events that affect a structure. The objective of a structural analysis is to determine the forces and displacements pertaining to the structure and to analyze their relationships as specified by the geometric and material properties of structural elements. Structural analysis in a broader sense can then be divided into two categories: the force method and the displacement method. In the force method, we treat the forces as the basic unknowns and express the displacements in terms of forces, whereas in the displacement method we regard the displacements as the fundamental unknowns and express the forces in terms of displacements. In matrix analysis of linear structures, the force method is often referred to as the flexibility method, and the displacement method is called the stiffness method.

The fundamental step in the application of the matrix displacement method is the determination of the stiffness characteristics of structural elements into which the structure is idealized for the purpose of the analysis. In the same way as the displacement method, the fundamental consideration in the matrix force method is the determination of the flexibility properties of structural elements.

The flexibility properties and stiffness properties can be solved by the following methods:

- Unit-displacement theorem
- Virtual force method
- Solution of differential equations for the element displacements
- Inversion of the displacement-force relationships.

Of these methods, the first one, the application of the unit-displacement theorem, is undoubtedly the most convenient since it leads directly to the required matrix equations relating element forces to their corresponding displacement. In the second method, instead of using the displacement, the force to obtain the equations is used, relating the displacement to their corresponding forces. In the third method, the solutions of the differential equations for displacements are used to derive the required stiffness relationships. In the last method, the equations for the displacement-force relationships are determined first, and then these equations are inverted to find the force-displacement relationships.

To exemplify these methods, we obtain the flexibility coefficient, and subsequently the flexibility matrix, by the virtual force method, while the differential equations will be used to determine the stiffness coefficients and the stiffness ma-

trix. Finally, we will use the displacement-force relationships to demonstrate the correlation between the flexibility matrix and the stiffness matrix.

A1.2 Flexibility coefficient and flexibility matrix

A flexibility coefficient f_{ij} is the displacement at point i due to a unit action at point j . Actually, the flexibility coefficient constitutes a relationship between deformations and forces.

Let us consider the simply supported beam shown in Figure A1.1, the relation between the generalized deformation $\{\Phi_b\}$ and the generalized stress vector $\{\mathbf{M}_b\}$ can be defined as:

$$\{\Phi_b\} = [\mathbf{F}_b]\{\mathbf{M}_b\} \quad (\text{A1.1})$$

Where the matrix $[\mathbf{F}_b]$ is defined as the flexibility matrix of a member.

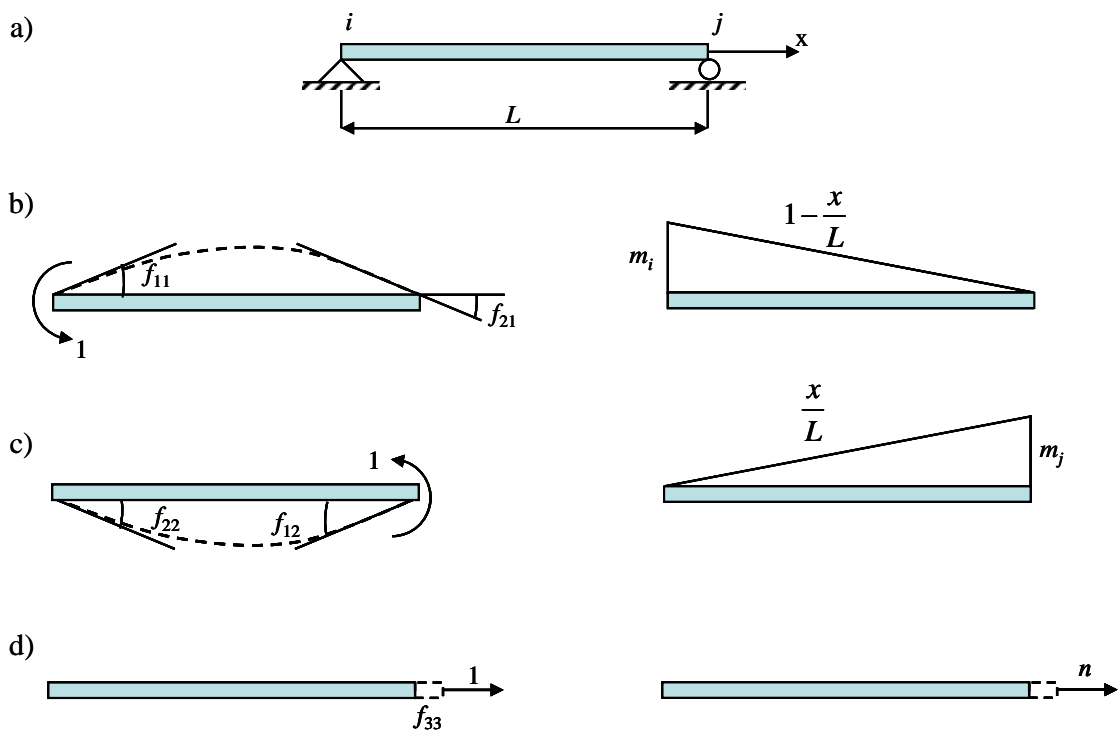


Figure A1.1 – Example for Flexibility Method –b) unitary bending moment at the node i ; c) unitary bending moment at the node j ; c) unitary axial force.

Rewritten the equation (A1.1) into matrix form:

$$\underbrace{\begin{Bmatrix} \phi_i \\ \phi_j \\ \delta \end{Bmatrix}}_{\{\Phi\}} = \underbrace{\begin{bmatrix} f_{11} & f_{12} & f_{13} \\ f_{21} & f_{22} & f_{23} \\ f_{31} & f_{32} & f_{33} \end{bmatrix}}_{[F]} \underbrace{\begin{Bmatrix} m_i \\ m_j \\ n \end{Bmatrix}}_{\{M\}} \quad (\text{A1.2})$$

Using the flexibility coefficients, we may express each of the member deformations in terms of the separate influences of the whole set of member forces:

$$\begin{aligned} \phi_i &= m_i f_{11} + m_j f_{12} + n f_{13} \\ \phi_j &= m_i f_{21} + m_j f_{22} + n f_{23} \\ \delta &= m_i f_{31} + m_j f_{32} + n f_{33} \end{aligned} \quad (\text{A1.3})$$

To obtain the flexibility terms, the use of the virtual work will be necessary, or more specifically, the virtual force method to analyze this problem.

Using the virtual work for a frame element defined in the equation (3.31), and assuming that we have a linear elastic material ($\sigma = E\varepsilon$) then:

$$\begin{aligned} \delta w_b &= \int_{\omega_b} \varepsilon \delta \sigma d\omega_b = \int_{\omega_i} \varepsilon_x \underbrace{E \delta \varepsilon_x}_{\delta \sigma_x} d\omega_i + \int_{\omega_j} \varepsilon_x \underbrace{E \delta \varepsilon_x}_{\delta \sigma_x} d\omega_j + \int_{\omega_n} \varepsilon \underbrace{E \delta \varepsilon}_{\delta \sigma} d\omega_n \\ \delta w_b &= \int_{\omega_i} \varepsilon_x \delta \sigma_x d\omega_i + \int_{\omega_j} \varepsilon_x \delta \sigma_x d\omega_j + \int_{\omega_n} \varepsilon \delta \sigma d\omega_n \end{aligned} \quad (\text{A1.4})$$

Being σ the stress tensor, ε the strain tensor, and ω the volume of a member b , and E the elastic modulus.

For flexural force, the stress σ_x in the section can be defined as:

$$\sigma_x = \frac{m_z y}{I_z} \quad (\text{A1.5})$$

where m_z is the bending moment in the section at the point z , y is the distance until the neutral axis, and I_z is the moment of inertia of the section.

Likewise, the strain ε_x in the section can be redefined as

$$\varepsilon = \frac{\sigma}{E} = \frac{m_z y}{EI_z} \quad (\text{A1.6})$$

the volume ω of a flexural member can be defined as

$$\omega = dA dx \quad (\text{A1.7})$$

while the moment of inertia I_z is defined as

$$\int_A y^2 dA = I_z \quad (\text{A1.8})$$

Replacing the definitions (A1.5), (A1.6), (A1.7), and (A1.8) into (A1.4) leads to the virtual work for flexural element:

$$\delta w_i = \int_0^L \underbrace{\delta m_z}_{\delta \sigma} \underbrace{\frac{m_i}{EI_z}}_{\varepsilon} dx \quad ; \quad \delta w_j = \int_0^L \underbrace{\delta m_z}_{\delta \sigma} \underbrace{\frac{m_j}{EI_z}}_{\varepsilon} dx \quad (\text{A1.9})$$

For axial force, the stress σ in the section can be defined as:

$$\sigma = \frac{n}{A} \quad (\text{A1.10})$$

where n and A are the axial force and the area of the section, respectively. While the strain ε is defined as

$$\varepsilon = \frac{\sigma}{E} = \frac{n}{AE} \quad (\text{A1.11})$$

the volume ω of a member can be defined as

$$\omega = A dx \quad (\text{A1.12})$$

Thus, the virtual work for axial element can be expressed as

$$\delta w_n = \int_0^L \underbrace{\delta n}_{\delta \sigma} \underbrace{\frac{n}{EA}}_{\varepsilon} dx \quad (\text{A1.13})$$

therefore, the internal energy can be rewritten in matrix form:

$$\{\delta w_b^T\} = \left\{ \int_0^L \delta m_z \frac{m_i}{EI_z} dx \quad \int_0^L \delta m_z \frac{m_j}{EI_z} dx \quad \int_0^L \delta n \frac{n}{EA} dx \right\} \quad (\text{A1.14})$$

We can define the virtual work due a virtual external force $\{\delta \mathbf{M}_b\}$ as

$$\underbrace{\{\delta w\}}_{\text{Internal Forces}} = \underbrace{[\mathbf{F}_b]}_{\text{External Forces}} \{\delta \mathbf{M}_b\} \quad (\text{A1.15})$$

expanding the equation (A1.15) leads to:

$$\underbrace{\left\{ \int_0^L \delta m_z \frac{m_i}{EI_z} dx \quad \int_0^L \delta m_z \frac{m_j}{EI_z} dx \quad \int_0^L \delta n \frac{n}{EA} dx \right\}^T}_{\text{Internal Forces}} = \underbrace{\begin{Bmatrix} \delta m_i f_{11} + \delta m_j f_{12} + \delta n f_{13} \\ \delta m_i f_{21} + \delta m_j f_{22} + \delta n f_{23} \\ \delta m_i f_{31} + \delta m_j f_{32} + \delta n f_{33} \end{Bmatrix}}_{\text{External Forces}} \quad (\text{A1.16})$$

In the beam shown in Figure A1.1a, we apply in the node i one unitary virtual moment, $\delta m_z = \delta m_i = 1$ (Figure A1.1b), while $\delta m_j = 0$ and $\delta n = 0$, and recalling that the bending moment expression in the length of the beam is defined as $m_i = (1 - \frac{x}{L})$ and $m_j = (\frac{x}{L})$, the equation (A1.16) reduces to:

$$\left\{ \int_0^L (1 - \frac{x}{L}) \frac{(1 - \frac{x}{L})}{EI_z} dx \quad \int_0^L (1 - \frac{x}{L}) \frac{(\frac{x}{L})}{EI_z} dx \quad \underbrace{\int_0^L \delta n \frac{n}{EA} dx}_0 \right\}^T = \begin{Bmatrix} \delta m_i f_{11} + \cancel{\delta m_j f_{12}} + \cancel{\delta n f_{13}} \\ \delta m_i f_{21} + \cancel{\delta m_j f_{22}} + \cancel{\delta n f_{23}} \\ \delta m_i f_{31} + \cancel{\delta m_j f_{32}} + \cancel{\delta n f_{33}} \end{Bmatrix} \quad (\text{A1.17})$$

this leads to:

$$\begin{aligned} f_{11} &= \int_0^L \left(1 - \frac{x}{L}\right) \left(1 - \frac{x}{L}\right) \frac{1}{EI_z} dx \Rightarrow f_{11} = \frac{L}{3EI_z} \\ f_{21} &= \int_0^L \left(1 - \frac{x}{L}\right) \left(\frac{x}{L}\right) \frac{1}{EI_z} dx \Rightarrow f_{21} = -\frac{L}{6EI_z} \\ f_{31} &= 0 \end{aligned} \quad (\text{A1.18})$$

If now we apply one unitary virtual moment at the node j , $\delta m_z = \delta m_j = 1$ (Figure A1.1.c), we obtain:

$$\left\{ \int_0^L \left(\frac{x}{L}\right) \frac{(1-\frac{x}{L})}{EI_z} dx \quad \int_0^L \left(\frac{x}{L}\right) \frac{(\frac{x}{L})}{EI_z} dx \quad \underbrace{\int_0^L \delta n \frac{n}{EA} dx}_0 \right\}^T = \left\{ \begin{array}{l} \cancel{\delta m_i f_{11}} + \delta m_j f_{12} + \cancel{\delta n f_{13}} \\ \cancel{\delta m_i f_{21}} + \delta m_j f_{22} + \cancel{\delta n f_{23}} \\ \cancel{\delta m_i f_{31}} + \delta m_j f_{32} + \cancel{\delta n f_{33}} \end{array} \right\} \quad (\text{A1.19})$$

thus:

$$\begin{aligned} f_{12} &= \int_0^L \left(\frac{x}{L}\right) \left(1 - \frac{x}{L}\right) \frac{1}{EI_z} dx \Rightarrow f_{12} = -\frac{L}{6EI_z} \\ f_{22} &= \int_0^L \left(\frac{x}{L}\right) \left(\frac{x}{L}\right) \frac{1}{EI_z} dx \Rightarrow f_{22} = \frac{L}{3EI_z} \\ f_{32} &= 0 \end{aligned} \quad (\text{A1.20})$$

If now we only consider the influence of the unitary axial force, $\delta n = \delta n = 1$ (Figure A1.1.d), we have:

$$\left\{ \underbrace{\int_0^L \delta m_z \frac{m}{EI_z} dx}_0 \quad \underbrace{\int_0^L \delta m_z \frac{m_j}{EI_z} dx}_0 \quad \int_0^L \delta n \frac{n}{EA} dx \right\}^T = \left\{ \begin{array}{l} \cancel{\delta m_i f_{11}} + \cancel{\delta m_j f_{12}} + \delta n f_{13} \\ \cancel{\delta m_i f_{21}} + \cancel{\delta m_j f_{22}} + \delta n f_{23} \\ \cancel{\delta m_i f_{31}} + \cancel{\delta m_j f_{32}} + \delta n f_{33} \end{array} \right\} \quad (\text{A1.21})$$

consequently:

$$\begin{aligned} f_{13} &= 0 \\ f_{23} &= 0 \\ f_{33} &= \int_0^L \delta n \frac{n}{EA} dx \Rightarrow f_{33} = \frac{L}{EA} \end{aligned} \quad (\text{A1.22})$$

If we summarized the results(A1.18),(A1.20) and (A1.22) into a matrix form, as

$$[\mathbf{F}_b] = \begin{bmatrix} \frac{L}{3EI} & -\frac{L}{6EI} & 0 \\ -\frac{L}{6EI} & \frac{L}{3EI} & 0 \\ 0 & 0 & \frac{L}{EA} \end{bmatrix} \quad (\text{A1.23})$$

which leads to the flexibility matrix $[F]$.

A1.3 Stiffness coefficient and Stiffness matrix

Before determining the stiffness coefficients, it will be necessary determine the differential equation applicable to the beams, in our case the classic Euler-Bernoulli beam will be adopted. Therefore, there are some Euler-Bernoulli beam assumptions that will be taken into account to obtain the differential equation:

- The beam is long and slender.
- The beam cross-section is constant along its axis.
- Deformations remain small.
- Material is isotropic.
- Plane sections of the beam remain plane.

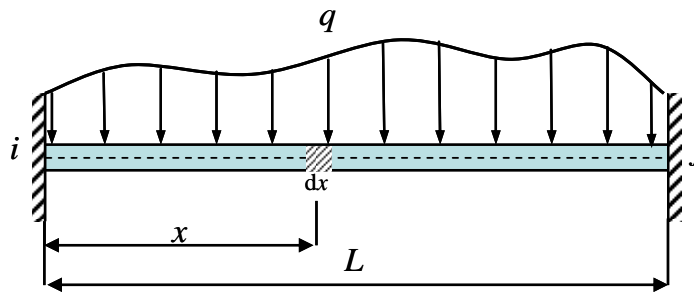


Figure A1.2 – A Euler-Bernoulli beam

Let us consider a plan beam, with length L and a distributed load q composed of an elastic material as shown in Figure A1.2. If we suppose that the deformations are small, and the axes are straight and unstretched, we can safely assume that there is negligible strain in the y direction dependence in $u(x, y)$ explicit via a simple geometric expression,

$$u(x, y) = \chi(x)y + u(x) \quad (\text{A1.24})$$

where $\chi(x)$ is the cross section rotation, and $u(x)$ is the deformation by the axial effect disconnect of the flexion.

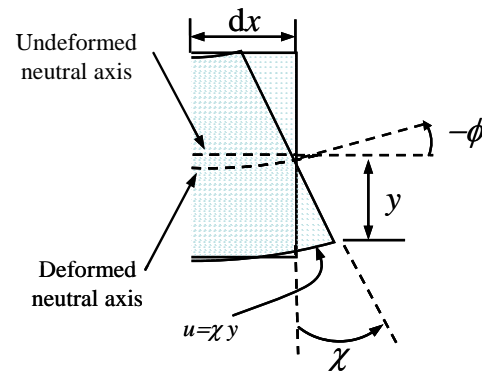


Figure A 1.3 – Deflection displacement and rotation of the beam's neutral axis.

The direct strain throughout the beam can be defined as:

$$\varepsilon = \frac{du(x)}{dx} \quad (\text{A1.25})$$

The relation between the cross section rotation $\chi(x)$ to the neutral plane rotation ϕ , and eventually to the beam's deflection displacement $v(x)$:

$$\chi = -\phi = \frac{dv}{dx} \quad (\text{A1.26})$$

So, the equation (A1.25) can be rewritten as:

$$\varepsilon = \frac{\partial u}{\partial x} = -y \frac{d^2v(x)}{dx^2} + \frac{dv(x)}{dx} \quad (\text{A1.27})$$

The force resultants concept enables us to determine the stresses in a beam. If we were to cut a beam at a point x , we would find a distribution of normal stresses $\sigma_x(x)$ and shear stress $\sigma_{xy}(x)$. Each little portion of direct stress acting on the cross section creates a moment about the neutral plane ($y = 0$). Summing these individual moments over the area of the cross-section the result is the moment resultant $m(x)$:

$$m(x) = \iint_A -y \sigma_x(x) dA \quad (\text{A1.28})$$

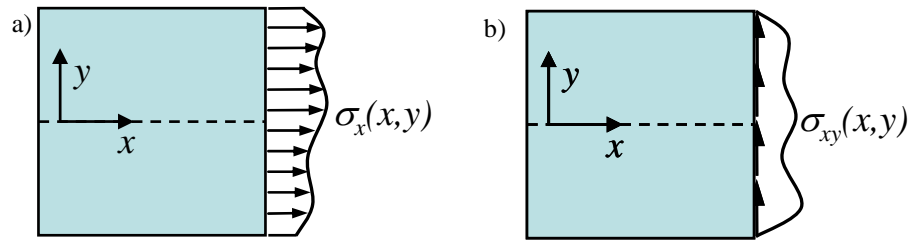


Figure A1.4 – Stresses in a beam- a) normal stresses $\sigma_x(x, y)$; b) shear stresses $\sigma_{xy}(x, y)$

Similarly, summing the shear stresses on the cross-section is the definition of the shear resultant $V(x)$:

$$V(x) = \iint_A \sigma_{xy}(x) dA \quad (\text{A1.29})$$

The last force resultant that we can define for completeness is the sum of all normal stresses acting on the cross section, and is known as axial stress $n(x)$:

$$n(x) = \iint_A \sigma_x(x) dA \quad (\text{A1.30})$$

The axial force $n(x)$ does not yet play a role in (linear) beam theory since it does not cause a deflection displacement $v(x)$. Instead, it plays a role in the axial displacement of the rods and bars.

Considering the balance of forces and moments acting on a small section of beam (Figure A1.5), the equilibrium in the y -directions gives the equation for the shear resultant $V(x)$:

$$\frac{dV(x)}{dx} = -q(x) \quad (\text{A1.31})$$

Moment equilibrium about a point on the right side of the beam gives the equation for the moment resultant $m(x)$

$$\frac{dm(x)}{dx} = -V(x) \quad (\text{A1.32})$$

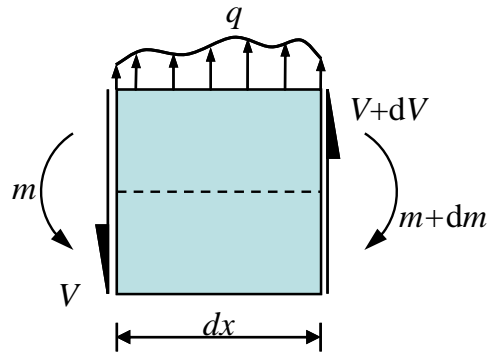


Figure A1.5 – Balance of forces and moments into a section dx of beam.

Now, assuming that the beam typically uses the simple 1-dimensional Hooke's equation $\sigma_x(x) = E\varepsilon_x(x)$, we can rewrite equation (A1.28) in terms of the equation (A1.27), so

$$m(x) = \iint_A -y\sigma_x dA = \iint_A -yE\varepsilon_x dA = \iint_A E \left(y^2 \frac{d^2v}{dx^2} - y \frac{dv}{dx} \right) dA = E \frac{d^2v}{dx^2} \underbrace{\iint_A y^2 dA}_I$$

$$m(x) = EI \frac{d^2v}{dx^2}$$
(A1.33)

Our assumption that $\frac{du(x)}{dx} = 0$, is based in the consideration that the axial force does not influence the bending moment in the (linear) beam theory. Combining the equations (A1.31), (A1.32), (A1.33):

$$\left. \begin{aligned} \frac{dV(x)}{dx} &= -q(x) \\ \frac{dm(x)}{dx} &= -V(x) \\ m(x) &= EI \frac{d^2v}{dx^2} \end{aligned} \right\} \frac{d^2m(x)}{dx^2} = q(x) \Rightarrow \frac{d^2}{dx^2} \left(EI \frac{d^2v(x)}{dx^2} \right) = q(x)$$
(A1.34)

The result obtained in the equation (A1.34) is known as the Euler-Bernoulli beam equation:

$$EI \frac{d^4v(x)}{dx^4} = q(x)$$
(A1.35)

In the same way, we can obtain the axial force in terms of the displacement as:

$$\begin{aligned}
n(x) &= \iint_A \sigma_x dA = \iint_A E \varepsilon_x dA = \iint_A E \left(-y \frac{dv}{dx^2} + y \frac{du}{dx} \right) dA = E \frac{du}{dx} \underbrace{\iint_A dA}_A - \frac{dv}{dx^2} \underbrace{\iint_A y dA}_0 \\
n(x) &= EA \frac{du}{dx}
\end{aligned} \tag{A1.36}$$

For axial force, there is not influence of the bending moments, the term $\iint_A y dA$, the static moment, will be assumed as null.

Finally, we can express the relation between the out-of-plane (deflection) displacement $v(x)$, the external distributed loading q , the axial displacement $u(x)$, and the axial force $n(x)$, as:

$$EI \frac{d^4 v(x)}{d x^4} = q(x) \tag{A1.37}$$

$$EA \frac{du(x)}{d x} = n \tag{A1.38}$$

The solution of the differential equation (A1.37) can be expressed as a cubic polynomial plus one particular solution due to the external distributed loading $q(x)$

$$v(x) = \iiint \frac{q(x)}{EI} dx + C_1 \frac{x^3}{6EI} + C_2 \frac{x^2}{2EI} + C_3 x + C_4 \tag{A1.39}$$

For the solution of the parameters, we will assume that the distributed loading $q(x)$ is null. When deformations $\{\Phi\}$ take place in the frame element due to the movement into the structure, we have the follow border conditions:

- On the node i ($x = 0$):

$$v(x) = 0 \quad ; \quad -\phi_i = \frac{dv(x)}{dx} \quad ; \quad m_i = EI \left(\frac{d^2 v(x)}{dx^2} \right) \tag{A1.40}$$

- On the node j ($x = L$):

$$v(x) = 0 \quad ; \quad -\phi_j = \frac{dv(x)}{dx} \quad ; \quad -m_j = EI \left(\frac{d^2 v(x)}{dx^2} \right) \tag{A1.41}$$

The assumptions of the null deflection at the edges can be justified because it is assumed that the axis x follows the chord in its movement. So, the parameter can be obtained as:

$$v(x)|_{x=0} = 0 \Rightarrow C_4 = 0 \quad (\text{A1.42})$$

$$\left. \frac{dv(x)}{dx} \right|_{x=0} = -\phi_i = C_3 \quad (\text{A1.43})$$

$$\left. \frac{dv(x)}{dx} \right|_{x=L} = -\phi_j = \frac{L^2}{2EI} C_1 + \frac{L}{EI} C_2 + C_3 \Rightarrow C_2 = \frac{2EI(\phi_i - \phi_j)}{L} - C_1 \frac{L}{2} \quad (\text{A1.44})$$

$$v(x)|_{x=L} = 0 = C_1 \frac{L^3}{6EI} + C_2 \frac{L^2}{2EI} + C_3 L + C_4 \Rightarrow C_1 = -\frac{6}{L^2} EI (\phi_i + \phi_j) \quad (\text{A1.45})$$

this can be summarized as:

$$\begin{aligned} C_1 &= -\frac{6}{L^2} EI (\phi_i + \phi_j) \\ C_2 &= \frac{2EI}{L} (2\phi_i + \phi_j) \\ C_3 &= -\phi_i \\ C_4 &= 0 \end{aligned} \quad (\text{A1.46})$$

so, the expression (A1.39) becomes:

$$v(x) = -(\phi_i + \phi_j) \frac{x^3}{L^2} + (2\phi_i + \phi_j) \frac{x^2}{L} - \phi_i x \quad (\text{A1.47})$$

For those cases where the distributed loading $q(x)$ is assumed uniform and not null:

$$v(x) = \frac{q}{EI} \left(\frac{x^4}{24} - \frac{Lx^3}{12} + \frac{L^2 x^2}{24} \right) + \phi_i \left(-\frac{x^3}{L^2} + 2\frac{x^2}{L} - x \right) + \phi_j \left(-\frac{x^3}{L^2} + \frac{x^2}{L} \right) \quad (\text{A1.48})$$

Therefore, the bending moment in terms of the rotations can be expressed as:

$$m_i = EI \left(\frac{d^2 v(x)}{dx^2} \right) \Big|_{x=0} \Rightarrow \frac{4EI}{L} \phi_i + \frac{2EI}{L} \phi_j + \frac{qL^3}{12} \quad (\text{A1.49})$$

$$m_j = EI \left(\frac{d^2 v(x)}{dx^2} \right) \Big|_{x=L} \Rightarrow \frac{2EI}{L} \phi_i + \frac{4EI}{L} \phi_j - \frac{qL^3}{12} \quad (\text{A1.50})$$

The same procedure can be followed for the axial deformation differential equation

$$EA \frac{du(x)}{dx} = n \quad (\text{A1.51})$$

Once it is assumed that the axial force is constant, the solution of the equation (A1.51), can be expressed as a polynomial expression:

$$EAu(x) = nx + C_5 \quad (\text{A1.52})$$

The solution of the parameters can be obtained by the edges conditions:

$$\begin{aligned} u(x) \Big|_{x=0} = 0 &\Rightarrow C_5 = 0 \\ u(x) \Big|_{x=L} = \delta &\Rightarrow n = \frac{EA}{L} \delta \end{aligned} \quad (\text{A1.53})$$

The condition of the null axial displacement for $x=0$ is due to the fact that the coordinate's origin are attached to the join i during its movement.

Grouping the equations (A1.49),(A1.50),and (A1.53) into a matrix form:

$$\begin{Bmatrix} m_i \\ m_j \\ n \end{Bmatrix}_b = \begin{bmatrix} \frac{4EI}{L} & \frac{4EI}{L} & 0 \\ \frac{4EI}{L} & \frac{4EI}{L} & 0 \\ 0 & 0 & \frac{EA}{L} \end{bmatrix}_b \begin{Bmatrix} \phi_i \\ \phi_j \\ \delta \end{Bmatrix}_b + \begin{Bmatrix} \frac{qL^3}{12} \\ -\frac{qL^3}{12} \\ 0 \end{Bmatrix}_b \quad (\text{A1.54})$$

$$\{\mathbf{M}_b\} = [\mathbf{S}_b] \{\Phi_b\} + \{\mathbf{M}_b^0\} \quad (\text{A1.55})$$

Where the quadratic matrix $[S_b]$ is called the stiffness matrix of a member, and the vector $\{\mathbf{M}_b^0\}$ is called the vector of initial generalized forces, which depends on the type of the forces applied in the frame element.

A1.4 Flexibility and stiffness relation

If we consider one beam with a couple bending moment applied in the extremities as shown in Figure A1.6, the expression which represents the moment at the point x can be:

$$m_f|_x = -m_i \left(1 - \frac{x}{L}\right) + m_j \left(\frac{x}{L}\right) \quad (\text{A1.56})$$

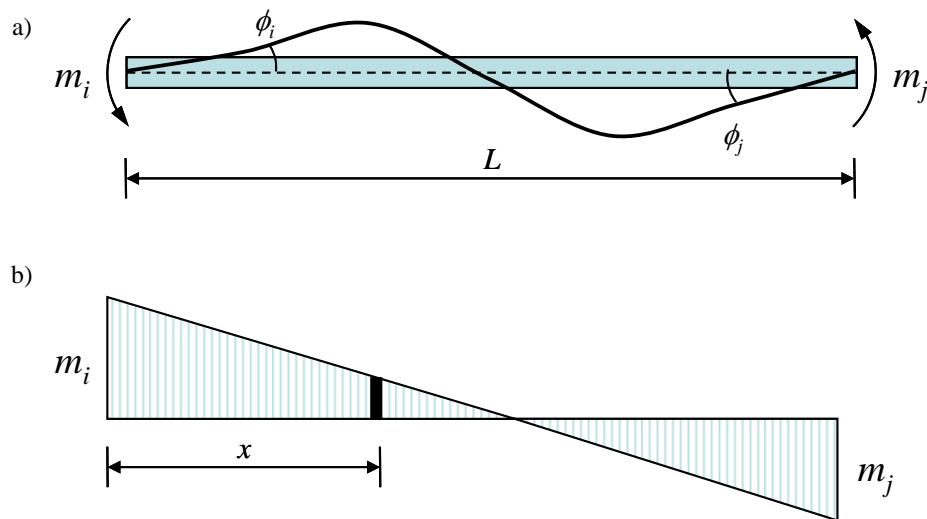


Figure A1.6 – Beam subjected to end moments and moment diagram.

The work done by the moment m_f to turn an angular displacement $d\phi$ is:

$$m_f d\phi \quad (\text{A1.57})$$

Using the internal energy definition (equation (3.17)), the total work done by m_f can be expressed as:

$$W = \int_{\phi_i}^{\phi_j} m_f d\phi \quad (\text{A1.58})$$

As long the linear relationship between the load and the deflections holds, all external work will be converted into internal work or elastic energy. Let dW be the strain energy restored in an infinitesimal element of the beam (fig.). We have

$$dW = \overset{\text{def}}{\frac{1}{2}} m_f d\phi \quad (\text{A1.59})$$

If only the bending moment m_f produced by the forces on the element is considered significant, the angular displacement $d\phi$ can be expressed as:

$$\frac{d\phi}{dx} = \frac{d^2v}{dx^2} \quad (\text{A1.60})$$

once the $\frac{dv}{dx} = \frac{m_f}{EI}$ (equation (A1.33)). The equation (A1.59) can be rewritten as

$$dW = \frac{m_f^2}{2EI} dx \quad (\text{A1.61})$$

The total strain energy restored in the beam of length L is given, therefore, by

$$W = \int_0^L \frac{m_f^2}{2EI} dx \quad (\text{A1.62})$$

By the expressions (A1.58) and (A1.59) we can obtain the rotations ϕ_i and ϕ_j , as

$$\begin{aligned} \phi_i &= \frac{\partial W}{\partial m_i} = \int_0^L m_f \frac{\partial m_f}{\partial m_i} dx \\ \phi_j &= \frac{\partial W}{\partial m_j} = \int_0^L m_f \frac{\partial m_f}{\partial m_j} dx \end{aligned} \quad (\text{A1.63})$$

Replacing the value of m_f (equation (A1.56)) and expanding:

$$\phi_i = \int_0^L m_f \frac{\partial m_f}{\partial m_i} \frac{dx}{EI} = \int_0^L \left[-m_i \left(1 - \frac{x}{L} \right) + m_j \left(\frac{x}{L} \right) \right] \left[- \left(1 - \frac{x}{L} \right) \right] \frac{dx}{EI} = \frac{m_i L}{3EI} - \frac{m_j L}{6EI} \quad (\text{A1.64})$$

$$\phi_j = \int_0^L m_f \frac{\partial m_f}{\partial m_j} \frac{dx}{EI} = \int_0^L \left[-m_i \left(1 - \frac{x}{L} \right) + m_j \left(\frac{x}{L} \right) \right] \left[\left(\frac{x}{L} \right) \right] \frac{dx}{EI} = -\frac{m_i L}{6EI} + \frac{m_j L}{3EI}$$

If the axial influence is included, the equation (A1.64) can be expressed as the flexibility matrix obtained in the equation (A1.23).

$$\begin{Bmatrix} \phi_i \\ \phi_j \\ n \end{Bmatrix} = \underbrace{\begin{bmatrix} \frac{L}{3EI} & -\frac{L}{6EI} & 0 \\ -\frac{L}{6EI} & \frac{L}{3EI} & 0 \\ 0 & 0 & \frac{L}{EA} \end{bmatrix}}_{[\mathbf{F}]} \begin{Bmatrix} m_i \\ m_j \\ n \end{Bmatrix} \quad (\text{A1.65})$$

The equations (A1.64) can be also expressed in terms of the bending moments as:

$$m_i = \frac{4EI}{L} \phi_i + \frac{2EI}{L} \phi_j \quad (\text{A1.66})$$

$$m_j = \frac{2EI}{L} \phi_i + \frac{4EI}{L} \phi_j$$

Similarly, including the axial influence, the equation (A1.66) can be expressed as the stiffness matrix defined in (A1.54), so.

$$\begin{Bmatrix} m_i \\ m_j \\ n \end{Bmatrix} = \underbrace{\begin{bmatrix} \frac{4EI}{L} & \frac{2EI}{L} & 0 \\ \frac{2EI}{L} & \frac{4EI}{L} & 0 \\ 0 & 0 & \frac{EA}{L} \end{bmatrix}}_{[\mathbf{S}]} \begin{Bmatrix} \phi_i \\ \phi_j \\ n \end{Bmatrix} \quad (\text{A1.67})$$

By analyzing the equations (A1.65) and (A1.67), we can conclude the relationship between the flexibility matrix and the stiffness:

$$\begin{aligned} [\mathbf{S}] &= [\mathbf{F}]^{-1} \\ [\mathbf{F}] &= [\mathbf{S}]^{-1} \end{aligned} \quad (\text{A1.68})$$

This relationship will be valid only for elastic material.

A1.4.1 Frame Elements with internal hinges

In some structures, there are elements that can be connected by hinges on the ends (Figure A1.7). These hinges have only axial and shear reactions, leading the bending moment on edges to be equal to zero.

For those cases, the stiffness matrix, or the flexibility matrix for a frame member can be determined by the equation (A1.64), assuming that the bending moment is zero where the hinge is settled.

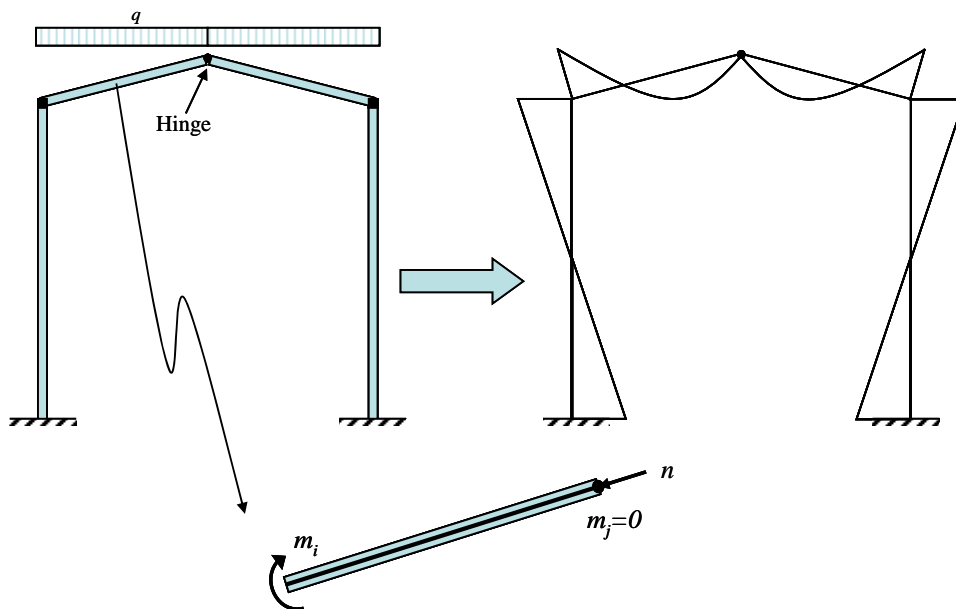


Figure A1.7 – Frame structures with an internal hinge and the moment diagram.

For example, let us suppose that the hinge is located at the node j , Figure A1.7, which leads to the $m_j = 0$, so the equation (A1.64) reduces to:

$$\phi_i = \int_0^L m_f \frac{\partial m_f}{\partial m_i} \frac{dx}{EI} = \int_0^L \left[-m_i \left(1 - \frac{x}{L} \right) + \underbrace{m_j \left(\frac{x}{L} \right)}_0 \right] \left[-m_i \left(1 - \frac{x}{L} \right) \right] \frac{dx}{EI} = \frac{m_i L}{3EI}$$
(A1.69)

$$\phi_j = \int_0^L m_f \frac{\partial m_f}{\partial m_j} \frac{dx}{EI} = \int_0^L \left[-m_i \left(1 - \frac{x}{L} \right) + \right] \left[\underbrace{m_j \left(\frac{x}{L} \right)}_0 \right] \frac{dx}{EI} = 0$$

so:

$$m_i = \frac{3EI}{L} \phi_i$$
(A1.70)

expressed as matrix form, we obtain the stiffness matrix for hinge at the node j :

$$[\mathbf{S}_b]_j^* = \frac{1}{L} \begin{bmatrix} 3EI & 0 & 0 \\ 0 & 0 & 0 \\ 0 & 0 & EA \end{bmatrix}$$
(A1.71)

If we suppose the hinge to be located at the node i , the stiffness matrix become:

$$[\mathbf{S}_b]_i^* = \frac{1}{L} \begin{bmatrix} 0 & 0 & 0 \\ 0 & 3EI & 0 \\ 0 & 0 & EA \end{bmatrix}$$
(A1.72)

It is also possible to describe the hinge matrix as a flexibility matrix.

A1.5 Stiffness and Flexibility Matrices of Beam-Columns

If the axial load in a frame member is negligible, the member is commonly referred to as a beam. If bending moment and shear are negligible and the axial load is compressive, the member is referred to as a column. Members subjected to bending moments, shears, and compressive axial forces are typically called beam-columns. In reality, all members in a frame are beam-columns. There are some cases where the axial force effect in a member is negligible compared to the bending effect. In this case the equations presented in sections A1.2 and A1.3 are adequate to solve the problem.

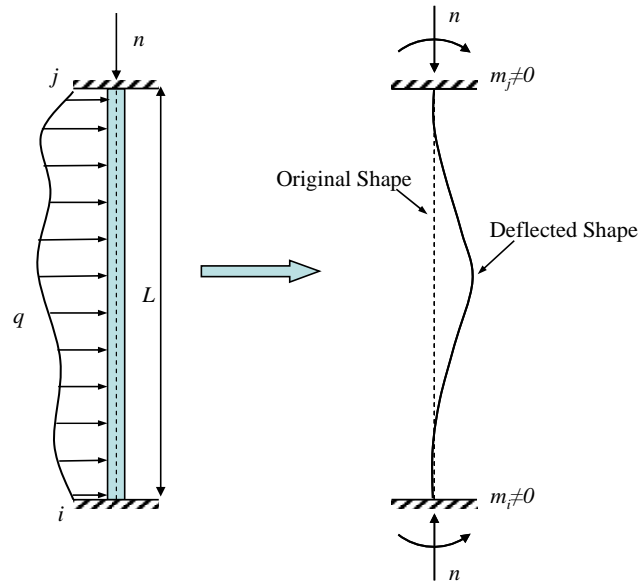


Figure A1.8 – Symmetric buckling mode of a fixed-fixed column.

However, if the bending effect in a member is secondary compared to the axial force effect, it is more convenient to treat such a member as a column and analyze and design it accordingly (Most vertical members are called columns, although technically they behave as beam-columns).

A1.5.1 Differential equations of the Beam-Columns

Let us determine the resultant bending moment $m(x)$ and assume that $\frac{du(x)}{dx} \neq 0$, so the equation (A1.33) becomes:

$$m(x) = \iint_A -y\sigma_x dA = \iint_A -yE\varepsilon_x dA = \iint_A E \left(y^2 \frac{d^2v}{dx^2} - y \frac{du}{dx} \right) dA = E \frac{d^2v}{dx^2} \underbrace{\iint_A y^2 dA}_I - yE \frac{du}{dx} \underbrace{\iint_A dA}_A =$$

$$m(x) = EI \frac{d^2v}{dx^2} - yEA \frac{du}{dx} \tag{A1.73}$$

once $EA \frac{du}{dx} = n(x)$ and $-y = v$, the equation (A1.73) can be rewritten as:

$$m(x) = EI \frac{d^2v}{dx^2} + nv \tag{A1.74}$$

The differential equation can be defined similarly as defined in the equation(A1.34):

$$\left. \begin{aligned} \frac{dV(x)}{dx} &= -q(x) \\ \frac{dm(x)}{dx} &= -V(x) \\ m(x) &= EI \frac{d^2v}{dx^2} + nv \end{aligned} \right\} \frac{d^2m(x)}{dx^2} = q(x) \Rightarrow \frac{d^2}{dx^2} \left(EI \frac{d^2v(x)}{dx^2} \right) + n \frac{d^2v(x)}{dx^2} = q(x) \quad (\text{A1.75})$$

$$EI \frac{d^4v(x)}{dx^4} + n \frac{d^2v(x)}{dx^2} = q(x) \quad (\text{A1.76})$$

To make simple solutions possible, consider that the axial (normal) force n and the bending rigidity EI are constant along the beam. The differential equation has constant coefficients, and the fundamental solutions of the associated equation ($q(x) = 0$) may be sought in the form $v = e^{\lambda x}$. Upon substitution into the equation (A1.76) we see that $e^{\lambda x}$ cancels out and we obtain the characteristic equation $EI\lambda^4 + n\lambda^2 = 0$ or $\lambda^2(\lambda^2 + k^2) = 0$, where $k^2 = |n|/EI$. The roots are $\lambda = ik, -ik, 0, 0$ provided that $n > 0$ (compression). Since $\sin kx$ and $\cos kx$ are linear combinations of $e^{i\lambda x}$ and $e^{-i\lambda x}$, the general solution of the equation (A1.76) for EI and n constants can be expressed as:

$$v(x) = C_1 \sin kx + C_2 \cos kx + C_3 x + v_p(x) \quad (n > 0) \quad (\text{A1.77})$$

in which $C_1, C_2, C_3,$ and C_4 are arbitrary constants and $v_p(x)$ is a particular solution corresponding to the distributed loads $q(x)$.

For columns in structures, it is sometimes also necessary to take into account the effect of an axial tensile force $n < 0$ on the deflections. In that case the general solution then is:

$$v(x) = C_1 \sinh kx + C_2 \cosh kx + C_3 x + v_p(x) \quad (n < 0) \quad (\text{A1.78})$$

A1.5.2 Stiffness matrix

In this section, we will develop the stiffness matrix for a beam-column. Using the same boundary conditions defined in (A1.42), we can determine the constants of the equation (A1.77), so:

$$v(x)|_{x=0} = 0 \Rightarrow C_2 + C_4 = 0 \quad (\text{A1.79})$$

$$\left. \frac{dv(x)}{dx} \right|_{x=0} = C_1 k + C_3 = -\phi_i \quad (\text{A1.80})$$

$$v(x)|_{x=L} = C_1 \sin kl + C_2 \cos kl + C_3 L + C_4 = 0 \quad (\text{A1.81})$$

$$\left. \frac{dv(x)}{dx} \right|_{x=L} = C_1 k \cos kl - C_2 k \sin kl + C_3 = -\phi_j \quad (\text{A1.82})$$

eliminating C_3 , and C_4 from equations (A1.81) and (A1.82) we obtain the equations:

$$C_1(\sin kl - kl) + C_2(\cos kl - 1) = \phi_i L \quad (\text{A1.83})$$

$$C_1(\cos kl - 1) - C_2(\sin kl) = \frac{\phi_i - \phi_j}{k} \quad (\text{A1.84})$$

Isolating the term C_1 and substituting this into the equation (A1.83), we obtain the expression for C_2 . The final solution will be given by the bending moment expressions (A1.49) and (A1.50), so:

$$m_i = EI \left(\frac{d^2 v(x)}{dx^2} \right) \Big|_{x=0} \Rightarrow \left(\frac{EI}{L} \right) s_{11} \phi_i + s_{12} \phi_j \quad (\text{A1.85})$$

$$m_j = EI \left(\frac{d^2 v(x)}{dx^2} \right) \Big|_{x=L} \Rightarrow \left(\frac{EI}{L} \right) s_{21} \phi_i + s_{22} \phi_j \quad (\text{A1.86})$$

where

$$s_{11} = s_{22} = \frac{kL \sin kL - (kL)^2 \cos kL}{2 - 2 \cos kL - kL \sin kL} \quad (\text{A1.87})$$

$$s_{12} = s_{21} = \frac{(kL)^2 - kL \sin kL}{2 - 2 \cos kL - kL \sin kL} \quad (\text{A1.88})$$

The same procedure can be followed for the case of $n < 0$, thus, the resolution of the equation (A1.78) is:

$$s_{11} = s_{22} = \frac{(kL)^2 \cosh kL - kL \sinh kL}{2 - 2 \cosh kL + kL \sinh kL} \quad (\text{A1.89})$$

$$s_{12} = s_{21} = \frac{kL \sinh kL - (kL)^2}{2 - 2 \cosh kL + kL \sinh kL} \quad (\text{A1.90})$$

the stiffness matrix for beam-column can be written in matrix form as:

$$[\mathbf{S}_b] = \frac{1}{L} \begin{bmatrix} EIs_{11} & EIs_{12} & 0 \\ EIs_{21} & EIs_{22} & 0 \\ 0 & 0 & EA \end{bmatrix} \left\{ \begin{array}{l} s_{11} = s_{22} = \begin{cases} \frac{kL \sin kL - (kL)^2 \cos kL}{2 - 2 \cos kL - kL \sin kL} & \Leftrightarrow n > 0 \\ 4 & \Leftrightarrow n = 0 \\ \frac{(kL)^2 \cosh kL - kL \sinh kL}{2 - 2 \cosh kL + kL \sinh kL} & \Leftrightarrow n < 0 \end{cases} \\ s_{12} = s_{21} = \begin{cases} \frac{(kL)^2 - kL \sin kL}{2 - 2 \cos kL - kL \sin kL} & \Leftrightarrow n > 0 \\ 2 & \Leftrightarrow n = 0 \\ \frac{kL \sinh kL - (kL)^2}{2 - 2 \cosh kL + kL \sinh kL} & \Leftrightarrow n < 0 \end{cases} \end{array} \right. \quad (\text{A1.91})$$

A1.6 Generalized Stress and Stiffness relationship

The relation between generalized stress and the history of deformations can be expressed as follows (Cipollina, *et al.* 1993):

$$\{\mathbf{M}_b\} = [\mathbf{S}_b^e(\Phi_b)] \{\Phi_b^e\} \text{ or } \{\Phi_b^e\} = [\mathbf{F}_b^e(\mathbf{M}_b)] \{\mathbf{M}_b\} \quad (\text{A1.92})$$

where $[\mathbf{S}_b^e(\Phi_b)]$ and $[\mathbf{F}_b^e(\mathbf{M}_b)]$ indicates the local elastic stiffness and flexibility matrices of a beam-column element, respectively. They are defined according to the deformed configuration of the member, using the stiffness or flexibility matrices defined in section A1.5. In the case of small deformations, the elastic stiffness and flexibility matrices remain constant, and can be defined as proposed in (A1.23), for the flexibility matrix, or by (A1.54), for stiffness matrix. In this context, the equation (A1.92) can be rewritten as:

$$\{\mathbf{M}_b\} = [\mathbf{S}_b^e] \{\Phi_b^e\} \text{ or } \{\Phi_b^e\} = [\mathbf{F}_b^e] \{\mathbf{M}_b\} \quad (\text{A1.93})$$

Since the generalized deformation $\{\Phi_b^e\}$ is defined in terms of the global displacement $\{U\}$, the generalized stress of a member can be rewritten as

$$\{\mathbf{M}_b\} = [\mathbf{S}_b^e][\mathbf{B}_b]\{U\} \quad (\text{A1.94})$$

Despite the fact that equation (A1.93) can be used for both structural elements, beams and columns, unlike beam elements, the deformation of columns is influenced by axial load. For this reason, equation (A1.92) should be used to represent the effect of the axial force at columns. However, the variation of axial forces in the interior columns of a bending moment resisting frame is, usually, small, since the axial force caused by the shear in the right hand side beam cancels that caused by the shear of the left hand side beam.

This is especially true if the frame has bays of approximately equal length. Exterior columns exhibit much larger variation of axial forces than interior columns. Consequently, we can assume that constant axial load will not significantly affect the global response. However, the column shear history under constant axial load might be different from that due to variable load, if axial loads fluctuate greatly in exterior columns. Although the axial load variation in slender bending moment resisting frames could be important, these effects are not very significant in well-designed frame structures of typical dimensions, because columns of typical mid-rise frame buildings are oversized to control drift. The axial load level, therefore, will be a small fraction of the column capacity and the fluctuation of this already small axial load level will not be very significant. Since accounting for axial load variation leads to considerable increase in computational effort, due to the necessity of calculation of the stiffness (equation (A1.91)) in function of the axial force for each time, the variation of column axial forces due to lateral load reversals will be neglected. Therefore, we consider that the columns will be subjected to axial loads below the balanced load.

Appendix 2

One-Dimensional Plasticity.

A2.1 Introduction

In physics and engineering, plasticity is a property of a material to undergo a non-reversible change of shape in response to an applied force. Plastic deformation occurs under shear stress, as opposed to brittle fractures, which occur under normal stress.

For many ductile metals, tensile loading applied to a sample will cause it to behave in an elastic manner. Each increment of load is accompanied by a proportional increment in extension, and when the load is removed, the piece returns exactly to its original size. However, once the load exceeds some threshold (the

yield strength), the extension increases more rapidly than in the elastic region, and when the load is removed, some amount of the extension remains.

The main purpose of this appendix is to review the principal concepts in plasticity, applied to the uniaxial stress.

A2.2 Uniaxial Elastoplasticity

With most materials, as we increase the strain ε , the stress σ first increases linearly until a certain critical value, the elastic limit, is reached. This level is characterized by a stress value σ_y called the yield stress, plastic stress or yield limit. For materials that do not exhibit a significant proportional limit, the elastic limit is an arbitrary approximation (apparent elastic limit). Thus, an abrupt change in the stiffness or in the elastic modulus can be observed for the material beyond yield point (this change may not be so abrupt for brittle materials). Moreover, when all forces acting on the material are removed, the material does not return to its original shape, but has some permanent plastic deformations associated with it. This behaviour can be represented by a stress-strain curve.

The nature of the curve varies from material to material. Figure A2.1 shows the engineering stress* versus engineering strain† relationship typical of low-carbon steel loaded in tension.

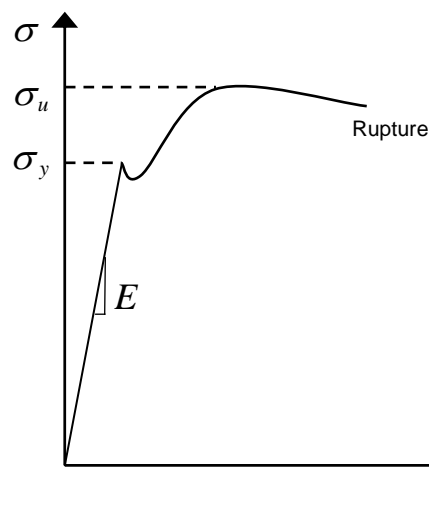


Figure A2.1 - Typical stress-strain curve of low-carbon steel

* Engineering stress is used to indicate the rating the strength of materials loaded in one dimension.

† Engineering strain is used to indicate the change in length of a line or by the change in angle between two lines

Steel exhibits a very linear stress-strain relationship up to a well-defined yield point. The slope of this initial portion of the curve is known as the modulus of elasticity E . After the yield point σ_y , the curve typically decreases slightly and then increases to the ultimate strength σ_u . This increase is known as strain hardening or work hardening. After the point of ultimate strength, the curve decreases until the specimen ruptures. The cause of this decrease is known as necking, which results from a decrease in specimen area as it is plastically deformed. If the curve is plotted in units of true stress and true strain this decrease is not observed.

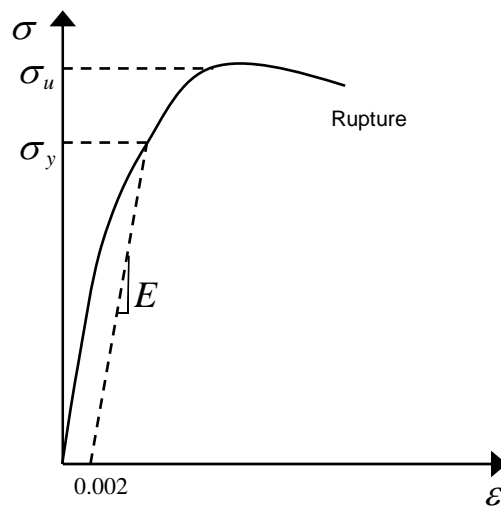


Figure A2.2 - Stress-strain curve for ductile metals.

Most ductile metals other than steel do not have a well-defined yield point. For these materials, the yield strength is typically determined by the "0.2% offset method", by which a line is drawn parallel to the initial portion of the curve and intersecting the abscissa at 0.002. The intersection of this line and the stress-strain curve is considered to be the yield point σ_y . This method is shown in Figure A2.2.

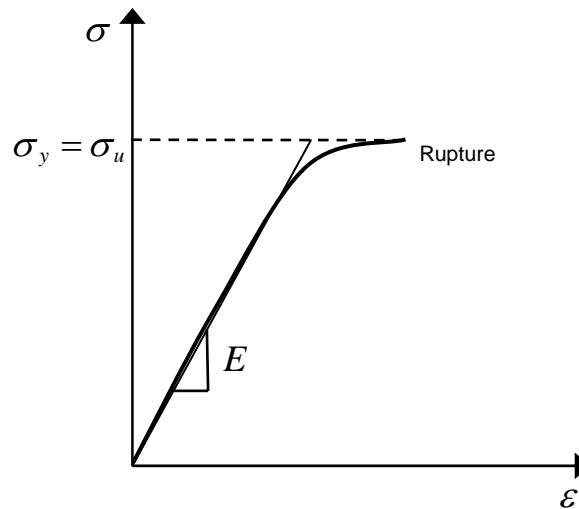


Figure A2.3 - Stress-strain curve for brittle materials.

Brittle materials such as concrete or ceramics do not have a yield point σ_y . For these materials, the rupture strength and the ultimate strength σ_u are the same. Figure A2.3 shows an example of a stress-strain curve for a brittle material.

The area underneath the stress-strain curve is the toughness of the material- i.e. the energy the material can absorb prior to rupture.

Since each material has a different stress-strain curve, for the purposes of the structural analysis, we idealize the stress-strain curves of all these material shown above, by the “idealized” assumptions of a perfectly straight and horizontal yield plateau, the elastic-perfectly plastic (or elastic-ideal plastic). The material behaviour is assumed to be elastic-perfectly plastic when, after reaching the yield stress, the material starts flowing plastically without any further increase in stress.

Figure A2.4 shows an idealized stress-strain for an elastic-perfectly plastic material. The material is first loaded to point a , where it reaches the yield stress σ_y . Beyond this, the material flows plastically without any increase in the stress it carries. At point b , we begin unloading until we reach a zero-load condition at point c . However, because we have loaded the material beyond the yield point, we observe that a permanent deformation or a permanent strain has been introduced into the material. In other words, the material does not have the same shape as at the start of the test. The permanent strain is called plastic strain ϵ_p .

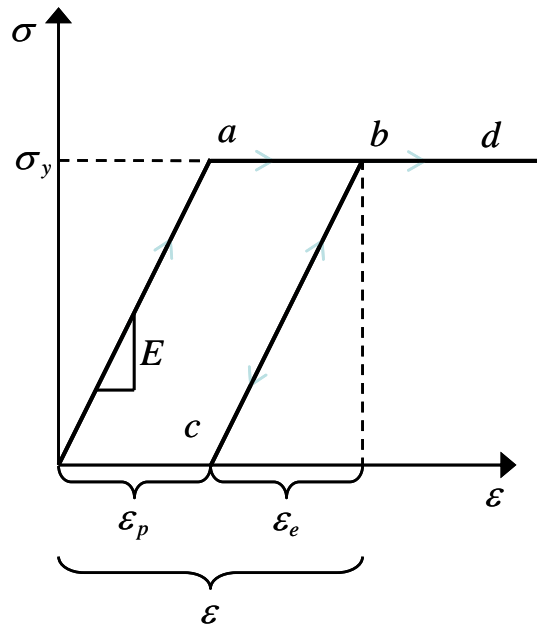


Figure A2.4 – Stress-strain response of elastic-perfectly plastic material.

The total strain ε at point B is the sum of the elastic (reversible) strain ε_e and the plastic (irreversible) strain ε_p :

$$\varepsilon = \varepsilon_e + \varepsilon_p \quad (\text{A2.1})$$

Hooke's law gives the stress in the material:

$$\sigma = E\varepsilon_e \quad (\text{A2.2})$$

where E is Young's modulus of elasticity. Substituting (A2.1) into (A2.2), we obtain:

$$\sigma = E(\varepsilon - \varepsilon_p) \quad (\text{A2.3})$$

Note that for elastic behaviour, the plastic strain vanishes and equation (A2.3) reduces to the standard Hooke's law.

During the elastic loading (or unloading), the mechanical work done on the material is converted to the stored elastic energy. During the plastic yield, a part of this work is dissipated by irreversible plastic process in the material, usually as heat. For perfect elastoplastic material, the rate of dissipation per unit volume is:

$$W = \sigma \dot{\varepsilon} \quad (\text{A2.4})$$

Under uniaxial stress, the stress during plastic yielding is either $\sigma = \sigma_y$, and the plastic strain rate $\dot{\varepsilon}_p$ must be positive, or $\sigma = -\sigma_y$, and then the plastic strain rate $\dot{\varepsilon}_p$ must be negative. In either case, the elastic strain ε_e remains constant. Consequently, $\dot{\varepsilon}_p = \dot{\varepsilon}$ and so:

$$W = \sigma |\dot{\varepsilon}_p| \quad (\text{A2.5})$$

A2.3 Simple elastoplastic constitutive models

In uniaxial elastoplasticity concepts, defined in the previous section, for perfect plasticity, the stress σ cannot be greater in absolute value than the uniaxial yield stress of the material $\sigma_y > 0$. This means that the admissible stresses are constrained to lie in the close interval $[-\sigma_y, \sigma_y] \subset \mathbb{R}$. Expressed as a function

$$f(\sigma) = |\sigma| - \sigma_y \leq 0 \quad (\text{A2.6})$$

called the yield function (Simo and Hughes (1998)). The definitions of $f(\sigma) \leq 0$ is referred to as the yield condition.

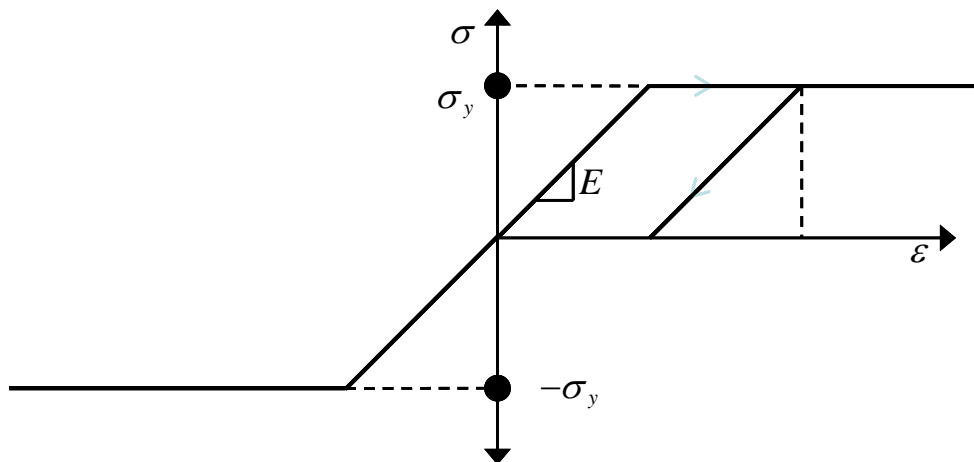


Figure A2.5 – Perfect Plasticity.

The yield condition, defines the behaviour of material. The material is said to be elastic when

$$f(\sigma) < 0 \quad (\text{A2.7})$$

corresponds to elastic stress states. The material is elastoplastic if

$$f(\sigma) = 0 \quad (\text{A2.8})$$

which defines the stress states for which the material exhibits plastic flow. The set stress states that satisfy the yield condition (A2.8) form the so-called yield surface in the stress space. Stress states for which $f(\sigma) > 0$ cannot be supported by the material. All the stress states for which $f(\sigma) \leq 0$ are called plastically admissible.

A2.3.1 Flow theory

Let us now analysis the stress-strain response of elastic-perfectly plastic plotted using the elastoplastic relationship $\sigma = E(\varepsilon - \varepsilon_p)$, defined in section A2.2, (equation (A2.3)). We assume that the material exhibits plastic flow, without damage, the elastic modulus E remains unchanged. We assume also that the change in the configuration of the material is possible only if $\dot{\varepsilon}_p = \frac{\partial}{\partial t} \varepsilon_p \neq 0$, called the flow rule (Jirásek and Bazant (2002)).

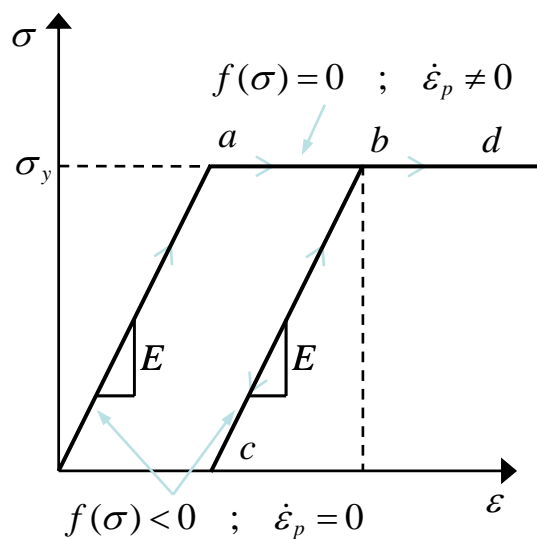


Figure A2.6 – Schematic representation of the mechanical response of one-dimensional elastoplastic model

Let us analyze the load-unload stress-strain response of elastic-perfectly plastic material in Figure A2.6. During the load interval $0-a$, the absolute value of the applied stress σ is less than the yield stress σ_y , consequently the $\dot{\varepsilon}_p = 0$. This implies $f(\sigma) < 0$, the material behaviour is elastic, the stress can be calculated by Hooke's law, $\sigma = E\varepsilon$, and the slope is equal to E . At point a ($\varepsilon = \frac{\sigma_y}{E}$ and $\sigma = \sigma_y$) is the beginning of the elastoplastic behaviour, $f(\sigma) = 0$. During the elastoplastic interval $a-b$, the increment of the applied stress remains constant,

$\dot{\sigma} = 0$, and equal to σ_y , which implies that $\dot{\varepsilon}_p \neq 0$. The interval $b-c$ corresponds to an elastic unload, $f(\sigma) < 0$, with slope equal to E . During unload; the flow rule $\dot{\varepsilon}_p$ is equal to zero, while the plastic strain ε_p is nonzero. Now the stress must be calculated by the elastoplastic equation $\sigma = E(\varepsilon - \varepsilon_p)$. During the second load process $c-d-e$, the behaviour remains elastic while the yield functions are negative, interval $c-d$. At point d the elastoplastic behaviour begin again, $f(\sigma) = 0$, with stress constant and equal to σ_y .

With the observations made above, shown that the flow rule $\dot{\varepsilon}_p$ is dependent of the yield function, because a change in ε_p can take place only if $f(\sigma) = |\sigma| - \sigma_y = 0$. So, the flow rule $\dot{\varepsilon}_p$ is related to the yield condition through the potential relationship

$$\dot{\varepsilon}_p = \dot{\lambda} \frac{\partial f(\sigma)}{\partial \sigma} \quad (\text{A2.9})$$

which is called the associated flow rule[‡]. The symbol λ , the plastic multiplier, is a scalar factor that controls the magnitude of the plastic strain, and the superior dot explicitly that $\dot{\lambda}$ has the meaning of the rate, proportional to the strain rate. For simplify notation, the rate form of the flow rule can be replaced by the incremental form:

$$\Delta \varepsilon_p = \Delta \lambda \frac{\partial f(\sigma)}{\partial \sigma} \quad (\text{A2.10})$$

We already have demonstrated that in the elastic regime, the yield function must remain negative $f(\sigma) < 0$ and the rate of the plastic strain is zero $\dot{\varepsilon}_p = 0$ (plastic strain remains constant). This implies that the plastic multiplier is zero ($\dot{\lambda} \frac{\partial f}{\partial \sigma} = 0 \Rightarrow \dot{\lambda} = 0$). While in the elastoplastic regime the yield function must be equal to zero $f(\sigma) = 0$ (stress remains on the yield surface) and the rate of the plastic strain is nonzero ($\dot{\varepsilon}_p \neq 0$), which implies that the plastic multiplier is positive ($\dot{\lambda} \frac{\partial f}{\partial \sigma} \geq 0 \Rightarrow \dot{\lambda} \geq 0$). Both cases can be simultaneously covered by the loading-unloading conditions

$$\dot{\lambda} \geq 0 \quad ; \quad f(\sigma) \leq 0 \quad ; \quad \dot{\lambda} f(\sigma) = 0 \quad (\text{A2.11})$$

[‡] Associated flow rule in stress space is often called normality rule.

called the Kuhn-Tucker conditions. Based on these three conditions, it can be briefly deduced (Simo and Hughes, 1998):

$$\left\{ \begin{array}{ll} f(\sigma) < 0 \Rightarrow \dot{\lambda} = 0 & \text{elastic behaviour or unload} \\ f(\sigma) = 0 \Rightarrow \left\{ \begin{array}{ll} \dot{\lambda} > 0 & \text{elastoplastic behaviour or load} \\ \dot{\lambda} = 0 & \text{neutral elastoplastic load} \end{array} \right. & \\ f(\sigma) > 0 \Rightarrow & \text{incompatible state} \end{array} \right. \quad (\text{A2.12})$$

During the plastic flow the stress remains on the yield surface, and so the yield function remains equal to zero for a certain period of time. Consequently, the time derivative of the yield function $\dot{f}(\sigma)$ vanishes whenever the rate of the plastic multiplier $\dot{\lambda}$ is nonzero. Therefore, we may state the consistency condition

$$\dot{\lambda} \dot{f}(\sigma) = 0 \quad (\text{A2.13})$$

Condition (A2.13) is also called the persistency condition.

A2.3.2 Isotropic Hardening

Experimentally, under uniaxial loading in some metals, the stress transmitted by a yielding material can increase. An increase of the yield stress is referred to as hardening or strain hardening. During the hardening, the elastic domain undergoes a certain evolution, expanding with the amount of the plastic flow. Due to the changes in the material induced by plastic flow, the elastoplastic domain changes its size in a loading surface.

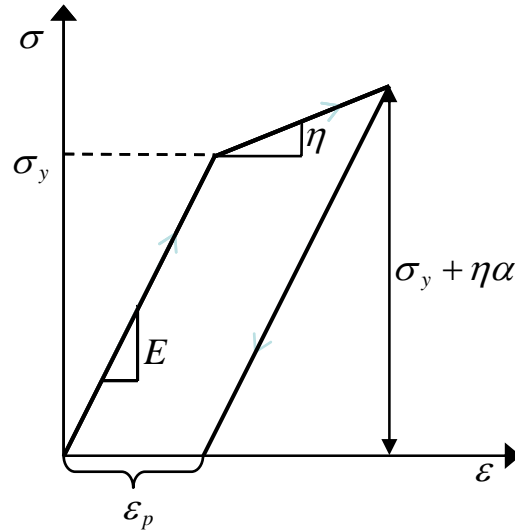


Figure A2.7 – Uniaxial stress-strain diagram of a material with isotropic hardening

For the isotropic hardening, we are obliged too make some assumptions:

- At any state of loading, the centre of the yield surface remains at the origin.
- The hardening is linear in the amount of plastic flow (linear in $|\varepsilon_p|$) and independent of the sign of plastic strain ε_p .

The first assumption leads to a yield criterion of the form

$$f(\sigma, \alpha) = |\sigma| - (\sigma_y + \eta\alpha) \leq 0 \quad (\text{A2.14})$$

where yield stress of the material $\sigma_y > 0$ and $\eta > 0$ are given constants. η is often called the plastic modulus. The variable α is a nonnegative function of the amount of the plastic flow, called an internal hardening variable. Taking into account the second assumption, we consider the simplest evolutionary equation for α as

$$\alpha = |\varepsilon_p| \quad (\text{A2.15})$$

so the equation (A2.14) can be rewritten as

$$f(\sigma, \varepsilon_p) = |\sigma| - (\sigma_y + \eta|\varepsilon_p|) \quad (\text{A2.16})$$

The behaviour of the equation (A2.16) can be expressed by means of the Kuhn-Tucker loading-unloading conditions ((A2.11)), as

$$\dot{\lambda} \geq 0 \quad ; \quad f(\sigma, \varepsilon_p) \leq 0 \quad ; \quad \dot{\lambda} f(\sigma, \varepsilon_p) = 0 \quad (\text{A2.17})$$

where once more λ is determined by the consistency condition

$$\lambda \dot{f}(\sigma, \varepsilon_p) = 0 \quad (\text{A2.18})$$

A2.3.3 Kinematic Hardening law.

In many metals subjected to cyclic loading, it is often experimentally observed that the centre of the yield surface have a motion in the direction of the plastic flow. Even if the magnitudes of the yield stress in tension and in compression are initially the same, this is no longer the case when the material is pre-loaded into the plastic range and then unloaded. In metal, this effect is known as the Baushinger's effect[§].

When kinematic hardening leads to a translation of the loading surface (shift the origin of the initial yield surface), the shifted surface can be described as

$$f(\sigma, \varepsilon_p) = |\sigma - q| - \sigma_y \quad (\text{A2.19})$$

where q is called the back stress, which defines the location of the center of the yield surface. The evolution of the back stress q is defined as

$$\dot{q} = H \dot{\varepsilon}_p \quad (\text{A2.20})$$

where H is called the kinematic hardening modulus.

[§] The Baushinger effect refers to a property of materials where the material's stress-strain characteristics change because of the microscopic stress distribution of the material. I.e., an increase in compressive yield strength at the expense of tensile yield strength.

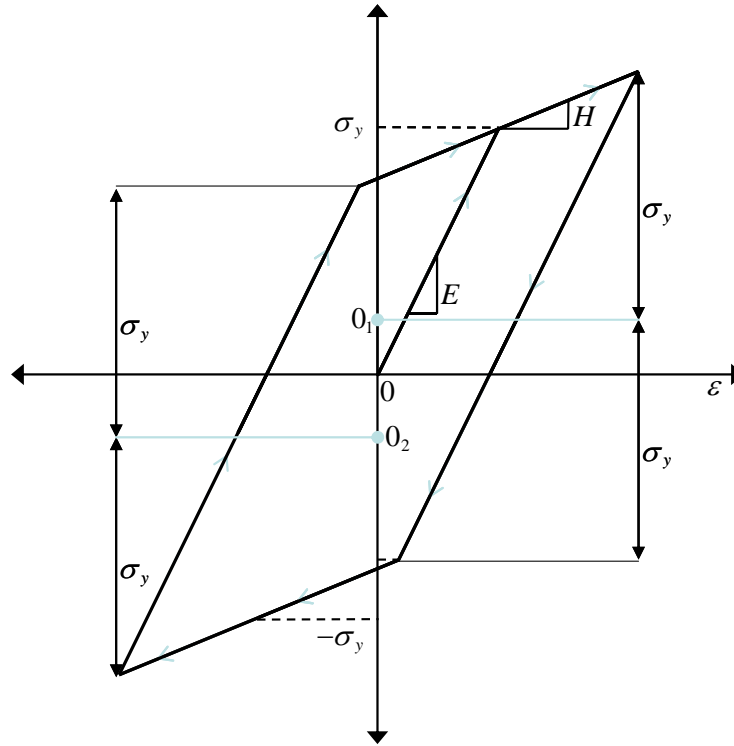


Figure A2.8 – Uniaxial stress-strain diagram of kinematic hardening behaviour.

The equation (A2.19) is still ruled by the Kuhn-Tucker loading-unloading conditions (A2.11), and by consistency condition (A2.13). With this consideration, we are able to solve explicitly for $\dot{\lambda}$ and relate stress rates to strain rates as follows. From (A2.16), and (A2.9), along with the elastoplastic stress-strain relationship $\sigma = E(\varepsilon - \varepsilon_p)$:

$$\begin{aligned} \dot{f}(\sigma, q) &= \frac{\partial f}{\partial \sigma} \dot{\sigma} + \frac{\partial f}{\partial q} \dot{q} = \frac{\partial f}{\partial \sigma} E(\dot{\varepsilon} - \dot{\varepsilon}_p) + \frac{\partial f}{\partial q} H \dot{\varepsilon}_p \leq 0 \\ \dot{f}(\sigma, q) &= \frac{\partial f}{\partial \sigma} E \dot{\varepsilon} - \left(\frac{\partial f}{\partial \sigma} E - \frac{\partial f}{\partial q} H \right) \underbrace{\dot{\varepsilon}_p}_{\dot{\lambda} \frac{\partial f}{\partial \sigma}} \leq 0 \\ \dot{f}(\sigma, q) &= \frac{\partial f}{\partial \sigma} E \dot{\varepsilon} - \dot{\lambda} \left(\frac{\partial f}{\partial \sigma} E \frac{\partial f}{\partial \sigma} - \frac{\partial f}{\partial q} H \frac{\partial f}{\partial \sigma} \right) \leq 0 \end{aligned} \quad (\text{A2.21})$$

Although the term $\frac{\partial f}{\partial \sigma}$ could be reduced to $\text{sign}(\sigma)$, we follow the traditional notation of the finite element method. Furthermore, once $\frac{\partial f}{\partial q} = -\frac{\partial f}{\partial \sigma}$, (A2.21) can be written as

$$\dot{f}(\sigma, \varepsilon_p) = \frac{\partial f}{\partial \sigma} E \dot{\varepsilon} - \dot{\lambda} \left(\frac{\partial f}{\partial \sigma} E \frac{\partial f}{\partial \sigma} + \frac{\partial f}{\partial \sigma} H \frac{\partial f}{\partial \sigma} \right) \leq 0 \quad (\text{A2.22})$$

$\dot{f}(\sigma) > 0$ cannot hold. From (A2.11) and (A2.13) it follows that $\dot{\lambda}$ can be nonzero only if

$$\dot{f}(\sigma, q) = 0 \Rightarrow \dot{\lambda} = \frac{\frac{\partial f}{\partial \sigma} E \dot{\varepsilon}}{\frac{\partial f}{\partial \sigma} E \frac{\partial f}{\partial \sigma} + \frac{\partial f}{\partial \sigma} H \frac{\partial f}{\partial \sigma}} \geq 0 \quad (\text{A2.23})$$

then the rate form of the elastoplastic relationship $\dot{\sigma} = \frac{d\sigma}{d\varepsilon} \dot{\varepsilon}$ along with (A2.23) yields:

$$\frac{d\sigma}{d\varepsilon} = \begin{cases} E & \Leftrightarrow \dot{\lambda} = 0 \\ \frac{\left(\frac{\partial f}{\partial \sigma} E \right) \left(\frac{\partial f}{\partial \sigma} E \right)}{\frac{\partial f}{\partial \sigma} E \frac{\partial f}{\partial \sigma} + \frac{\partial f}{\partial \sigma} H \frac{\partial f}{\partial \sigma}} & \Leftrightarrow \dot{\lambda} > 0 \end{cases} \quad (\text{A2.24})$$

(A2.24) defines the so-called elastoplastic tangent modulus.

A2.3.4 Return-Mapping Algorithms

The evolution laws often have the form of differential equations, and their integration in a closed form is possible only in very special cases. Most material models require special numerical integration schemes providing approximate solutions of the constitutive equations. In plasticity, such procedures are well known as return-mapping algorithms**.

Let us suppose that the elastoplastic stress-strain relationship, the total strain, the flow rule, the back stress, and the yield surface at the step $n+1$ must be

$$\sigma^{n+1} = E(\varepsilon^{n+1} - \varepsilon_p^{n+1}) \quad (\text{A2.25})$$

$$\varepsilon^{n+1} = \varepsilon^{n+1} + \Delta \varepsilon^{n+1} \quad (\text{A2.26})$$

** The return-mapping algorithms are often referred to as the stress return algorithms, because the stress must be "returned" to yield surface. Some authors also refer to them as backward Euler difference scheme.

$$\Delta \varepsilon_p^{n+1} = \Delta \lambda \frac{\partial f}{\partial \varphi^{n+1}} \Rightarrow \varepsilon_p^{n+1} - \varepsilon_p^n = \Delta \lambda \frac{\partial f}{\partial \varphi^{n+1}} \quad (\text{A2.27})$$

$$\Delta q^{n+1} = \Delta \lambda H \frac{\partial f}{\partial \varphi^{n+1}} \Rightarrow q^{n+1} - q^n = \Delta \lambda H \frac{\partial f}{\partial \varphi^{n+1}} \quad (\text{A2.28})$$

$$f(\varphi^{n+1}) = f^{n+1} = |\varphi^{n+1}| - \sigma_y \quad (\text{A2.29})$$

where

$$\varphi^{n+1} = \sigma^{n+1} - q^{n+1} \quad (\text{A2.30})$$

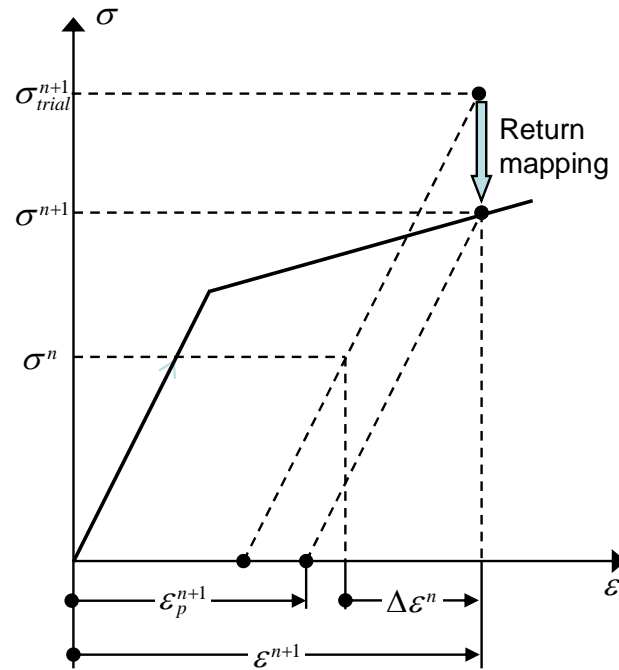


Figure A2.9 – The final stress obtained by return mapping.

Note that the yield function is evaluated for the stress at the end of the instant $n+1$. Finally, the loading-unloading conditions (A2.11), and the yield function (A2.29) are redefined as

$$\Delta \lambda \geq 0 \quad ; \quad f(\varphi^{n+1}) \leq 0 \quad ; \quad \Delta \lambda f(\varphi^{n+1}) = 0 \quad (\text{A2.31})$$

Substituting (A2.27) into (A2.25) we obtain

$$\sigma^{n+1} = E(\varepsilon^{n+1} - \varepsilon_p^n) - \Delta\lambda E \frac{\partial f}{\partial \sigma^{n+1}} \quad (\text{A2.32})$$

If we assume one trial^{††} stress where $\Delta\lambda = 0$ (elastic step), the equation (A2.32) reduces to

$$\sigma_{trial}^{n+1} = E(\varepsilon^{n+1} - \varepsilon_p^n) \quad (\text{A2.33})$$

For the case where $\Delta\lambda \neq 0$, the equation (A2.32) can be rewritten as

$$\sigma^{n+1} = \sigma_{trial}^{n+1} - \Delta\lambda E \frac{\partial f}{\partial \varphi^{n+1}} \quad (\text{A2.34})$$

Replacing (A2.34), and (A2.28) into (A2.30), we obtain:

$$\varphi^{n+1} = (\sigma_{trial}^{n+1} - q^n) - \Delta\lambda (E + H) \frac{\partial f}{\partial \varphi^{n+1}} \quad (\text{A2.35})$$

We can assume that $\varphi_{trial}^{n+1} = (\sigma_{trial}^{n+1} - q^n)$, so the equation (A2.35) becomes

$$\varphi^{n+1} = \varphi_{trial}^{n+1} - \Delta\lambda (E + H) \frac{\partial f}{\partial \varphi^{n+1}} \quad (\text{A2.36})$$

Multiplying by the differential of the yield function, we obtain

$$\varphi^{n+1} \frac{\partial f}{\partial \varphi^{n+1}} = \varphi_{trial}^{n+1} \frac{\partial f}{\partial \varphi_{trial}^{n+1}} - \frac{\partial f}{\partial \varphi_{trial}^{n+1}} \Delta\lambda (E + H) \frac{\partial f}{\partial \varphi^{n+1}} \quad (\text{A2.37})$$

Since $\Delta\lambda > 0$ and $E + H > 0$, we can conclude that $\frac{\partial f}{\partial \varphi^{n+1}} = \frac{\partial f}{\partial \varphi_{trial}^{n+1}}$, so the equation (A2.37) reduces to:

$$|\varphi^{n+1}| = |\varphi_{trial}^{n+1}| - \Delta\lambda \frac{\partial f}{\partial \varphi_{trial}^{n+1}} (E + H) \frac{\partial f}{\partial \varphi^{n+1}} \quad (\text{A2.38})$$

substituting (A2.38) into the yield function (A2.29), we can determine the plastic consistency parameter $\Delta\lambda > 0$ when $f(\varphi^{n+1}) = 0$, as

^{††} The adjective "trial" refers to the fact that, not knowing whether plastic flow takes place or not, we first try a purely elastic step.

$$\begin{aligned}
f(\varphi^{n+1}) &= |\varphi_{trial}^{n+1}| - \Delta\lambda \frac{\partial f}{\partial \varphi_{trial}^{n+1}}(E+H) \frac{\partial f}{\partial \varphi_{trial}^{n+1}} - \sigma_y = 0 \\
&= |\varphi_{trial}^{n+1}| - \sigma_y - \Delta\lambda \frac{\partial f}{\partial \varphi_{trial}^{n+1}}(E+H) \frac{\partial f}{\partial \varphi_{trial}^{n+1}} = 0 \\
&= f(\varphi_{trial}^{n+1}) - \Delta\lambda \frac{\partial f}{\partial \varphi_{trial}^{n+1}}(E+H) \frac{\partial f}{\partial \varphi_{trial}^{n+1}} = 0
\end{aligned} \tag{A2.39}$$

solving this algebraic equation for $f^{n+1} = 0$, the plastic multiplier $\Delta\lambda > 0$ is obtained as:

$$\Delta\lambda = \frac{f_{trial}^{n+1}}{\frac{\partial f_{trial}^{n+1}}{\partial \varphi_{trial}^{n+1}} E \frac{\partial f_{trial}^{n+1}}{\partial \varphi_{trial}^{n+1}} + \frac{\partial f_{trial}^{n+1}}{\partial \varphi_{trial}^{n+1}} H \frac{\partial f_{trial}^{n+1}}{\partial \varphi_{trial}^{n+1}}} \tag{A2.40}$$

We can observe the similitude with the equation (A2.23)

So, the equations (A2.25), (A2.27), (A2.28) and (A2.29) can be rewritten in terms of $\varphi_{trial}^{n+1} = (\sigma_{trial}^{n+1} - q^n)$ as

$$\sigma^{n+1} = \sigma_{trial}^{n+1} - \Delta\lambda E \frac{\partial f_{trial}^{n+1}}{\partial \varphi_{trial}^{n+1}} \tag{A2.41}$$

$$\varepsilon_p^{n+1} = \varepsilon_p^n + \Delta\lambda \frac{\partial f_{trial}^{n+1}}{\partial \varphi_{trial}^{n+1}} \tag{A2.42}$$

$$q^{n+1} = q^n + \Delta\lambda H \frac{\partial f_{trial}^{n+1}}{\partial \varphi_{trial}^{n+1}} \tag{A2.43}$$

$$f_{trial}^{n+1} = |\varphi_{trial}^{n+1}| - \sigma_y \tag{A2.44}$$

In general, the solution of the equations (A2.41), (A2.42), (A2.43), and (A2.44) will require an interactive solution procedure, which can be based on the Newton-Raphson technique, for example. Evaluation of the trial stress is sometimes referred to as the elastic predictor, and the procedure that returns the stress to the yield surface is then called the plastic corrector.

Appendix 3

Plastic Analysis Theory

A3.1 Introduction

One of the classical theories used in structural analysis was the theory of the plastic analysis, also called limit theorems of plasticity. This analysis assumes that structural elements remain elastic except at critical regions, the plastic hinges, where the plasticity and the deformation are concentrated. The limit theorems of plasticity provide a fast way to determine the collapse load of frame structures.

We review all elastoplastic concepts that are necessary for the plastic theory; furthermore, we revise the procedures used to determine the limit (plastic) load in accordance with the theory of plastic analysis.

Moreover, these concepts will also serve like foundations for the subjects expounded in Chapter 4.

A3.2 Bending stresses and strains in beam-column

A straight beam subjected to lateral loads exhibits bending, and the relation between the bending moment and the curvature of the deformed middle axis is then of interest. Consider the uniformly load beam with a symmetrical cross section in Figure A3.1.a with two supporting ends, one of which is hinged and the other is on rollers. The plane cross section remains plane, and remains normal to the deflected middle axis of the beam, as defined in the classical Euler-Bernoulli assumptions. This assumption has been demonstrated by numerous experiments, for elastic as well as inelastic bending.

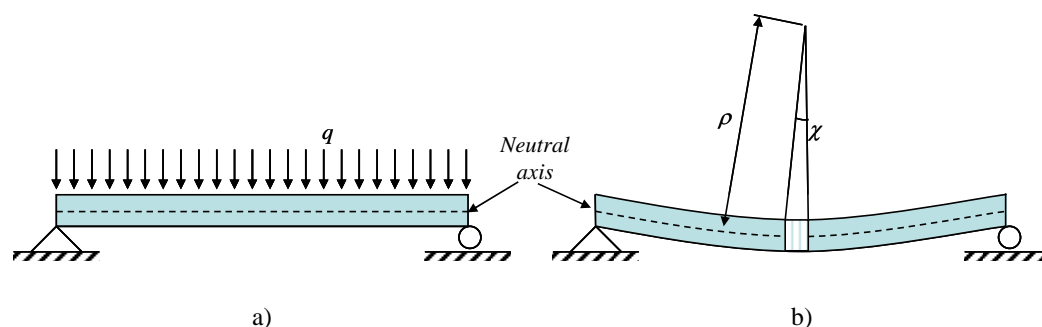


Figure A3.1 – Simple supported beam: a) uniform load, b) deformed shape.

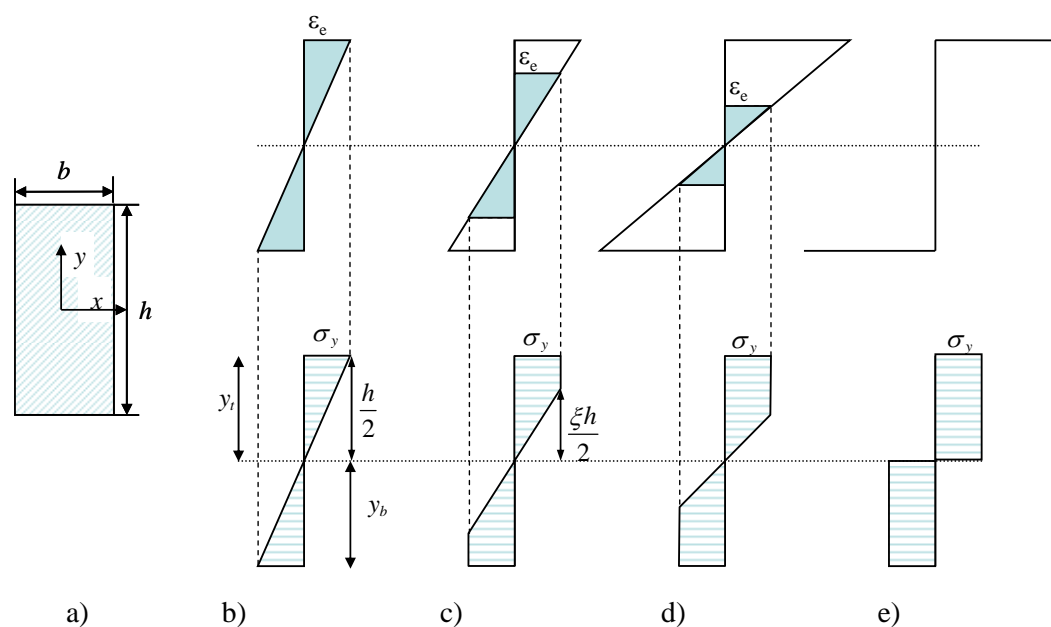


Figure A3.2 – Rectangular cross section under pure bending: a) the cross section, b) the stress and strain at the elastic limit state, c) stress and strain at an elastoplastic state, d) the stress and strain at an increase of the elastoplastic state, e) stress and strain at the limit state.

Let us suppose that Figure A3.2.a shows the symmetric cross section of the beam shown in Figure A3.1. The strain varies linearly along the beam depth (Figure A3.2.b). The strain at the top section is compressive and decreases with depth, becoming zero at certain distance below the top. The plane where the strain is zero is called the neutral axis. Below the neutral axis, tensile strains act, increasing in magnitude downward.

Based on the foregoing assumptions, the strain deformation shown in Figure A3.1.b can be expressed as

$$\varepsilon = \frac{y}{\rho} = y\chi \quad (\text{A3.1})$$

here ρ is the radius of the curved segment, $\chi = \frac{1}{\rho}$ is the curvature (the cross section rotation), and y is the depth coordinate measured from the neutral axis x . The bending moment in the beam due to internal forces may be computed from the stresses function $\sigma_x(y)$ as

$$m = \int_A y\sigma_x(y)dA = \int_{y_b}^{y_t} \sigma_x(y)y \underbrace{b(y)dy}_{dA} \quad (\text{A3.2})$$

in which $\sigma_x(y)$ is the distribution of normal stresses as function of y . dA is the differential unit of cross-section area of the differential depth dy and a width $b(y)$ of the beam at the distance y from the neutral axis.

A3.2.1 Bending in the elastic range

If we assume the stress-strain is linear, the stress would be linearly distributed along the depth of the beam, the distribution of normal stresses $\sigma_x(y)$ in the Figure A3.2.b can be expressed as:

$$\sigma_x(y) = \frac{\sigma_y}{y_t} y \quad (\text{A3.3})$$

where σ_y is the yield stress, y_t is the distance from the neutral axis to beam top. Substituting the equation (A3.3) into (A3.2) gives

$$m = \int_{y_b}^{y_t} \frac{\sigma_y}{y_t} b(y) y^2 dy = \frac{\sigma_y}{y_t} \int_{y_b}^{y_t} b(y) y^2 dy = \sigma_y \frac{I}{y_t} \quad (\text{A3.4})$$

$$m = \sigma_y Z_e$$

where $I = \int b(y) y^2 dy$ is the moment of the inertia of the cross section about the neutral axis. The factor $Z_e = I/y_t$ is the elastic section modulus, for the top of the surface. If we consider that the section of the beam is a rectangular section with b and depth h , as shown in Figure A3.2.a, the moment of inertia I is:

$$I = \int_{y_b}^{y_t} b(y) y^2 dy = \int_{-h/2}^{h/2} b y^2 dy = \frac{1}{12} b h^3 \quad (\text{A3.5})$$

and the elastic section modulus will be Z_e :

$$Z_e = \frac{I}{y_t} = \frac{\frac{1}{12} b h^3}{\frac{1}{2} h} = \frac{1}{6} b h^2 \quad (\text{A3.6})$$

The corresponding bending moment

$$m_e = \sigma_y Z_e = \sigma_y \frac{1}{6} b h^2 \quad (\text{A3.7})$$

is called the elastic limit moment.

A3.2.2 Bending in plastic range

When all the cross-section reaches the yield stress σ_y the stress diagram would take the form as shown in Figure A3.2.e. Although the strains would still vary linearly with depth, the moment becomes the plastic moment and would be the sum of the diagram areas, as

$$m = \sigma_y \int_0^{y_t} b(y) y dy + \sigma_y \int_0^{y_b} b(y) y dy = \sigma_y Z_p \quad (\text{A3.8})$$

where $Z_p = \int_0^{y_t} b(y) y dy + \int_0^{y_b} b(y) y dy$ is the plastic section modulus. For a rectangular section, the plastic section modulus Z_p can be expressed as:

$$Z_p = \int_0^{y_t} b(y)ydy + \int_0^{y_b} b(y)ydy = \int_0^{\frac{h}{2}} bydy + \int_0^{-\frac{h}{2}} bydy = \frac{bh^2}{4} \quad (\text{A3.9})$$

and the plastic moment m_p becomes

$$m_p = \sigma_y Z_p = \sigma_y \frac{bh^2}{4} \quad (\text{A3.10})$$

A3.3 Moment-Curvature diagram of a beam-column

Now let us try to obtain the law of variation of the bending moment with the curvature defined in the equation (A3.1). Since we have assumed the beam to have a linear elastic material, which complies with Hooke's law ($\sigma = E\varepsilon$), this relationship is valid as long as the strain at the extreme points (at the top or bottom surface) remains at or below the elastic limit strain $\varepsilon_e = \frac{\sigma_y}{E}$ (Figure A3.2.b). With the equations (A3.1) and (A3.2) the moment-curvature is given as:

$$m = \int_A y\sigma_x(y)dA = \int_A yE\varepsilon(y)dA = \int_A yEy\chi dA = E \underbrace{\int_A y^2 dA}_I \chi = EI\chi \quad (\text{A3.11})$$

the product EI is called the bending stiffness.

When the stress exceeds the yield stress σ_y , the elastic part of the cross section, over which stress distribution is linear, Figure A3.2c, has the depth ξh with $\xi < 1$. In the remaining (plastic) part of the section, the normal stress is at the positive or negative yield limit. Evaluating the moment from the stress distribution drawn in Figure A3.2c, through the integration of the equation (A3.2), we have for a rectangular section de formulation proposed by (Jirasék and Bazant, 2002):

$$m = 2 \left[\sigma_y b \frac{1}{2} \left(\frac{\xi h}{2} \right) \left(\frac{2}{3} \frac{\xi h}{2} \right) \right] + 2 \left[\sigma_y b \left(\frac{h}{2} - \frac{\xi h}{2} \right) \frac{1}{2} \left(\frac{\xi h}{2} + \frac{h}{2} \right) \right] = \frac{1}{4} \sigma_y b h^2 \left(1 - \frac{\xi^2}{3} \right) \quad (\text{A3.12})$$

$$m = m_p \left(1 - \frac{\xi^2}{3} \right)$$

Observing in the elastoplastic limit (Figure A3.2.c), we can assume that in the remaining plastic part of the section there is one elastic strain $\varepsilon_e = \frac{\sigma_y}{E}$. Analyzing the equation (A3.1) at $y = \frac{\xi h}{2}$, the parameter ξ can be expressed as

$$\varepsilon_e = y\chi = \frac{\sigma_y}{E} \Leftrightarrow \frac{\xi h}{2} \chi = \frac{\sigma_y}{E} \Leftrightarrow \xi = \frac{2\sigma_0}{\underbrace{Eh}_{\chi_e}} \chi \quad (\text{A3.13})$$

$$\xi = \frac{\chi_e}{\chi}$$

where χ_e is the curvature at the elastic limit. Substituting (A3.13) into (A3.12) leads to the moment-curvature relation:

$$m(\chi) = m_p \left(1 - \frac{\chi_e^2}{3\chi} \right) \quad (\text{A3.14})$$

which is valid above the elastic limit, i.e. for $\chi \geq \chi_e$. Plotting (A3.11) for $\chi \leq \chi_e$ and (A3.14) for $\chi \geq \chi_e$ we obtain the moment curvature diagram drawn in Figure A3.3.

We have seen that for bending moments in the range $m_e \leq m \leq m_p$, a beam section comprises fully plastic regions and a central elastic middle. Thus yielding occurs in the plastic regions with no increase in stress, whereas in the elastic middle increases in deformation are accompanied by increases in stress. The elastic middle therefore controls the deformation of the beam; a state sometimes termed contained *plastic flow*. As m approaches m_p , the moment-curvature diagram is asymptotic to the line $m = m_p$ so that large increases in deformation occur without any increase in moment, a condition known as *unrestricted plastic flow*.

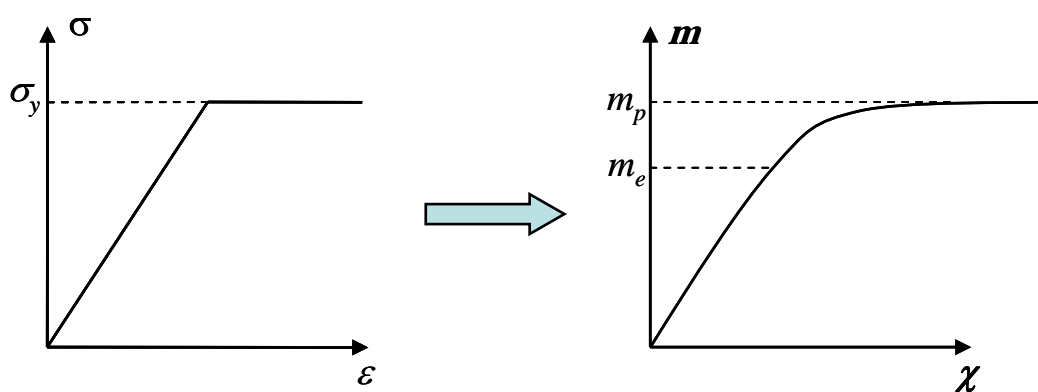


Figure A3.3 - Stress strain and moment curvature in a beam.

A3.4 Plastic Hinge

The presence of unrestricted plastic flow at a section of a beam leads us to the concept of the formation of plastic hinges in beams and other structures.

A plastic hinge is said to form in a structural member when the cross-section is fully yielded, i.e. Figure A3.2.e. If the material strain hardening is not yet considered in the analysis, a fully yielded cross-section can undergo indefinite rotation at a constant restraining plastic moment m_p .

Let us analyze the elastic behaviour of a simply supported beam with a rectangular section with b and depth h , loaded up to collapse by a concentrated load P at midspan (Figure A3.4).

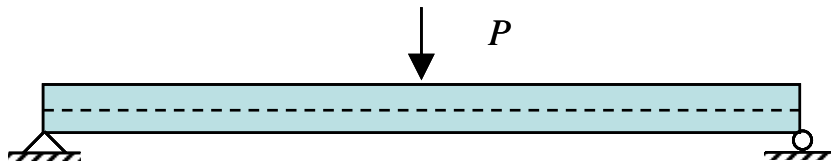


Figure A3.4 – Beam loaded at midspan

During the increasing of the load P , the cross section at midspan, at which the bending moment is the highest, will go through some stages before the complete plastification. When the load is $P = P_e$, consequently $m = m_e$, the stress at the cross section takes the value σ_y at the surface, while the rest of the section remains elastic, as shown in Figure A3.5.

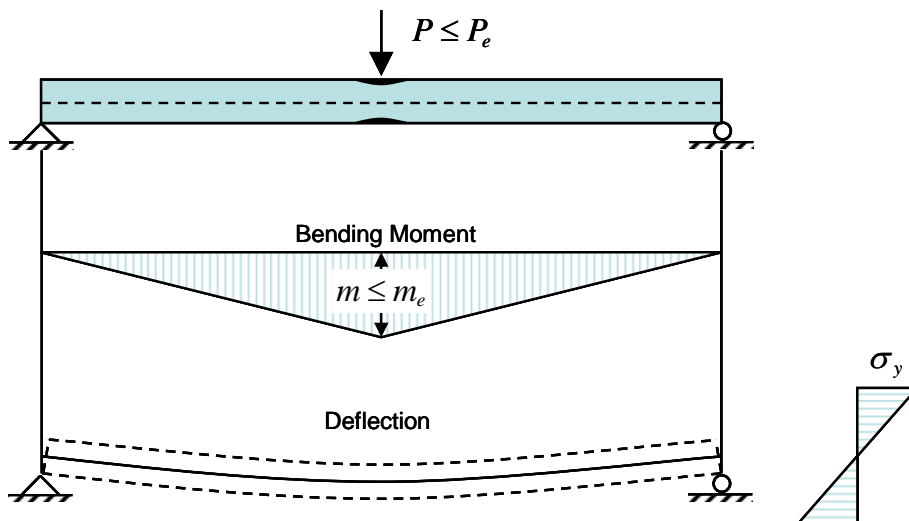


Figure A3.5 -- Bending moment and deflection at $P \leq P_e$

During the step $P_e \leq P < P_p$, Figure A3.6, bending moment within $m_e \leq m < m_p$, the cross section (at the midspan) becomes plastic across its depth, with the increase of the deflections.

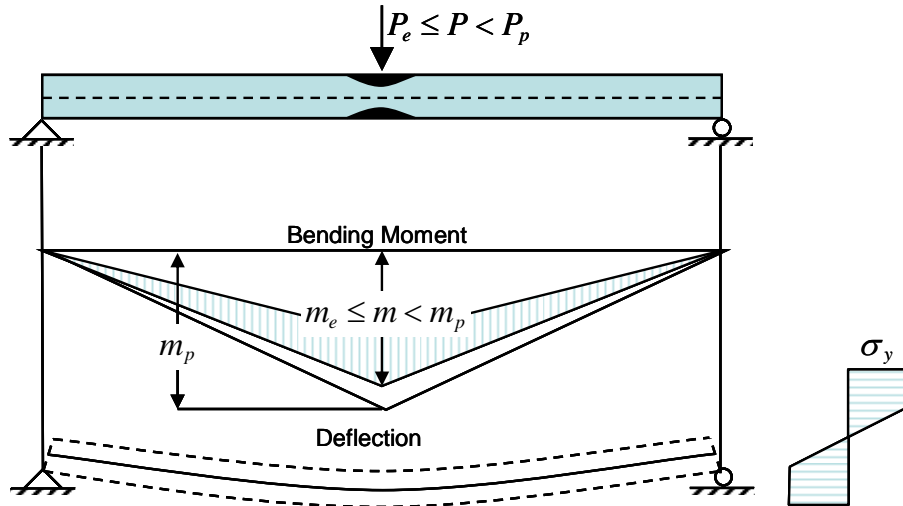


Figure A3.6 – Bending moment and deflection at $P_e \leq P < P_p$

When one cross section becomes plastic across the full depth, Figure A3.7, with $P_p \leq P < P_l$, the value of the bending moment reaches its maximum value $m = m_p$. At that point, an arbitrary further increase of curvature at that cross section is possible (at least within the geometrical theory).

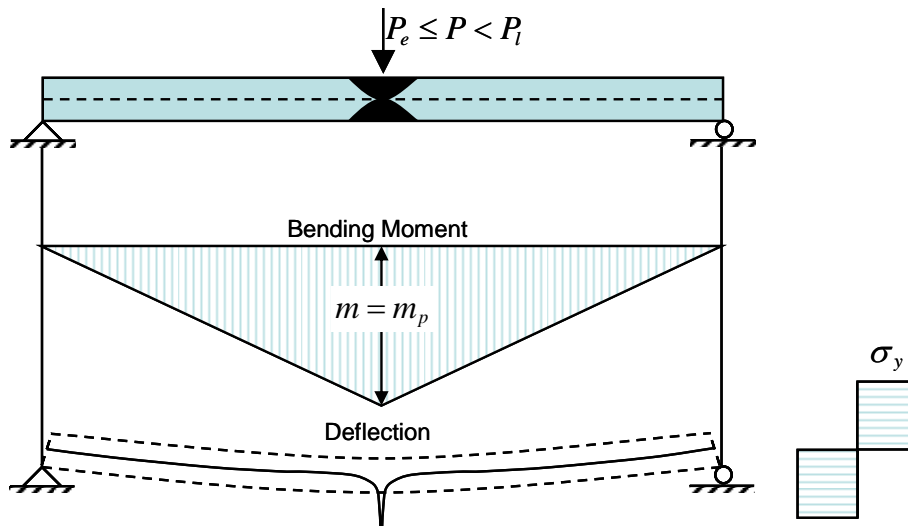


Figure A3.7 -- Bending moment and deflection at $P_p \leq P < P_l$

Since the curvature can increase greatly, mathematically infinitely, we have at the midspan an equivalent of a hinge, called a plastic hinge or yield hinge. An infinite increase of the curvature at this hinge is equivalent to a finite rotation at

this cross section, which leads to the collapse of the beam with the load P equal the maximum value P_l .

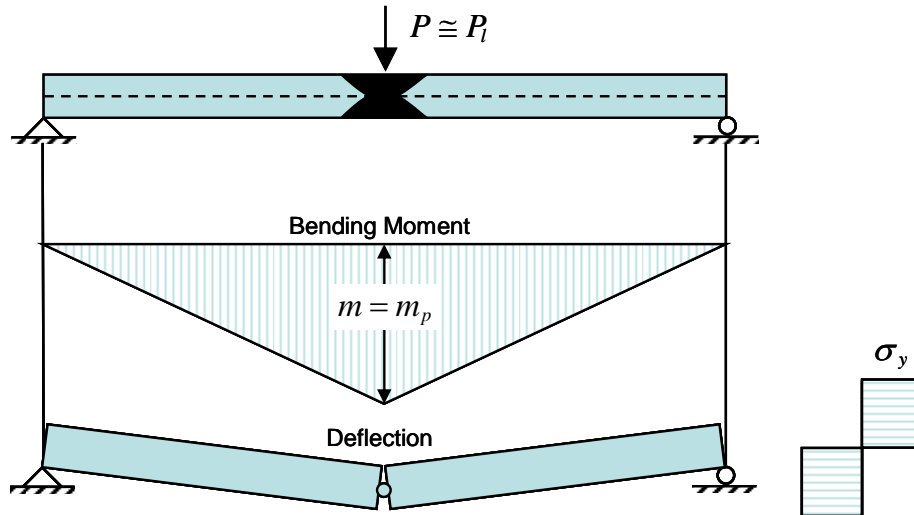


Figure A3.8 -- Bending moment and deflection at $P \cong P_p$

Note that the concept of plastic hinge does not require the plastic rotation to be large. During the collapse, the load is constant, and so the elastic deformations do not change. Therefore, all the structural parts whose cross section is not fully plasticized behave as a rigid body.

As already stated, the idealized yield hinge lumps all the plastic deformation into a single cross section. The real plastic zone occupies a certain volume, and its shape can be estimated if the elastoplastic state of the cross sections carrying bending moments between m_e and m_p is taken into account.

The exact length and shape of the plasticized zone has only a small effect on the global response of the structure, and so we can lump the plastic hinge into one single cross section. The total plastic deformation is replaced by a rotation ϕ , in an idealized hinge (Figure A3.9). From kinematic considerations, it follows that the plastic extension at an arbitrary point of the cross section can be expressed by a linear function:

$$\varepsilon_p(y) = \phi y \quad (\text{A3.15})$$

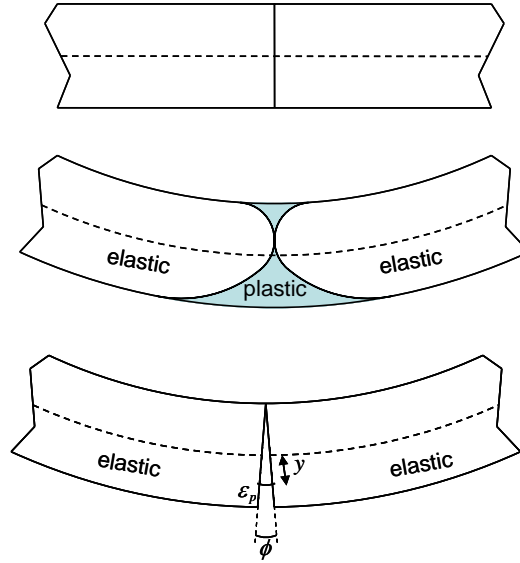


Figure A3.9 – Idealized plastic hinge.

The energy dissipated by a plastic hinge, defined by the volume integral

$$W_{int} = \int_{\Omega} \sigma \dot{\varepsilon}_p \, d\Omega \quad (\text{A3.16})$$

can be evaluated as expressed by the integral over the fully plasticized cross section,

$$W_{int} = \int_A \sigma(y) \dot{\varepsilon}_p(y) \, dA \quad (\text{A3.17})$$

Substituting the equation (A3.15) into (A3.17), and recalling the stress-bending moment relationship, (equation(A3.2)), we obtain:

$$W_{int} = \int_A \sigma(y) \underbrace{\dot{\phi} y}_{\varepsilon_p} \, dA = \underbrace{\int_A \sigma(y) y \, dA}_m \dot{\phi} = m \dot{\phi} \quad (\text{A3.18})$$

which can be expressed as:

$$W_{int} = m \dot{\phi} = m_p \left| \dot{\phi} \right| \quad (\text{A3.19})$$

provided that the magnitude of the plastic moment does not depend on the sign of curvature.

A3.5 Theory of Plastic Analysis

As shown in the A3.4, for the case of a simply supported beam the attainment of the collapse load can be easily calculated. However, for more complicated, statically indeterminate structures is not. In this case, we can use some plastic analysis procedure to obtain the solutions.

The analysis procedure described in this section is approximate because of some assumptions proposed in Deierlein *et al.* (2001):

- The response of all members are elastic perfectly plastic
- The plasticity is concentrated at specific points in the member (spread of plasticity is not accounted for)
- The interaction between force and moments is not considered, the yield of a cross section is governed uniquely by the plastic moment capacity m_p of that cross section.

Together with these assumptions, an “exact” plastic analysis solution must satisfy three basic conditions. They are equilibrium, mechanism and plastic moment conditions, well known as the Uniqueness Theorem. The plastic analysis disregards the continuity condition as required by the elastic analysis of indeterminate structures. The formation of a plastic hinge in members leads to discontinuity of slope. If sufficient plastic hinges are formed to allow the structure to deform into a mechanism, this is a mechanism condition. Since plastic hinge analysis utilizes the limit of resistance of the member’s plastic strength, the plastic moment condition is required to ensure that the resistance of the cross section is not violated anywhere in the structure. Lastly, the equilibrium condition, which is the same condition to be satisfied in elastic analysis, requires that the sum of all applied forces and reactions be equal to zero and that all internal forces be self-balanced.

When all three conditions are satisfied, the resulting plastic analysis for the limiting load is the “correct” limit load. The collapse loads for simple structures such as beams and portal frames can be solved easily using a direct approach or through visualization of the formation of “correct” collapse mechanism. However, for more complex structures, the exact solution satisfying all three conditions may be difficult to predict.

Once a mechanism has formed, the structure continues to deform (mechanism motion) without an increase in load. Mechanism motion causes concentrated rotations at the plastic hinge locations, but no changes in deformations (curva-

tures) in the elements between plastic hinges (rigid body mechanism), as shown in Figure A3.10.

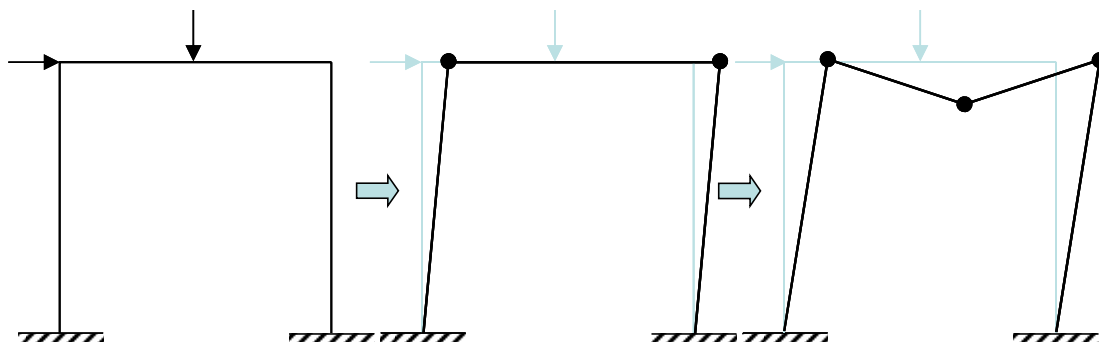


Figure A3.10 – Mechanism of formation and motion.

To determine the mechanism load for the structure, we use the limit theorems of plastic analysis, i.e. the upper bound theorem, and the lower bound theorem.

- Lower bound theorem
Any set of loads in equilibrium with an assumed moment diagram, which is statically admissible and consistent with a given loading condition and for which the moments do not exceed m_p , is smaller than or at most equal to the set of loads that produces collapse of the structure.
- Upper bound theorem
Any set of loads in equilibrium with an assumed kinematically admissible field[‡] is larger than or at least equal to the set of loads that produces collapse of the structure.

There are two approaches based on the lower and upper bound theorem to determine the mechanism load of the structure: a statical approach, and a kinematical approach.

[‡] Kinematically admissible field is a mechanism in which the external work (W_e) done by the forces F on the deformations δF and the internal work (W_{int}) done by the moments $m_p(x)$ on the rotations $\phi(x)$ are positive. In particular, at each plastic hinge, $m_p(x)$ and $\phi(x)$ must be of the same sign.

A3.5.1 Statical Approach

In the statical approach, also called equilibrium method, which employs the lower bound theorem, the structure is analyzed under the forces it is subjected to, and the forces are gradually increased until any one member reaches its moment capacity. The point in the member that reaches its capacity now becomes a plastic hinge, and the structure is analyzed for further incremental loads, assuming this point to behave like a hinge.

Though the hinge carries moment equal to the plastic capacity of the cross section, for incremental loads, it behaves like a perfect hinge; that is, incremental rotations of the hinge do not cause additional forces. This incremental loading is continued until another cross section reaches its plastic moment capacity. At this stage, this second cross section also becomes a plastic hinge, and for further incremental loads, it is treated as a hinge.

We continue these processes until sufficient plastic hinges have been created to cause the structure to become unstable (the stiffness matrix becomes singular due to the introduction of so many hinges), and we can no longer analyze the structure statically. Since the method of analysis is based on statics (the moments do not exceed m_p), and at the point of mechanism formation, it also satisfies the kinematically admissible field, thus the load given by this method is the mechanism load.

A3.5.2 Kinematic Approach

This method, also called mechanism method, which is based on the upper bound theorem, states that the load computed on the basis of an assumed failure mechanism is never less than the exact plastic limit load of a structure. Thus, it always predicts the upper bound solution of the collapse limit load. It can also be shown that the minimum upper bound is the limit load itself. The procedure of using the mechanism method has the following two steps:

1. Assume a failure mechanism and form the corresponding work equation from which an upper bound value of the plastic limit load can be estimated.
 2. Write the equilibrium equations for the assumed mechanism and check the moments to see whether the plastic moment condition is met everywhere in the structure.
-

To obtain the true limit load using the mechanism method, it is necessary to determine every possible collapse mechanism, some of which are the combinations of a certain number of independent mechanisms.

Once the independent mechanisms have been identified, a work equation may be established for each combination, and the corresponding collapse load is determined. The lowest load among those obtained by considering all the possible combinations of independent mechanisms is the correct plastic limit load.

References

- Álvares, M. S. (1993). "Estudo de um modelo de dano para o concreto: formulação indentificação paramétrica e aplicação com emprego do método dos elementos finitos." Departamento de Estruturas, Escola de Engenharia de São Carlos – USP, São Carlos, Brazil.
- Álvares, M. S. (2004). "Aplicação de um Modelo de Dano Localizado a Estruturas de Barras em Concreto Armado."
- Argyris, J. H., Boni, B., and Kleiber, M. (1982). "Finite Element Analysis of Two and Three – Dimensional Elasto-Plastic Frames – The Natural Approach." *Computer Methods in Applied Mechanics an Engineering*, 35, 221-248.
- Ayala, G., and Xianguo, Y. "Analytical evaluation of the structural seismic damage of reinforced concrete frames." *7th Canadian Conference on Earthquake Engineering*, Montreal, Canada, 389-396
- Banon, H., Biggs, J., and Irvine, M. (1981). "Seismic Damage in Concrete Frames." *Journal of Structural Engineering, ASCE*, 107(9), 1713-1729.

- Banon, H., and Veneziano, D. (1982). "Seismic safety of reinforced members and structures." *Earthquake Engineering & Structural Dynamics*, 10(2), 179-193.
- Barbat, A. H., and Canet, J. M. (1994). *Estructuras Sometidas a Acciones Sísmicas.*, CIMNE, Barcelona.
- Barbat, A. H., Cervera, M., Hanganu, A., Cirauqui, C., and Oñate, E. (1998). "Failure pressure evaluation of the containment building of a large dry nuclear power plant." *Nuclear Engineering and Design*, 180, 251-270.
- Barbat, A. H., Oller, S., Oñate, E., and Hanganu, A. (1997). "Viscous Damage Model for Timoshenko Beam Structures." *International Journal of Solids Structures*, 34(30), 3953-3976.
- CEB. (1998). "Task Group 2.2, Ductility Requirements for Structural Concrete - Reinforcement , Ductibility of reinforced concrete structures." Comité Euro-International du Béton T. G. 2.2, ed., Thomas Telford.
- Cervera, M., Oliver, J., and Faria, R. (1995). "Seismic evaluation of concrete dams via continuum damage models " *Earthquake Engineering and Structure Dynamics*, 24, 1225 - 1245.
- Cipolina, A., López Inojosa, A., and Flórez-López, J. (1995). "A Simplified Damage Mechanics Approach to Nonlinear Analysis of Frames. ." *Computer & Structures*, 54(6), 1113-1126.
- Clough, R., and Benuska, L. (1967). "Nonlinear Earthquake Behavior of Tall Buildings." *Journal of Mechanical Engineering, ASCE*, 93(3), 129-146.
- Clough, R., and Johnston, S. "Effect of Stiffness Degradation on Earthquake Ductility Requirements " *Japan Earthquake Engineering Symposium*, Tokyo, Japan, 195-198.
- Clough, R., and Penzien, J. (1993). *Dynamics of Structures*, McGraw-Hill, New York
- Cohn, M. Z., and Franchi, A. (1979). "Structural Plasticity Computer System: STRUPL. ." *Journal of Structural Division ASCE* 105(4), 789 – 804.
- Chen, W. E. (1994). *Constitutive equations for engineering materials*, Elsevier, New York, N.Y.
- Chen, W. F. (1982). *Plasticity in Reinforce Concrete*, MacGraw Hill.
-

-
- Chen, W. F., and Chan, S. L. (1995). "Second-order Inelastic Análisis of Steel Frames Using Element with Midspan and end Springs." *Journal of Structural Engineering* – Vol. 121, nº 3, 530 -541, 121(3), 530 -541.
- Chung, Y. S., Meyer, C., and Shinozuka, M. (1987). "Seismic damage assessment of reinforced concrete members." *NCEER-87-0022*, National Center for Earthquake Engineering Research, State University of New York at Bufalo, Bufalo, NY.
- Deierlein, G. G., Hajjar, J. F., and Kavinde, A. (2001). "Material Nonlienar Analysis of Strutres: A Concentrated Plasticity Approach. ." S. E. Report *ST-01-10*, Department of Civil Engineering, University of Minesota.
- DiPasquale, E., and Çakmak, A. S. (1987). "Detection and assessment of seismic structural damage." *NCEER-87-0015*, National Center for Earthquake Engineering Research, State University of New York at Buffalo.
- DiPasquale, E., and Çakmak, A. S. (1998). "Identification of the serviceability limit state and detection of seismic structural damage." *NCEER-88-0022*, National Center for Earthquake Engineering Research, State University of New York at Bufalo, Bufalo, NY.
- Dubé, J., Pijaudier-Cabot, G., and Laborderie, C. (1996). "Rate dependent damage model for concrete in dynamics." *Journal of Engineering Mechanics ASCE*, 122(10), 939-947.
- Felippa, C. A. (2000). "A Historical Outline of Matrix Structural Analysis: A Play in Three Acts." *CU-CAS-00-13*, Center for Aerospace Structures, College of Engineering University of Colorado, Boulder, Colorado.
- Filippou, F. C., D'Ambrisi, A., and Issa, A. (1992). "Nonlinear Static and Dymanic Analysis of Reinforced Concrete Subassembles." *UCB/EERC-92/08*, Earthquake Engineering Research Center, College of Engineering, University of California, Berkeley.
- Filippou, F. C., and Issa, A. (1998). "Nonlinear Analysis of Reinforced Concrete Frames Under Cyclic Load Reversals " *EERC 88/12*, Earthquake Engineering Research Center, University of California Berkeley.
- Flórez-López, J. (1993). "Modelos de Daño Concentrado para la Similacion Numérica del Colapso de Pórticos Planos." *Revista Internacional de Métodos Numéricos Para Cálculo y Diseño en Ingeniería* 9(2), 123-139.
-

- Flórez-López, J. (1995). "Simplified Model of Unilateral Damage for RC Frames. ." *Journal of Structural Engineering, ASCE*, 121(12), 1765-1771.
- Flórez-López, J. (1999). "Plasticidad y Fractura en Estructuras Aporticadas." A. H. Barbat, CIMNE - Centro Internacional de Metodos Numéricos en Ingeniería, Barcelona.
- Giberson, M. (1967). "The Response of Nonlinear Multi-Story Structures Subjected to Earthquake Excitations ", Earthquake Engineering Research Laboratory, Pasadena.
- Hanganu, A., Oñate, E., and Barbat, A. H. (2002). "A finite element methodology for local/global damage evaluation in civil engineering structures." *Computer and Structures*, 80, 1667-1687.
- Jirásek, M. (1997). "Analytical and Numerical Solutions for Frames with Softening Hinges." *Journal of Structural Engineering* 123(1), 8-14.
- Jirásek, M., and Bazant, Z. P. (2002). *Inelastic analysis of structures. : ,* John Willey & Sons, New York.
- Kachanov, L. M. (1958). "On Creep Rupture Time." *Proc. Acad. Sci., USSR, Div. Eng. Sci*, 8, 26–31.
- Kachanov, L. M. (1986). *Introduction to continuum damage mechanics*, Martinus Nijhoff Publishers, Dordrecht, The Netherlands.
- Karsan, I. D., and Jirsa, J. (1969). "Behavior of concrete under compressive loadings." *Journal of Structural Division ASCE* 95(12), 2535-2563.
- Kondoh, K., and Atluri, S. N. (1987). "Large-deformation, Elasto-plastic Análisis of Frames Nonconservative Loading, Using Explicit Derived Tangent Stiffnesses based on Assumed Stress. ." *Computational Mechanis, Vol. 2*, 1-25, 2(1-25).
- Kondoh, K., Tanaka, K., and Atluri, S. N. (1986). "An Explicit Expresión for the Tangent-Stiffness of a Finitely Deformad 3-D Beam and its use in the Análisis of Space Frames." *Computers & Structures*, 24(2), 253-271.
- Kwak, H. G., and Filippou, F. C. (1997). "Nonlinear FE Analysis of Reinforced Concrete Structures under Monotonic Loads." *Computer & Structures*, 65.(4), 585-592.
-

-
- Lemaitre, J., and Chaboche, J. L. (1990). *Mechanics of Solid Materials*, Cambridge University Press, New York, N.Y.
- Lemaitre, J., and Lippmann, H. (1996). *A Course on damage mechanics* Springer, Berlin.
- Lubliner, J. (1990). *Plasticity theory*, Macmillan Publishing.
- Lubliner, J., Oliver, J., Oller, S., and Onate, E. (1989). "A plastic-damage model for concrete." *International Journal of Solids and Structures*, 25(3), 299-326.
- Luccioni, B. (2003). "Apuntes de Mecánica de Daño Continuo. ." Departamento de Resistencia de los Materiales y Estructuras a la Ingeniería, Universidad Politécnica de Catalunya.
- Luccioni, B., Oller, S., and Danesi, R. "Plastic damaged model for anisotropic materials ; ." *Fourth Pan American Congress of Applied Mechanics (PACAM IV)*, Buenos Aires
- Luccioni, B., Oller, S., and Danesi, R. (1996). "Coupled Plastic-Damage Model." *Computer Methods in Applied Mechanics and Engineering*, 129, 81-89.
- Mahin, S., and Bertero, V. V. (1981). "An Evaluation of Inelastic Seismic Design Spectra." *Journal of Structural Engineering, ASCE*, 107(9), 1777-1795.
- Makode, P. V., Corotis, R. B., and Ramírez, M. R. (1999a). "Geometric Nonlinear Análisis of Frame Structures by Pseudodistortions." *Journal of Structural Engineering*, 125(11), 1318-1327.
- Makode, P. V., Corotis, R. B., and Ramírez, M. R. (1999b). "Nonlinear Analysis of Frame Structures by Pseudodistortions." *Journal of Structural Engineering, ASCE*, 125(11), 1309-1317.
- Malvern, L. (1969). *Introduction to the Mechanics of a Continuos Medium* Prentice Hall.
- Massonnet, C. E., and Save, M. A. (1966). *Cálculo plástico de las construcciones*, L. I. Morlán, translator, Montaner y Simón, DL Barcelona.
- Mazars, J. (1986). "A model of a unilateral elastic damageable material and its application to concrete." *Fracture toughness andfiacture energy of concrete*, E. S. Publishers, ed., E H. Wittmann, Amsterdam, The Netherlands, 61 -71.
-

- Mazars, J., and Pijaudier-Cabot, G. (1989). "Continuum damage theory: application to concrete." *Journal of Engineering Mechanics ASCE*, 115(2), 345-365.
- Newmark, N. M., and Rosenblueth, E. (1971). *Fundamentals of Earthquake Engineering*, Prentice-Hall, Englewood Clis, N.J.
- Ohtani, Y., and Chen, W. F. (1988). "Multiple hardening for plasticity materials." *Journal of Engineering Mechanics ASCE*, 114, 1890-1810.
- Oliver, J., Cervera, M., Oller, S., and Lubliner, J. "Isotropic Damage Models and Smeared Crack Analysis of Concrete." *Computer Aided Analysis and Design of Concrete Structures*, Zell Am See, 945-957.
- Oller, S. (2001a). *Dinámica no Lineal*, CIMNE, Barcelona.
- Oller, S. (2001b). *Fractura Mecánica – Un Enfoque Global*, CIMNE, Barcelona.
- Oller, S., and Barbat, A. H. (2005). "Moment–curvature damage model for bridges subjected to seismic loads " *Computer Methods in Applied Mechanics and Engineering*, , In Press, Corrected Proof, Available online 28 November 2005 www.sciencedirect.com.
- Oller, S., Barbat, A. H., Oñate, E., and Hanganu, A. "A damage model for the seismic analysis of building structures." *A Proceedings of the Tenth World Conference on Earthquake Engineering*, Madrid, Spain, 2593-2598.
- Oller, S., Luccioni, B., and Barbat, A. H. (1996). "Un Método de Evaluación del Daño Sísmico en Estructuras de Hormigón Armado." *Revista Internacional de Métodos Numéricos para Cálculo y Diseño en Ingeniería*, 12(2), 215-238.
- Otani, S. (1974). "Inelastic Analysis of R/C Frame Structures." *Journal of the Structural Division, ASCE*, 100(7).
- Otani, S., and Sozen, M. A. (1972). "Behaviour of multi-story reinforced concrete frames during earthquakes. ." S. R. Series 392, University of Illinois, Urbana, IL.
- Park, R., and Paulay, T. (1975). *Reinforced concrete structures*, John Wiley and Sons.
- Park, Y. J., and Ang, A. H. (1985). "Mechanistic Seismic Damage Model for Reinforced Concrete." *Journal of Structural Engineering, ASCE*, 111(4), 722-739.
- Paz, M. (1992). *Dinámica estructural : teoría y cálculo* Reverté, Barcelona.
-

-
- Powell, G. H. (1975). "Supplement to computer program DRAIN-2D." *DRAIN-2D user's guide*, University of California Berkeley, CA.
- Prager, W., and Hodge, P. (1951). *Theory of Perfectly Plastic Solids*, John Wiley and Sons, New York.
- Riva, P., and Cohn, M. Z. (1990). "Engineering Approach to Nonlinear Analysis of Concrete Structures." *Journal of Structural Engineering, ASCE*, 116(8), 2163-2186.
- Roufaiel, M. S. L., and Meyer, C. (1981). "Analysis of damaged concrete frame buildings." *NSF-CEE-81-21359-1*, Columbia University, New York, NY.
- Salamy, M. R., Kobayashi, H., and Unjoh, S. "Experimental and analytical study on RC deep beams." *Second International Conference on Concrete & Development*.
- Shi, G., and Alturi, S. N. (1998). "Elasto-plastic Large Deformation Analysis of Space-Frames: A Plastic-Hinge and Stress-Based Explicit Derivation of Tangent Stiffnesses." *International Journal for Numerical Methods in Engineering*, 26, 589-615.
- Simo, J. C., and Hughes, T. J. R. (1998). *Computational Inelasticity* Springer – Verlag
- Simo, J. C., and Ju, J. W. (1987). "Stress and strain based continuum damage models-I. Formulation." *International Journal of Solids and Structure*, 23, 821 -840.
- Sozen, M. A. (1981). "Review of Earthquake response of reinforced concrete buildings with a view to drift control - State-of-the-Art in Earthquake Engineering." Turkish National Committee on Earthquake Engineering, Istanbul, Turkey
- Takeda, T., Sozen, M. A., and Nielsen, N. (1970). "Reinforced Concrete Response to Simulated Earthquakes." *Journal of Structural Engineering, ASCE*, 96(12), 2557-2573.
- Taucer, F., Spacone, E., and Filippou, F. C. (1991). "A Fiber Beam-Column Element for Seismic. Response Analysis of Reinforced Concrete Structures." EERC 91/17, Earthquake Engineering Research Center, University of California.
- Taylor, W. M. S. (2004). "Análise elastoplástica de estruturas metálicas utilizando algoritmos de retorno radial." *Revista Internacional de Métodos Numéricos Para Cálculo y Diseño en Ingeniería*, 20(3), 297-317.
-

Thomson, E., Benito, A., and Flórez, J. L. (1998). "Simplified Model of Low Cycle Fatigue for RC Frames." *Journal of Structural Engineering*, 124(9), 1082-1085.

Toussi, S., and Yao, J. T. P. (1982). "Hysteresis identification of existing structures " *Journal of Engineering Mechanics ASCE* 109(5), 1189-1203.

Vecchio, F. J., and Emara, M. B. (1992). "Shear Deformations in Reinforced Concrete Frames." *ACI Structural Journal*, 89(1), 45-46.
